ISSN 1948-0210 (online)

World Journal of *Stem Cells*

Monthly Volume 17 Number 3 March 26, 2025

Published by Baishideng Publishing Group Inc

WJSC

World Journal of Stem Cells

Contents

Monthly Volume 17 Number 3 March 26, 2025

REVIEW

Yi YF, Fan ZQ, Liu C, Ding YT, Chen Y, Wen J, Jian XH, Li YF. Immunomodulatory effects and clinical application of exosomes derived from mesenchymal stem cells. *World J Stem Cells* 2025; 17(3): 103560 [DOI: 10.4252/wjsc.v17.i3.103560]

MINIREVIEWS

Wang JJ, Zheng Y, Li YL, Xiao Y, Ren YY, Tian YQ. Emerging role of mesenchymal stem cell-derived exosomes in the repair of acute kidney injury. *World J Stem Cells* 2025; 17(3): 103360 [DOI: 10.4252/wjsc.v17.i3.103360]

ORIGINAL ARTICLE

Basic Study

Liu WJ, Wang JX, Li QF, Zhang YH, Ji PF, Jin JH, Zhang YB, Yuan ZH, Feng P, Wu YF, Shen HY, Wang P. Fat mass and obesity-associated protein in mesenchymal stem cells inhibits osteoclastogenesis *via* lnc NORAD/miR-4284 axis in ankylosing spondylitis. *World J Stem Cells* 2025; 17(3): 98911 [DOI: 10.4252/wjsc.v17.i3.98911]

Cao XZ, Zhang YF, Song YW, Yuan L, Tang HL, Li JY, Qiu YB, Lin JZ, Ning YX, Wang XY, Xu Y, Lin SQ. DNA methyltransferase 1/miR-342-3p/Forkhead box M1 signaling axis promotes self-renewal in cervical cancer stem-like cells *in vitro* and nude mice models. *World J Stem Cells* 2025; 17(3): 99472 [DOI: 10.4252/wjsc.v17.i3.99472]

Shen YZ, Yang GP, Ma QM, Wang YS, Wang X. Regulation of lncRNA-ENST on Myc-mediated mitochondrial apoptosis in mesenchymal stem cells: *In vitro* evidence implicated for acute lung injury therapeutic potential. *World J Stem Cells* 2025; 17(3): 100079 [DOI: 10.4252/wjsc.v17.i3.100079]

Jin JJ, Liu RH, Chen JY, Wang K, Han JY, Nie DS, Gong YQ, Lin B, Weng GX. MiR-21-5p-enriched exosomes from hiPSC-derived cardiomyocytes exhibit superior cardiac repair efficacy compared to hiPSC-derived exosomes in a murine MI model. *World J Stem Cells* 2025; 17(3): 101454 [DOI: 10.4252/wjsc.v17.i3.101454]

Fu Y, Han YT, Xie JL, Liu RQ, Zhao B, Zhang XL, Zhang J, Zhang J. Mesenchymal stem cell exosomes enhance the development of hair follicle to ameliorate androgenetic alopecia. *World J Stem Cells* 2025; 17(3): 102088 [DOI: 10.4252/wjsc.v17.i3.102088]

SYSTEMATIC REVIEWS

Safwan M, Bourgleh MS, Haider KH. Clinical experience with cryopreserved mesenchymal stem cells for cardiovascular applications: A systematic review. *World J Stem Cells* 2025; 17(3): 102067 [DOI: 10.4252/wjsc.v17.i3.102067]

LETTER TO THE EDITOR

Guo MQ, Hu P, Huang ZW. Cyclodextrin host-guest complex to facilitate sinomenine-based osteoporosis therapy. *World J Stem Cells* 2025; 17(3): 101376 [DOI: 10.4252/wjsc.v17.i3.101376]

Lin F, Ma KX, Ding Y, Liang XT. Efficacy equivalence but hidden hurdles: Can serum-free human umbilical cord mesenchymal stem cells translate to clinically superior osteoarthritis therapy. *World J Stem Cells* 2025; 17(3): 104566 [DOI: 10.4252/wjsc.v17.i3.104566]

World Journal of Stem Cells

Monthly Volume 17 Number 3 March 26, 2025

Contents

ABOUT COVER

Peer Review of *World Journal of Stem Cells*, Rafael Moreno-Gómez-Toledano, Assistant Professor, PhD, Department of Surgery, Medical, and Social Sciences, Universidad de Alcalá, Alcalá de Henares 28806, Madrid, Spain. rafael.moreno@uah.es

AIMS AND SCOPE

The primary aim of *World Journal of Stem Cells* (*WJSC*, *World J Stem Cells*) is to provide scholars and readers from various fields of stem cells with a platform to publish high-quality basic and clinical research articles and communicate their research findings online. *WJSC* publishes articles reporting research results obtained in the field of stem cell biology and regenerative medicine, related to the wide range of stem cells including embryonic stem cells, germline stem cells, tissue-specific stem cells, adult stem cells, mesenchymal stromal cells, induced pluripotent stem cells, embryonal carcinoma stem cells, hemangioblasts, lymphoid progenitor cells, *etc*.

INDEXING/ABSTRACTING

The *WJSC* is now abstracted and indexed in Science Citation Index Expanded (SCIE, also known as SciSearch®), Journal Citation Reports/Science Edition, PubMed, PubMed Central, Scopus, Biological Abstracts, BIOSIS Previews, Reference Citation Analysis, China Science and Technology Journal Database, and Superstar Journals Database. The 2024 Edition of Journal Citation Reports® cites the 2023 journal impact factor (JIF) for *WJSC* as 3.6; JIF without journal self cites: 3.5; 5-year JIF: 4.2; JIF Rank: 105/205 in cell biology; JIF Quartile: Q3; and 5-year JIF Quartile: Q2. The *WJSC*'s CiteScore for 2023 is 7.8 and Scopus CiteScore rank 2023: Histology is 11/62; Genetics is 78/347; Genetics (clinical) is 19/99; Molecular Biology is 131/410; Cell Biology is 104/285.

RESPONSIBLE EDITORS FOR THIS ISSUE

Production Editor: *Xiang-Di Zhang*; **Production Department Director:** *Xu Guo*; **Cover Editor:** *Jia-Ru Fan*.

NAME OF JOURNAL
World Journal of Stem Cells

ISSN
ISSN 1948-0210 (online)

LAUNCH DATE
December 31, 2009

FREQUENCY
Monthly

EDITORS-IN-CHIEF
Shengwen Calvin Li

EDITORIAL BOARD MEMBERS
https://www.wjgnet.com/1948-0210/editorialboard.htm

PUBLICATION DATE
March 26, 2025

INSTRUCTIONS TO AUTHORS
https://www.wjgnet.com/bpg/gerinfo/204

GUIDELINES FOR ETHICS DOCUMENTS
https://www.wjgnet.com/bpg/GerInfo/287

GUIDELINES FOR NON-NATIVE SPEAKERS OF ENGLISH
https://www.wjgnet.com/bpg/gerinfo/240

PUBLICATION ETHICS
https://www.wjgnet.com/bpg/GerInfo/288

PUBLICATION MISCONDUCT
https://www.wjgnet.com/bpg/gerinfo/208

ARTICLE PROCESSING CHARGE
https://www.wjgnet.com/bpg/gerinfo/242

STEPS FOR SUBMITTING MANUSCRIPTS
https://www.wjgnet.com/bpg/GerInfo/239

ONLINE SUBMISSION
https://www.f6publishing.com

World Journal of Stem Cells

Submit a Manuscript: https://www.f6publishing.com

World J Stem Cells 2025 March 26; 17(3): 103560

DOI: 10.4252/wjsc.v17.i3.103560

ISSN 1948-0210 (online)

REVIEW

Immunomodulatory effects and clinical application of exosomes derived from mesenchymal stem cells

Yang-Fei Yi, Zi-Qi Fan, Can Liu, Yi-Tong Ding, Yao Chen, Jie Wen, Xiao-Hong Jian, Yu-Fei Li

Specialty type: Cell and tissue engineering

Provenance and peer review: Invited article; Externally peer reviewed.

Peer-review model: Single blind

Peer-review report's classification
Scientific Quality: Grade B, Grade C, Grade C, Grade C, Grade D
Novelty: Grade B, Grade B, Grade B, Grade C
Creativity or Innovation: Grade B, Grade B, Grade B, Grade C
Scientific Significance: Grade B, Grade B, Grade B, Grade B

P-Reviewer: Cui YX; Ding G; Hussain MS; Ventura C

Received: November 25, 2024
Revised: January 16, 2025
Accepted: February 17, 2025
Published online: March 26, 2025
Processing time: 118 Days and 16.8 Hours

Yang-Fei Yi, Zi-Qi Fan, Can Liu, Yi-Tong Ding, Yao Chen, Jie Wen, Xiao-Hong Jian, Yu-Fei Li, Department of Anatomy, Hunan Normal University School of Medicine, Changsha 410005, Hunan Province, China

Jie Wen, Department of Pediatric Orthopedics, Hunan Provincial People's Hospital, Changsha 410013, Hunan Province, China

Co-first authors: Yang-Fei Yi and Zi-Qi Fan.

Co-corresponding authors: Jie Wen and Yu-Fei Li.

Corresponding author: Jie Wen, PhD, Associate Professor, Department of Pediatric Orthopedics, Hunan Provincial People's Hospital, No. 61 West Jiefang Road, Changsha 410013, Hunan Province, China. cashwj@qq.com

Abstract

Exosomes (Exos) are extracellular vesicles secreted by cells and serve as crucial mediators of intercellular communication. They play a pivotal role in the pathogenesis and progression of various diseases and offer promising avenues for therapeutic interventions. Exos derived from mesenchymal stem cells (MSCs) have significant immunomodulatory properties. They effectively regulate immune responses by modulating both innate and adaptive immunity. These Exos can inhibit excessive inflammatory responses and promote tissue repair. Moreover, they participate in antigen presentation, which is essential for activating immune responses. The cargo of these Exos, including ligands, proteins, and microRNAs, can suppress T cell activity or enhance the population of immunosuppressive cells to dampen the immune response. By inhibiting lymphocyte proliferation, acting on macrophages, and increasing the population of regulatory T cells, these Exos contribute to maintaining immune and metabolic homeostasis. Furthermore, they can activate immune-related signaling pathways or serve as vehicles to deliver microRNAs and other bioactive substances to target tumor cells, which holds potential for immunotherapy applications. Given the immense therapeutic potential of MSC-derived Exos, this review comprehensively explores their mechanisms of immune regulation and therapeutic applications in areas such as infection control, tumor suppression, and autoimmune disease management. This article aims to provide valuable insights into the mechanisms behind the actions of MSC-derived Exos, offering theoretical references for their future clinical utilization as cell-free drug preparations.

Key Words: Mesenchymal stem cells; Exosomes; Immunomodulatory effects; Clinical application; Therapeutic potential

Core Tip: Exosomes (Exos) are extracellular vesicles secreted by cells, and they serve as crucial mediators of intercellular communication, playing a pivotal role in the pathogenesis, progression, and therapeutic interventions for various diseases. Given the immense therapeutic potential of Exos derived from mesenchymal stem cells (MSC-Exos), this review article comprehensively explores mechanisms underlying their immune regulation as well as their therapeutic applications in infection control measures and tackling tumors or autoimmune diseases among others. This article aims to provide valuable insights into further investigations regarding the mechanism behind MSC-Exo actions while offering theoretical references for future clinical utilization of MSC-Exos as cell-free drug preparations.

Citation: Yi YF, Fan ZQ, Liu C, Ding YT, Chen Y, Wen J, Jian XH, Li YF. Immunomodulatory effects and clinical application of exosomes derived from mesenchymal stem cells. *World J Stem Cells* 2025; 17(3): 103560
URL: https://www.wjgnet.com/1948-0210/full/v17/i3/103560.htm
DOI: https://dx.doi.org/10.4252/wjsc.v17.i3.103560

INTRODUCTION

Exosomes (Exos) were first discovered in 1983 as 50-nm vesicles released by reticulocytes carrying transferrin receptors extracellularly[1]. Since then, the understanding of the mechanisms and functions of Exos has exponentially expanded[2]. Exos are extracellular vesicles (EVs) with a diameter ranging from 40 to 160 nm (mean, ~100 nm) that originate from endosomes[3]. Depending on the specific cell type that they derive from, Exos contain various components such as DNA, RNA, lipids, metabolites, cytoplasmic contents, and cell-surface proteins[4]. The exact physiological role of Exo production by cells remains elusive and requires further investigation[5]. Due to their functional and targeted nature as cellular constituents, Exos play a crucial role in intercellular communication[6]. Mesenchymal stem cells (MSCs) are a class of adult stem cells first identified by Friedenstein in mouse bone marrow and characterized by their multilineage differentiation potential. Caplan subsequently coined the term "mesenchymal stem cells"[7], although their definitive stem cell properties have yet to be rigorously demonstrated *in vivo*[8]. MSCs have been shown to originate from perivascular and pericytic progenitors in almost all tissues[9]. These cells possess trilineage differentiation potential, enabling them to differentiate into osteoblasts, adipocytes, and chondrocytes. They express positive cell surface markers CD90, CD105, and CD73, while lacking CD45, CD34, CD14, CD79a, and HLA-DR[10]. Under specific conditions, MSCs can also differentiate into other cell types, such as neurons and cardiomyocytes[11].

MSCs possess a certain self-renewal capacity and can be propagated through multiple generations *in vitro* while maintaining their phenotype and differentiation potential[12]. They secrete a variety of cytokines and growth factors, which inhibit the proliferation of B cells and T cells, suppress monocyte maturation, and promote the generation of regulatory T cells (Tregs) and M2 macrophages[13]. These characteristics endow MSCs with immunomodulatory functions, forming the foundation for their application in treating various immune-related diseases. The primary clinical value of MSCs appears to stem from secreted EVs (including Exos) and a range of cytokines and growth factors[14]. The immunoregulatory effects of these secreted Exos have demonstrated therapeutic potential in numerous clinical studies. These studies encompass conditions such as myocardial infarction, stroke, graft-*versus*-host disease (GvHD), systemic lupus erythematosus (SLE), rheumatoid arthritis (RA), Crohn's disease, acute lung injury, chronic obstructive pulmonary disease, liver cirrhosis, multiple sclerosis (MS), amyotrophic lateral sclerosis, and diabetes[15].

A substantial body of evidence suggests that MSCs exert their immunomodulatory functions primarily through paracrine pathways, particularly *via* Exos[16]. Exos derived from MSCs (MSC-Exos) exhibit comparable biological activities to MSCs and possess several advantageous characteristics such as rapid passage through capillaries, inherent stability, and robust information transfer capacity compared to MSCs[17]. Furthermore, the utilization of Exos can circumvent issues associated with ectopic osteogenesis, tumor formation, pulmonary capillary blockade, and immune rejection commonly encountered in cell therapy. The low immunogenicity and high stability of Exos make them a promising alternative strategy for cell therapy[18]. Notably, Exos play pivotal roles in inflammation, tumors, and autoimmune diseases, as well as graft rejection[19]. MSC-Exos have achieved several significant breakthroughs in recent years. Research has demonstrated their ability to cross the blood-brain barrier, exert neuroprotective effects, and facilitate nerve regeneration. This approach offers novel insights and potential strategies for the treatment of brain injuries, stroke, and neurodegenerative diseases such as Alzheimer's and Parkinson's disease. MSC-Exos play a crucial role in immune regulation by modulating immune responses and mitigating inflammation, which holds potential for treating autoimmune diseases such as RA and SLE[20,21]. Additionally, MSC-Exos are being explored for cancer treatment, including metastatic cancers. Studies have demonstrated their utility as drug delivery vectors to enhance the efficacy of anticancer drugs while minimizing side effects. In cardiovascular disease and skin wound repair, MSC-Exos have exhibited the capacity to promote tissue repair and regeneration, supporting myocardial cell survival and functional recovery, as well as accelerating skin wound healing[22]. Recent technological advancements have improved the

production efficiency and functional customization of MSC-Exos. For instance, genetic engineering and optimized culture conditions have enhanced specific therapeutic properties of Exos[23]. These innovations highlight the significant potential of MSC-Exos as a novel biologic therapeutic tool. Several clinical studies on Exos have been approved by the Food and Drug Administration (FDA), including investigations into the molecular mechanisms of Exos in melanoma pathogenesis (FDA lot number: NCT02310451), the clinical correlation of glioma exosomal molecular abnormalities (FDA batch No.: NCT06116903), and the effect of Exo administration in preventing early leakage in patients with low anterior resection rectal cancer (FDA Lot No.: NCT06536712). As research progresses, the application prospects for MSC-Exos will continue to broaden[24]. Therefore, this article comprehensively reviews the mechanisms underlying immune regulation by MSC-Exos along with their therapeutic applications in infection control, tumor management, and autoimmune diseases. This article serves as a valuable reference for further investigations into the mechanisms governing MSC-Exo function while providing theoretical support for future clinical implementation of MSC-Exos as cell-free drug preparations.

BIOLOGICAL CHARACTERISTICS OF EXOS DERIVED FROM MSCS

MSCs can be isolated from various tissues, and Exos derived from different tissues and cell types may carry distinct biomolecules that confer unique immune properties and potential therapeutic applications. MSC-Exos exhibit significant immunomodulatory effects, capable of downregulating inflammatory responses and promoting immune tolerance. They are widely utilized in the treatment of inflammatory diseases and autoimmune conditions such as SLE and RA, as well as in promoting tissue repair and regeneration[25]. Exos derived from tumor cells are frequently utilized as biomarkers and therapeutic targets for developing novel cancer immunotherapies and diagnostic approaches[26]. Exos secreted by cardiomyocytes can modulate cardiac inflammatory responses, enhance cardiomyocyte survival, and facilitate cardiac tissue regeneration. In studies of myocardial infarction and other cardiovascular diseases, these Exos have demonstrated potential therapeutic benefits[22]. Exos from adipose-derived stem cells are employed to treat conditions such as impaired wound healing and skin disorders, promoting the regeneration process. Exos derived from neural stem cells exhibit neuroprotective and anti-inflammatory properties, provide neurotrophic support, and regulate immune responses within the nervous system, showing promise in treating neurodegenerative diseases like Alzheimer's and Parkinson's[27,28]. These cells can be derived from diverse tissues depending on their origin. Exos are small vesicles released into the extracellular space following fusion between intracellular multivesicular bodies and the cellular membrane[29]. This secretory process involves recognition and trafficking of specific proteins and lipids[30], such as the ESCRT system (endosomal sorting complex)[31]. Exos typically range in size from 40 to 160 nm[32] with a lipid bilayer membrane structure that provides stability and protection[33], conferring them potential therapeutic utility due to their stable structure and precise targeting ability[34,35]. Exos transport distinct proteins and RNA molecules that mirror the cellular origin and exert an impact on the functionality of recipient cells[36]. They assume pivotal roles in intercellular communication by transferring informational molecules to regulate immune response, inflammation, and tissue repair, among other processes[37]. Consequently, owing to their inherent structural stability and precise targeting capabilities, Exos are regarded as promising therapeutic tools[38] (Figure 1).

MSC-Exos not only express protein markers commonly found in all Exos[39], but also exhibit specific membrane surface molecules on MSCs[40]. These Exos contain bioactive molecules such as microRNAs (miRNAs), mRNA, and proteins that play a crucial role in regulating gene expression and function in target cells. Lai *et al*[41] first investigated the role of MSC-Exos in a mouse model of myocardial ischemia-reperfusion injury in 2010, followed by studies conducted across various disease models[42]. MSC-Exos have been shown to facilitate tissue regeneration through intercellular communication, particularly following kidney, liver, cardiovascular, and nervous system injuries[43]. By secreting Exos, MSCs modulate immune responses by reducing inflammatory factors while increasing anti-inflammatory factor levels [44]. These Exos carry miRNAs and proteins that regulate apoptotic pathways to enhance the survival of target cells and mitigate oxidative stress damage[45]. In heart disease models specifically, MSC-Exos improve cardiac function and morphology by augmenting survival signaling pathways while suppressing inflammatory responses[46]. Therefore, the clinical potential for utilizing MSC-Exos as a cell replacement therapy is extensive. However, MSC-Exos encounter several practical challenges during the isolation process. For instance, Exo production can be influenced by multiple factors such as the diversity of cell sources, variations in culture conditions, and differences in cell states. This variability introduces uncertainty in Exo yield for each isolation procedure, thereby impacting its consistent supply[47]. Additionally, efficiently extracting high-purity Exos from other cellular components remains a significant challenge. Existing separation techniques may introduce impurities, compromising the efficacy and safety of research outcomes and clinical applications. Scaling up from laboratory to clinical use presents numerous difficulties. To address these issues, it is essential not only to optimize the production process to enhance yield and purity but also to ensure stringent quality control and standardization to meet rigorous clinical application requirements. Overcoming these challenges may involve optimizing culture conditions, refining separation techniques, and developing innovative processes to facilitate the widespread and effective utilization of MSC-Exos in practical applications.

ROLE OF MSC-EXOS IN IMMUNE REGULATION

MSC-Exos play a pivotal role in immunomodulation, which has been associated with their capacity to influence various immune cell functions[48]. MSC-Exos possess the ability to regulate both innate and adaptive immune responses. In terms of innate immunity, they modulate the polarization and cytokine secretion of macrophages and dendritic cells

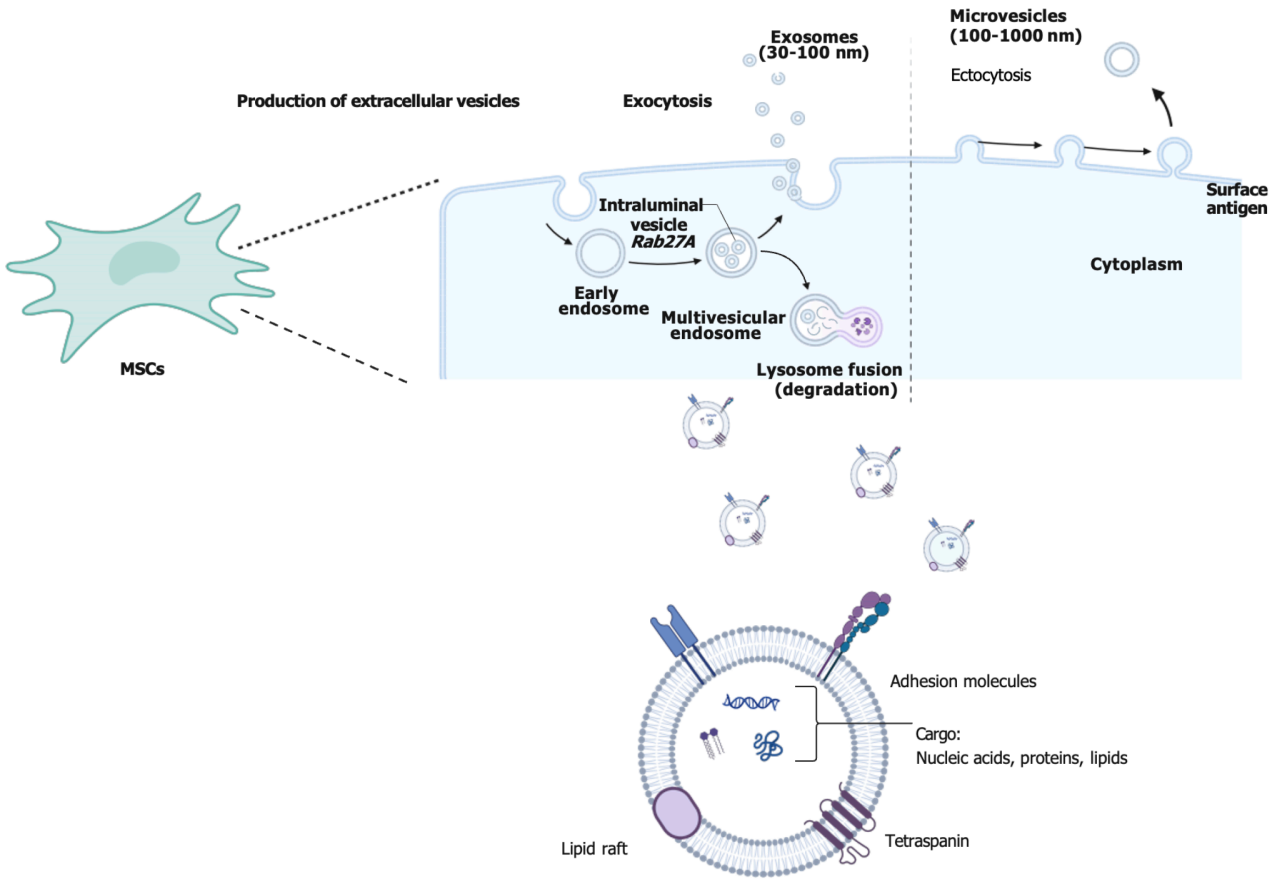

Figure 1 Exocytosis of exosomes derived from mesenchymal stem cells. The diagram illustrates the process of exosome biogenesis: From early endosomes to multivesicular bodies, and finally the secretion of exosomes containing various components such as nucleic acids, proteins, lipids, cell adhesion molecules, and transmembrane proteins. MSC: Mesenchymal stem cells.

(DCs) through interactions with these cells, thereby suppressing inflammatory responses[49]. Specifically, MSC-Exos can attenuate inflammatory damage by polarizing macrophages towards an anti-inflammatory M2 phenotype rather than a pro-inflammatory M1 phenotype[50]. Concerning adaptive immunity, MSC-Exos achieve immunosuppression by regulating the activity of T cells and B cells. They inhibit the proliferation and cytotoxic functions of T cells while promoting the generation of Tregs, which are crucial for maintaining immune tolerance and preventing autoimmune diseases[51]. Through these mechanisms, MSC-Exos are capable of maintaining immune tolerance and preventing or treating autoimmune diseases. This capability is especially valuable in scenarios where excessive immune responses must be modulated in disease states such as RA and other autoimmune conditions[52]. MSC-Exos also have the ability to modulate humoral immune responses by influencing the antibody-producing function of B cells[53]. The miRNAs, proteins, and other bioactive molecules encapsulated within MSC-Exos can transmit signals between cells *via* various pathways including direct targeting of specific mRNAs to regulate gene expression or activation/inhibition of immune signaling pathways[54]. MiRNAs are a class of short non-coding RNA molecules that regulate gene expression. MiRNAs encapsulated in Exos can modulate protein expression levels by targeting specific mRNAs, leading to their inhibition or degradation[55]. Specific miRNAs can influence both pro-inflammatory and anti-inflammatory pathways. For instance, certain miRNAs can downregulate the expression of pro-inflammatory factors in M1-type macrophages, thereby promoting their transition to the M2-type (anti-inflammatory) phenotype[56]. Notably, miRNAs such as miR-223 and miR-146a alter the functional state of macrophages by affecting key signaling nodes like nuclear factor-kappaB (NF-κB), signal transducer and activator of transcription (STAT), and phosphatidylinositol 3-kinase/protein kinase B. NF-κB plays a crucial role in the development, differentiation, and responsiveness of immune cells. Exos can modulate the function of immune cells, including T cells, B cells, and macrophages, by regulating the NF-κB pathway. Exos secreted by tumor cells can promote tumor growth and immune escape through the activation of the NF-κB pathway, whereas Exos derived from stem cells may inhibit this pathway and enhance anti-tumor immunity[57]. By modulating the NF-κB signaling pathway, Exos regulate inflammatory responses. For instance, MSC-Exos can exert anti-inflammatory effects by inhibiting NF-κB activity and reducing the production of pro-inflammatory cytokines such as tumor necrosis factor-α (TNF-α) and interleukin (IL)-1β[58]. Cytokines within Exos directly influence immune cell behavior; for example, anti-inflammatory cytokines like IL-10 or transforming growth factor-beta (TGF-β) delivered *via* Exos can modulate immune responses and promote immune tolerance. Additionally, membrane proteins and signaling molecules in Exos can bind to receptors on target cells, initiate intracellular signaling cascades, and regulate cellular behavior. Specific proteins within Exos can directly modulate the immune response, such as by inhibiting immune cell activation or inducing immune cell apoptosis to achieve immune regulatory effects[59]. As natural vectors for signal transduction, MSC-Exos possess significant

regulatory capabilities in controlling immune system homeostasis by inhibiting excessive inflammatory responses while promoting tissue repair.

MSC-Exos regulate immunity by delivering immunoactive substances

In recent years, it has been discovered that MSCs play a crucial role in intercellular communication through the secretion of Exos[45]. These Exos possess the ability to modulate immune cell function and response. Through packaging and transportation of signaling molecules, a diverse range of bioactive compounds can be encapsulated within Exos, ensuring protection against degradation while enabling specific delivery to target cells[60]. Furthermore, Exo surfaces are adorned with various membrane proteins involved in target cell recognition and binding[61]. Upon fusion with the target cell membrane, the contents of Exos are released into the cytoplasm, thereby activating relevant signaling pathways[62]. MSC-Exos exhibit an abundance of miRNAs that specifically target and regulate immune-related gene expression[63]. Certain miRNAs have demonstrated their capability to shift macrophage polarization from proinflammatory M1 phenotype towards an anti-inflammatory M2 phenotype by regulating Toll-like receptor and NF-κB signaling pathways, ultimately leading to inflammation reduction[64].

Proteins present in Exos, such as cytokines and signaling proteins, have a direct impact on the functionality of target cells. Exos can deliver anti-inflammatory cytokines to inhibit the proliferation of T cells and B cells or facilitate the generation of Tregs by delivering immunomodulatory proteins. Moreover, they can transport specific signaling molecules that activate or suppress signaling pathways in target cells, thereby influencing the cellular immune response[65]. This mechanism plays a crucial role in regulating immune system homeostasis and preventing potential damage caused by excessive immune activity[66]. The utilization of MSC-Exos offers novel insights and potential applications for treating various immune-related disorders through efficient delivery of diverse immunoactive substances while modulating immune system responses (Figure 1).

MSC-Exos achieve immunosuppression through different mechanisms

Immunosuppression refers to the process of suppressing or reducing immune system activity through various mechanisms. MSC-Exos modulate cytokines, such as IL-10 and prostaglandin E2, thereby regulating macrophage polarization from a pro-inflammatory M1 to an anti-inflammatory M2 type, which reduces inflammation and promotes tissue repair[67]. The role of MSC-Exos in immune regulation is primarily towards immunosuppression rather than activation[68]. These Exos contain a variety of molecules that can regulate T cell function, including specific miRNAs and proteins that downregulate T-cell receptor signaling, and inhibit T-cell proliferation and activation, thus reducing the intensity of the immune response[69].

Exos contain specific components that can impede the maturation and antigen presentation capacity of DCs, thereby diminishing their potential to activate T cells. Consequently, this effect mitigates the hyperactive response of the immune system towards tissues or grafts[70]. Additionally, MSC-Exos exhibit inhibitory effects on B cell proliferation, differentiation, and antibody production, thus contributing to the amelioration of pathological immune responses. Furthermore, MSC-Exos possess the ability to attenuate inflammation and tissue damage by suppressing the cytotoxic activity of natural killer cells and restraining aggressive behavior within their own tissues[71]. Although Exos can effectively suppress unwanted immune responses and aid in the treatment of autoimmune diseases, prolonged immunosuppression may render the body more susceptible to infections and certain diseases[72]. This is because some protective functions of the immune system may also be compromised. Excessive immunosuppression could negatively impact the body's immune surveillance function, thereby increasing the risk of cancer or other abnormal cell proliferation. In cases of immune suppression, this function may be weakened. Additionally, different tissues may respond variably to Exo therapy. Improper immune regulation may result in incomplete or aberrant tissue repair. Long-term treatment might lead to a decrease in Exo adaptability and efficacy. In addition, there are dosing and delivery challenges: Determining the appropriate dose to avoid excessive suppression of immune system function remains a challenge. Efficiently delivering Exos to specific target cells is also technically challenging. Therefore, when developing Exo-based therapies, thorough research and clinical trials are essential to evaluate these potential risks and ensure their safety and efficacy for long-term applications. Despite these challenges, Exos remain promising candidates for treating tumor-related diseases and immune disorders such as autoimmune diseases, transplant rejection, and inflammatory diseases (Table 1).

ROLE OF MSC-EXOS IN DISEASES

Inflammatory diseases

MSC-Exos have the ability to mitigate inflammatory responses by modulating immune reactions in inflammatory diseases. They facilitate the transportation of anti-inflammatory molecules and inhibit the release of pro-inflammatory cytokines, thereby attenuating excessive immune responses triggered by bacterial or viral infections. These Exos express multiple adhesion molecules (CD29, CD44, and CD73), enabling them to home in on injured and inflamed tissues[15]. Several studies have indicated that macrophages are the primary cellular targets of MSC-Exos for reducing colonic inflammation. The activation of the NF-κB signaling pathway in colonic macrophages induced by damage-associated molecular patterns released from damaged epithelial cells leads to increased expression of inducible nitric oxide synthase, as well as elevated levels of inflammatory factors such as TNF-α, IL-1β, nitric oxide, and chemokines involved in lymphocyte and monocyte recruitment (CCL-17 and CCL-24)[55]. Macrophages are considered pivotal cells responsible for initiating colonic inflammation[73]. Cao *et al*'s study demonstrated that MSC-derived EVs significantly ameliorated dextran sulfate sodium-induced colitis in mice by inducing polarization towards immunosuppressive M2 phenotype in

colonic macrophages[74]. The therapeutic effect exerted by these EVs on ulcerative colitis repair seems to be associated with JAK1/STAT1/STAT6 signaling[74]. Yang *et al*'s findings suggested that modulation of antioxidant/oxidative balance within the affected gut is accountable for MSC-EV-induced phenotypic and functional effects on macrophages [75]. Additionally, MSC-EV treatment resulted in a reduction in the cleavage of caspases-3, -8, and -9 as well as attenuated release of damage-associated molecular patterns from damaged intestinal epithelial cells. This led to the attenuation of NF-κB signaling pathway activation in colonic macrophages and subsequently promoted the generation of an immunosuppressive M2 phenotype[75].

MSC-Exos exhibit a protective effect on hepatocytes in cases of acute liver injury and fibrosis. In hepatitis, MSC-Exos inhibit natural killer T cells, $CD4^+$ T lymphocytes, and hepatic stellate cells, thereby attenuating acute liver failure and fibrosis[76]. Furthermore, they safeguard stem cells by suppressing pyroptosis, inhibiting hepatocyte death, and reducing IL-1β- and IL-18-mediated inflammation[77]. Accumulating evidence suggests that MSC-Exos can shield lung epithelial cells from reactive oxidants and proteolytic enzymes released by infiltrating neutrophils and monocytes[78]. Mansouri *et al*[79] demonstrated that a single intravenous injection of Exos derived from human bone marrow-derived MSC (BM-MSC) significantly mitigated bleomycin-induced pulmonary fibrosis in mice through modulation of the phenotype and function of alveolar macrophages. Additionally, MSC-Exos alleviate inflammation at the site of nerve injury by inhibiting microglial production of inflammatory factors (TNF-α and IL-1β) while promoting synthesis of anti-inflammatory factors (IL-10 and TGF-β)[80].

Tumor immunity and cancer therapy

The role of MSC-Exos in tumor immunity is dual, primarily determined by the bioactive molecular composition of the Exos and their interaction with the tumor microenvironment[81]. They can deliver immunosuppressive molecules that facilitate immune evasion by tumors, while also containing specific miRNAs and proteins that potentially exert immunostimulatory effects[82], enhancing immune recognition and cytotoxicity against tumor cells. MSC-Exos possess the ability to modulate the immune balance within the tumor microenvironment and shape its characteristics[83]. Consequently, their impact on tumor immunity is intricate and multifaceted, potentially providing both anti-tumor support or promoting tumorigenesis[84]. Biswas *et al*[85] demonstrated *in vivo* that MSC-Exos upregulate programmed death-ligand 1 expression in bone marrow cells while downregulating programmed cell death-1 expression in T cells, thereby suppressing protective antitumor immunity specifically in breast cancer models. Furthermore, MSC-Exos have been shown to suppress proinflammatory responses and oxidative stress mediated by immune system cells as well as humoral factors under both *in vitro* and *in vivo* conditions, creating a conducive environment for tissue regeneration[86].

Exos derived from human adipose-derived MSCs have been shown to exert inhibitory effects on ovarian cancer cells by inducing cell cycle arrest and activating mitochondrial-mediated apoptotic signaling pathways[87]. Exo miR-187 derived from human BM-MSCs was found to suppress malignant characteristics in prostate cancer cells[88] by targeting CD276, thereby inhibiting the JAK3-STAT3-Slug pathway in PCa[89]. Exos derived from human umbilical cord MSCs were utilized for paclitaxel loading and their effect on cervical cancer cell line (HeLa) was evaluated. These Exos accelerated cancer cell death through modulation of Bax, BCL2, cleaved Caspase-3, and cleaved Caspase-9 levels, while reducing chemotherapy resistance *via* regulation of epithelial-mesenchymal transition-related proteins such as TGF-β and catenin-β [90]. MSC-Exos have emerged as a valuable tool for cancer suppression, exhibiting the potential to inhibit hepatocellular carcinoma progression through blockade of the C5orf66-AS1/miR-127-3p/DUSP1/ERK axis[91].

Autoimmune diseases

It has been observed that MSC-Exos exhibit significant inhibitory effects on various effector cells involved in both innate and adaptive immune responses. Remarkable progress has been achieved in the treatment of autoimmune disorders, such as MS, SLE, type 1 diabetes mellitus, uveitis, and RA[92]. MSC-Exos demonstrate the ability to replicate MSC functionality while surpassing the limitations associated with conventional cell therapies.

MS is the most prevalent inflammatory disease of the central nervous system (CNS). Microglia, as the primary immune cells in the CNS, play a crucial role in maintaining tissue homeostasis under normal physiological conditions[93]. Glial cells contribute to both neurodestructive and neuroprotective functions[94]. An imbalance between M1/M2 phenotypes inhibiting neuroprotective functions can promote MS development. Isik *et al*[95] demonstrated that treatment with BM-MSC-Exos suppressed microglial polarization towards the M1 phenotype while promoting polarization towards the M2 phenotype, leading to secretion of anti-inflammatory cytokines such as IL-10 and TGF-β. Notably, BM-MSC-Exos treatment significantly ameliorated neurobehavioral symptoms of experimental autoimmune encephalomyelitis and alleviated inflammation and demyelination within the CNS.

Uveitis, a leading cause of global visual impairment, is believed to be primarily driven by autoimmunity. Numerous studies have demonstrated the beneficial effects of MSC-Exos on inflammatory ocular diseases. In autoimmune uveitis mice, retinal photoreceptors exhibited severe damage accompanied by infiltration of inflammatory cells; however, when MSC-Exos were administered *via* tail vein injection in autoimmune uveitis mice, their retinas resembled those of normal mice with minimal structural damage and inflammatory infiltration[96,97]. Notably, T helper 1 (Th1) and Th17 cells play crucial roles in the pathogenesis of autoimmune uveitis. Treatment with MSC-Exos resulted in significantly reduced numbers of interferon-gamma+$CD4^+$ cells (Th1) and IL-17+$CD4^+$ cells (Th17) compared to phosphate buffered saline-treated mice[98]. These findings suggest that MSC-Exos possess the ability to suppress the development of autoimmune uveitis through inhibition of Th1 and Th17 cell responses.

RA is a chronic inflammatory disease characterized by synovial hyperplasia and immune-cell infiltration, leading to joint destruction[99]. Studies have found that exosomal miRNAs also play an important role in alleviating the development of RA. MSC-Exos expressing miRNA-150-5p reduced the migration and invasion of RA fibroblast-like synoviocytes and downregulated human umbilical vein endothelial cell tube formation by targeting matrix metallopro-

teinase 14 and vascular endothelial growth factor[100]. MSC-EV provides new insights into the treatment of RA and may provide new opportunities and strategies for the treatment of this autoimmune disease. SLE is a chronic autoimmune disease characterized by immune inflammation and multiple organ damage. The pathogenesis of SLE is extremely complex. With the help of follicular helper T (Tfh) cells, antinuclear antibodies are produced, leading to the deposition of immune complexes in important organs. It has been found that the infusion of human BM-MSCs into a mouse model of lupus nephritis improved the survival of mice and alleviated the clinical symptoms of glomerulonephritis by inhibiting the development of Tfh cells and reducing the levels of autoantibodies[87].

Organ transplantation

Immune rejection is a crucial factor limiting the prognosis of organ transplantation and represents an urgent problem that needs to be addressed. Previous studies have demonstrated that the inflammatory environment can influence the characteristics and expression of biomolecules, such as proteins and nucleic acids, within Exos. Conversely, stem cells can effectively modulate inflammatory responses by transferring genetic information, including miRNA, *via* Exos, thereby playing an immunomodulatory role in tissue repair processes. Exosomal miRNAs serve as key regulators of islet cell function encompassing insulin expression, processing, and secretion. These exosomal miRNAs act as valuable biomarkers for assessing islet cell function and survival with significant implications for the outcome of islet transplantation[101]. Furthermore, they may be closely associated with vascular remodeling and immune regulation following islet transplantation. Notably, miR-21-5p derived from BM-MSC-Exos has been found to prevent islet apoptosis by suppressing PDCD4 expression, thus offering potential therapeutic applications as a cell-free agent to minimize beta-cell apoptosis during early stages of islet transplantation[102]. The team led by Mahato successfully delivered Exos into a rat model following islet transplantation, while co-culturing with peripheral blood mononuclear cells. This intervention significantly downregulated the expression levels of Fas and miR-375 in the rat model post-transplantation, thereby enhancing Tregs function through peripheral blood mononuclear cell proliferation. These findings highlight the significant immunomodulatory potential of MSC-Exos in improving immune tolerance after islet transplantation. Consequently, this study suggests that utilizing Exos as a means of immunomodulation holds great promise for advancing research in organ transplantation[103].

Currently, the direct application of MSC-Exos in organ transplantation indicates a promising potential for MSCs in the field of organ transplantation. Graft-infiltrating DCs and $CD8^+$ T lymphocytes play crucial roles in immune regulation following liver transplantation (LT). Exos also emerge as a significant factor involved in transplantation immunity. Exos derived from $CD80^+$ DCs negatively regulate CD8 T cells by suppressing nucleotide-binding domain, leucine-rich repeat, and pyrin domain-containing protein 3 expression, thereby playing an essential role in attenuating acute LT rejection. These findings unveil a novel function of Exos derived from $CD80^+$ DCs associated with the induction of LT tolerance [104].

CLINICAL POTENTIAL AND APPLICATION OF MSC-DERIVED EXOS

MSCs have been extensively utilized in cell therapy due to their potent immunomodulatory and regenerative properties [105]. The paracrine activity of MSCs, particularly the production of various factors through EVs, notably Exos, has been demonstrated as a crucial determinant of their primary efficacy after infusion[106]. MSC-Exos possess significant advantages over MSCs themselves and effectively mitigate adverse side effects such as infusion-related toxicity[107]. Consequently, MSC-Exos are emerging as a promising cell-free therapeutic tool with an increasing number of clinical studies evaluating their therapeutic efficacy in diverse diseases[48]. MSC-Exos exhibit immense potential for clinical application as cell-free agents[108].

MSC-Exos from diverse sources exhibit conserved biological functions; however, they may also display functional disparities[109]. For instance, adipose tissue-derived MSC-Exos demonstrate superior angiogenic capacity compared to those derived from bone marrow[110]. Conversely, BM-MSC-Exos possess immunomodulatory and anti-inflammatory effects by inhibiting interferon-gamma secretion in T cells[111]. The route of administration is another crucial factor influencing the therapeutic efficacy of MSC-Exos, with various routes being evaluated. Although intravenous injection remains the most commonly employed route in preclinical studies[112], alternative approaches such as intraperitoneal and subcutaneous administration result in enhanced accumulation of MSC-Exos within organs like the pancreas[113].

Clinical applications of MSC-Exos in different diseases

MSC-Exos were evaluated as therapeutic agents for various conditions, including acute respiratory distress syndrome, renal disease, GvHD, osteoarthritis (OA), stroke, Alzheimer's disease, and type 1 diabetes[46].

In neoplastic diseases, MSC-Exos, as natural nanocarriers, can serve as effective delivery vehicles for anticancer drugs and gene therapy tools such as small interfering RNA or miRNA, directly targeting cancer cells. This approach enhances treatment precision and mitigates the side effects associated with conventional chemotherapy. By modulating immune cells within the tumor microenvironment, MSC-Exos can augment the immune system's ability to recognize and attack tumors. Additionally, MSC-Exos can transport anti-tumor molecules that inhibit tumor cell proliferation or induce apoptosis[114]. Chronic kidney diseases are progressive and irreversible disorders that occur when renal function declines below a certain threshold[115]. Progressive tubulointerstitial fibrosis is a common characteristic of end-stage renal disease caused by chronic kidney disease. Nassar *et al*[116] utilized umbilical cord blood MSC-Exos to ameliorate the progression of the disease. The umbilical cord blood MSC-Exos group exhibited significant improvements in glomerular filtration rate, serum creatinine level, blood urea nitrogen levels, and urinary albumin-to-creatinine ratio. These

Table 1 Applications of exosomes from different sources in various diseases

Source cell	Disease	Effect	Year	Ref.
Bone marrow mesenchymal stromal cells	Acute kidney injury	Promote renal tubular epithelial cell regeneration	2017	[42]
Mesenchymal stem cells	Ischemic myocardium	Cardioprotection	2015	[43]
Bone marrow mesenchymal stromal/stem cell	Acute graft-*versus*-host disease	Prolonged the survival of acute graft-*versus*-host disease mice and reduced pathological damage in multiple graft-*versus*-host disease target organs	2018	[52]
Tumor	Colorectal cancer	Promote liver metastasis	2020	[53]
Mesenchymal stromal cells	Myocardial ischaemia-reperfusion	Attenuate myocardial ischaemia-reperfusion injury	2019	[54]
Bone marrow mesenchymal stem cells	Acute lung injury	Ameliorate LPS-induced acute lung injury	2024	[56]
M1 macrophages	Tumor	Enhance antitumor immunity to inhibit tumor growth	2021	[57]
Mesenchymal stem cells	Multiple sclerosis	Reduce demyelination, decrease neuroinflammation, and increase the number of regulatory T cells in the spinal cord of EAE mice	2019	[63]
Mesenchymal stem cells	Acquired aplastic anemia	Play a key role in immune dysregulation	2023	[65]
Hypoxic mesenchymal stem cells	Bone fracture	Promote bone fracture healing	2020	[66]
Mesenchymal stem cells	Osteochondral defects	Mediate cartilage repair	2018	[67]
Mesenchymal stem cells	Temporomandibular joint osteoarthritis	Alleviate temporomandibular joint osteoarthritis	2019	[69]
Bone marrow mesenchymal stem cells	Ulcerative colitis	Alleviate ulcerative colitis	2019	[74]
Mesenchymal stem cells	Ischemia/reperfusion injury	Alleviate ischemia/reperfusion injury	2019	[78]
Mesenchymal stromal cells	Pulmonary fibrosis	Alleviated the core features of pulmonary fibrosis and lung inflammation	2019	[79]
Umbilical cord mesenchymal stem cells	Nerve injury-induced pain	Possess anti-inflammatory and neurotrophic abilities	2019	[80]
Mesenchymal stem cells	Intrauterine adhesion	Modify intrauterine adhesion	2022	[81]
Bone marrow-derived mesenchymal stem cells	Prostate cancer	Restrained prostate cancer	2022	[89]
Wharton jelly-derived mesenchymal stem cells	Cervical cancer	As drug delivery systems for cervical cancer	2022	[90]
Olfactory ecto-mesenchymal stem cells	Murine Sjögren's syndrome	Ameliorate murine Sjögren's syndrome	2021	[96]
Mesenchymal stem cells	Autoimmune uveoretinitis	Inhibit activation of antigen-presenting cells and suppress development of T helper 1 and 17 cells	2017	[97]
Mesenchymal stem cells	Islet transplantation	Improve islet transplantation	2016	[103]
Dendritic cells	Liver transplantation	Negatively regulate $CD8^+$ T cells *via* inhibition of NLRP3	2022	[104]
Endothelial cells	ARDS	Modulate the therapeutic efficacy of mesenchymal stem cells through IDH2/TET pathway in ARDS	2024	[107]

LPS: Lipopolysaccharide; NLRP3: Nucleotide-binding domain, leucine-rich repeat, and pyrin domain-containing protein 3; ARDS: Acute respiratory distress syndrome; IDH2: Isocitrate dehydrogenase 2; TET: Ten-eleven translocation.

improvements may be attributed to an elevation in circulating anti-inflammatory cytokines and a reduction in pro-inflammatory cytokines; specifically, there was a notable increase in plasma TGF-β1 and IL-10 levels in the treatment group. Skin pigmentation is a dermatological disorder that affects skin color through discoloration or darkening of the skin. Studies have investigated the therapeutic effects of Exos derived from adipose tissue-derived MSCs on skin pigmentation by potentially inducing ceramide or sphingosine 1-phosphate synthesis which regulates melanogenesis in melanocytes and reduces melanin content in the treated group[117].

Allogeneic hematopoietic stem cell transplantation is a potentially life-saving treatment for patients with hematological malignancies. One of the most serious complications associated with hematopoietic stem cell transplantation is acute or chronic GvHD. A study utilized Exos derived from bone marrow MSCs in patients with GvHD, resulting in reduced

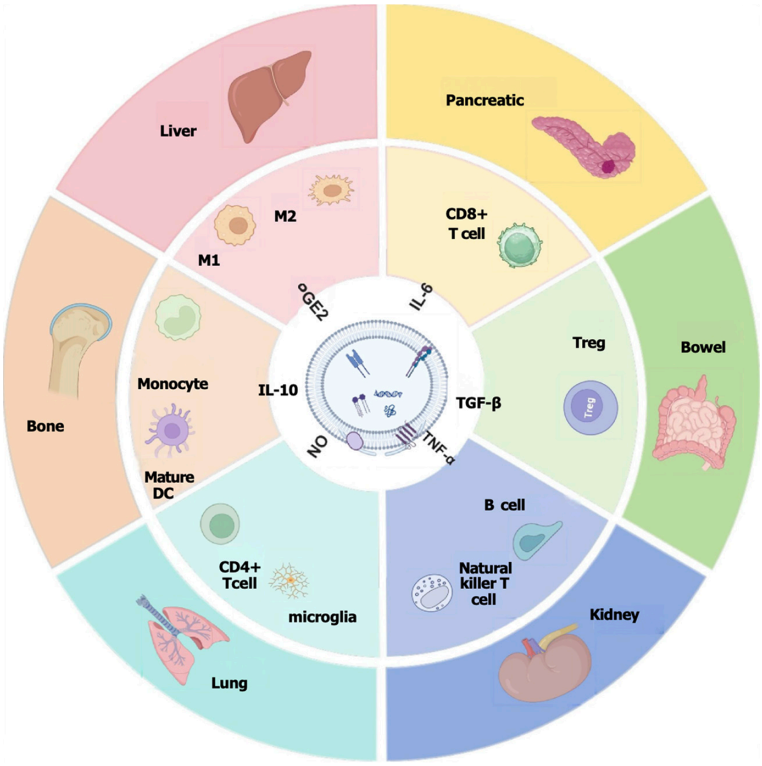

Figure 2 Mesenchymal stem cell-derived exosomes regulate immune responses in diseases through different cytokines. PGE2: Prostaglandin E2; IL-6: Interleukin 6; TGF-β: Transforming growth factor-beta; TNF-α: Tumour necrosis factor-alpha; IL-10: Interleukin-10; NO: Nitric oxide; DC: Dendritic cell.

secretion of pro-inflammatory cytokines and significant improvement in symptoms, including a reduction in diarrhea and inhibition of skin and mucosal GvHD within 14 days. However, it should be noted that one patient died of pneumonia seven months after treatment. Nevertheless, these results are promising and demonstrate potential efficacy in the treatment of GvHD[118].

Exos derived from MSCs in infectious diseases mitigate tissue damage caused by excessive immune responses through immune regulation. These Exos can transport antibacterial molecules or regulatory factors that either directly exert antibacterial effects or enhance the body's innate immunity, thereby enabling a more effective combat against pathogens [119]. Coronavirus disease 2019 (COVID-19) is a respiratory disease caused by the coronavirus severe acute respiratory syndrome coronavirus 2, which was discovered in 2020[120]. Inhalation of Exos is believed to reduce inflammation and lung injury while inducing regenerative processes, suggesting a potential therapeutic role in treating COVID-19. In a clinical study using BM-MSC-Exos, lymphopenia significantly improved and $CD3^+$, $CD4^+$, and $CD8^+$ T cells increased following MSC-Exos injection, indicating the immunomodulatory effects as the therapeutic mechanism of MSC-Exos [121]. Therefore, the authors consider MSC-Exos to hold promise as a treatment for COVID-19.

In autoimmune diseases, MSC-Exos can restore immune homeostasis and mitigate disease symptoms by suppressing hyperactive immune cells, including T cells and B cells, and promoting the generation of Tregs. The bioactive molecules within these Exos can attenuate chronic inflammatory responses in various autoimmune conditions, thereby alleviating symptoms associated with diseases such as arthritis and SLE[118]. OA is an arthritic condition affecting joints that leads to pain and stiffness. BM-MSC-Exos have been investigated as a therapeutic agent for OA across various joints. At six months post-infusion, both Brief Pain Scale scores along with Upper Extremity Function Scale and Lower Extremity Function Scale scores demonstrated improvement following treatment with BM-MSC-Exos. These findings indicate that utilizing BM-MSC-Exos effectively improves OA joint conditions while ensuring safety[122].

CONCLUSION

MSC-Exos have the ability to regulate immune responses through various mechanisms, including modulation of both innate and adaptive immune systems, inhibition of excessive inflammatory responses, and promotion of tissue repair. They exert their effects by delivering immunoactive substances such as miRNAs and proteins directly to target cells, playing a crucial role in maintaining immune system homeostasis. Additionally, Exos play a regulatory role in inflammatory diseases, tumors, autoimmune diseases, and organ transplantation. Due to their outstanding performance in regulating inflammatory responses, inhibiting tumor growth, and promoting immune tolerance, Exos hold great therapeutic potential for various pathological conditions as a cell-free therapy tool that offers higher safety and stability compared to traditional cell therapy (Figure 2).

However, challenges remain before clinical applications can be fully realized. These challenges include the standardization and characterization of Exos, optimization of preparation processes, and determining the optimal route for administration. Additionally, long-term safety and efficacy need to be thoroughly verified. Future research must focus on bridging these gaps by developing strategies such as engineering Exos to enhance their functionality or to target specific tissues more effectively.

To address these challenges, it will be essential to innovate methods for Exo engineering, enabling precise modulation of their cargo and surface properties for targeted delivery. Techniques such as genetic modification or surface marker manipulation could be employed to direct Exos specifically to disease sites, enhancing therapeutic outcomes. Further, large-scale production techniques need to be optimized to ensure consistency and quality in Exo preparations.

More preclinical and clinical studies are necessary to advance this novel cell-free therapy into clinical use. Future studies should continue exploring the mechanisms of action, optimizing production and preparation processes, and verifying efficacy through more rigorous clinical trials. By addressing these knowledge gaps and developing robust methodologies, the application of Exos as a novel cell-free therapy in clinical treatment can be promoted. Advancing their application in regenerative medicine and other fields will require ongoing research and development to unlock their full therapeutic potential.

FOOTNOTES

Author contributions: Yi YF and Fan ZQ contributed equally to this study as co-first authors. Yi YF contributed to the conceptualization; Fan ZQ contributed to the methodology; Liu C participated in the formal analysis; Ding YT took part in investigation; Chen Y curated the data; Wen J contributed to the resources; Jian XH was involved in validation of the manuscript; Li YF contributed to the supervision. Jian XH and Li YF contributed equally to this study as co-corresponding authors, and they revised the paper.

Supported by the National Natural Science Foundation of China, No. 82072537; and the General Project of Hunan Natural Science Foundation, No. 2022JJ30412 and No. 2021JJ30464.

Conflict-of-interest statement: All the authors report no relevant conflicts of interest for this article.

Country of origin: China

ORCID number: Jie Wen 0000-0002-5734-4678.

S-Editor: Wang JJ
L-Editor: Wang TQ
P-Editor: Zhang XD

REFERENCES

1 **Zhang L**, Yu D. Exosomes in cancer development, metastasis, and immunity. *Biochim Biophys Acta Rev Cancer* 2019; **1871**: 455-468 [PMID: 31047959 DOI: 10.1016/j.bbcan.2019.04.004]

2 **Krylova SV**, Feng D. The Machinery of Exosomes: Biogenesis, Release, and Uptake. *Int J Mol Sci* 2023; **24**: 1337 [PMID: 36674857 DOI: 10.3390/ijms24021337]

3 **Tang J**, Jia X, Li Q, Cui Z, Liang A, Ke B, Yang D, Yao C. A DNA-based hydrogel for exosome separation and biomedical applications. *Proc Natl Acad Sci U S A* 2023; **120**: e2303822120 [PMID: 37399419 DOI: 10.1073/pnas.2303822120]

4 **Théry C**, Witwer KW, Aikawa E, Alcaraz MJ, Anderson JD, Andriantsitohaina R, Antoniou A, Arab T, Archer F, Atkin-Smith GK, Ayre DC, Bach JM, Bachurski D, Baharvand H, Balaj L, Baldacchino S, Bauer NN, Baxter AA, Bebawy M, Beckham C, Bedina Zavec A, Benmoussa A, Berardi AC, Bergese P, Bielska E, Blenkiron C, Bobis-Wozowicz S, Boilard E, Boireau W, Bongiovanni A, Borràs FE, Bosch S, Boulanger CM, Breakefield X, Breglio AM, Brennan MÁ, Brigstock DR, Brisson A, Broekman ML, Bromberg JF, Bryl-Górecka P, Buch S, Buck AH, Burger D, Busatto S, Buschmann D, Bussolati B, Buzás EI, Byrd JB, Camussi G, Carter DR, Caruso S, Chamley LW, Chang YT, Chen C, Chen S, Cheng L, Chin AR, Clayton A, Clerici SP, Cocks A, Cocucci E, Coffey RJ, Cordeiro-da-Silva A, Couch Y, Coumans FA, Coyle B, Crescitelli R, Criado MF, D'Souza-Schorey C, Das S, Datta Chaudhuri A, de Candia P, De Santana EF, De Wever O, Del Portillo HA, Demaret T, Deville S, Devitt A, Dhondt B, Di Vizio D, Dieterich LC, Dolo V, Dominguez Rubio AP, Dominici M, Dourado MR, Driedonks TA, Duarte FV, Duncan HM, Eichenberger RM, Ekström K, El Andaloussi S, Elie-Caille C, Erdbrügger U, Falcón-Pérez JM, Fatima F, Fish JE, Flores-Bellver M, Försönits A, Frelet-Barrand A, Fricke F, Fuhrmann G, Gabrielsson S, Gámez-Valero A, Gardiner C, Gärtner K, Gaudin R, Gho YS, Giebel B, Gilbert C, Gimona M, Giusti I, Goberdhan DC, Görgens A, Gorski SM, Greening DW, Gross JC, Gualerzi A, Gupta GN, Gustafson D, Handberg A, Haraszti RA, Harrison P, Hegyesi H, Hendrix A, Hill AF, Hochberg FH, Hoffmann KF, Holder B, Holthofer H, Hosseinkhani B, Hu G, Huang Y, Huber V, Hunt S, Ibrahim AG, Ikezu T, Inal JM, Isin M, Ivanova A, Jackson HK, Jacobsen S, Jay SM, Jayachandran M, Jenster G, Jiang L, Johnson SM, Jones JC, Jong A, Jovanovic-Talisman T, Jung S, Kalluri R, Kano SI, Kaur S, Kawamura Y, Keller ET, Khamari D, Khomyakova E, Khvorova A, Kierulf P, Kim KP, Kislinger T, Klingeborn M, Klinke DJ 2nd, Kornek M, Kosanović MM, Kovács

ÁF, Krämer-Albers EM, Krasemann S, Krause M, Kurochkin IV, Kusuma GD, Kuypers S, Laitinen S, Langevin SM, Languino LR, Lannigan J, Lässer C, Laurent LC, Lavieu G, Lázaro-Ibáñez E, Le Lay S, Lee MS, Lee YXF, Lemos DS, Lenassi M, Leszczynska A, Li IT, Liao K, Libregts SF, Ligeti E, Lim R, Lim SK, Linē A, Linnemannstöns K, Llorente A, Lombard CA, Lorenowicz MJ, Lörincz ÁM, Lötvall J, Lovett J, Lowry MC, Loyer X, Lu Q, Lukomska B, Lunavat TR, Maas SL, Malhi H, Marcilla A, Mariani J, Mariscal J, Martens-Uzunova ES, Martin-Jaular L, Martinez MC, Martins VR, Mathieu M, Mathivanan S, Maugeri M, McGinnis LK, McVey MJ, Meckes DG Jr, Meehan KL, Mertens I, Minciacchi VR, Möller A, Møller Jørgensen M, Morales-Kastresana A, Morhayim J, Mullier F, Muraca M, Musante L, Mussack V, Muth DC, Myburgh KH, Najrana T, Nawaz M, Nazarenko I, Nejsum P, Neri C, Neri T, Nieuwland R, Nimrichter L, Nolan JP, Nolte-'t Hoen EN, Noren Hooten N, O'Driscoll L, O'Grady T, O'Loghlen A, Ochiya T, Olivier M, Ortiz A, Ortiz LA, Osteikoetxea X, Østergaard O, Ostrowski M, Park J, Pegtel DM, Peinado H, Perut F, Pfaffl MW, Phinney DG, Pieters BC, Pink RC, Pisetsky DS, Pogge von Strandmann E, Polakovicova I, Poon IK, Powell BH, Prada I, Pulliam L, Quesenberry P, Radeghieri A, Raffai RL, Raimondo S, Rak J, Ramirez MI, Raposo G, Rayyan MS, Regev-Rudzki N, Ricklefs FL, Robbins PD, Roberts DD, Rodrigues SC, Rohde E, Rome S, Rouschop KM, Rughetti A, Russell AE, Saá P, Sahoo S, Salas-Huenuleo E, Sánchez C, Saugstad JA, Saul MJ, Schiffelers RM, Schneider R, Schøyen TH, Scott A, Shahaj E, Sharma S, Shatnyeva O, Shekari F, Shelke GV, Shetty AK, Shiba K, Siljander PR, Silva AM, Skowronek A, Snyder OL 2nd, Soares RP, Sódar BW, Soekmadji C, Sotillo J, Stahl PD, Stoorvogel W, Stott SL, Strasser EF, Swift S, Tahara H, Tewari M, Timms K, Tiwari S, Tixeira R, Tkach M, Toh WS, Tomasini R, Torrecilhas AC, Tosar JP, Toxavidis V, Urbanelli L, Vader P, van Balkom BW, van der Grein SG, Van Deun J, van Herwijnen MJ, Van Keuren-Jensen K, van Niel G, van Royen ME, van Wijnen AJ, Vasconcelos MH, Vechetti IJ Jr, Veit TD, Vella LJ, Velot É, Verweij FJ, Vestad B, Viñas JL, Visnovitz T, Vukman KV, Wahlgren J, Watson DC, Wauben MH, Weaver A, Webber JP, Weber V, Wehman AM, Weiss DJ, Welsh JA, Wendt S, Wheelock AM, Wiener Z, Witte L, Wolfram J, Xagorari A, Xander P, Xu J, Yan X, Yáñez-Mó M, Yin H, Yuana Y, Zappulli V, Zarubova J, Žėkas V, Zhang JY, Zhao Z, Zheng L, Zheutlin AR, Zickler AM, Zimmermann P, Zivkovic AM, Zocco D, Zuba-Surma EK. Minimal information for studies of extracellular vesicles 2018 (MISEV2018): a position statement of the International Society for Extracellular Vesicles and update of the MISEV2014 guidelines. *J Extracell Vesicles* 2018; **7**: 1535750 [PMID: 30637094 DOI: 10.1080/20013078.2018.1535750]

5 **Arya SB**, Collie SP, Parent CA. The ins-and-outs of exosome biogenesis, secretion, and internalization. *Trends Cell Biol* 2024; **34**: 90-108 [PMID: 37507251 DOI: 10.1016/j.tcb.2023.06.006]

6 **Mathieu M**, Martin-Jaular L, Lavieu G, Théry C. Specificities of secretion and uptake of exosomes and other extracellular vesicles for cell-to-cell communication. *Nat Cell Biol* 2019; **21**: 9-17 [PMID: 30602770 DOI: 10.1038/s41556-018-0250-9]

7 **Caplan AI**. Mesenchymal stem cells. *J Orthop Res* 1991; **9**: 641-650 [PMID: 1870029 DOI: 10.1002/jor.1100090504]

8 **Bernardo ME**, Fibbe WE. Mesenchymal stromal cells: sensors and switchers of inflammation. *Cell Stem Cell* 2013; **13**: 392-402 [PMID: 24094322 DOI: 10.1016/j.stem.2013.09.006]

9 **Prockop DJ**. Concise review: two negative feedback loops place mesenchymal stem/stromal cells at the center of early regulators of inflammation. *Stem Cells* 2013; **31**: 2042-2046 [PMID: 23681848 DOI: 10.1002/stem.1400]

10 **Samsonraj RM**, Raghunath M, Nurcombe V, Hui JH, van Wijnen AJ, Cool SM. Concise Review: Multifaceted Characterization of Human Mesenchymal Stem Cells for Use in Regenerative Medicine. *Stem Cells Transl Med* 2017; **6**: 2173-2185 [PMID: 29076267 DOI: 10.1002/sctm.17-0129]

11 **Naji A**, Eitoku M, Favier B, Deschaseaux F, Rouas-Freiss N, Suganuma N. Biological functions of mesenchymal stem cells and clinical implications. *Cell Mol Life Sci* 2019; **76**: 3323-3348 [PMID: 31055643 DOI: 10.1007/s00018-019-03125-1]

12 **Ankrum JA**, Ong JF, Karp JM. Mesenchymal stem cells: immune evasive, not immune privileged. *Nat Biotechnol* 2014; **32**: 252-260 [PMID: 24561556 DOI: 10.1038/nbt.2816]

13 **Al-Ghadban S**, Bunnell BA. Adipose Tissue-Derived Stem Cells: Immunomodulatory Effects and Therapeutic Potential. *Physiology (Bethesda)* 2020; **35**: 125-133 [PMID: 32027561 DOI: 10.1152/physiol.00021.2019]

14 **de Castro LL**, Lopes-Pacheco M, Weiss DJ, Cruz FF, Rocco PRM. Current understanding of the immunosuppressive properties of mesenchymal stromal cells. *J Mol Med (Berl)* 2019; **97**: 605-618 [PMID: 30903229 DOI: 10.1007/s00109-019-01776-y]

15 **Shokri MR**, Bozorgmehr M, Ghanavatinejad A, Falak R, Aleahmad M, Kazemnejad S, Shokri F, Zarnani AH. Human menstrual blood-derived stromal/stem cells modulate functional features of natural killer cells. *Sci Rep* 2019; **9**: 10007 [PMID: 31292483 DOI: 10.1038/s41598-019-46316-3]

16 **Zhu YG**, Shi MM, Monsel A, Dai CX, Dong X, Shen H, Li SK, Chang J, Xu CL, Li P, Wang J, Shen MP, Ren CJ, Chen DC, Qu JM. Nebulized exosomes derived from allogenic adipose tissue mesenchymal stromal cells in patients with severe COVID-19: a pilot study. *Stem Cell Res Ther* 2022; **13**: 220 [PMID: 35619189 DOI: 10.1186/s13287-022-02900-5]

17 **Liu Y**, Li C, Wang S, Guo J, Guo J, Fu J, Ren L, An Y, He J, Li Z. Human umbilical cord mesenchymal stem cells confer potent immunosuppressive effects in Sjögren's syndrome by inducing regulatory T cells. *Mod Rheumatol* 2021; **31**: 186-196 [PMID: 31859545 DOI: 10.1080/14397595.2019.1707996]

18 **Wang Z**, Yang C, Yan S, Sun J, Zhang J, Qu Z, Sun W, Zang J, Xu D. Emerging Role and Mechanism of Mesenchymal Stem Cells-Derived Extracellular Vesicles in Rheumatic Disease. *J Inflamm Res* 2024; **17**: 6827-6846 [PMID: 39372581 DOI: 10.2147/JIR.S488201]

19 **Harrell CR**, Jovicic N, Djonov V, Arsenijevic N, Volarevic V. Mesenchymal Stem Cell-Derived Exosomes and Other Extracellular Vesicles as New Remedies in the Therapy of Inflammatory Diseases. *Cells* 2019; **8**: 1605 [PMID: 31835680 DOI: 10.3390/cells8121605]

20 **Ala M**. The beneficial effects of mesenchymal stem cells and their exosomes on myocardial infarction and critical considerations for enhancing their efficacy. *Ageing Res Rev* 2023; **89**: 101980 [PMID: 37302757 DOI: 10.1016/j.arr.2023.101980]

21 **Giovannelli L**, Bari E, Jommi C, Tartara F, Armocida D, Garbossa D, Cofano F, Torre ML, Segale L. Mesenchymal stem cell secretome and extracellular vesicles for neurodegenerative diseases: Risk-benefit profile and next steps for the market access. *Bioact Mater* 2023; **29**: 16-35 [PMID: 37456581 DOI: 10.1016/j.bioactmat.2023.06.013]

22 **Yu H**, Wang Z. Cardiomyocyte-Derived Exosomes: Biological Functions and Potential Therapeutic Implications. *Front Physiol* 2019; **10**: 1049 [PMID: 31481897 DOI: 10.3389/fphys.2019.01049]

23 **Cao Q**, Huang C, Chen XM, Pollock CA. Mesenchymal Stem Cell-Derived Exosomes: Toward Cell-Free Therapeutic Strategies in Chronic Kidney Disease. *Front Med (Lausanne)* 2022; **9**: 816656 [PMID: 35386912 DOI: 10.3389/fmed.2022.816656]

24 **Bian D**, Wu Y, Song G, Azizi R, Zamani A. The application of mesenchymal stromal cells (MSCs) and their derivative exosome in skin wound healing: a comprehensive review. *Stem Cell Res Ther* 2022; **13**: 24 [PMID: 35073970 DOI: 10.1186/s13287-021-02697-9]

25 **Fujii S**, Miura Y. Immunomodulatory and Regenerative Effects of MSC-Derived Extracellular Vesicles to Treat Acute GVHD. *Stem Cells* 2022; **40**: 977-990 [PMID: 35930478 DOI: 10.1093/stmcls/sxac057]

26 **Qiu G**, Zheng G, Ge M, Wang J, Huang R, Shu Q, Xu J. Mesenchymal stem cell-derived extracellular vesicles affect disease outcomes *via*

transfer of microRNAs. *Stem Cell Res Ther* 2018; **9**: 320 [PMID: 30463593 DOI: 10.1186/s13287-018-1069-9]

27 **Zhang H**, Wang L, Li C, Yu Y, Yi Y, Wang J, Chen D. Exosome-Induced Regulation in Inflammatory Bowel Disease. *Front Immunol* 2019; **10**: 1464 [PMID: 31316512 DOI: 10.3389/fimmu.2019.01464]

28 **Arabpour M**, Saghazadeh A, Rezaei N. Anti-inflammatory and M2 macrophage polarization-promoting effect of mesenchymal stem cell-derived exosomes. *Int Immunopharmacol* 2021; **97**: 107823 [PMID: 34102486 DOI: 10.1016/j.intimp.2021.107823]

29 **Ocansey DKW**, Zhang L, Wang Y, Yan Y, Qian H, Zhang X, Xu W, Mao F. Exosome-mediated effects and applications in inflammatory bowel disease. *Biol Rev Camb Philos Soc* 2020; **95**: 1287-1307 [PMID: 32410383 DOI: 10.1111/brv.12608]

30 **Shen Z**, Huang W, Liu J, Tian J, Wang S, Rui K. Effects of Mesenchymal Stem Cell-Derived Exosomes on Autoimmune Diseases. *Front Immunol* 2021; **12**: 749192 [PMID: 34646275 DOI: 10.3389/fimmu.2021.749192]

31 **Lin Z**, Wu Y, Xu Y, Li G, Li Z, Liu T. Mesenchymal stem cell-derived exosomes in cancer therapy resistance: recent advances and therapeutic potential. *Mol Cancer* 2022; **21**: 179 [PMID: 36100944 DOI: 10.1186/s12943-022-01650-5]

32 **Skotland T**, Hessvik NP, Sandvig K, Llorente A. Exosomal lipid composition and the role of ether lipids and phosphoinositides in exosome biology. *J Lipid Res* 2019; **60**: 9-18 [PMID: 30076207 DOI: 10.1194/jlr.R084343]

33 **Pascual M**, Ibáñez F, Guerri C. Exosomes as mediators of neuron-glia communication in neuroinflammation. *Neural Regen Res* 2020; **15**: 796-801 [PMID: 31719239 DOI: 10.4103/1673-5374.268893]

34 **Yin T**, Xin H, Yu J, Teng F. The role of exosomes in tumour immunity under radiotherapy: eliciting abscopal effects? *Biomark Res* 2021; **9**: 22 [PMID: 33789758 DOI: 10.1186/s40364-021-00277-w]

35 **Franco da Cunha F**, Andrade-Oliveira V, Candido de Almeida D, Borges da Silva T, Naffah de Souza Breda C, Costa Cruz M, Faquim-Mauro EL, Antonio Cenedeze M, Ioshie Hiyane M, Pacheco-Silva A, Aparecida Cavinato R, Torrecilhas AC, Olsen Saraiva Câmara N. Extracellular Vesicles isolated from Mesenchymal Stromal Cells Modulate CD4(+) T Lymphocytes Toward a Regulatory Profile. *Cells* 2020; **9**: 1059 [PMID: 32340348 DOI: 10.3390/cells9041059]

36 **Ou Q**, Dou X, Tang J, Wu P, Pan D. Small extracellular vesicles derived from PD-L1-modified mesenchymal stem cell promote Tregs differentiation and prolong allograft survival. *Cell Tissue Res* 2022; **389**: 465-481 [PMID: 35688948 DOI: 10.1007/s00441-022-03650-9]

37 **Lotfy A**, AboQuella NM, Wang H. Mesenchymal stromal/stem cell (MSC)-derived exosomes in clinical trials. *Stem Cell Res Ther* 2023; **14**: 66 [PMID: 37024925 DOI: 10.1186/s13287-023-03287-7]

38 **Zheng G**, Huang R, Qiu G, Ge M, Wang J, Shu Q, Xu J. Mesenchymal stromal cell-derived extracellular vesicles: regenerative and immunomodulatory effects and potential applications in sepsis. *Cell Tissue Res* 2018; **374**: 1-15 [PMID: 29955951 DOI: 10.1007/s00441-018-2871-5]

39 **Qiu G**, Zheng G, Ge M, Wang J, Huang R, Shu Q, Xu J. Functional proteins of mesenchymal stem cell-derived extracellular vesicles. *Stem Cell Res Ther* 2019; **10**: 359 [PMID: 31779700 DOI: 10.1186/s13287-019-1484-6]

40 **Keshtkar S**, Azarpira N, Ghahremani MH. Mesenchymal stem cell-derived extracellular vesicles: novel frontiers in regenerative medicine. *Stem Cell Res Ther* 2018; **9**: 63 [PMID: 29523213 DOI: 10.1186/s13287-018-0791-7]

41 **Lai RC**, Arslan F, Lee MM, Sze NS, Choo A, Chen TS, Salto-Tellez M, Timmers L, Lee CN, El Oakley RM, Pasterkamp G, de Kleijn DP, Lim SK. Exosome secreted by MSC reduces myocardial ischemia/reperfusion injury. *Stem Cell Res* 2010; **4**: 214-222 [PMID: 20138817 DOI: 10.1016/j.scr.2009.12.003]

42 **Bruno S**, Tapparo M, Collino F, Chiabotto G, Deregibus MC, Soares Lindoso R, Neri F, Kholia S, Giunti S, Wen S, Quesenberry P, Camussi G. Renal Regenerative Potential of Different Extracellular Vesicle Populations Derived from Bone Marrow Mesenchymal Stromal Cells. *Tissue Eng Part A* 2017; **23**: 1262-1273 [PMID: 28471327 DOI: 10.1089/ten.TEA.2017.0069]

43 **Yu B**, Kim HW, Gong M, Wang J, Millard RW, Wang Y, Ashraf M, Xu M. Exosomes secreted from GATA-4 overexpressing mesenchymal stem cells serve as a reservoir of anti-apoptotic microRNAs for cardioprotection. *Int J Cardiol* 2015; **182**: 349-360 [PMID: 25590961 DOI: 10.1016/j.ijcard.2014.12.043]

44 **Kim YG**, Choi J, Kim K. Mesenchymal Stem Cell-Derived Exosomes for Effective Cartilage Tissue Repair and Treatment of Osteoarthritis. *Biotechnol J* 2020; **15**: e2000082 [PMID: 32559340 DOI: 10.1002/biot.202000082]

45 **Rezaie J**, Rahbarghazi R, Pezeshki M, Mazhar M, Yekani F, Khaksar M, Shokrollahi E, Amini H, Hashemzadeh S, Sokullu SE, Tokac M. Cardioprotective role of extracellular vesicles: A highlight on exosome beneficial effects in cardiovascular diseases. *J Cell Physiol* 2019; **234**: 21732-21745 [PMID: 31140622 DOI: 10.1002/jcp.28894]

46 **Tan F**, Li X, Wang Z, Li J, Shahzad K, Zheng J. Clinical applications of stem cell-derived exosomes. *Signal Transduct Target Ther* 2024; **9**: 17 [PMID: 38212307 DOI: 10.1038/s41392-023-01704-0]

47 **Yang D**, Zhang W, Zhang H, Zhang F, Chen L, Ma L, Larcher LM, Chen S, Liu N, Zhao Q, Tran PHL, Chen C, Veedu RN, Wang T. Progress, opportunity, and perspective on exosome isolation - efforts for efficient exosome-based theranostics. *Theranostics* 2020; **10**: 3684-3707 [PMID: 32206116 DOI: 10.7150/thno.41580]

48 **Wang S**, Lei B, Zhang E, Gong P, Gu J, He L, Han L, Yuan Z. Targeted Therapy for Inflammatory Diseases with Mesenchymal Stem Cells and Their Derived Exosomes: From Basic to Clinics. *Int J Nanomedicine* 2022; **17**: 1757-1781 [PMID: 35469174 DOI: 10.2147/IJN.S355366]

49 **Yan L**, Li J, Zhang C. The role of MSCs and CAR-MSCs in cellular immunotherapy. *Cell Commun Signal* 2023; **21**: 187 [PMID: 37528472 DOI: 10.1186/s12964-023-01191-4]

50 **Zhao Y**, Zhong X, Du F, Wu X, Li M, Wen Q, Shen J, Chen Y, Zhang X, Yang Z, Deng Y, Liu X, Zou C, Du Y, Xiao Z. The Role of Mesenchymal Stem Cells in Cancer Immunotherapy. *Curr Stem Cell Res Ther* 2023; **18**: 1056-1068 [PMID: 36597604 DOI: 10.2174/1574888X18666230103120302]

51 **Ong HS**, Riau AK, Yam GH, Yusoff NZBM, Han EJY, Goh TW, Lai RC, Lim SK, Mehta JS. Mesenchymal Stem Cell Exosomes as Immunomodulatory Therapy for Corneal Scarring. *Int J Mol Sci* 2023; **24**: 7456 [PMID: 37108619 DOI: 10.3390/ijms24087456]

52 **Fujii S**, Miura Y, Fujishiro A, Shindo T, Shimazu Y, Hirai H, Tahara H, Takaori-Kondo A, Ichinohe T, Maekawa T. Graft-Versus-Host Disease Amelioration by Human Bone Marrow Mesenchymal Stromal/Stem Cell-Derived Extracellular Vesicles Is Associated with Peripheral Preservation of Naive T Cell Populations. *Stem Cells* 2018; **36**: 434-445 [PMID: 29239062 DOI: 10.1002/stem.2759]

53 **Zhao S**, Mi Y, Guan B, Zheng B, Wei P, Gu Y, Zhang Z, Cai S, Xu Y, Li X, He X, Zhong X, Li G, Chen Z, Li D. Tumor-derived exosomal miR-934 induces macrophage M2 polarization to promote liver metastasis of colorectal cancer. *J Hematol Oncol* 2020; **13**: 156 [PMID: 33213490 DOI: 10.1186/s13045-020-00991-2]

54 **Zhao J**, Li X, Hu J, Chen F, Qiao S, Sun X, Gao L, Xie J, Xu B. Mesenchymal stromal cell-derived exosomes attenuate myocardial ischaemia-reperfusion injury through miR-182-regulated macrophage polarization. *Cardiovasc Res* 2019; **115**: 1205-1216 [PMID: 30753344 DOI: 10.1093/cvr/cvz040]

55 **Jiao Y**, Zhang T, Zhang C, Ji H, Tong X, Xia R, Wang W, Ma Z, Shi X. Exosomal miR-30d-5p of neutrophils induces M1 macrophage polarization and primes macrophage pyroptosis in sepsis-related acute lung injury. *Crit Care* 2021; **25**: 356 [PMID: 34641966 DOI: 10.1186/s13054-021-03775-3]

56 **Xu H**, Nie X, Deng W, Zhou H, Huang D, Wang Z. Bone marrow mesenchymal stem cells-derived exosomes ameliorate LPS-induced acute lung injury by miR-223-regulated alveolar macrophage M2 polarization. *J Biochem Mol Toxicol* 2024; **38**: e23568 [PMID: 37899695 DOI: 10.1002/jbt.23568]

57 **Gunassekaran GR**, Poongkavithai Vadevoo SM, Baek MC, Lee B. M1 macrophage exosomes engineered to foster M1 polarization and target the IL-4 receptor inhibit tumor growth by reprogramming tumor-associated macrophages into M1-like macrophages. *Biomaterials* 2021; **278**: 121137 [PMID: 34560422 DOI: 10.1016/j.biomaterials.2021.121137]

58 **Ou X**, Wang H, Tie H, Liao J, Luo Y, Huang W, Yu R, Song L, Zhu J. Novel plant-derived exosome-like nanovesicles from Catharanthus roseus: preparation, characterization, and immunostimulatory effect *via* TNF-α/NF-κB/PU.1 axis. *J Nanobiotechnology* 2023; **21**: 160 [PMID: 37210530 DOI: 10.1186/s12951-023-01919-x]

59 **Li C**, Guo F, Wang X, Liu D, Wu B, Wang F, Chen W. Exosome-based targeted RNA delivery for immune tolerance induction in skin transplantation. *J Biomed Mater Res A* 2020; **108**: 1493-1500 [PMID: 32170897 DOI: 10.1002/jbm.a.36919]

60 **Mendt M**, Rezvani K, Shpall E. Mesenchymal stem cell-derived exosomes for clinical use. *Bone Marrow Transplant* 2019; **54**: 789-792 [PMID: 31431712 DOI: 10.1038/s41409-019-0616-z]

61 **Jahangiri B**, Khalaj-Kondori M, Asadollahi E, Kian Saei A, Sadeghizadeh M. Dual impacts of mesenchymal stem cell-derived exosomes on cancer cells: unravelling complex interactions. *J Cell Commun Signal* 2023; **17**: 1229-1247 [PMID: 37973719 DOI: 10.1007/s12079-023-00794-3]

62 **Oveili E**, Vafaei S, Bazavar H, Eslami Y, Mamaghanizadeh E, Yasamineh S, Gholizadeh O. The potential use of mesenchymal stem cells-derived exosomes as microRNAs delivery systems in different diseases. *Cell Commun Signal* 2023; **21**: 20 [PMID: 36690996 DOI: 10.1186/s12964-022-01017-9]

63 **Riazifar M**, Mohammadi MR, Pone EJ, Yeri A, Lässer C, Segaliny AI, McIntyre LL, Shelke GV, Hutchins E, Hamamoto A, Calle EN, Crescitelli R, Liao W, Pham V, Yin Y, Jayaraman J, Lakey JRT, Walsh CM, Van Keuren-Jensen K, Lotvall J, Zhao W. Stem Cell-Derived Exosomes as Nanotherapeutics for Autoimmune and Neurodegenerative Disorders. *ACS Nano* 2019; **13**: 6670-6688 [PMID: 31117376 DOI: 10.1021/acsnano.9b01004]

64 **Naaldijk Y**, Sherman LS, Turrini N, Kenfack Y, Ratajczak MZ, Souayah N, Rameshwar P, Ulrich H. Mesenchymal Stem Cell-Macrophage Crosstalk Provides Specific Exosomal Cargo to Direct Immune Response Licensing of Macrophages during Inflammatory Responses. *Stem Cell Rev Rep* 2024; **20**: 218-236 [PMID: 37851277 DOI: 10.1007/s12015-023-10612-3]

65 **Wang S**, Huo J, Liu Y, Chen L, Ren X, Li X, Wang M, Jin P, Huang J, Nie N, Zhang J, Shao Y, Ge M, Zheng Y. Impaired immunosuppressive effect of bone marrow mesenchymal stem cell-derived exosomes on T cells in aplastic anemia. *Stem Cell Res Ther* 2023; **14**: 285 [PMID: 37794484 DOI: 10.1186/s13287-023-03496-0]

66 **Liu W**, Li L, Rong Y, Qian D, Chen J, Zhou Z, Luo Y, Jiang D, Cheng L, Zhao S, Kong F, Wang J, Zhou Z, Xu T, Gong F, Huang Y, Gu C, Zhao X, Bai J, Wang F, Zhao W, Zhang L, Li X, Yin G, Fan J, Cai W. Hypoxic mesenchymal stem cell-derived exosomes promote bone fracture healing by the transfer of miR-126. *Acta Biomater* 2020; **103**: 196-212 [PMID: 31857259 DOI: 10.1016/j.actbio.2019.12.020]

67 **Zhang S**, Chuah SJ, Lai RC, Hui JHP, Lim SK, Toh WS. MSC exosomes mediate cartilage repair by enhancing proliferation, attenuating apoptosis and modulating immune reactivity. *Biomaterials* 2018; **156**: 16-27 [PMID: 29182933 DOI: 10.1016/j.biomaterials.2017.11.028]

68 **Qiu W**, Guo Q, Guo X, Wang C, Li B, Qi Y, Wang S, Zhao R, Han X, Du H, Zhao S, Pan Z, Fan Y, Wang Q, Gao Z, Li G, Xue H. Mesenchymal stem cells, as glioma exosomal immunosuppressive signal multipliers, enhance MDSCs immunosuppressive activity through the miR-21/SP1/DNMT1 positive feedback loop. *J Nanobiotechnology* 2023; **21**: 233 [PMID: 37481646 DOI: 10.1186/s12951-023-01997-x]

69 **Zhang S**, Teo KYW, Chuah SJ, Lai RC, Lim SK, Toh WS. MSC exosomes alleviate temporomandibular joint osteoarthritis by attenuating inflammation and restoring matrix homeostasis. *Biomaterials* 2019; **200**: 35-47 [PMID: 30771585 DOI: 10.1016/j.biomaterials.2019.02.006]

70 **Del Papa B**, Sportoletti P, Cecchini D, Rosati E, Balucani C, Baldoni S, Fettucciari K, Marconi P, Martelli MF, Falzetti F, Di Ianni M. Notch1 modulates mesenchymal stem cells mediated regulatory T-cell induction. *Eur J Immunol* 2013; **43**: 182-187 [PMID: 23161436 DOI: 10.1002/eji.201242643]

71 **Kim JY**, Park M, Kim YH, Ryu KH, Lee KH, Cho KA, Woo SY. Tonsil-derived mesenchymal stem cells (T-MSCs) prevent Th17-mediated autoimmune response *via* regulation of the programmed death-1/programmed death ligand-1 (PD-1/PD-L1) pathway. *J Tissue Eng Regen Med* 2018; **12**: e1022-e1033 [PMID: 28107610 DOI: 10.1002/term.2423]

72 **Bansal S**, Rahman M, Ravichandran R, Canez J, Fleming T, Mohanakumar T. Extracellular Vesicles in Transplantation: Friend or Foe. *Transplantation* 2024; **108**: 374-385 [PMID: 37482627 DOI: 10.1097/TP.0000000000004693]

73 **Lee SH**, Kwon JE, Cho ML. Immunological pathogenesis of inflammatory bowel disease. *Intest Res* 2018; **16**: 26-42 [PMID: 29422795 DOI: 10.5217/ir.2018.16.1.26]

74 **Cao L**, Xu H, Wang G, Liu M, Tian D, Yuan Z. Extracellular vesicles derived from bone marrow mesenchymal stem cells attenuate dextran sodium sulfate-induced ulcerative colitis by promoting M2 macrophage polarization. *Int Immunopharmacol* 2019; **72**: 264-274 [PMID: 31005036 DOI: 10.1016/j.intimp.2019.04.020]

75 **Yang J**, Liu XX, Fan H, Tang Q, Shou ZX, Zuo DM, Zou Z, Xu M, Chen QY, Peng Y, Deng SJ, Liu YJ. Extracellular Vesicles Derived from Bone Marrow Mesenchymal Stem Cells Protect against Experimental Colitis *via* Attenuating Colon Inflammation, Oxidative Stress and Apoptosis. *PLoS One* 2015; **10**: e0140551 [PMID: 26469068 DOI: 10.1371/journal.pone.0140551]

76 **Gazdic M**, Simovic Markovic B, Vucicevic L, Nikolic T, Djonov V, Arsenijevic N, Trajkovic V, Lukic ML, Volarevic V. Mesenchymal stem cells protect from acute liver injury by attenuating hepatotoxicity of liver natural killer T cells in an inducible nitric oxide synthase- and indoleamine 2,3-dioxygenase-dependent manner. *J Tissue Eng Regen Med* 2018; **12**: e1173-e1185 [PMID: 28488390 DOI: 10.1002/term.2452]

77 **Chen L**, Lu FB, Chen DZ, Wu JL, Hu ED, Xu LM, Zheng MH, Li H, Huang Y, Jin XY, Gong YW, Lin Z, Wang XD, Chen YP. BMSCs-derived miR-223-containing exosomes contribute to liver protection in experimental autoimmune hepatitis. *Mol Immunol* 2018; **93**: 38-46 [PMID: 29145157 DOI: 10.1016/j.molimm.2017.11.008]

78 **Li JW**, Wei L, Han Z, Chen Z. Mesenchymal stromal cells-derived exosomes alleviate ischemia/reperfusion injury in mouse lung by transporting anti-apoptotic miR-21-5p. *Eur J Pharmacol* 2019; **852**: 68-76 [PMID: 30682335 DOI: 10.1016/j.ejphar.2019.01.022]

79 **Mansouri N**, Willis GR, Fernandez-Gonzalez A, Reis M, Nassiri S, Mitsialis SA, Kourembanas S. Mesenchymal stromal cell exosomes prevent and revert experimental pulmonary fibrosis through modulation of monocyte phenotypes. *JCI Insight* 2019; **4**: e128060 [PMID: 31581150 DOI: 10.1172/jci.insight.128060]

80 **Shiue SJ**, Rau RH, Shiue HS, Hung YW, Li ZX, Yang KD, Cheng JK. Mesenchymal stem cell exosomes as a cell-free therapy for nerve injury-induced pain in rats. *Pain* 2019; **160**: 210-223 [PMID: 30188455 DOI: 10.1097/j.pain.0000000000001395]

81 **Li J**, Pan Y, Yang J, Wang J, Jiang Q, Dou H, Hou Y. Tumor necrosis factor-α-primed mesenchymal stem cell-derived exosomes promote M2 macrophage polarization *via* Galectin-1 and modify intrauterine adhesion on a novel murine model. *Front Immunol* 2022; **13**: 945234 [PMID: 36591221 DOI: 10.3389/fimmu.2022.945234]

82 **Saadh MJ**, K Abdulsahib W, Ashurova D, Sanghvi G, Ballal S, Sharma R, Kumar Pathak P, Aman S, Kumar A, Feez Sead F, Chaitanya MVNL. FLT3-mutated AML: immune evasion through exosome-mediated mechanisms and innovative combination therapies targeting immune escape. *Expert Rev Anticancer Ther* 2025; **25**: 143-150 [PMID: 39885639 DOI: 10.1080/14737140.2025.2461632]

83 **Lee YJ**, Shin KJ, Jang HJ, Ryu JS, Lee CY, Yoon JH, Seo JK, Park S, Lee S, Je AR, Huh YH, Kong SY, Kwon T, Suh PG, Chae YC. GPR143 controls ESCRT-dependent exosome biogenesis and promotes cancer metastasis. *Dev Cell* 2023; **58**: 320-334.e8 [PMID: 36800996 DOI: 10.1016/j.devcel.2023.01.006]

84 **Harrell CR**, Volarevic A, Djonov VG, Jovicic N, Volarevic V. Mesenchymal Stem Cell: A Friend or Foe in Anti-Tumor Immunity. *Int J Mol Sci* 2021; **22**: 12429 [PMID: 34830312 DOI: 10.3390/ijms222212429]

85 **Biswas S**, Mandal G, Roy Chowdhury S, Purohit S, Payne KK, Anadon C, Gupta A, Swanson P, Yu X, Conejo-Garcia JR, Bhattacharyya A. Exosomes Produced by Mesenchymal Stem Cells Drive Differentiation of Myeloid Cells into Immunosuppressive M2-Polarized Macrophages in Breast Cancer. *J Immunol* 2019; **203**: 3447-3460 [PMID: 31704881 DOI: 10.4049/jimmunol.1900692]

86 **Börger V**, Bremer M, Ferrer-Tur R, Gockeln L, Stambouli O, Becic A, Giebel B. Mesenchymal Stem/Stromal Cell-Derived Extracellular Vesicles and Their Potential as Novel Immunomodulatory Therapeutic Agents. *Int J Mol Sci* 2017; **18**: 1450 [PMID: 28684664 DOI: 10.3390/ijms18071450]

87 **Reza AMMT**, Choi YJ, Yasuda H, Kim JH. Human adipose mesenchymal stem cell-derived exosomal-miRNAs are critical factors for inducing anti-proliferation signalling to A2780 and SKOV-3 ovarian cancer cells. *Sci Rep* 2016; **6**: 38498 [PMID: 27929108 DOI: 10.1038/srep38498]

88 **Colombo M**, Moita C, van Niel G, Kowal J, Vigneron J, Benaroch P, Manel N, Moita LF, Théry C, Raposo G. Analysis of ESCRT functions in exosome biogenesis, composition and secretion highlights the heterogeneity of extracellular vesicles. *J Cell Sci* 2013; **126**: 5553-5565 [PMID: 24105262 DOI: 10.1242/jcs.128868]

89 **Li C**, Sun Z, Song Y, Zhang Y. Suppressive function of bone marrow-derived mesenchymal stem cell-derived exosomal microRNA-187 in prostate cancer. *Cancer Biol Ther* 2022; **23**: 1-14 [PMID: 36245088 DOI: 10.1080/15384047.2022.2123675]

90 **Abas BI**, Demirbolat GM, Cevik O. Wharton jelly-derived mesenchymal stem cell exosomes induce apoptosis and suppress EMT signaling in cervical cancer cells as an effective drug carrier system of paclitaxel. *PLoS One* 2022; **17**: e0274607 [PMID: 36108271 DOI: 10.1371/journal.pone.0274607]

91 **Gu H**, Yan C, Wan H, Wu L, Liu J, Zhu Z, Gao D. Mesenchymal stem cell-derived exosomes block malignant behaviors of hepatocellular carcinoma stem cells through a lncRNA C5orf66-AS1/microRNA-127-3p/DUSP1/ERK axis. *Hum Cell* 2021; **34**: 1812-1829 [PMID: 34431063 DOI: 10.1007/s13577-021-00599-9]

92 **Gao C**, Jiang J, Tan Y, Chen S. Microglia in neurodegenerative diseases: mechanism and potential therapeutic targets. *Signal Transduct Target Ther* 2023; **8**: 359 [PMID: 37735487 DOI: 10.1038/s41392-023-01588-0]

93 **Dendrou CA**, Fugger L, Friese MA. Immunopathology of multiple sclerosis. *Nat Rev Immunol* 2015; **15**: 545-558 [PMID: 26250739 DOI: 10.1038/nri3871]

94 **Zhang W**, Xiao D, Mao Q, Xia H. Role of neuroinflammation in neurodegeneration development. *Signal Transduct Target Ther* 2023; **8**: 267 [PMID: 37433768 DOI: 10.1038/s41392-023-01486-5]

95 **Isik S**, Yeman Kiyak B, Akbayir R, Seyhali R, Arpaci T. Microglia Mediated Neuroinflammation in Parkinson's Disease. *Cells* 2023; **12**: 1012 [PMID: 37048085 DOI: 10.3390/cells12071012]

96 **Rui K**, Hong Y, Zhu Q, Shi X, Xiao F, Fu H, Yin Q, Xing Y, Wu X, Kong X, Xu H, Tian J, Wang S, Lu L. Olfactory ecto-mesenchymal stem cell-derived exosomes ameliorate murine Sjögren's syndrome by modulating the function of myeloid-derived suppressor cells. *Cell Mol Immunol* 2021; **18**: 440-451 [PMID: 33408339 DOI: 10.1038/s41423-020-00587-3]

97 **Shigemoto-Kuroda T**, Oh JY, Kim DK, Jeong HJ, Park SY, Lee HJ, Park JW, Kim TW, An SY, Prockop DJ, Lee RH. MSC-derived Extracellular Vesicles Attenuate Immune Responses in Two Autoimmune Murine Models: Type 1 Diabetes and Uveoretinitis. *Stem Cell Reports* 2017; **8**: 1214-1225 [PMID: 28494937 DOI: 10.1016/j.stemcr.2017.04.008]

98 **Jang E**, Jeong M, Kim S, Jang K, Kang BK, Lee DY, Bae SC, Kim KS, Youn J. Infusion of Human Bone Marrow-Derived Mesenchymal Stem Cells Alleviates Autoimmune Nephritis in a Lupus Model by Suppressing Follicular Helper T-Cell Development. *Cell Transplant* 2016; **25**: 1-15 [PMID: 25975931 DOI: 10.3727/096368915X688173]

99 **Noack M**, Miossec P. Selected cytokine pathways in rheumatoid arthritis. *Semin Immunopathol* 2017; **39**: 365-383 [PMID: 28213794 DOI: 10.1007/s00281-017-0619-z]

100 **Chen Z**, Wang H, Xia Y, Yan F, Lu Y. Therapeutic Potential of Mesenchymal Cell-Derived miRNA-150-5p-Expressing Exosomes in Rheumatoid Arthritis Mediated by the Modulation of MMP14 and VEGF. *J Immunol* 2018; **201**: 2472-2482 [PMID: 30224512 DOI: 10.4049/jimmunol.1800304]

101 **Minhua Q**, Bingzheng F, Zhiran X, Yingying Z, Yuwei Y, Ting Z, Jibing C, Hongjun G. Exosomal-microRNAs Improve Islet Cell Survival and Function In Islet Transplantation. *Curr Stem Cell Res Ther* 2024; **19**: 669-677 [PMID: 37165494 DOI: 10.2174/1574888X18666230510105947]

102 **Wang J**, Wang J, Wang Y, Ma R, Zhang S, Zheng J, Xue W, Ding X. Bone Marrow Mesenchymal Stem Cells-Derived miR-21-5p Protects Grafted Islets Against Apoptosis by Targeting PDCD4. *Stem Cells* 2023; **41**: 169-183 [PMID: 36512434 DOI: 10.1093/stmcls/sxac085]

103 **Wen D**, Peng Y, Liu D, Weizmann Y, Mahato RI. Mesenchymal stem cell and derived exosome as small RNA carrier and Immunomodulator to improve islet transplantation. *J Control Release* 2016; **238**: 166-175 [PMID: 27475298 DOI: 10.1016/j.jconrel.2016.07.044]

104 **Cui B**, Sun J, Li SP, Zhou GP, Chen XJ, Sun LY, Wei L, Zhu ZJ. CD80(+) dendritic cell derived exosomes inhibit CD8(+) T cells through down-regulating NLRP3 expression after liver transplantation. *Int Immunopharmacol* 2022; **109**: 108787 [PMID: 35490667 DOI: 10.1016/j.intimp.2022.108787]

105 **Sababathy M**, Ramanathan G, Ganesan S, Sababathy S, Yasmin AR, Ramasamy R, Foo JB, Looi QH, Nur-Fazila SH. Multipotent mesenchymal stromal/stem cell-based therapies for acute respiratory distress syndrome: current progress, challenges, and future frontiers. *Braz J Med Biol Res* 2024; **57**: e13219 [PMID: 39417447 DOI: 10.1590/1414-431X2024e13219]

106 **Gorman E**, Millar J, McAuley D, O'Kane C. Mesenchymal stromal cells for acute respiratory distress syndrome (ARDS), sepsis, and COVID-

19 infection: optimizing the therapeutic potential. *Expert Rev Respir Med* 2021; **15**: 301-324 [PMID: 33172313 DOI: 10.1080/17476348.2021.1848555]

107 **Wu X**, Tang Y, Lu X, Liu Y, Liu X, Sun Q, Wang L, Huang W, Liu A, Liu L, Chao J, Zhang X, Qiu H. Endothelial cell-derived extracellular vesicles modulate the therapeutic efficacy of mesenchymal stem cells through IDH2/TET pathway in ARDS. *Cell Commun Signal* 2024; **22**: 293 [PMID: 38802896 DOI: 10.1186/s12964-024-01672-0]

108 **Zhang H**, Wan X, Tian J, An Z, Liu L, Zhao X, Zhou Y, Zhang L, Ge C, Song X. The therapeutic efficacy and clinical translation of mesenchymal stem cell-derived exosomes in cardiovascular diseases. *Biomed Pharmacother* 2023; **167**: 115551 [PMID: 37783149 DOI: 10.1016/j.biopha.2023.115551]

109 **Tang Y**, Zhou Y, Li HJ. Advances in mesenchymal stem cell exosomes: a review. *Stem Cell Res Ther* 2021; **12**: 71 [PMID: 33468232 DOI: 10.1186/s13287-021-02138-7]

110 **Kang IS**, Suh J, Lee MN, Lee C, Jin J, Lee C, Yang YI, Jang Y, Oh GT. Characterization of human cardiac mesenchymal stromal cells and their extracellular vesicles comparing with human bone marrow derived mesenchymal stem cells. *BMB Rep* 2020; **53**: 118-123 [PMID: 31964470 DOI: 10.5483/BMBRep.2020.53.2.235]

111 **Benecke L**, Coray M, Umbricht S, Chiang D, Figueiró F, Muller L. Exosomes: Small EVs with Large Immunomodulatory Effect in Glioblastoma. *Int J Mol Sci* 2021; **22**: 3600 [PMID: 33808435 DOI: 10.3390/ijms22073600]

112 **Hassanzadeh A**, Rahman HS, Markov A, Endjun JJ, Zekiy AO, Chartrand MS, Beheshtkhoo N, Kouhbanani MAJ, Marofi F, Nikoo M, Jarahian M. Mesenchymal stem/stromal cell-derived exosomes in regenerative medicine and cancer; overview of development, challenges, and opportunities. *Stem Cell Res Ther* 2021; **12**: 297 [PMID: 34020704 DOI: 10.1186/s13287-021-02378-7]

113 **Wiklander OP**, Nordin JZ, O'Loughlin A, Gustafsson Y, Corso G, Mäger I, Vader P, Lee Y, Sork H, Seow Y, Heldring N, Alvarez-Erviti L, Smith CI, Le Blanc K, Macchiarini P, Jungebluth P, Wood MJ, Andaloussi SE. Extracellular vesicle in vivo biodistribution is determined by cell source, route of administration and targeting. *J Extracell Vesicles* 2015; **4**: 26316 [PMID: 25899407 DOI: 10.3402/jev.v4.26316]

114 **Zou J**, Yang W, Cui W, Li C, Ma C, Ji X, Hong J, Qu Z, Chen J, Liu A, Wu H. Therapeutic potential and mechanisms of mesenchymal stem cell-derived exosomes as bioactive materials in tendon-bone healing. *J Nanobiotechnology* 2023; **21**: 14 [PMID: 36642728 DOI: 10.1186/s12951-023-01778-6]

115 **Luyckx VA**, Cherney DZI, Bello AK. Preventing CKD in Developed Countries. *Kidney Int Rep* 2020; **5**: 263-277 [PMID: 32154448 DOI: 10.1016/j.ekir.2019.12.003]

116 **Nassar W**, El-Ansary M, Sabry D, Mostafa MA, Fayad T, Kotb E, Temraz M, Saad AN, Essa W, Adel H. Umbilical cord mesenchymal stem cells derived extracellular vesicles can safely ameliorate the progression of chronic kidney diseases. *Biomater Res* 2016; **20**: 21 [PMID: 27499886 DOI: 10.1186/s40824-016-0068-0]

117 **Cho BS**, Lee J, Won Y, Duncan DI, Jin RC, Lee J, Kwon HH, Park GH, Yang SH, Park BC, Park KY, Youn J, Chae J, Jung M, Yi YW. Skin Brightening Efficacy of Exosomes Derived from Human Adipose Tissue-Derived Stem/Stromal Cells: A Prospective, Split-Face, Randomized Placebo-Controlled Study. *Cosmetics* 2020; **7**: 90 [DOI: 10.3390/cosmetics7040090]

118 **Kordelas L**, Rebmann V, Ludwig AK, Radtke S, Ruesing J, Doeppner TR, Epple M, Horn PA, Beelen DW, Giebel B. MSC-derived exosomes: a novel tool to treat therapy-refractory graft-versus-host disease. *Leukemia* 2014; **28**: 970-973 [PMID: 24445866 DOI: 10.1038/leu.2014.41]

119 **Noonin C**, Thongboonkerd V. Exosome-inflammasome crosstalk and their roles in inflammatory responses. *Theranostics* 2021; **11**: 4436-4451 [PMID: 33754070 DOI: 10.7150/thno.54004]

120 **Lim SK**, Giebel B, Weiss DJ, Witwer KW, Rohde E. Re: "Exosomes Derived from Bone Marrow Mesenchymal Stem Cells as Treatment for Severe COVID-19" by Sengupta *et al*. *Stem Cells Dev* 2020; **29**: 877-878 [PMID: 32520641 DOI: 10.1089/scd.2020.0089]

121 **Sengupta V**, Sengupta S, Lazo A, Woods P, Nolan A, Bremer N. Exosomes Derived from Bone Marrow Mesenchymal Stem Cells as Treatment for Severe COVID-19. *Stem Cells Dev* 2020; **29**: 747-754 [PMID: 32380908 DOI: 10.1089/scd.2020.0080]

122 **Jin Y**, Xu M, Zhu H, Dong C, Ji J, Liu Y, Deng A, Gu Z. Therapeutic effects of bone marrow mesenchymal stem cells-derived exosomes on osteoarthritis. *J Cell Mol Med* 2021; **25**: 9281-9294 [PMID: 34448527 DOI: 10.1111/jcmm.16860]

World Journal of Stem Cells

Submit a Manuscript: https://www.f6publishing.com

World J Stem Cells 2025 March 26; 17(3): 103360

DOI: 10.4252/wjsc.v17.i3.103360

ISSN 1948-0210 (online)

MINIREVIEWS

Emerging role of mesenchymal stem cell-derived exosomes in the repair of acute kidney injury

Juan-Juan Wang, Yu Zheng, Yan-Lin Li, Yin Xiao, Yang-Yang Ren, Yi-Qing Tian

Specialty type: Cell and tissue engineering

Provenance and peer review: Invited article; Externally peer reviewed.

Peer-review model: Single blind

Peer-review report's classification
Scientific Quality: Grade A, Grade B, Grade B, Grade C, Grade C, Grade D, Grade D
Novelty: Grade A, Grade B, Grade B, Grade B, Grade C, Grade C
Creativity or Innovation: Grade A, Grade B, Grade B, Grade B, Grade C, Grade C
Scientific Significance: Grade A, Grade A, Grade B, Grade B, Grade C, Grade C

P-Reviewer: Liang ZF; Li SC; Lyu FJ; Pan ZJ

Received: November 18, 2024
Revised: December 26, 2024
Accepted: February 13, 2025
Published online: March 26, 2025
Processing time: 124 Days and 17.8 Hours

Juan-Juan Wang, Yu Zheng, Yan-Lin Li, Clinical Laboratory, The First People's Hospital of Yancheng, Yancheng First Hospital, Affiliated Hospital of Nanjing University Medical School, Yancheng 224000, Jiangsu Province, China

Yin Xiao, Department of Medical Imaging, The Affiliated Xuzhou Municipal Hospital of Xuzhou Medical University, Xuzhou 221000, Jiangsu Province, China

Yang-Yang Ren, Clinical Laboratory, Xinyi People's Hospital, Xuzhou 221000, Jiangsu Province, China

Yi-Qing Tian, Clinical Laboratory, Xuzhou Central Hospital, Xuzhou 221000, Jiangsu Province, China

Co-first authors: Juan-Juan Wang and Yu Zheng.

Co-corresponding authors: Yang-Yang Ren and Yi-Qing Tian.

Corresponding author: Yi-Qing Tian, Dr, Clinical Laboratory, Xuzhou Central Hospital, No. 199 Jiefang South Road, Xuzhou 221000, Jiangsu Province, China. 824303893@qq.com

Abstract

Acute kidney injury (AKI) is a clinical syndrome characterized by a rapid deterioration in kidney function and has a significant impact on patient health and survival. Mesenchymal stem cells (MSCs) have the potential to enhance renal function by suppressing the expression of cell cycle inhibitors and reducing the expression of senescence markers and microRNAs *via* paracrine and endocrine mechanisms. MSC-derived exosomes can alleviate AKI symptoms by regulating DNA damage, apoptosis, and other related signaling pathways through the delivery of proteins, microRNAs, long-chain noncoding RNAs, and circular RNAs. This technique is both safe and effective. MSC-derived exosomes may have great application prospects in the treatment of AKI. Understanding the underlying mechanisms will foster the development of new and promising therapeutic strategies against AKI. This review focused on recent advancements in the role of MSCs in AKI repair as well as the mechanisms underlying the role of MSCs and their secreted exosomes. It is anticipated that novel and profound insights into the functionality of MSCs and their derived exosomes will emerge.

Key Words: Mesenchymal stem cells; Exosomes; Delivery of molecules; Acute kidney injury; Repair

Core Tip: Exosomes secreted by mesenchymal stem cells are increasingly recognized for their small size, lack of cellular components, stability, enhanced biocompatibility, and reduced toxicity. In studies of experimental acute kidney injury, exosomes have shown great potential in terms of their safety and efficacy as well as their ability to modulate gene expression and transcription in recipient cells.

Citation: Wang JJ, Zheng Y, Li YL, Xiao Y, Ren YY, Tian YQ. Emerging role of mesenchymal stem cell-derived exosomes in the repair of acute kidney injury. *World J Stem Cells* 2025; 17(3): 103360
URL: https://www.wjgnet.com/1948-0210/full/v17/i3/103360.htm
DOI: https://dx.doi.org/10.4252/wjsc.v17.i3.103360

INTRODUCTION

Acute kidney injury (AKI) covers a range of clinical conditions characterized by a sudden and prolonged decline in renal function. It is defined by an increase in serum creatinine by ≥ 0.3 mg/dL (≥ 26.5 μmol/L) over a 48-h period or an increase in serum creatinine to at least 1.5 times the baseline, which is either known or presumed to have occurred within the preceding 7 days. Additionally, AKI may be indicated by a urine output of less than 0.5 mL/kg/hour for a duration of 6 h [1,2]. AKI may present with oliguria (defined as urine output of less than 400 mL over 24 h or 17 mL/hour) or anuria (defined as urine output of less than 100 mL over 24 h).

Identified risk factors for the development of AKI include advanced age, chronic hypertension, diabetes mellitus, a high percentage of total body surface area burned, an elevated abbreviated burn severity index score, inhalation injury, rhabdomyolysis, surgical intervention, a high Acute Physiology and Chronic Health Evaluation II score, an increased Sequential Organ Failure Assessment score, sepsis, mechanical ventilation, hypoalbuminemia, specific genetic polymorphisms, and drug-induced AKI[3-5]. AKI poses a significant threat to human health, with recent findings indicating that approximately 30% of patients exhibited preadmission renal dysfunction. The period prevalence of acute renal failure necessitating renal replacement therapy in the intensive care unit was 5.0%-6.0%, with an overall hospital mortality rate of 60.3% (95% confidence interval: 58.0%-62.6%)[6].

Mesenchymal stem cells (MSCs) are stromal cells with the ability for self-renewal and multidirectional differentiation. They can be isolated from various tissues, including adipose tissue, the umbilical cord, endometrial polyps, menstrual blood, and bone marrow[7,8]. MSCs possess the ability to differentiate into various cell lineages, which has significantly advanced the field of stem cell therapy and has become an innovative treatment method. As a key cellular component, exosomes can replicate the biological potential of MSCs. Compared to MSCs, exosomes secreted by MSCs offer substantial advantages, notably in reducing adverse side effects such as infusion-related toxicities and immunogenicity[9,10]. Exosomes are emerging as a novel cell-free therapeutic modality, prompting an increasing number of studies to evaluate their therapeutic efficacy and capabilities in different diseases including AKI[11]. In this review, we summarized the research progress on MSCs and their secreted exosomes in the context of AKI to highlight the latest developments in this field.

AKI

The pivotal factors contributing to AKI encompass ischemia, hypoxia, immunological reactions, and nephrotoxicity[12,13]. Inflammation is a significant supplementary aspect in AKI, orchestrating the progression to the extension phase of renal damage. The kidney, a highly complex organ, is vulnerable to numerous injuries due to its intricate structure, which includes tubules, glomeruli, interstitium, and intrarenal blood vessels. Consequently, kidney injury is classified into four main categories: Tubular; glomerular; interstitial; and vascular damage. The progress in contemporary renal treatment strategies includes two major approaches. One is to repair the damaged organ to restore its function, and the other is to replace it with cells, bioengineering devices, or engineered tissues. In the event of kidney injury, diverse cellular demise pathways manifest, including apoptosis, necroptosis, pyroptosis, and ferroptosis[14-17]. These intricate mechanisms paradoxically act as protective shields for renal tissue against further insult. However, the kidney repair process, which is highly complex, is mainly controlled by paracrine communication within the microenvironment.

Transforming growth factor-β, a cornerstone cytokine, plays a critical role in tissue repair and fibrosis[18]. Its profibrotic signaling pathway converges at the activation of β-catenin. Remarkably, the β-catenin/Foxo interaction redirects transforming growth factor-β signaling away from fibrosis towards physiological epithelial healing. In the intricate process of renal injury repair, a wide range of cytokines and growth factors play crucial roles. Among these, insulin-like growth factor-1[19], stromal cell-derived factor-1[20], vascular endothelial growth factor[21], and hepatocyte growth factor (HGF)[22] are all intricately involved. These potent molecules work together to create a conducive environment for kidney function restoration, tubular repair, and regeneration, thereby ensuring a smoother process. By enhancing cellular proliferation, promoting angiogenesis, and facilitating the migration of reparative cells, they

contribute significantly to the overall recovery from kidney injury[23]. Recently, the therapeutic potential of MSCs and extracellular vesicles (EVs) has garnered significant attention among researchers exploring avenues to combat kidney diseases[24]. These innovative therapeutic approaches offer the promise of revolutionizing the treatment of kidney diseases.

AKI is now widely recognized as an expansive clinical syndrome with a diverse array of causative factors. This expansive syndrome encompasses acute tubular necrosis, acute interstitial nephritis, prerenal azotemia, acute glomerular, vasculitic renal disorders, and acute postrenal obstructive nephropathy, all of which contribute to its complex nature[25]. Based on the anatomical site of injury, AKI can be neatly categorized into three distinct groups, including prerenal, intrinsic renal, and postrenal. Prerenal AKI stems from hypoperfusion of the kidneys, a condition colloquially known as prerenal azotemia. This reduction in glomerular filtration rate arises from diminished blood flow to the kidneys, occurring in the absence of any discernible parenchymal damage. Intrinsic AKI, the most prevalent form among these categories, encompasses a broad spectrum of processes that inflict injury upon glomerular, interstitial, tubular, or endothelial cells within the kidney itself[26]. These insults can be multifarious, ranging from inflammatory processes to direct cellular damage. Lastly, postrenal AKI arises as a consequence of either partial or complete obstruction within the venous outflow or urinary tract, impeding the normal flow of fluids and waste products. To provide a comprehensive understanding, the underlying reasons for each category of AKI have been meticulously summarized in the Table 1, offering a detailed glimpse into the intricacies of this complex clinical syndrome.

MSCS AND EVS

In recent years, the EVs that are liberated by MSCs have emerged as the epicenter of intense scientific inquiry. This shift in focus underscores the growing recognition of the pivotal role that EVs play in mediating a myriad of biological processes. Emerging evidence have definitively demonstrated that MSCs and their exosomes have therapeutic effects on AKI. This section elaborates on the origin, function, and characteristics of MSCs and EVs and compares the therapeutic effects of MSCs and EVs from different sources on AKI.

Source of MSCs

MSCs, which are also known as mesenchymal stromal cells, were first discovered within the bone marrow stroma of pigs in the 1960s[27]. MSCs are paramount in mitigating the harmful effects and promoting the body's natural recovery mechanisms in organ injury diseases[28]. MSCs are characterized by a distinct set of surface molecules, including CD73, CD90, and CD105 as the prominent and key identifiers. Conversely, they are devoid of the expression of certain surface molecules that are characteristic of other cell types, including CD34, CD45, human leukocyte antigen-D related, CD14, CD11b, CD79a, and CD19[29,30]. MSCs possess an extraordinary plasticity including a high self-renewal capacity, multilineage differentiation potential, and immunomodulatory properties[31].

A diverse array of human sources has been harnessed for the generation of differentiated MSC populations, spanning across various tissues and organs. These include but are not limited to: bone and bone marrow, which offer a rich repository[32-36]; cartilage, noted for its unique regenerative potential[37]; tendon, with its inherent strength and flexibility[38]; muscle, for its dynamic properties[39]; liver, as a vital metabolic hub[40]; adipose tissue and skin, which are abundant and accessible sources[41-43]; placenta and fetal membrane, representing early developmental stages[44]; the umbilical cord, serving as a bridge connecting mother and child; and even deciduous and permanent teeth[45], highlighting the vast regenerative capabilities embedded within our bodies. This broad spectrum of sources underscores the remarkable versatility of MSCs and their potential for use in diverse therapeutic applications, where each source may confer unique advantages depending on the specific requirements of the targeted tissue or condition. Historically, bone marrow has been the primary and well-established source of MSCs in human research and clinical applications[46]. However, umbilical cord tissue has proven to be a rich source of MSCs, and it is characterized by its pristine stemness, making it a prominent alternative[34].

Characteristics and functionalities of MSCs

Many studies have illuminated the changes in MSC characteristics and functionalities across various settings, including cell phenotype, proliferation, differentiation, migration, apoptosis, and factor secretion. Furthermore, their low immunogenicity coupled with their trophic properties underscores their remarkable therapeutic potential[47,48]. These distinctive properties of MSCs endow them with immense potential for the development of innovative MSC-based or MSC-derived therapeutic interventions. MSCs have a remarkable ability to enhance cell viability and proliferation, which is crucial for tissue repair and regeneration.

Studies have shown that MSCs can promote the proliferation of muscle cells and enhance their differentiation. They can also improve the contractile ability of muscle cells. Additionally, the effect of MSCs on angiogenesis and endothelial cell proliferation is significant, particularly under hypoxic conditions, which further supports their role in tissue repair. Moreover, they effectively inhibit cell apoptosis, thereby preserving vital cellular functions in the affected tissues. In some cases, MSCs exhibit the capacity to modulate immune responses, orchestrating a healing environment that aids in the restoration of injured and diseased tissues[28,49-53]. The broad therapeutic potential underscores the crucial role MSCs could play in advancing the realm of regenerative medicine.

Table 1 The causes of acute kidney injury

Causes of AKI	Specific causes
Prerenal	Renal hypoperfusion, such as acute bleeding or diarrhea, dehydration, shock
Intrinsic	Renal ischemia, drug nephrotoxicity, glomerulonephritis, infection, ischemia-reperfusion injury, different group blood transfusion, vasculitis, *etc.*
Postrenal	Lithiasis, tumor, prostatomegaly

AKI: Acute kidney injury.

Comparison of therapeutic effects of MSCs from different sources on AKI

AKI likely leads to cellular senescence, which may be closely related to mechanisms such as cell cycle arrest and downregulation of Klotho protein expression[54]. Notably, human umbilical cord-derived MSCs (HucMSCs) are more effective than bone marrow-derived MSCs (BMMSCs) or adult adipose-derived MSCs (ADMSCs) in reducing the expression of cell cycle inhibitors[55]. In an experimental study on ischemia-reperfusion injury, the use of HucMSCs has recently been reported to improve renal function and downregulate the expression of senescence markers (β-galactosidase, p21Waf1/Cip1, and p16INK4a) and microRNAs (miRNA) (miR-29a and miR-34a) that are upregulated. Compared to adult ADMSCs, younger (postnatal) cells appear to be more effective in treating AKI[56]. It was found that MSCs derived from Wharton's jelly have a superior ability to increase Klotho protein levels compared to ADMSCs, thereby more effectively protecting tissues from the effects of aging. The younger the cells, the more factors associated with the youth they possess. By comparing cells collected from umbilical cords, newborns 4 days after birth, mothers, and adult volunteers, the results showed that the levels of soluble Klotho in cells from umbilical cords were significantly higher. Additionally, HucMSCs exhibited a higher expression of Klotho than ADMSCs[57,58].

MSC-derived EVs

Moreover, MSCs release EVs, which serve as vehicles for delivering crucial cargoes, enhancing their ability to promote tissue regeneration and healing[59,60]. The established classification framework for electric vehicles, metaphorically applied to membrane structures, meticulously segregates them into three distinct categories: Exosomes; ectosomes (herein designated as microvesicles, or MVs for brevity); and apoptotic bodies[61].

Exosomes, minute vesicles exquisitely defined by their diameter spanning 30-100 nm and a density meticulously calibrated within the range of 1.13-1.19 g/cm^2, have been meticulously identified as the product of a sophisticated process involving the fusion of multivesicular bodies with the plasma membrane[62]. This fusion event triggers their liberation into the extracellular milieu, indicating their pivotal role in intercellular communication and the dynamic exchange of biological molecules. EVs can be definitively discerned through the presence of distinctive markers that serve as hallmarks of their endocytic derivation, encompassing CD63, CD81, and CD9, among others[63].

MVs, whose dimensions range from 100-1000 nm, are elegantly expelled from the plasma membrane *via* a direct, outward budding process[64]. However, a definitive marker for identifying MVs remains elusive. Apoptotic bodies, arising as a consequence of cellular fragmentation during the terminal stages of apoptosis, are released into the surrounding environment. These bodies exhibit a remarkable range in their diameters, spanning from 1000-5000 nm[64].

EVs are nanoscale vehicles that encapsulate a wide range of bioactive molecules, including essential proteins such as cytokines, receptors, and their corresponding ligands, as well as a complex array of nucleic acids like DNA, mRNA, miRNA, and the elusive long-chain noncoding RNAs (lncRNAs). These vesicles play a crucial role in intercellular communication and have been extensively studied for their potential in drug delivery, leveraging their natural biocompatibility, biodegradability, low toxicity, and non-immunogenic properties. Additionally, they carry sugars and lipids, forming a comprehensive repertoire that underscores their intricate biological makeup and functional potential[65]. The intricate interplay between MSCs and their EV cargo, which encompasses a treasure trove of bioactive molecules, has sparked a renaissance in the field, fostering novel insights into regenerative medicine, immunology, and intercellular communication.

Comparison of therapeutic effects of EVs from different MSC sources in AKI

The initial proof of the advantageous impact of EVs released by BMMSCs was provided by Bruno *et al*[66] in 2009, using a model of AKI caused by glycerol injection in SCID mice. The impact of EVs was found to be comparable to that of the original MSCs, suggesting that EVs could potentially replace cell therapy. Furthermore, EVs isolated from liver-resident MSCs were administered intravenously in an AKI model induced by glycerol, resulting in improved renal function and morphology[67]. In the ischemia/reperfusion injury model, EVs released by BMMSCs have proven to be effective[68]. The use of exosomes released by fetal tissue-derived MSCs, such as umbilical cord blood-derived MSCs and Wharton's jelly-derived MSCs, has also yielded similarly positive effects, despite their different mechanisms of action[69-71].

Through the induction of rat HGF and the transfer of human HGF, EVs secreted by umbilical cord blood-derived MSCs accelerated the dedifferentiation and growth of renal tubular cells. Conversely, EVs released by Wharton's jelly-derived MSCs have the ability to stimulate cell proliferation through mitochondrial protective effects and to reduce inflammation and apoptosis[69,70]. Furthermore, it was found that exosomes derived from ADMSCs and those from BMMSCs can

reduce oxidative stress and inflammation and have a significant impact on the autophagy levels of kidney tissue. Additionally, compared to exosomes derived from BMMSCs, exosomes derived from ADMSCs are more significant in improving kidney function and structure, combating lipopolysaccharide (LPS)-induced AKI by inhibiting oxidative stress and inflammation[72]. In summary, we can see that EVs derived from various MSC sources demonstrate potent therapeutic effects in all models of AKI. The mechanism of action appears to be multifaceted, promoting proliferation and survival of resident cells while also limiting inflammation, oxidative stress, and angiogenesis.

ROLE OF MSCS AND THEIR SECRETED EXOSOMES IN THE TREATMENT OF AKI

A multitude of exhaustive studies have definitively demonstrated that MSCs and their exosomes can significantly alleviate the severity of AKI. However, the complex mechanisms responsible for these therapeutic effects exhibit considerable variation between MSCs and their exosomes. Yun and Lee[73] delved into the promising potential and therapeutic efficacy of MSC-based treatments, specifically addressing their application in the management of both acute and chronic kidney diseases. They comprehensively outlined how the mechanisms of MSCs in fostering renal recovery, in optimizing the cellular microenvironment, and in regulating inflammatory responses are intricately linked to their intricate interactions within the compromised kidney milieu. These multifaceted interactions are believed to underlie the therapeutic potential of MSCs, as they not only promote tissue regeneration but also modulate the surrounding environment to facilitate a more conducive healing process. In this comprehensive review, we have meticulously synthesized the most recent advancements in elucidating the intricate mechanisms underlying the therapeutic potential of MSC-derived exosomes for the treatment of AKI.

MSC-secreted exosome delivery of proteins

Proteins are important components of exosomes and play a crucial role in various cellular processes. The traditional perspective holds that the primary methods of repair by MSCs involve paracrine and endocrine effects, including their anti-apoptotic, anti-inflammatory, and angiogenic influences. However, Wang *et al*[74] demonstrated that exosomes transported by HucMSCs, specifically containing the protein 14-3-3ζ, can potentially enhance autophagic activity to protect HK-2 cells from cisplatin-induced injury. This suggests a more complex and multifaceted role of exosomes in cellular repair processes than previously thought. The protein 14-3-3ζ is a crucial functional molecule that plays a role in numerous vital biological processes.

Recently, 14-3-3ζ was shown to have protective effects against cisplatin-induced AKI by enhancing mitochondrial function and restoring the balance between cellular proliferation and apoptosis through the facilitation of β-catenin nuclear translocation[75]. Jia *et al*[76] also conclusively demonstrated that the 14-3-3ζ protein, encapsulated within exosomes derived from HucMSCs, engages in a pivotal interaction with autophagy-related protein 16 L, thereby triggering the activation of autophagy. This intricate mechanism serves as a potent safeguard against cisplatin-induced nephrotoxicity, offering a novel therapeutic avenue for mitigating the adverse renal effects associated with this chemotherapy agent[76].

The intricate interplay between cellular signaling pathways and the promising potential of exosome-mediated therapies in protecting against chemotherapy-induced organ damage is supported by recent studies, such as the one highlighting the protective role of exosomes in acute organ injuries, including the heart and kidneys. Moreover, Yin *et al*[77] uncovered a pivotal role of protein 14-3-3ζ in diabetic kidney disease. Notably, this protein could effectively promote the cytoplasmic sequestration of Yes-associated protein 1, thereby preventing its nuclear translocation, and it could augment the level of autophagy in the cytoplasm. These studies have shown that the delivery of 14-3-3ζ by MSC-derived exosomes could be a critical mechanism through which MSCs exert their therapeutic effects on AKI. A different study found that the use of ADMSC therapy could enhance the expression of tubular Sry-related HMG box 9, actively stimulate tubular regeneration, and effectively reduce the severity of AKI[78].

MSC-secreted exosome delivery of miRNA

MiRNAs are a complex class of endogenous non-coding RNAs, serving as crucial genetic regulators. Recently, numerous studies have been dedicated to examining the delivery of miRNAs *via* exosomes secreted by MSCs in AKI. Cao *et al*[79] investigated the role of miR-125b-5p, a molecule prominently abundant in HucMSC-derived exosomes, in suppressing p53 to facilitate tubular repair during ischemic AKI. This downregulation not only elicited a stimulatory effect on CDK1 and cyclin B1, thereby alleviating the G2/M cell cycle arrest, but also meticulously orchestrated the balance between Bcl-2 and Bax, two key regulators of apoptosis. This discovery offered important insights into the intricate mechanisms underlying renal recovery after injury[79].

Wang *et al*[80] demonstrated that the presence of miRNA let-7b-5p in MSC-derived exosomes effectively mitigated tubular epithelial cell apoptosis by inhibiting p53 expression. This process subsequently reduced DNA damage and apoptosis pathway activity, highlighting the potential role of miRNAs in promoting cell survival through MSC-derived exosomes[80].

Furthermore, HucMSC-derived exosomes may be a promising therapeutic agent capable of precisely modulating necroptosis through the complex targeting of miR-874-3p to the receptor-interacting protein kinase 1/phosphoglycerate mutase family member 5 pathway. This complex interaction not only alleviates renal tubular epithelial cell injury but also promotes robust repair mechanisms, thus presenting a potential therapeutic strategy[81]. HucMSCs have also been found to exhibit a remarkable ability in suppressing interleukin-1 receptor associated kinase 1 expression, a key regulatory factor, by significantly upregulating the level of miR-146b. This complex molecular interplay subsequently leads to the

inhibition of nuclear factor-kappa B activity, a key mediator of inflammatory cascades. Consequently, sepsis-associated AKI is effectively alleviated, and the survival rates of mice with sepsis are improved[82].

Another study showed that miR-199a-3p was notably abundant in exosomes derived from BMMSCs. These exosomes reduced the expression of semaphorin 3A and activated both the protein kinase B and extracellular-signal-regulated kinase pathways. Consequently, they play a protective role in mitigating the effects of hypoxia/reoxygenation injury[83]. Excitingly, it has been observed that exosomes derived from miR-1-184 agomir-treated MSCs effectively counteract cisplatin-induced suppression of cell growth by mitigating apoptosis. Simultaneously, these treated MSCs have demonstrated a significant induction of G1 phase arrest in HK-2 cells through the regulation of Forkhead box protein O 4, p27 Kip1, and CDK2 while also mitigating inflammatory responses[84].

Zhang *et al*[85] found that human urine-derived stem cells harbor an abundance of miR-216a-5p, which significantly downregulates the expression of phosphatase and tensin homolog and orchestrates a cascade of events, ultimately regulating cell apoptosis through the intricate protein kinase B signaling pathway[85]. A study revealed that exosomes derived from ADMSCs, carrying miR-342-5p, can ameliorate sepsis-associated AKI. Specifically, this research demonstrated that miR-342-5p exerts its protective effect by inhibiting toll-like receptor 9, thereby promoting autophagy, mitigating inflammation, and reducing kidney damage[86].

The therapeutic value of miRNAs in MSCs-derived exosome lies in tissue recovery, renal protection and regeneration, modulation of inflammatory responses, and mitigation of the devastating consequences of sepsis, among others. This holds great significance and prospect for the treatment of clinical kidney injury-related diseases.

MSC-secreted exosome delivery of lncRNA

LncRNAs represent a class of RNA molecules that, contrary to their protein-coding counterparts, do not directly encode for proteins. Instead, they play pivotal roles in modulating gene expression across diverse levels and through intricate mechanisms. These versatile molecules orchestrate the intricate dance of gene regulation, influencing not only the maturation of mRNA transcripts but also the intricate architecture of chromatin. Furthermore, lncRNAs engage in competitive interactions with miRNAs, vying for binding sites on endogenous RNAs, thereby adding another layer of complexity to the intricate web of gene regulatory networks[87].

The delivery of lncRNA *via* exosomes derived from MSCs plays a pivotal role in safeguarding AKI. A study has shown that exosomes secreted by HucMSCs are rich in lncRNA TUG1. This lncRNA has been found to interact with RNA-binding proteins, such as serine/arginine-rich splicing factor 1, which is crucial for the regulation of mRNA stability, as seen in the context of acyl-CoA synthetase long-chain family member 4 mRNA. Consequently, it curtails ferroptosis in HK-2 cells subjected to conditions of hypoxia followed by reoxygenation. A comparable phenomenon is also observed in cases of ischemia/reperfusion-induced AKI in mice[88]. The lncRNA delivery by MSCs through exosomes indicates a profound mechanism in mitigating kidney damage, pointing to potential therapeutic strategies in the future.

MSC-secreted exosome delivery of circular RNA

Circular RNAs constitute a distinct category of RNA molecules that are formed through a covalent bond due to the back-splicing of linear RNA sequences. Specifically, circVMA21 plays a pivotal role as a regulator in sepsis-associated AKI[89]. ADMSCs protected LPS-induced AKI in mice by increasing circVMA21 expression and decreasing miR-16-5p expression, which provided a potential molecular target for treating sepsis-related AKI. ADMSCs were found to offer protection against LPS-induced AKI in mice. The protective effect against AKI was achieved by enhancing the expression of circVMA21 and simultaneously suppressing the expression of miR-16-5p. The modulation of circVMA21 and miR-16-5p expression may serve as a promising therapeutic strategy for the treatment of sepsis-associated AKI, providing hope for patients afflicted with this condition.

Another notable discovery reveals that circular RNA circ DENND4C, when delivered *via* exosomes secreted from HucMSCs, possesses the capability to inhibit pyroptosis and effectively alleviate ischemia-reperfusion-induced AKI[90]. In this context, we have comprehensively summarized the experimental findings pertaining to the molecular cargoes transmitted by MSC-derived exosomes (Figure 1, Table 2), which have been shown to significantly improve functional recovery in a rat model of intracerebral hemorrhage and hold immense potential for future clinical applications.

CONCLUSION

Despite ongoing research efforts, no effective treatment options for AKI have been discovered thus far, emphasizing the need for heightened awareness and proactive measures to combat this menace[91]. In recent years, research on biological therapy has been a key focus, particularly for a new star in this field: MSCs[92]. The diversity and pluripotency of MSCs make them promising candidates for developing innovative clinical applications. Cellular therapy encompasses a diverse array of mechanisms, intricately woven to address various physiological challenges. These mechanisms not only alleviate inflammation but also exert immunomodulatory effects, delicately modulating the response of the immune system. Furthermore, they demonstrate antiapoptotic properties, safeguarding cells from premature death and fostering their survival. In addition, they combat oxidative stress, mitigating the harmful effects of reactive oxygen species[80,91,93-95].

Although numerous studies have consistently shown the safety and efficacy of MSCs therapy, potential hidden safety concerns that necessitate further attention may remain[96-98]. Moreover, MSC-derived exosomes have shown significant promise in experimental AKI, not only for their safety and efficacy but also for their ability to modulate gene expression and transcription in recipient cells, which could have significant implications on cellular function and the overall therapeutic outcome. Therefore, it is imperative to conduct comprehensive research on the long-term effects of MSC-

Table 2 Molecules delivered by mesenchymal stem cells derived exosomes for acute kidney injury therapy

Molecules	Source	AKI types	Conditions		Ref.
Protein	14-3-3ζ	HucMSC	Cisplatin-induced	Upregulating autophagic level	[74]
		HucMSC	Cisplatin-induced	Interacting with ATG16 L to activate autophagy	[75]
		HucMSC	Diabetic kidney disease	Promoting YAP cytoplasmic retention instead of entering the nucleus, enhancing autophagy in the cytoplasm	[76]
	Sox9	ADMSC	Ischemia/reperfusion	Upregulating Sox9 and promoting tubular regeneration	[78]
MiRNA	MiR-125b-5p	HucMSC	Ischemia/reperfusion	Repressing p53, upregulating CDK1 and cyclin B1 to rescue G2/M arrest, and inhibiting tubular epithelial cell apoptosis	[79]
	let-7b-5p	HBMMSC	Cisplatin-induced	Inhibiting P53 and reducing DNA damage and apoptosis	[80]
	MiR-874-3p	HucMSC	Cisplatin-induced	Targeting RIPK1/PGAM5 pathway	[81]
	MiR-146b	HucMSC	Sepsis-associated	Upregulating miR-146b levels and reducing IRAK1 expression resulting in inhibition of NF-κB activity	[82]
	MiR-199a-3p	HBMMSC	Hypoxia/reoxygenation injury	Decreasing Sema3A and activating the AKT and ERK pathways	[83]
	MiR-1184	HucMSC	Cisplatin-induced	Inducing G1 phase arrest in HK-2 cells by regulating FOXO4, p27 Kip1, and CDK2. Inhibiting cisplatin-induced inflammatory responses	[84]
	MiR-216a-5p	USC	Ischemia/reperfusion	Targeting PTEN and regulating cell apoptosis through the AKT pathway	[85]
	MiR-342-5p	ADMSC	Sepsis-related	Inhibiting TLR9, thereby promoting autophagy, mitigating inflammation, and reducing kidney damage	[86]
LncRNA	LncRNA TUG1	HucMSC	Ischemia/reperfusion	Interacting with SRSF1 to regulate ACSL4-mediated ferroptosis	[88]
CircRNA	CircVMA21	ADMSC	Sepsis-related	Increasing circVMA21 expression and decreasing miR-16-5p expression	[89]
	Circ DENND4C	USC	Ischemia/reperfusion	Inhibiting pyroptosis	[90]

AKI: Acute kidney injury; MiRNA: MicroRNA; LncRNA: Long-chain noncoding RNA; CircRNA: Circular RNA; Sox9: Sry-related HMG box 9; HucMSC: Human umbilical cord-derived mesenchymal stem cell; ADMSC: Adipose-derived mesenchymal stem cell; HBMMSC: Human bone marrow-derived mesenchymal stem cell; USC: Urine-derived stem cell; ATG16: Autophagy-related protein 16; YAP: Yes-associated protein 1; RIPK1: Receptor-interacting protein kinase 1; PGAM5: Phosphoglycerate mutase family member 5; IRAK1: Interleukin-1 receptor associated kinase 1; NF-κB: Nuclear factor-kappaB; Sema3A: Semaphorin 3A; AKT: Protein kinase B; ERK: Extracellular-signal-regulated kinase; FOXO4: Forkhead box protein O 4; PTEN: Phosphatase and tensin homolog; TLR9: Toll-like receptor 9; SRSF1: Serine/arginine-rich splicing factor 1; ACSL4: Acyl-CoA synthetase long-chain family member 4.

derived exosomes in order to assess their efficacy and safety profile, which should encompass a variety of areas, including the identification of potential side effects, evaluation of dose-response relationships, and examination of the interactions between exosomes and the recipient's immune system. In summary, MSC-derived exosomes have demonstrated promising outcomes in experiments, yet their use in stem cell therapies necessitates further research and clinical trials to confirm long-term safety and effectiveness.

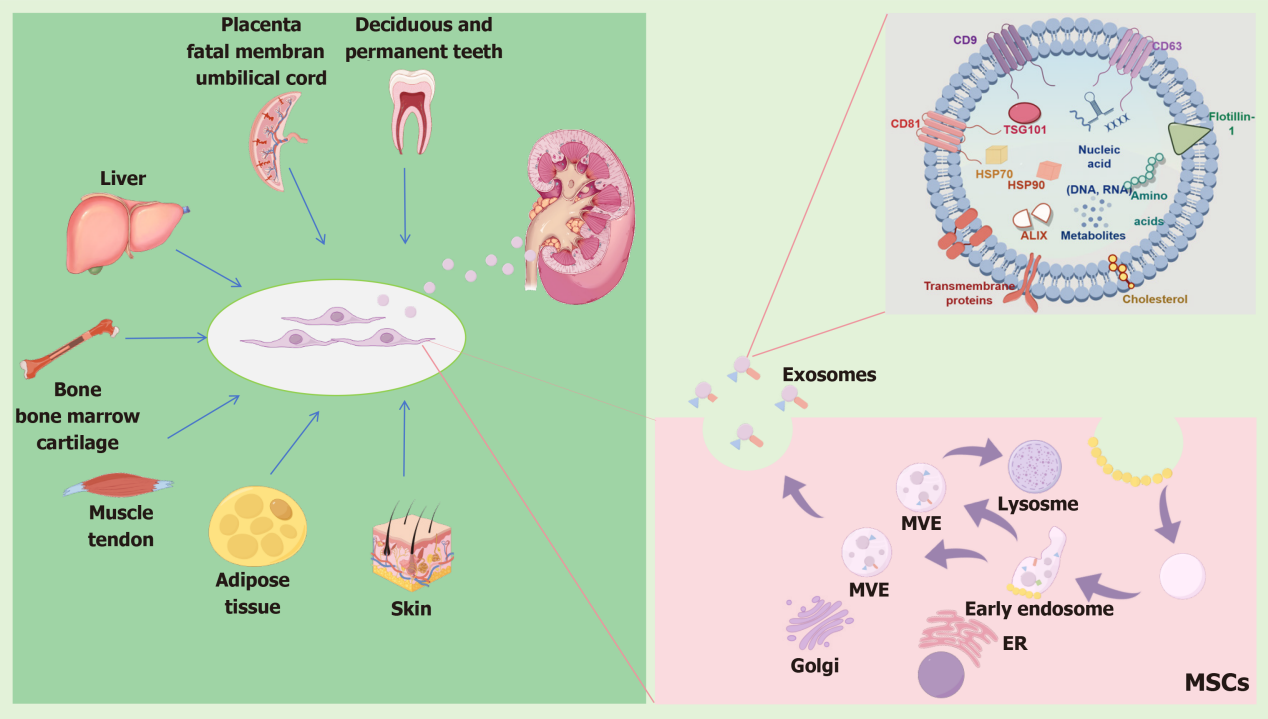

Figure 1 Sources of mesenchymal stem cells and molecular factors delivered by mesenchymal stem cell exosomes. Mesenchymal stem cells can come from a variety of tissues and organs in humans, covering a wide range of sources. These sources include skin, fat, muscle, bone, bone marrow, liver, placenta and fetal membranes, deciduous teeth, and permanent teeth. Extracellular vesicles are nanoscale vehicles that encapsulate a wide array of bioactive molecules, including essential proteins such as cytokines, receptors, and their corresponding ligands, as well as a complex array of nucleic acids like DNA, mRNA, microRNA, and the elusive long-chain noncoding RNA. These vesicles play a crucial role in intercellular communication and have been extensively studied for their potential in drug delivery, leveraging their natural biocompatibility, biodegradability, low toxicity, and non-immunogenic properties. TSG101: Tumor susceptibility gene 101; HSP70: 70-kDa heat shock protein; HSP90: 90-kDa heat shock protein; ALIX: Apoptosis-linked gene 2-interacting protein X; MVE: Multivesicular emulsion; ER: Endoplasmic reticulum; MSCs: Mesenchymal stem cells. The figure was drawn by Figdraw.

FOOTNOTES

Author contributions: Wang JJ and Zheng Y drafted the initial manuscript and contributed equally to this manuscript as co-first authors; Li YL and Xiao Y contributed to the figure and table artwork and illustrations; Ren YY and Tian YQ conceptualized and designed the review and contributed equally to this manuscript as co-corresponding authors. All authors critically reviewed the manuscript for important intellectual content, approved the final manuscript as submitted, and agreed to be accountable for work.

Conflict-of-interest statement: All the authors report no relevant conflicts of interest for this article.

Country of origin: China

ORCID number: Yi-Qing Tian 0000-0002-5184-5615.

S-Editor: Wang JJ
L-Editor: Filipodia
P-Editor: Zhang L

REFERENCES

1 **Kellum JA**, Lameire N; KDIGO AKI Guideline Work Group. Diagnosis, evaluation, and management of acute kidney injury: a KDIGO summary (Part 1). *Crit Care* 2013; **17**: 204 [PMID: 23394211 DOI: 10.1186/cc11454]
2 **Pickkers P**, Darmon M, Hoste E, Joannidis M, Legrand M, Ostermann M, Prowle JR, Schneider A, Schetz M. Acute kidney injury in the critically ill: an updated review on pathophysiology and management. *Intensive Care Med* 2021; **47**: 835-850 [PMID: 34213593 DOI: 10.1007/s00134-021-06454-7]
3 **Kim JY**, Yee J, Yoon HY, Han JM, Gwak HS. Risk factors for vancomycin-associated acute kidney injury: A systematic review and meta-

analysis. *Br J Clin Pharmacol* 2022; **88**: 3977-3989 [PMID: 35665530 DOI: 10.1111/bcp.15429]
4 **Varrier M**, Ostermann M. Novel risk factors for acute kidney injury. *Curr Opin Nephrol Hypertens* 2014; **23**: 560-569 [PMID: 25162200 DOI: 10.1097/MNH.0000000000000061]
5 **Rey A**, Gras-Champel V, Choukroun G, Masmoudi K, Liabeuf S. Risk factors for and characteristics of community- and hospital-acquired drug-induced acute kidney injuries. *Fundam Clin Pharmacol* 2022; **36**: 750-761 [PMID: 35037310 DOI: 10.1111/fcp.12758]
6 **Uchino S**, Kellum JA, Bellomo R, Doig GS, Morimatsu H, Morgera S, Schetz M, Tan I, Bouman C, Macedo E, Gibney N, Tolwani A, Ronco C; Beginning and Ending Supportive Therapy for the Kidney (BEST Kidney) Investigators. Acute renal failure in critically ill patients: a multinational, multicenter study. *JAMA* 2005; **294**: 813-818 [PMID: 16106006 DOI: 10.1001/jama.294.7.813]
7 **Ding DC**, Shyu WC, Lin SZ. Mesenchymal stem cells. *Cell Transplant* 2011; **20**: 5-14 [PMID: 21396235 DOI: 10.3727/096368910X]
8 **Al-Ghadban S**, Bunnell BA. Adipose Tissue-Derived Stem Cells: Immunomodulatory Effects and Therapeutic Potential. *Physiology (Bethesda)* 2020; **35**: 125-133 [PMID: 32027561 DOI: 10.1152/physiol.00021.2019]
9 **Lotfy A**, AboQuella NM, Wang H. Mesenchymal stromal/stem cell (MSC)-derived exosomes in clinical trials. *Stem Cell Res Ther* 2023; **14**: 66 [PMID: 37024925 DOI: 10.1186/s13287-023-03287-7]
10 **Wang S**, Guo L, Ge J, Yu L, Cai T, Tian R, Jiang Y, Zhao RCh, Wu Y. Excess Integrins Cause Lung Entrapment of Mesenchymal Stem Cells. *Stem Cells* 2015; **33**: 3315-3326 [PMID: 26148841 DOI: 10.1002/stem.2087]
11 **Huang J**, Cao H, Cui B, Ma X, Gao L, Yu C, Shen F, Yang X, Liu N, Qiu A, Cai G, Zhuang S. Mesenchymal Stem Cells-Derived Exosomes Ameliorate Ischemia/Reperfusion Induced Acute Kidney Injury in a Porcine Model. *Front Cell Dev Biol* 2022; **10**: 899869 [PMID: 35686052 DOI: 10.3389/fcell.2022.899869]
12 **Basile DP**, Anderson MD, Sutton TA. Pathophysiology of acute kidney injury. *Compr Physiol* 2012; **2**: 1303-1353 [PMID: 23798302 DOI: 10.1002/cphy.c110041]
13 **Molitoris BA**, Sandoval R, Sutton TA. Endothelial injury and dysfunction in ischemic acute renal failure. *Crit Care Med* 2002; **30**: S235-S240 [PMID: 12004242 DOI: 10.1097/00003246-200205001-00011]
14 **Li N**, Lin G, Zhang H, Sun J, Gui M, Liu Y, Li W, Zhan Z, Li Y, Pan S, Liu J, Tang J. Lyn attenuates sepsis-associated acute kidney injury by inhibition of phospho-STAT3 and apoptosis. *Biochem Pharmacol* 2023; **211**: 115523 [PMID: 37003346 DOI: 10.1016/j.bcp.2023.115523]
15 **Wang F**, Wang JN, He XY, Suo XG, Li C, Ni WJ, Cai YT, He Y, Fang XY, Dong YH, Xing T, Yang YR, Zhang F, Zhong X, Zang HM, Liu MM, Li J, Meng XM, Jin J. Stratifin promotes renal dysfunction in ischemic and nephrotoxic AKI mouse models *via* enhancing RIPK3-mediated necroptosis. *Acta Pharmacol Sin* 2022; **43**: 330-341 [PMID: 33833407 DOI: 10.1038/s41401-021-00649-w]
16 **Wang Y**, Zhang H, Chen Q, Jiao F, Shi C, Pei M, Lv J, Zhang H, Wang L, Gong Z. TNF-α/HMGB1 inflammation signalling pathway regulates pyroptosis during liver failure and acute kidney injury. *Cell Prolif* 2020; **53**: e12829 [PMID: 32419317 DOI: 10.1111/cpr.12829]
17 **Sun X**, Huang N, Li P, Dong X, Yang J, Zhang X, Zong WX, Gao S, Xin H. TRIM21 ubiquitylates GPX4 and promotes ferroptosis to aggravate ischemia/reperfusion-induced acute kidney injury. *Life Sci* 2023; **321**: 121608 [PMID: 36958437 DOI: 10.1016/j.lfs.2023.121608]
18 **Rao P**, Qiao X, Hua W, Hu M, Tahan M, Chen T, Yu H, Ren X, Cao Q, Wang Y, Yang Y, Wang YM, Lee VW, Alexander SI, Harris DC, Zheng G. Promotion of β-Catenin/Forkhead Box Protein O Signaling Mediates Epithelial Repair in Kidney Injury. *Am J Pathol* 2021; **191**: 993-1009 [PMID: 33753026 DOI: 10.1016/j.ajpath.2021.03.005]
19 **Imberti B**, Morigi M, Tomasoni S, Rota C, Corna D, Longaretti L, Rottoli D, Valsecchi F, Benigni A, Wang J, Abbate M, Zoja C, Remuzzi G. Insulin-like growth factor-1 sustains stem cell mediated renal repair. *J Am Soc Nephrol* 2007; **18**: 2921-2928 [PMID: 17942965 DOI: 10.1681/ASN.2006121318]
20 **Sun Z**, Li X, Zheng X, Cao P, Yu B, Wang W. Stromal cell-derived factor-1/CXC chemokine receptor 4 axis in injury repair and renal transplantation. *J Int Med Res* 2019; **47**: 5426-5440 [PMID: 31581874 DOI: 10.1177/0300060519876138]
21 **Yuan L**, Wu MJ, Sun HY, Xiong J, Zhang Y, Liu CY, Fu LL, Liu DM, Liu HQ, Mei CL. VEGF-modified human embryonic mesenchymal stem cell implantation enhances protection against cisplatin-induced acute kidney injury. *Am J Physiol Renal Physiol* 2011; **300**: F207-F218 [PMID: 20943766 DOI: 10.1152/ajprenal.00073.2010]
22 **Liu Y**. Hepatocyte growth factor in kidney fibrosis: therapeutic potential and mechanisms of action. *Am J Physiol Renal Physiol* 2004; **287**: F7-16 [PMID: 15180923 DOI: 10.1152/ajprenal.00451.2003]
23 **Lameire N**. The pathophysiology of acute renal failure. *Crit Care Clin* 2005; **21**: 197-210 [PMID: 15781157 DOI: 10.1016/j.ccc.2005.01.001]
24 **Huang Y**, Yang L. Mesenchymal stem cells and extracellular vesicles in therapy against kidney diseases. *Stem Cell Res Ther* 2021; **12**: 219 [PMID: 33789750 DOI: 10.1186/s13287-021-02289-7]
25 **Bellomo R**, Ronco C, Kellum JA, Mehta RL, Palevsky P; Acute Dialysis Quality Initiative workgroup. Acute renal failure - definition, outcome measures, animal models, fluid therapy and information technology needs: the Second International Consensus Conference of the Acute Dialysis Quality Initiative (ADQI) Group. *Crit Care* 2004; **8**: R204-R212 [PMID: 15312219 DOI: 10.1186/cc2872]
26 **Molitoris BA**. Low-Flow Acute Kidney Injury: The Pathophysiology of Prerenal Azotemia, Abdominal Compartment Syndrome, and Obstructive Uropathy. *Clin J Am Soc Nephrol* 2022; **17**: 1039-1049 [PMID: 35584927 DOI: 10.2215/CJN.15341121]
27 **Friedenstein AJ**, Chailakhjan RK, Lalykina KS. The development of fibroblast colonies in monolayer cultures of guinea-pig bone marrow and spleen cells. *Cell Tissue Kinet* 1970; **3**: 393-403 [PMID: 5523063 DOI: 10.1111/j.1365-2184.1970.tb00347.x]
28 **Uccelli A**, Moretta L, Pistoia V. Mesenchymal stem cells in health and disease. *Nat Rev Immunol* 2008; **8**: 726-736 [PMID: 19172693 DOI: 10.1038/nri2395]
29 **Gong P**, Zhang W, He Y, Wang J, Li S, Chen S, Ye Q, Li M. Classification and Characteristics of Mesenchymal Stem Cells and Its Potential Therapeutic Mechanisms and Applications against Ischemic Stroke. *Stem Cells Int* 2021; **2021**: 2602871 [PMID: 34795764 DOI: 10.1155/2021/2602871]
30 **Mushahary D**, Spittler A, Kasper C, Weber V, Charwat V. Isolation, cultivation, and characterization of human mesenchymal stem cells. *Cytometry A* 2018; **93**: 19-31 [PMID: 29072818 DOI: 10.1002/cyto.a.23242]
31 **Min SY**, Desai A, Yang Z, Sharma A, DeSouza T, Genga RMJ, Kucukural A, Lifshitz LM, Nielsen S, Scheele C, Maehr R, Garber M, Corvera S. Diverse repertoire of human adipocyte subtypes develops from transcriptionally distinct mesenchymal progenitor cells. *Proc Natl Acad Sci U S A* 2019; **116**: 17970-17979 [PMID: 31420514 DOI: 10.1073/pnas.1906512116]
32 **Hou T**, Xu J, Wu X, Xie Z, Luo F, Zhang Z, Zeng L. Umbilical cord Wharton's Jelly: a new potential cell source of mesenchymal stromal cells for bone tissue engineering. *Tissue Eng Part A* 2009; **15**: 2325-2334 [PMID: 19231937 DOI: 10.1089/ten.tea.2008.0402]
33 **Fekete N**, Rojewski MT, Fürst D, Kreja L, Ignatius A, Dausend J, Schrezenmeier H. GMP-compliant isolation and large-scale expansion of bone marrow-derived MSC. *PLoS One* 2012; **7**: e43255 [PMID: 22905242 DOI: 10.1371/journal.pone.0043255]

34 **Voskamp C**, Koevoet WJLM, Somoza RA, Caplan AI, Lefebvre V, van Osch GJVM, Narcisi R. Enhanced Chondrogenic Capacity of Mesenchymal Stem Cells After TNFα Pre-treatment. *Front Bioeng Biotechnol* 2020; **8**: 658 [PMID: 32714905 DOI: 10.3389/fbioe.2020.00658]

35 **Ooi YY**, Rahmat Z, Jose S, Ramasamy R, Vidyadaran S. Immunophenotype and differentiation capacity of bone marrow-derived mesenchymal stem cells from CBA/Ca, ICR and Balb/c mice. *World J Stem Cells* 2013; **5**: 34-42 [PMID: 23362438 DOI: 10.4252/wjsc.v5.i1.34]

36 **Svensson S**, Palmer M, Svensson J, Johansson A, Engqvist H, Omar O, Thomsen P. Monocytes and pyrophosphate promote mesenchymal stem cell viability and early osteogenic differentiation. *J Mater Sci Mater Med* 2022; **33**: 11 [PMID: 35032239 DOI: 10.1007/s10856-021-06639-y]

37 **Sandrasaigaran P**, Algraittee SJR, Ahmad AR, Vidyadaran S, Ramasamy R. Characterisation and immunosuppressive activity of human cartilage-derived mesenchymal stem cells. *Cytotechnology* 2018; **70**: 1037-1050 [PMID: 29497876 DOI: 10.1007/s10616-017-0182-4]

38 **Al-Ani MKh**, Xu K, Sun Y, Pan L, Xu Z, Yang L. Study of Bone Marrow Mesenchymal and Tendon-Derived Stem Cells Transplantation on the Regenerating Effect of Achilles Tendon Ruptures in Rats. *Stem Cells Int* 2015; **2015**: 984146 [PMID: 26339252 DOI: 10.1155/2015/984146]

39 **Ćuti T**, Antunović M, Marijanović I, Ivković A, Vukasović A, Matić I, Pećina M, Hudetz D. Capacity of muscle derived stem cells and pericytes to promote tendon graft integration and ligamentization following anterior cruciate ligament reconstruction. *Int Orthop* 2017; **41**: 1189-1198 [PMID: 28299448 DOI: 10.1007/s00264-017-3437-y]

40 **Weiss MC**, Strick-Marchand H. Isolation and characterization of mouse hepatic stem cells in vitro. *Semin Liver Dis* 2003; **23**: 313-324 [PMID: 14722809 DOI: 10.1055/s-2004-815558]

41 **Yang XF**, He X, He J, Zhang LH, Su XJ, Dong ZY, Xu YJ, Li Y, Li YL. High efficient isolation and systematic identification of human adipose-derived mesenchymal stem cells. *J Biomed Sci* 2011; **18**: 59 [PMID: 21854621 DOI: 10.1186/1423-0127-18-59]

42 **Ciuffreda MC**, Malpasso G, Musarò P, Turco V, Gnecchi M. Protocols for in vitro Differentiation of Human Mesenchymal Stem Cells into Osteogenic, Chondrogenic and Adipogenic Lineages. *Methods Mol Biol* 2016; **1416**: 149-158 [PMID: 27236670 DOI: 10.1007/978-1-4939-3584-0_8]

43 **Danisovic L**, Varga I, Polák S, Ulicná M, Hlavacková L, Böhmer D, Vojtassák J. Comparison of in vitro chondrogenic potential of human mesenchymal stem cells derived from bone marrow and adipose tissue. *Gen Physiol Biophys* 2009; **28**: 56-62 [PMID: 19390137 DOI: 10.4149/gpb_2009_01_56]

44 **Raynaud CM**, Maleki M, Lis R, Ahmed B, Al-Azwani I, Malek J, Safadi FF, Rafii A. Comprehensive characterization of mesenchymal stem cells from human placenta and fetal membrane and their response to osteoactivin stimulation. *Stem Cells Int* 2012; **2012**: 658356 [PMID: 22701494 DOI: 10.1155/2012/658356]

45 **Anil S**, Thomas NG, Chalisserry EP, Dalvi YB, Ramadoss R, Vellappally S. Isolation, Culture, and Characterization of Dental Pulp Stem Cells from Human Deciduous and Permanent Teeth. *J Vis Exp* 2024 [PMID: 38829121 DOI: 10.3791/65767]

46 **Pittenger MF**, Mackay AM, Beck SC, Jaiswal RK, Douglas R, Mosca JD, Moorman MA, Simonetti DW, Craig S, Marshak DR. Multilineage potential of adult human mesenchymal stem cells. *Science* 1999; **284**: 143-147 [PMID: 10102814 DOI: 10.1126/science.284.5411.143]

47 **Spees JL**, Lee RH, Gregory CA. Mechanisms of mesenchymal stem/stromal cell function. *Stem Cell Res Ther* 2016; **7**: 125 [PMID: 27581859 DOI: 10.1186/s13287-016-0363-7]

48 **Kimbrel EA**, Lanza R. Next-generation stem cells - ushering in a new era of cell-based therapies. *Nat Rev Drug Discov* 2020; **19**: 463-479 [PMID: 32612263 DOI: 10.1038/s41573-020-0064-x]

49 **Li L**, Zhang S, Zhang Y, Yu B, Xu Y, Guan Z. Paracrine action mediate the antifibrotic effect of transplanted mesenchymal stem cells in a rat model of global heart failure. *Mol Biol Rep* 2009; **36**: 725-731 [PMID: 18368514 DOI: 10.1007/s11033-008-9235-2]

50 **Dexter TM**, Spooncer E, Toksoz D, Lajtha LG. The role of cells and their products in the regulation of in vitro stem cell proliferation and granulocyte development. *J Supramol Struct* 1980; **13**: 513-524 [PMID: 7230803 DOI: 10.1002/jss.400130410]

51 **Le Blanc K**, Tammik L, Sundberg B, Haynesworth SE, Ringdén O. Mesenchymal stem cells inhibit and stimulate mixed lymphocyte cultures and mitogenic responses independently of the major histocompatibility complex. *Scand J Immunol* 2003; **57**: 11-20 [PMID: 12542793 DOI: 10.1046/j.1365-3083.2003.01176.x]

52 **Aggarwal S**, Pittenger MF. Human mesenchymal stem cells modulate allogeneic immune cell responses. *Blood* 2005; **105**: 1815-1822 [PMID: 15494428 DOI: 10.1182/blood-2004-04-1559]

53 **Liu M**, He J, Zheng S, Zhang K, Ouyang Y, Zhang Y, Li C, Wu D. Human umbilical cord mesenchymal stem cells ameliorate acute liver failure by inhibiting apoptosis, inflammation and pyroptosis. *Ann Transl Med* 2021; **9**: 1615 [PMID: 34926659 DOI: 10.21037/atm-21-2885]

54 **Andrade L**, Rodrigues CE, Gomes SA, Noronha IL. Acute Kidney Injury as a Condition of Renal Senescence. *Cell Transplant* 2018; **27**: 739-753 [PMID: 29701108 DOI: 10.1177/0963689717743512]

55 **Jin HJ**, Bae YK, Kim M, Kwon SJ, Jeon HB, Choi SJ, Kim SW, Yang YS, Oh W, Chang JW. Comparative analysis of human mesenchymal stem cells from bone marrow, adipose tissue, and umbilical cord blood as sources of cell therapy. *Int J Mol Sci* 2013; **14**: 17986-18001 [PMID: 24005862 DOI: 10.3390/ijms140917986]

56 **Rodrigues CE**, Capcha JM, de Bragança AC, Sanches TR, Gouveia PQ, de Oliveira PA, Malheiros DM, Volpini RA, Santinho MA, Santana BA, Calado RD, Noronha IL, Andrade L. Human umbilical cord-derived mesenchymal stromal cells protect against premature renal senescence resulting from oxidative stress in rats with acute kidney injury. *Stem Cell Res Ther* 2017; **8**: 19 [PMID: 28129785 DOI: 10.1186/s13287-017-0475-8]

57 **Yang HC**, Rossini M, Ma LJ, Zuo Y, Ma J, Fogo AB. Cells derived from young bone marrow alleviate renal aging. *J Am Soc Nephrol* 2011; **22**: 2028-2036 [PMID: 21965376 DOI: 10.1681/ASN.2010090982]

58 **Conboy IM**, Conboy MJ, Wagers AJ, Girma ER, Weissman IL, Rando TA. Rejuvenation of aged progenitor cells by exposure to a young systemic environment. *Nature* 2005; **433**: 760-764 [PMID: 15716955 DOI: 10.1038/nature03260]

59 **Boomsma RA**, Geenen DL. Mesenchymal stem cells secrete multiple cytokines that promote angiogenesis and have contrasting effects on chemotaxis and apoptosis. *PLoS One* 2012; **7**: e35685 [PMID: 22558198 DOI: 10.1371/journal.pone.0035685]

60 **Li JK**, Yang C, Su Y, Luo JC, Luo MH, Huang DL, Tu GW, Luo Z. Mesenchymal Stem Cell-Derived Extracellular Vesicles: A Potential Therapeutic Strategy for Acute Kidney Injury. *Front Immunol* 2021; **12**: 684496 [PMID: 34149726 DOI: 10.3389/fimmu.2021.684496]

61 **Yáñez-Mó M**, Siljander PR, Andreu Z, Zavec AB, Borràs FE, Buzas EI, Buzas K, Casal E, Cappello F, Carvalho J, Colás E, Cordeiro-da Silva A, Fais S, Falcon-Perez JM, Ghobrial IM, Giebel B, Gimona M, Graner M, Gursel I, Gursel M, Heegaard NH, Hendrix A, Kierulf P, Kokubun K, Kosanovic M, Kralj-Iglic V, Krämer-Albers EM, Laitinen S, Lässer C, Lener T, Ligeti E, Linē A, Lipps G, Llorente A, Lötvall J, Manček-Keber M, Marcilla A, Mittelbrunn M, Nazarenko I, Nolte-'t Hoen EN, Nyman TA, O'Driscoll L, Olivan M, Oliveira C, Pállinger É, Del Portillo

HA, Reventós J, Rigau M, Rohde E, Sammar M, Sánchez-Madrid F, Santarém N, Schallmoser K, Ostenfeld MS, Stoorvogel W, Stukelj R, Van der Grein SG, Vasconcelos MH, Wauben MH, De Wever O. Biological properties of extracellular vesicles and their physiological functions. *J Extracell Vesicles* 2015; **4**: 27066 [PMID: 25979354 DOI: 10.3402/jev.v4.27066]

62 **Trajkovic K**, Hsu C, Chiantia S, Rajendran L, Wenzel D, Wieland F, Schwille P, Brügger B, Simons M. Ceramide triggers budding of exosome vesicles into multivesicular endosomes. *Science* 2008; **319**: 1244-1247 [PMID: 18309083 DOI: 10.1126/science.1153124]

63 **Cocucci E**, Racchetti G, Meldolesi J. Shedding microvesicles: artefacts no more. *Trends Cell Biol* 2009; **19**: 43-51 [PMID: 19144520 DOI: 10.1016/j.tcb.2008.11.003]

64 **György B**, Szabó TG, Pásztói M, Pál Z, Misják P, Aradi B, László V, Pállinger E, Pap E, Kittel A, Nagy G, Falus A, Buzás EI. Membrane vesicles, current state-of-the-art: emerging role of extracellular vesicles. *Cell Mol Life Sci* 2011; **68**: 2667-2688 [PMID: 21560073 DOI: 10.1007/s00018-011-0689-3]

65 **Kalluri R**, LeBleu VS. The biology, function, and biomedical applications of exosomes. *Science* 2020; **367**: eaau6977 [PMID: 32029601 DOI: 10.1126/science.aau6977]

66 **Bruno S**, Grange C, Deregibus MC, Calogero RA, Saviozzi S, Collino F, Morando L, Busca A, Falda M, Bussolati B, Tetta C, Camussi G. Mesenchymal stem cell-derived microvesicles protect against acute tubular injury. *J Am Soc Nephrol* 2009; **20**: 1053-1067 [PMID: 19389847 DOI: 10.1681/ASN.2008070798]

67 **Herrera Sanchez MB**, Bruno S, Grange C, Tapparo M, Cantaluppi V, Tetta C, Camussi G. Human liver stem cells and derived extracellular vesicles improve recovery in a murine model of acute kidney injury. *Stem Cell Res Ther* 2014; **5**: 124 [PMID: 25384729 DOI: 10.1186/scrt514]

68 **Gatti S**, Bruno S, Deregibus MC, Sordi A, Cantaluppi V, Tetta C, Camussi G. Microvesicles derived from human adult mesenchymal stem cells protect against ischaemia-reperfusion-induced acute and chronic kidney injury. *Nephrol Dial Transplant* 2011; **26**: 1474-1483 [PMID: 21324974 DOI: 10.1093/ndt/gfr015]

69 **Zou X**, Zhang G, Cheng Z, Yin D, Du T, Ju G, Miao S, Liu G, Lu M, Zhu Y. Microvesicles derived from human Wharton's Jelly mesenchymal stromal cells ameliorate renal ischemia-reperfusion injury in rats by suppressing CX3CL1. *Stem Cell Res Ther* 2014; **5**: 40 [PMID: 24646750 DOI: 10.1186/scrt428]

70 **Gu D**, Zou X, Ju G, Zhang G, Bao E, Zhu Y. Mesenchymal Stromal Cells Derived Extracellular Vesicles Ameliorate Acute Renal Ischemia Reperfusion Injury by Inhibition of Mitochondrial Fission through miR-30. *Stem Cells Int* 2016; **2016**: 2093940 [PMID: 27799943 DOI: 10.1155/2016/2093940]

71 **Ju GQ**, Cheng J, Zhong L, Wu S, Zou XY, Zhang GY, Gu D, Miao S, Zhu YJ, Sun J, Du T. Microvesicles derived from human umbilical cord mesenchymal stem cells facilitate tubular epithelial cell dedifferentiation and growth *via* hepatocyte growth factor induction. *PLoS One* 2015; **10**: e0121534 [PMID: 25793303 DOI: 10.1371/journal.pone.0121534]

72 **Zhang W**, Zhang J, Huang H. Exosomes from adipose-derived stem cells inhibit inflammation and oxidative stress in LPS-acute kidney injury. *Exp Cell Res* 2022; **420**: 113332 [PMID: 36084668 DOI: 10.1016/j.yexcr.2022.113332]

73 **Yun CW**, Lee SH. Potential and Therapeutic Efficacy of Cell-based Therapy Using Mesenchymal Stem Cells for Acute/chronic Kidney Disease. *Int J Mol Sci* 2019; **20**: 1619 [PMID: 30939749 DOI: 10.3390/ijms20071619]

74 **Wang J**, Jia H, Zhang B, Yin L, Mao F, Yu J, Ji C, Xu X, Yan Y, Xu W, Qian H. HucMSC exosome-transported 14-3-3ζ prevents the injury of cisplatin to HK-2 cells by inducing autophagy in vitro. *Cytotherapy* 2018; **20**: 29-44 [PMID: 28943243 DOI: 10.1016/j.jcyt.2017.08.002]

75 **Sun Z**, Ning Y, Wu H, Guo S, Jiao X, Ji J, Ding X, Yu X. 14-3-3ζ targets β-catenin nuclear translocation to maintain mitochondrial homeostasis and promote the balance between proliferation and apoptosis in cisplatin-induced acute kidney injury. *Cell Signal* 2023; **111**: 110878 [PMID: 37657586 DOI: 10.1016/j.cellsig.2023.110878]

76 **Jia H**, Liu W, Zhang B, Wang J, Wu P, Tandra N, Liang Z, Ji C, Yin L, Hu X, Yan Y, Mao F, Zhang X, Yu J, Xu W, Qian H. HucMSC exosomes-delivered 14-3-3ζ enhanced autophagy *via* modulation of ATG16L in preventing cisplatin-induced acute kidney injury. *Am J Transl Res* 2018; **10**: 101-113 [PMID: 29422997]

77 **Yin S**, Liu W, Ji C, Zhu Y, Shan Y, Zhou Z, Chen W, Zhang L, Sun Z, Zhou W, Qian H. hucMSC-sEVs-Derived 14-3-3ζ Serves as a Bridge between YAP and Autophagy in Diabetic Kidney Disease. *Oxid Med Cell Longev* 2022; **2022**: 3281896 [PMID: 36199425 DOI: 10.1155/2022/3281896]

78 **Zhu F**, Chong Lee Shin OLS, Pei G, Hu Z, Yang J, Zhu H, Wang M, Mou J, Sun J, Wang Y, Yang Q, Zhao Z, Xu H, Gao H, Yao W, Luo X, Liao W, Xu G, Zeng R, Yao Y. Adipose-derived mesenchymal stem cells employed exosomes to attenuate AKI-CKD transition through tubular epithelial cell dependent Sox9 activation. *Oncotarget* 2017; **8**: 70707-70726 [PMID: 29050313 DOI: 10.18632/oncotarget.19979]

79 **Cao JY**, Wang B, Tang TT, Wen Y, Li ZL, Feng ST, Wu M, Liu D, Yin D, Ma KL, Tang RN, Wu QL, Lan HY, Lv LL, Liu BC. Exosomal miR-125b-5p deriving from mesenchymal stem cells promotes tubular repair by suppression of p53 in ischemic acute kidney injury. *Theranostics* 2021; **11**: 5248-5266 [PMID: 33859745 DOI: 10.7150/thno.54550]

80 **Wang SY**, Xu Y, Hong Q, Chen XM, Cai GY. Mesenchymal stem cells ameliorate cisplatin-induced acute kidney injury *via* let-7b-5p. *Cell Tissue Res* 2023; **392**: 517-533 [PMID: 36543894 DOI: 10.1007/s00441-022-03729-3]

81 **Yu Y**, Chen M, Guo Q, Shen L, Liu X, Pan J, Zhang Y, Xu T, Zhang D, Wei G. Human umbilical cord mesenchymal stem cell exosome-derived miR-874-3p targeting RIPK1/PGAM5 attenuates kidney tubular epithelial cell damage. *Cell Mol Biol Lett* 2023; **28**: 12 [PMID: 36750776 DOI: 10.1186/s11658-023-00425-0]

82 **Zhang R**, Zhu Y, Li Y, Liu W, Yin L, Yin S, Ji C, Hu Y, Wang Q, Zhou X, Chen J, Xu W, Qian H. Human umbilical cord mesenchymal stem cell exosomes alleviate sepsis-associated acute kidney injury *via* regulating microRNA-146b expression. *Biotechnol Lett* 2020; **42**: 669-679 [PMID: 32048128 DOI: 10.1007/s10529-020-02831-2]

83 **Zhu G**, Pei L, Lin F, Yin H, Li X, He W, Liu N, Gou X. Exosomes from human-bone-marrow-derived mesenchymal stem cells protect against renal ischemia/reperfusion injury *via* transferring miR-199a-3p. *J Cell Physiol* 2019; **234**: 23736-23749 [PMID: 31180587 DOI: 10.1002/jcp.28941]

84 **Zhang J**, He W, Zheng D, He Q, Tan M, Jin J. ExosomalmiR1184 derived from mesenchymal stem cells alleviates cisplatinassociated acute kidney injury. *Mol Med Rep* 2021; **24**: 795 [PMID: 34515319 DOI: 10.3892/mmr.2021.12435]

85 **Zhang Y**, Wang J, Yang B, Qiao R, Li A, Guo H, Ding J, Li H, Ye H, Wu D, Cui L, Yang S. Transfer of MicroRNA-216a-5p From Exosomes Secreted by Human Urine-Derived Stem Cells Reduces Renal Ischemia/Reperfusion Injury. *Front Cell Dev Biol* 2020; **8**: 610587 [PMID: 33415108 DOI: 10.3389/fcell.2020.610587]

86 **Liu W**, Hu C, Zhang B, Li M, Deng F, Zhao S. Exosomal microRNA-342-5p secreted from adipose-derived mesenchymal stem cells mitigates acute kidney injury in sepsis mice by inhibiting TLR9. *Biol Proced Online* 2023; **25**: 10 [PMID: 37085762 DOI: 10.1186/s12575-023-00198-y]

87 **Zhang P**, Wu S, He Y, Li X, Zhu Y, Lin X, Chen L, Zhao Y, Niu L, Zhang S, Li X, Zhu L, Shen L. LncRNA-Mediated Adipogenesis in

Different Adipocytes. *Int J Mol Sci* 2022; **23**: 7488 [PMID: 35806493 DOI: 10.3390/ijms23137488]

88 **Sun Z**, Wu J, Bi Q, Wang W. Exosomal lncRNA TUG1 derived from human urine-derived stem cells attenuates renal ischemia/reperfusion injury by interacting with SRSF1 to regulate ASCL4-mediated ferroptosis. *Stem Cell Res Ther* 2022; **13**: 297 [PMID: 35841017 DOI: 10.1186/s13287-022-02986-x]

89 **He Y**, Li X, Huang B, Yang Y, Luo N, Song W, Huang B. Exosomal circvma21 derived from adipose-derived stem cells alleviates sepsis-induced acute kidney injury by targeting mir-16-5p. *Shock* 2023; **60**: 419-426 [PMID: 37493568 DOI: 10.1097/SHK.0000000000002179]

90 **Yang B**, Wang J, Qiao J, Zhang Q, Liu Q, Tan Y, Wang Q, Sun W, Feng W, Li Z, Wang C, Yang S, Cui L. Circ DENND4C inhibits pyroptosis and alleviates ischemia-reperfusion acute kidney injury by exosomes secreted from human urine-derived stem cells. *Chem Biol Interact* 2024; **391**: 110922 [PMID: 38412628 DOI: 10.1016/j.cbi.2024.110922]

91 **Lee PW**, Wu BS, Yang CY, Lee OK. Molecular Mechanisms of Mesenchymal Stem Cell-Based Therapy in Acute Kidney Injury. *Int J Mol Sci* 2021; **22**: 11406 [PMID: 34768837 DOI: 10.3390/ijms222111406]

92 **Sávio-Silva C**, Soinski-Sousa PE, Balby-Rocha MTA, Lira ÁO, Rangel ÉB. Mesenchymal stem cell therapy in acute kidney injury (AKI): review and perspectives. *Rev Assoc Med Bras (1992)* 2020; **66** Suppl 1: s45-s54 [PMID: 31939535 DOI: 10.1590/1806-9282.66.S1.45]

93 **Han Q**, Wang X, Ding X, He J, Cai G, Zhu H. Immunomodulatory Effects of Mesenchymal Stem Cells on Drug-Induced Acute Kidney Injury. *Front Immunol* 2021; **12**: 683003 [PMID: 34149721 DOI: 10.3389/fimmu.2021.683003]

94 **Burks SR**, Nagle ME, Bresler MN, Kim SJ, Star RA, Frank JA. Mesenchymal stromal cell potency to treat acute kidney injury increased by ultrasound-activated interferon-γ/interleukin-10 axis. *J Cell Mol Med* 2018; **22**: 6015-6025 [PMID: 30216653 DOI: 10.1111/jcmm.13874]

95 **Sun W**, Zhu Q, Yan L, Shao F. Mesenchymal stem cells alleviate acute kidney injury *via* miR-107-mediated regulation of ribosomal protein S19. *Ann Transl Med* 2019; **7**: 765 [PMID: 32042781 DOI: 10.21037/atm.2019.11.89]

96 **Makhlough A**, Shekarchian S, Moghadasali R, Einollahi B, Dastgheib M, Janbabaee G, Hosseini SE, Falah N, Abbasi F, Baharvand H, Aghdami N. Bone marrow-mesenchymal stromal cell infusion in patients with chronic kidney disease: A safety study with 18 months of follow-up. *Cytotherapy* 2018; **20**: 660-669 [PMID: 29580865 DOI: 10.1016/j.jcyt.2018.02.368]

97 **Peired AJ**, Sisti A, Romagnani P. Mesenchymal Stem Cell-Based Therapy for Kidney Disease: A Review of Clinical Evidence. *Stem Cells Int* 2016; **2016**: 4798639 [PMID: 27721835 DOI: 10.1155/2016/4798639]

98 **Aghajani Nargesi A**, Lerman LO, Eirin A. Mesenchymal stem cell-derived extracellular vesicles for kidney repair: current status and looming challenges. *Stem Cell Res Ther* 2017; **8**: 273 [PMID: 29202871 DOI: 10.1186/s13287-017-0727-7]

World Journal of Stem Cells

Submit a Manuscript: https://www.f6publishing.com

World J Stem Cells 2025 March 26; 17(3): 98911

DOI: 10.4252/wjsc.v17.i3.98911

ISSN 1948-0210 (online)

ORIGINAL ARTICLE

Basic Study

Fat mass and obesity-associated protein in mesenchymal stem cells inhibits osteoclastogenesis *via* lnc NORAD/miR-4284 axis in ankylosing spondylitis

Wen-Jie Liu, Jia-Xin Wang, Quan-Feng Li, Yun-Hui Zhang, Peng-Fei Ji, Jia-Hao Jin, Yi-Bin Zhang, Zi-Hao Yuan, Pei Feng, Yan-Feng Wu, Hui-Yong Shen, Peng Wang

Specialty type: Cell and tissue engineering

Provenance and peer review: Unsolicited article; Externally peer reviewed.

Peer-review model: Single blind

Peer-review report's classification
Scientific Quality: Grade A
Novelty: Grade A
Creativity or Innovation: Grade A
Scientific Significance: Grade A

P-Reviewer: Jia XL

Received: July 9, 2024
Revised: January 3, 2025
Accepted: February 26, 2025
Published online: March 26, 2025
Processing time: 254 Days and 22.6 Hours

Wen-Jie Liu, Jia-Xin Wang, Quan-Feng Li, Yun-Hui Zhang, Peng-Fei Ji, Jia-Hao Jin, Yi-Bin Zhang, Zi-Hao Yuan, Hui-Yong Shen, Peng Wang, Department of Orthopedics, The Eighth Affiliated Hospital, Sun Yat-sen University, Shenzhen 518033, Guangdong Province, China

Wen-Jie Liu, Jia-Xin Wang, Quan-Feng Li, Yun-Hui Zhang, Peng-Fei Ji, Jia-Hao Jin, Yi-Bin Zhang, Zi-Hao Yuan, Pei Feng, Yan-Feng Wu, Hui-Yong Shen, Peng Wang, Guangdong Provincial Clinical Research Center for Orthopedic Diseases, The Eighth Affiliated Hospital, Sun Yat-sen University, Shenzhen 518033, Guangdong Province, China

Pei Feng, Yan-Feng Wu, Center for Biotherapy, The Eighth Affiliated Hospital, Sun Yat-sen University, Shenzhen 518033, Guangdong Province, China

Co-first authors: Wen-Jie Liu and Jia-Xin Wang.

Co-corresponding authors: Hui-Yong Shen and Peng Wang.

Corresponding author: Peng Wang, PhD, Department of Orthopedics, The Eighth Affiliated Hospital, Sun Yat-sen University, No. 3025 Shennan Road, Shenzhen 518033, Guangdong Province, China. wangp57@mail.sysu.edu.cn

Abstract

BACKGROUND

Ankylosing spondylitis (AS) is recognized as a long-term inflammatory disorder that leads to inflammation in the spine and joints, alongside abnormal bone growth. In previous studies, we reported that mesenchymal stem cells (MSCs) derived from individuals with AS demonstrated a remarkable inhibition in the formation of osteoclasts compared to those obtained from healthy donors. The mechanism through which MSCs from AS patients achieve this inhibition remains unclear.

AIM

To investigate the potential underlying mechanism by which MSCs from individuals with ankylosing spondylitis (AS-MSCs) inhibit osteoclastogenesis.

METHODS
We analysed fat mass and obesity-associated (FTO) protein levels in AS-MSCs and MSCs from healthy donors and investigated the effects and mechanism by which FTO in MSCs inhibits osteoclastogenesis by coculturing and measuring the levels of tartrate-resistant acid phosphatase, nuclear factor of activated T cells 1 and cathepsin K.

RESULTS
We found that FTO, an enzyme responsible for removing methyl groups from RNA, was more abundantly expressed in MSCs from AS patients than in those from healthy donors. Reducing FTO levels was shown to diminish the capacity of MSCs to inhibit osteoclast development. Further experimental results revealed that FTO affects the stability of the long non-coding RNA activated by DNA damage (NORAD) by altering its N6-methyladenosine methylation status. Deactivating NORAD in MSCs significantly increased osteoclast formation by affecting miR-4284, which could regulate the MSC-mediated inhibition of osteoclastogenesis reported in our previous research.

CONCLUSION
This study revealed elevated FTO levels in AS-MSCs and found that FTO regulated the ability of AS-MSCs to inhibit osteoclast formation through the long noncoding RNA NORAD/miR-4284 axis.

Key Words: Ankylosing spondylitis; Mesenchymal stem cells; Osteoclastogenesis; Fat mass and obesity-associated protein; Non-coding RNA activated by DNA damage

Core Tip: This study explores how mesenchymal stem cells (MSCs) from ankylosing spondylitis (AS) patients inhibit osteoclastogenesis. We observed higher expression of fat mass and obesity-associated protein (FTO) in AS-MSCs compared to healthy controls. Reducing FTO expression diminished their osteoclast inhibitory effect. FTO regulates the long non-coding RNA activated by DNA damage (NORAD) by modulating its N6-methyladenosine methylation, and NORAD silencing increased osteoclast formation *via* miR-4284. These results highlight FTO as a key regulator of AS-MSC function and suggest the long noncoding RNA NORAD/miR-4284 axis as a novel mechanism of osteoclast inhibition in AS.

Citation: Liu WJ, Wang JX, Li QF, Zhang YH, Ji PF, Jin JH, Zhang YB, Yuan ZH, Feng P, Wu YF, Shen HY, Wang P. Fat mass and obesity-associated protein in mesenchymal stem cells inhibits osteoclastogenesis *via* lnc NORAD/miR-4284 axis in ankylosing spondylitis. *World J Stem Cells* 2025; 17(3): 98911
URL: https://www.wjgnet.com/1948-0210/full/v17/i3/98911.htm
DOI: https://dx.doi.org/10.4252/wjsc.v17.i3.98911

INTRODUCTION

Ankylosing spondylitis (AS) is an autoimmune disease characterized by chronic inflammation and pathological osteogenesis[1]. Currently, nonsteroidal anti-inflammatory drugs and biologics, such as tumor necrosis factor inhibitors and interleukin-17 inhibitors, have significantly enhanced the management of clinical symptoms related to chronic inflammation[2,3]. However, the molecular mechanisms underlying pathological osteogenesis in AS remain elusive, and the limited therapeutic options pose a significant threat to the quality of life of AS patients.

Mesenchymal stem cells (MSCs), as major sources of osteoblasts, play a crucial role in bone metabolism and homeostasis of the bone microenvironment[4]. Our prior investigation revealed that MSCs derived from individuals with AS (AS-MSCs) exhibited a greater propensity for osteogenic differentiation than MSCs sourced from healthy donors (HD-MSCs)[5]. Additionally, our research revealed that, compared with HD-MSCs, AS-MSCs notably suppressed osteoclastogenesis[6], suggesting that AS-MSCs might play a pivotal role in driving the imbalance between osteogenesis and osteoclastogenesis, thereby potentially contributing to the pathological osteogenesis observed in AS. Nevertheless, the mechanisms through which AS-MSCs promote this imbalance remain elusive.

N6-methyladenosine (m6A) methylation is the most prevalent RNA modification at the post-transcriptional level in eukaryotic cells, and plays a crucial role in various physiological and pathological processes[7]. Research has indicated that m6A modification plays a regulatory role in diverse biological functions of MSCs, including differentiation, senescence, and immune regulatory processes[8]. Moreover, our findings suggest that m6A modification may exacerbate the pathological progression of AS by modulating the direct migration of MSCs[9]. The role of m6A modifications in the ability of MSCs to suppress osteoclastogenesis remains poorly understood.

Long noncoding RNAs (lncRNAs) are a class of endogenous RNAs that exceed 200 nucleotides in length and lack protein-coding potential[10]. They have been implicated in numerous fundamental biological processes as well as various diseases[11]. Mounting evidence shows that lncRNAs can regulate gene expression through various mechanisms, such as

binding to proteins and microRNAs, or modulating interactions between proteins and DNA[12]. Furthermore, aberrant expression levels of lncRNAs have been observed in the progression of AS, rendering them promising biomarkers for the diagnosis and treatment of AS[13].

This study aimed to explore the impact of m6A modification on the enhanced ability of AS-MSCs to inhibit osteoclastogenesis compared with that of HD-MSCs. Our findings revealed that FTO, an RNA demethylase, was upregulated in AS-MSCs compared with HD-MSCs. Moreover, we demonstrated that suppressing FTO could attenuate the inhibitory effect of AS-MSCs on osteoclastogenesis by modulating the stability of long non-coding RNA activated by DNA damage (NORAD). This study may offer a novel perspective for understanding the pathologic osteogenesis of AS.

MATERIALS AND METHODS

Cell isolation and culture

The isolation and expansion of MSCs were carried out according to previously established methods[5], utilizing bone marrow obtained from the posterior superior iliac spine of healthy volunteers and individuals with AS. MSCs were cultured in Dulbecco's modified Eagle's medium (Gibco, NY, United States) supplemented with 10% fetal bovine serum (FBS, Gibco, NY, United States) at 37 °C. The culture medium was refreshed every 2 days. Peripheral blood mononuclear cells were isolated *via* density gradient centrifugation, followed by the further isolation and purification of $CD14^+$ monocytes from peripheral blood mononuclear cells using CD14 MicroBeads (Miltenyi Biotec, Germany). The isolated monocytes were subsequently cultured in Dulbecco's modified Eagle's medium containing 10% FBS at 37 °C under 5% CO_2.

Coculture system for osteoclast differentiation

$CD14^+$ monocytes were seeded at a density of 2.5×10^5 cells/cm^2 in the lower chamber of a six-well transwell plate, while MSCs (at a ratio of 10:1, monocyte: MSC) were plated in the upper chamber. The induction medium used for the experiment consisted of 90% alpha minimal essential medium, 10% FBS, 50 ng/mL recombinant human receptor activator of nuclear factor κB ligand, 25 ng/mL recombinant human macrophage-colony stimulating factor, and 50 μg/mL l-ascorbic acid (all from Peprotech, NJ, United States). The culture medium was changed every 3 days to ensure optimal conditions for cell growth and differentiation.

Tartrate resistant acid phosphatase staining

On the 9th day, the cells were washed three times with phosphate buffered saline (PBS). To assess osteoclastogenesis, tartrate resistant acid phosphatase (TRAP) staining was conducted *via* a leukocyte acid phosphatase assay kit (Sigma, Japan), in accordance with the manufacturer's guidelines. Cells exhibiting purple staining and possessing three or more nuclei were classified as TRAP-positive osteoclasts. The average number of osteoclasts was determined by evaluating a minimum of 9 fields that covered the entire well.

F-actin assay

On the 9th day, the cells were fixed with 4% paraformaldehyde for 5 minutes and thoroughly rinsed with PBS. The samples were subsequently stained with FITC-conjugated phalloidin (Sigma, Japan) and 4′,6-diamidino-2-phenylindole at room temperature for 40 minutes. Following three washes with PBS, the cells were examined *via* an Axio Observer fluorescence microscope (Carl Zeiss, Germany).

RNA interference

Targeted small interfering RNAs (siRNAs) specific to FTO and lncRNA NORAD, as well as a negative control, were procured from IGEbio (Guangzhou, China). When the cell confluence reached 60%-80%, MSCs were transfected with a mixture containing Opti-MEM reduced serum medium, Lipofectamine™ RNAiMAX (Invitrogen, CA, United States), and siRNA (at a concentration of 1.8×10^6 cells per 1 OD), following the manufacturer's instructions. After 5 hours of transfection, the transfection medium was removed. The efficiency of siRNA knockdown was evaluated 48 hours later using quantitative polymerase chain reaction (qPCR) and western blotting. The siRNA with the highest efficiency was selected for subsequent experiments.

Real-time quantitative reverse transcription-PCR

After the cells were washed three times with PBS, TRIzol (Invitrogen, CA, United States) was added for total RNA extraction. The extracted RNA was then reverse transcribed into complementary DNA using the PrimeScript RT Reagent Kit (TaKaRa, Japan). Subsequently, real-time quantitative reverse transcription-PCR detection was performed using SYBR Green Premix Ex Taq (TaKaRa, Japan) reagent. A real-time fluorescence quantitative PCR system was utilized to measure the gene expression levels. To determine the relative expression levels of the target genes, the $2^{-\Delta\Delta Ct}$ method was employed with GAPDH serving as the internal control. The detailed protocol for these steps can be found in our previously published research. Additionally, the forward and reverse primers for the target genes are below: *FTO*: Primer#1 5′-ACTTGGCTCCCTTATCTGACC-3′ and primer#2 5′-TGTGCAGTGTGAGAAAGGCTT-3′; *lnc NORAD*: Primer#1 5′-CTCTCAACTCCACCCCAACC-3′ and primer#2 5′-ACAAACGTGGACGTATCGCT-3′; *GAPDH*: Primer#1 5′-AAGGTGAAGGTCGGAGTCAA-3′ and primer#2 5′-AATGAAGGGGTCATTGATGG3′; *U6*: Primer#1 5′-CGCTTCG-GCAGCACATATAC-3′ and primer#2 5′-TTCACGAATTTGCGTGTCAT-3′; *miR-4284*: Primer#1 5′-TCGCCGACGGGCT-

CACATCA-3′ and primer#2 5′-CTCAACTGGTGTCGTGGAGTCGGC-3′; *miR-4284 RT* Primer: 5′-CTCAACTGGT-GTCGTGGAGTCGGCAATTCAGTTGAGATGGGGTG-3′.

Western blot

The cells were washed three times with cold PBS, followed by another wash with RIPA buffer containing a mixture of 1% phosphatase inhibitors and protease inhibitors to extract proteins. The cell lysate was collected and centrifuged at 14000 rpm for 30 minutes at 4 °C. The protein supernatant was collected, and the protein concentration was quantified using a BCA kit. The proteins were subsequently separated by sodium-dodecyl sulfate gel electrophoresis and transferred onto a polyvinylidene fluoride (PVDF) membrane. The PVDF membranes were blocked with 5% milk for 1 hour at room temperature and then incubated overnight with primary antibodies against nuclear factor of activated T cells 1 (NFATc1), TRAP, cathepsin K (CTSK), or beta-actin (dilution 1:1000). After being washed three times with Tris-buffered saline-Tween, the PVDF membrane was incubated with a horseradish peroxidase-conjugated secondary antibody (dilution 1:3000) at room temperature for 1 hour. Following another three washes, the target protein bands were detected *via* a chemiluminescent HRP substrate, and the density analysis of the bands was performed *via* ImageJ software.

m6A RNA immunoprecipitation-qPCR

The m6A RIP assay was conducted *via* the Magna MeRIP m6A Kit (Merck Millipore) following the protocol provided by the manufacturer. In brief, total RNA was isolated from pretreated MSCs and randomly broken into fragments of 100 or fewer nucleotides. Protein A/G magnetic beads conjugated with either an anti-m6A antibody (ab208577, Abcam, United Kingdon), an anti-FTO antibody (ab126605, Abcam, United Kingdom), or an immunoglobulin G control were added to the fragmented RNA and incubated overnight. Following the collection of the magnetic beads, the immunoprecipitated RNA was further collected to analyze m6A enrichment in target genes *via* qPCR. Non-immunoprecipitated RNA fragments were used as a control for input.

Luciferase reporter assay

A mutant (mut) NORAD variant with a mutation in the predicted miR-4284 binding site was constructed and named NORAD mut. The synthesized wild-type (luci-NORAD WT) or luci-NORAD mut sequences were cloned and inserted into the pmirGLO vector, which contains the firefly luciferase reporter gene. For the transfection experiments, 5000 MSCs were seeded per well in 96-well plates. Each construct was co-transfected with NORAD mimics or a negative control *via* Lipofectamine 3000 transfection reagent (Invitrogen, CA, United States). After 36 hours post-transfection, the cell lysates were collected, and the luciferase activity was measured *via* the Dual-Luciferase Reporter Assay System (Promega, WI, United States), following the manufacturer's instructions. The relative luciferase activity was determined by calculating the ratio of firefly to Renilla luciferase activity. This assay helps in assessing the impact of the mutation in the miR-4284 binding site on luciferase expression, shedding light on the regulatory role of miR-4284 in NORAD expression.

Mouse models

Male SKG mice were handled in compliance with the animal care guidelines approved by the Institutional Animal Care and Use Committee of Sun Yat-sen University. Disease induction commenced at 8 weeks of age through the intraperitoneal injection of 3 mg of curdlan. Adenoviruses encoding a specific shRNA targeting FTO (Av-shFTO) or adeno-associated virus of negative control for mouse experiments were procured from OBiO Technology. SKG mice were administered Av-shFTO or adeno-associated virus of negative control *via* intravenous tail vein injection upon disease onset. At the 8th week post-induction and treatment, the mice were euthanized, and tissue samples were collected for hematoxylin and eosin staining and Safranin O staining.

Statistical analysis

Each experiment was repeated three times. The data are presented as the mean ± SD. One-way analysis of variance (ANOVA) and Student's *t*-test were used for intergroup comparisons with SPSS 20.0 software (Chicago, IL, United States). A P-value < 0.05 was considered statistically significant.

RESULTS

FTO expression was upregulated in AS-MSCs compared with HD-MSCs

To investigate the involvement of m6A modifications in MSCs in AS, we first confirmed the protein-level differences in the expression of m6A-related methyltransferases and demethylases through western blot analysis. The results revealed a significant increase in the expression level of FTO in AS-MSCs compared with that in normal MSCs (Figure 1A and B). Furthermore, we extended this analysis to bone tissue samples from AS patients and normal controls. Immunofluorescence staining revealed a notably greater level of FTO expression in AS-MSCs marked with osteocalcin than in normal controls (Figure 1C). These findings suggest that FTO in MSCs may play a crucial role in the development of AS, indicating the potential involvement of FTO-mediated m6A modifications in the pathogenesis of AS.

FTO positively regulates the ability of MSCs to inhibit osteoclast formation

To investigate the effect of FTO upregulation in AS-MSCs, an siRNA was used to silence FTO in MSCs. Then, the MSCs were cocultured with CD14$^+$ monocytes in medium supplemented with macrophage colony-stimulating factor and

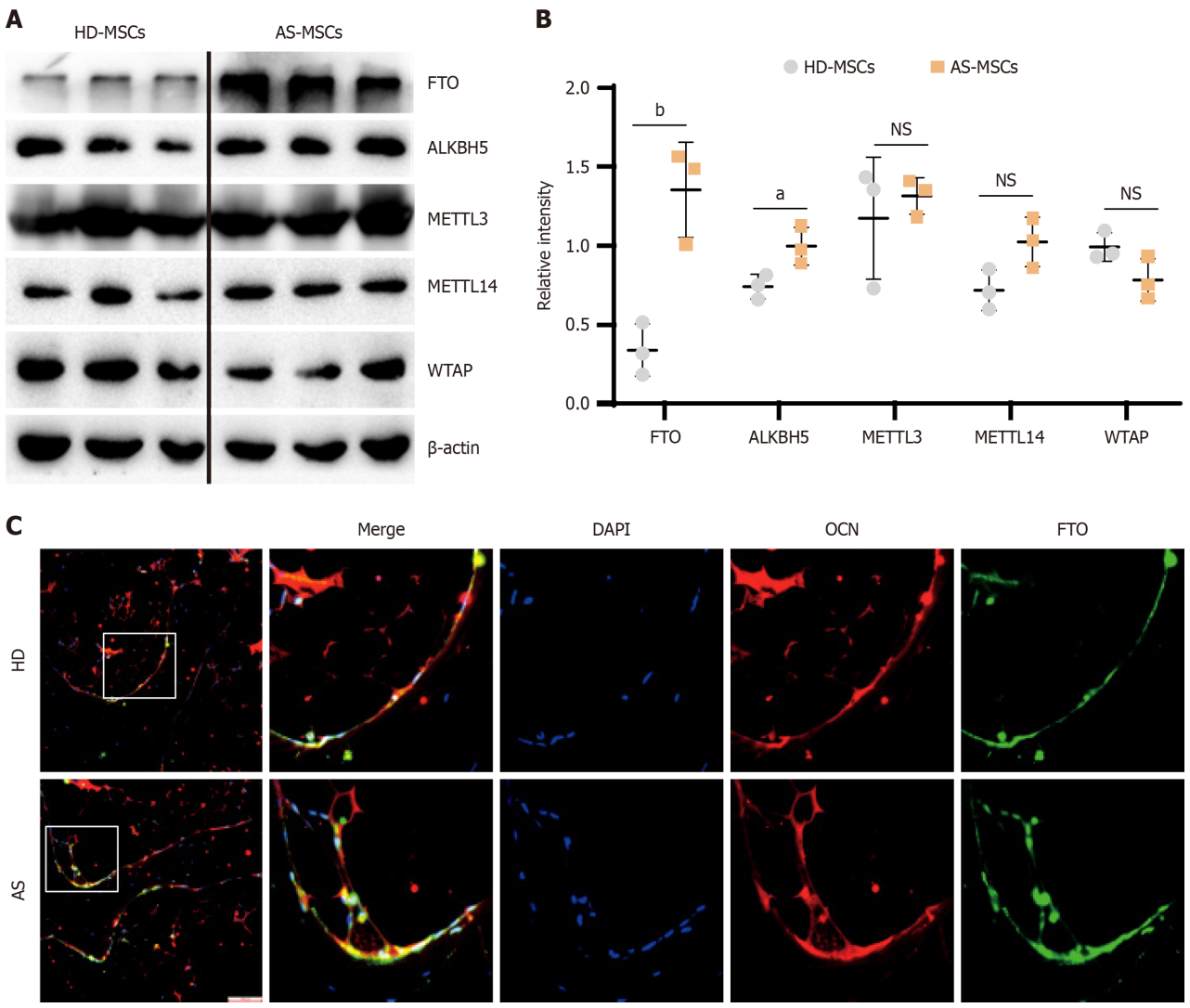

Figure 1 Fat mass and obesity-associated protein expression was upregulated in mesenchymal stem cells from individuals with ankylosing spondylitis compared with mesenchymal stem cells from healthy donors. A: Protein levels of N6-methyladenosine-related methyltransferase and demethylases in mesenchymal stem cells from individuals with ankylosing spondylitis and mesenchymal stem cells from healthy donors were determined by western blot; B: Quantitative data of protein levels of fat mass and obesity-associated, alkB homolog 5, methyltransferase 3, methyltransferase 14, and WT1 associated protein are shown; C: Immunofluorescence staining (scale bar = 100 mm) showed fat mass and obesity-associated expression in the osteocalcin positive mesenchymal stem cells in healthy donors group and ankylosing spondylitis group. The statistical data are represented as the means ± SDs, n = 3 in each group. NS: No significant difference, $^{a}P < 0.05$, $^{b}P < 0.01$. AS-MSCs: Mesenchymal stem cells from individuals with ankylosing spondylitis; HD-MSCs: Mesenchymal stem cells from healthy donors; ALKBH5: AlkB homolog 5; METTL3: Methyltransferase 3; METTL14: Methyltransferase 14; WTAP: WT1 associated protein; OCN: Osteocalcin; FTO: Fat mass and obesity-associated; AS: Ankylosing spondylitis; HD: Healthy donors.

receptor activator of nuclear factor κB ligand to induce osteoclast differentiation. TRAP staining and F-actin staining were employed to assess osteoclast formation. The results revealed that the number of osteoclasts in the HD-MSC group was greater than that in the AS-MSC group (Figure 2A-C). Following FTO knockdown, the number of osteoclasts increased significantly in both groups. Interestingly, the number of osteoclasts cultured with AS-MSCs recovered to the level observed in those cultured with HD-MSCs. Furthermore, the expression levels of osteoclast formation markers (NFATc1, TRAP, and CTSK) were evaluated *via* western blot analysis. The results revealed lower levels of NFATc1, TRAP, and CTSK in AS-MSCs and higher levels in the FTO-knockdown group (Figure 2D and E). To further confirm the influence of FTO in MSCs, we used lentiviruses to overexpress FTO. As shown by TRAP and F-actin staining and western blotting, overexpressing FTO in MSCs led to reduced osteoclast formation (Figure 2F-H). In summary, these findings suggest that FTO in MSCs positively regulates the ability of MSCs to inhibit osteoclast formation, highlighting the potential role of FTO in modulating osteoclastogenesis.

FTO regulated lnc NORAD stability

Previously, we demonstrated that miR-4284 could modulate the MSC-mediated inhibition of osteoclast formation[6]. We first examined the correlation between FTO and miR-4284 through qPCR. Our results revealed that the expression of miR-4284 was elevated after siFTO. Interestingly, suppressing miR-4284 did not affect the expression of FTO (Figure 3A). We thus wondered whether lncRNAs participate in the regulatory network between FTO and miR-4284. Next, we

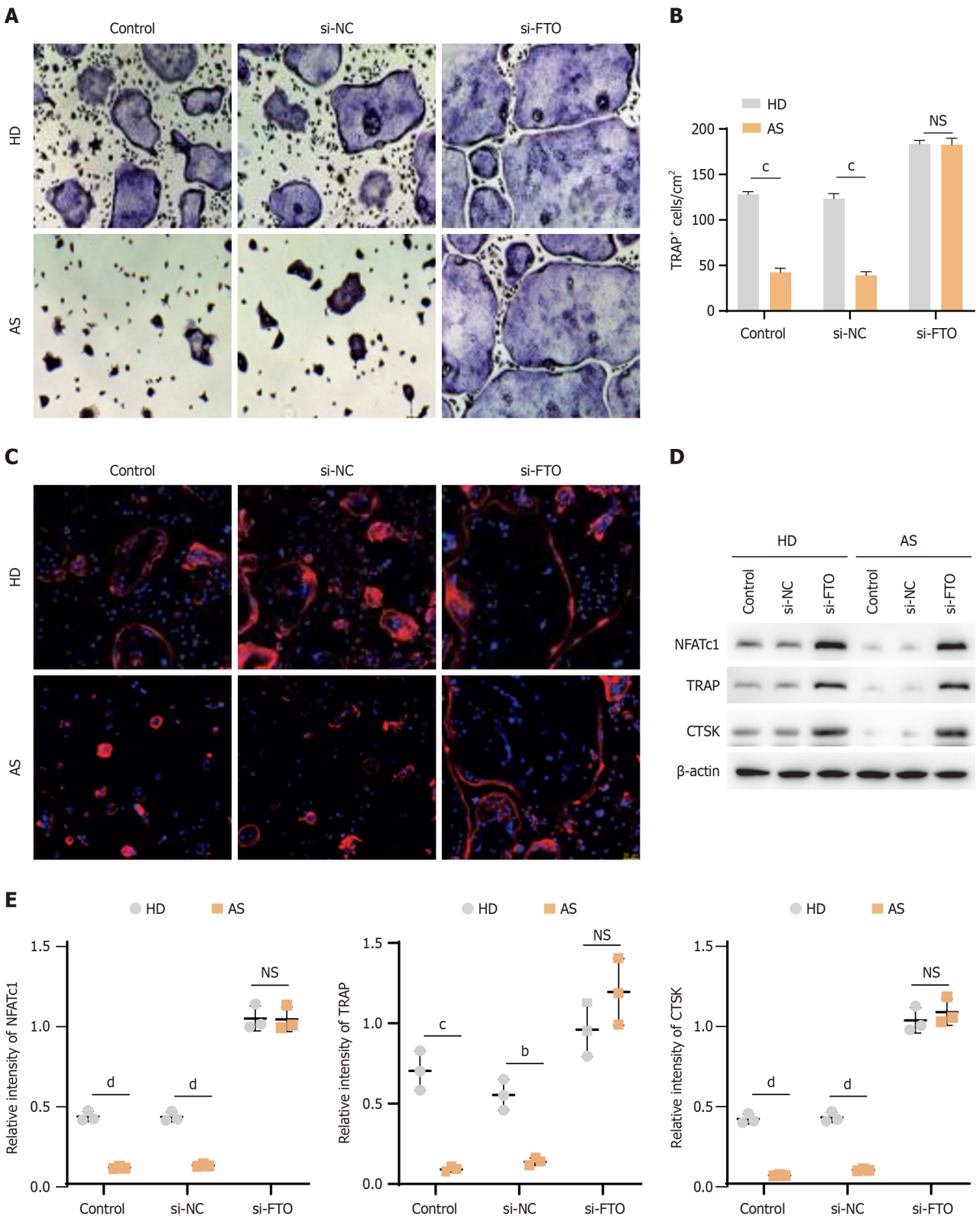
A
Control
si-NC
si-FTO
HD
AS
B
HD
AS
TRAP+ cells/cm2
200
150
100
50
0
c
c
NS
Control
si-NC
si-FTO
C
Control
si-NC
si-FTO
HD
AS
D
HD
AS
Control
si-NC
si-FTO
Control
si-NC
si-FTO
NFATc1
TRAP
CTSK
β-actin
E
HD
AS
Relative intensity of NFATc1
1.5
1.0
0.5
0.0
d
d
NS
Control
si-NC
si-FTO
Relative intensity of TRAP
c
b
NS
Relative intensity of CTSK
d
d
NS

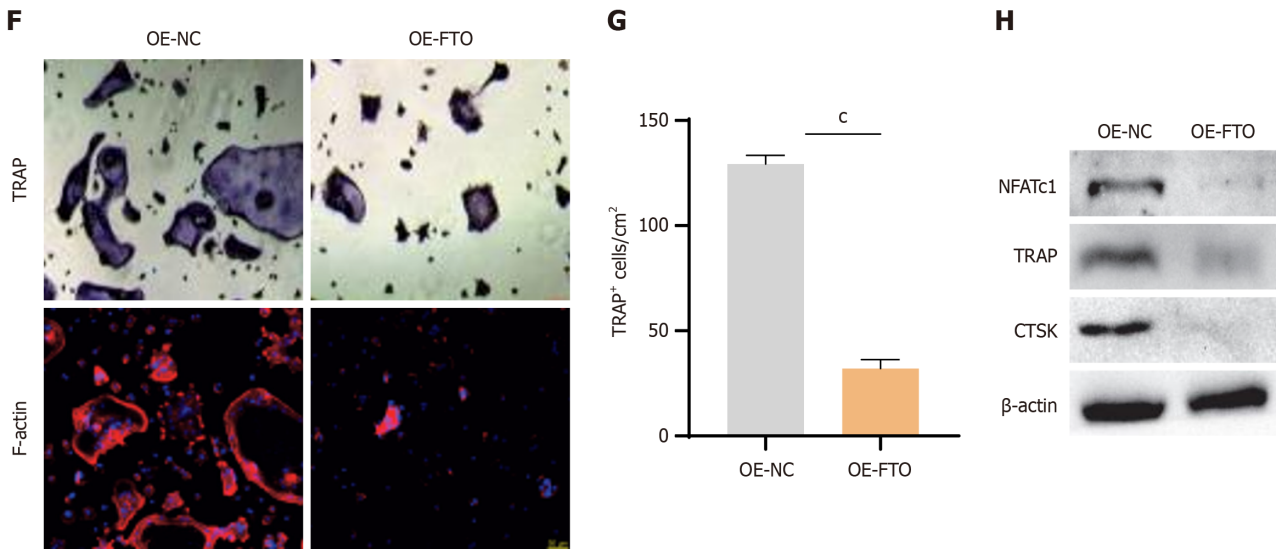

Figure 2 Fat mass and obesity-associated positively regulates the ability of mesenchymal stem cells to inhibit osteoclast formation. CD14⁺ monocytes were cultured with mesenchymal stem cells from healthy donors or mesenchymal stem cells from individuals with ankylosing spondylitis after knocking down fat mass and obesity-associated in the presence of macrophage colony-stimulating factor and receptor activator of nuclear factor κB ligand. A: Representative images of tartrate resistant acid phosphatase (TRAP) staining (× 100); B: Quantitative data of TRAP⁺ osteoclasts number in each well is shown; C: Representative images of F-actin assays (× 200); D: Western blot analysis was performed to detect protein levels of TRAP, nuclear factor of activated T cells 1 (NFATc1) and cathepsin K (CTSK); E: Quantitative data for NFATc1, TRAP, and CTSK protein levels determined by western blot analyses are shown; F: Representative images of TRAP staining (× 100) and F-actin assays (× 200); G: Quantitative data of TRAP⁺ osteoclasts number in each well is shown; H: Western blot analysis was performed to detect protein levels of NFATc1, TRAP, and CTSK. The statistical data are presented as the means ± SDs; $n = 3$ in each group. NS: No significant difference, $^{b}P < 0.01$, $^{c}P < 0.005$, $^{d}P < 0.001$. AS: Ankylosing spondylitis; HD: Healthy donors; si-NC: Small interfering RNA of negative control; si-FTO: Small interfering RNA targeting fat mass and obesity-associated; OE-NC: Overexpression of negative control; OE-FTO: Overexpression of fat mass and obesity-associated; TRAP: Tartrate resistant acid phosphatase; NFATc1: Nuclear factor of activated T cells 1; CTSK: Cathepsin K.

performed high-throughput sequencing to compare the lncRNA expression profiles of MSCs with or without FTO knockdown. The results revealed significant differential expression of the lncRNA NORAD in the profiles (Figure 3B), which further validated the interaction between miR-4284 and the lncRNA NORAD *via* DIANA TOOLS (Figure 3C). The qPCR results confirmed the downregulation of NORAD in the FTO-knockdown group (Figure 3D). Additionally, previous reports suggested that m6A modification could regulate the expression of the lncRNA NORAD[14]. To investigate this, we analysed the m6A levels on the lncRNA NORAD *via* m6A RNA immunoprecipitation-qPCR analysis. The results indicated that the m6A levels of the lncRNA NORAD in the FTO knockdown group were significantly greater than those in the control group, suggesting that FTO could reduce the m6A modification levels of the lncRNA NORAD (Figure 3E). To further understand how FTO regulates NORAD levels *via* m6A modification, RNA stability assays were performed using actinomycin D to inhibit RNA transcription. The results demonstrated that the half-life of NORAD in the control group was significantly longer than that in the FTO-knockdown group (Figure 3F). These findings collectively suggest that FTO regulates NORAD stability through m6A modification.

Lnc NORAD targets miR-4284

Next, we investigated the relationship between lnc NORAD and miR-4284. The results revealed that miR-4284 contains complementary binding sites with the lncRNA NORAD (Figure 3G). Luciferase assays revealed that the luciferase activity of WT NORAD was significantly increased when NORAD was cotransfected with the miR-4284 mimic, whereas there was no significant difference in the activity of the NORAD MUT (Figure 3H). Further analysis *via* qPCR demonstrated that lnc NORAD was upregulated after transfection with the miR-4284 mimic (Figure 3I). Additionally, the results from the RNA binding protein immunoprecipitation assay confirmed the interaction relationship between NORAD and miR-4284 (Figure 3J and K). Overall, these findings suggest that the lncRNA NORAD can bind with miR-4284 and potentially downregulate its expression. This finding indicates a regulatory mechanism in which the lncRNA NORAD may modulate the expression or activity of miR-4284, highlighting a potential regulatory axis in the context of MSC-mediated osteoclast formation.

Lnc NORAD in MSCs inhibits osteoclastogenesis

To investigate the effect of NORAD on MSC-mediated osteoclast formation, we cocultured CD14⁺ monocytes with AS-MSCs or HD-MSCs with or without NORAD knockdown. TRAP staining revealed an increased number of TRAP⁺ cells in the NORAD-knockdown group, and there was no significant difference in osteoclast formation between AS-MSCs and HD-MSCs after NORAD knockdown (Figure 4A and B). F-actin staining was consistent with the TRAP staining results (Figure 4C). Furthermore, western blot analysis was performed to evaluate the expression levels of osteoclast differentiation markers (NFATc1, TRAP, and CTSK). The results indicated that the lnc NORAD knockdown group presented higher expression levels of these markers than the control group. Additionally, NORAD knockdown abolished the

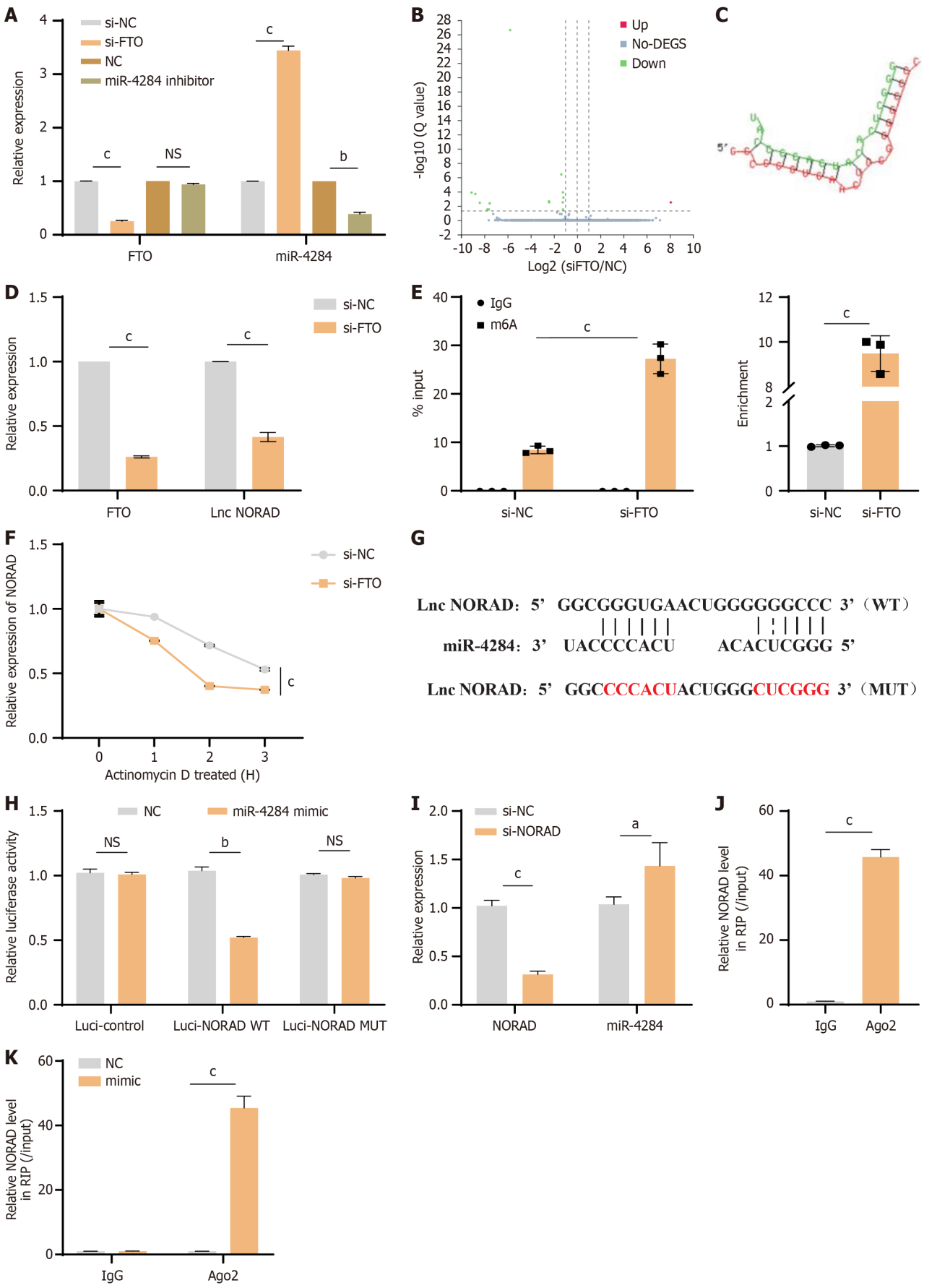

Figure 3 Fat mass and obesity-associated modulates the expression of microRNA-4284 by targeting ong non-coding RNA activated by DNA damage stability. A: Relative expression of fat mass and obesity-associated (FTO) and miR-4284 were quantified by quantitative reverse transcription polymerase chain reaction (qRT-PCR) in mesenchymal stem cells (MSCs) after small interfering RNA (siRNA) transfection; B: Volcano plots of long noncoding RNA

(lncRNA) high-throughput sequencing results for MSCs compared between control group and FTO knockdown group; C: The possible binding sites between long non-coding RNA activated by DNA damage (NORAD) and miR-4284 are predicted by DIANA TOOLS; D: The expression of FTO and lnc NORAD were quantified by qRT-PCR in MSCs after siRNA transfection; E: N6-methyladenosine modification level of lncRNA NORAD in si-NC or si-FTO treated MSCs (n = 3); F: Degradation curves of lncRNA NORAD in si-NC or si-FTO treated MSCs (n = 3); G: The possible binding sites between lncRNA NORAD and miR-4284 are shown, and a mutant lnc NORAD site was constructed; H: Luciferase reporter assay using empty luciferase vector (luci-control), wild type reporter with binding site (luci-NORAD wild type), and the vector containing mutated binding sequence (luci-NORAD mutant) in the presence of miR-4284 mimic (n = 3); I: The expression of lnc NORAD and miR-4284 were quantified by qRT-PCR in MSCs after siRNA transfection; J and K: RNA immunoprecipitation assays were used to detect the interaction between lnc NORAD and miR-4284. The statistical data are presented as the means ± SDs; n = 3 in each group. NS: No significant difference; $^{a}P < 0.05$, $^{b}P < 0.01$, $^{c}P < 0.005$. FTO: Fat mass and obesity-associated; NC: Negative control; si-NC: Small interfering RNA of negative control; si-FTO: Small interfering RNA targeting fat mass and obesity-associated; IgG: Immunoglobulin G; m6A: N6-methyladenosine; WT: Wild type; MUT: Mutant; Ago2: Argonaute 2; NORAD: Non-coding RNA activated by DNA damage.

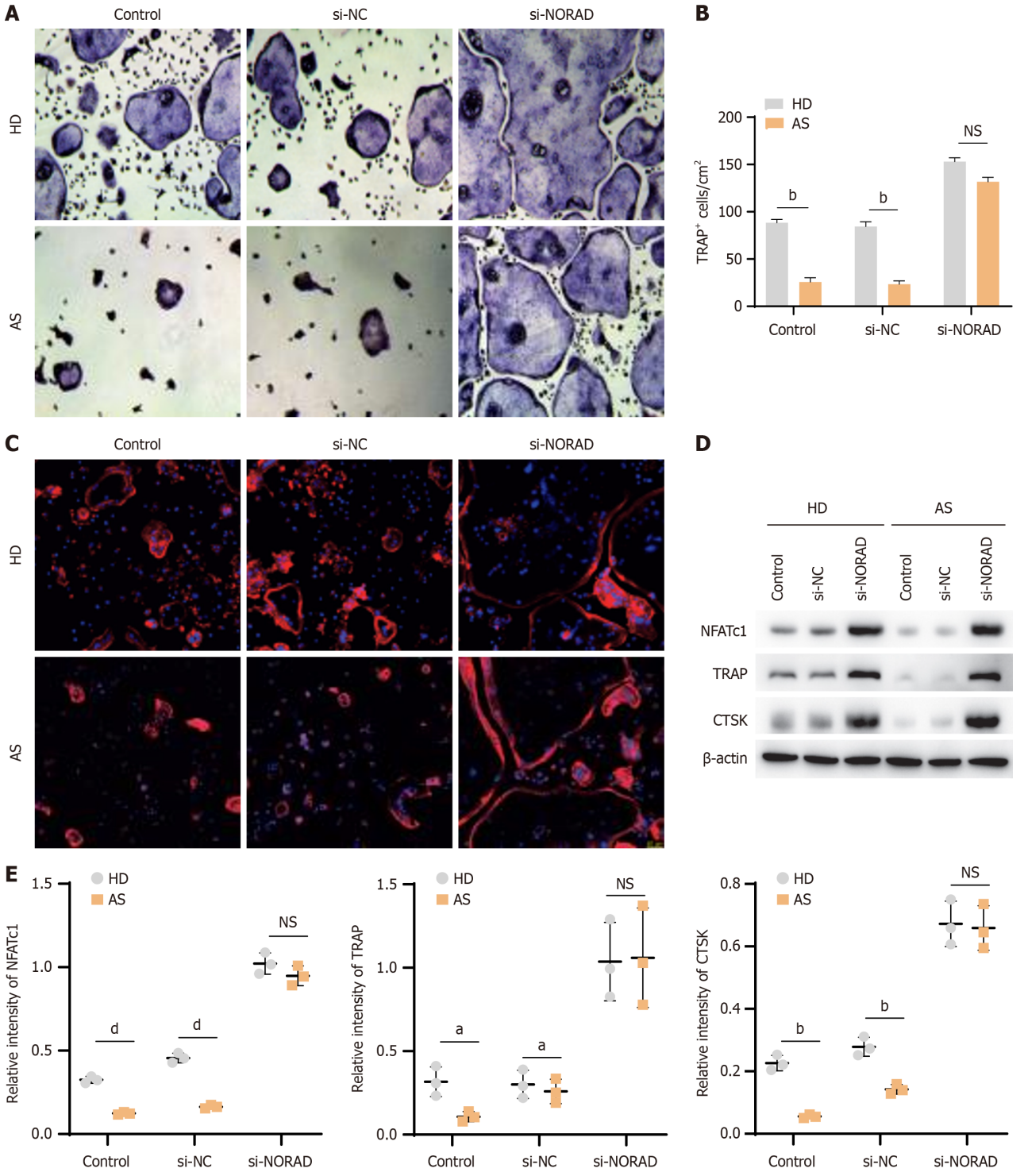

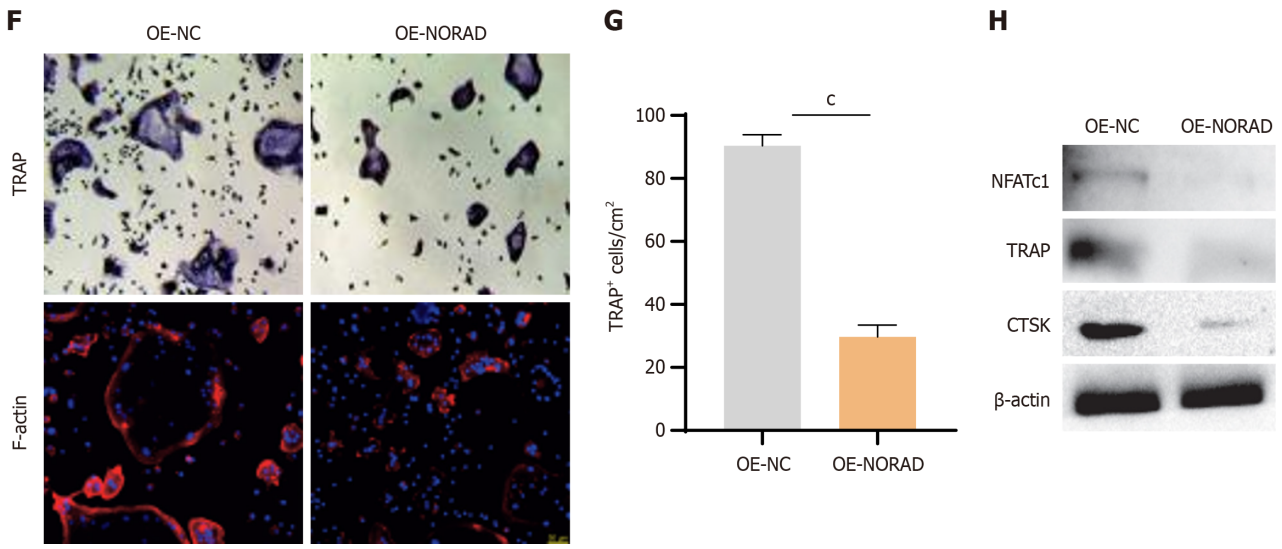

Figure 4 Long non-coding RNA activated by DNA damage in mesenchymal stem cells inhibits osteoclastogenesis. A: Representative images of tartrate resistant acid phosphatase (TRAP) staining of osteoclasts co-cultured with mesenchymal stem cells on day 9 after knocking down long non-coding RNA activated by DNA damage (× 100); B: Quantitative data of TRAP⁺ osteoclasts number in each well is shown; C: Representative images of osteoclasts stained with F-actin assays (× 200); D: Western blot analysis was performed to detect protein levels of nuclear factor of activated T cells 1 (NFATc1), TRAP, and cathepsin K (CTSK); E: Quantitative data for NFATc1, TRAP, and CTSK protein levels determined by western blot analyses are shown; F: Representative images of TRAP staining (× 100) and F-actin assays (× 200); G: Quantitative data of TRAP⁺ osteoclasts number in each well is shown; H: Western blot analysis was performed to detect protein levels of NFATc1, TRAP, and CTSK. The statistical data are presented as the means ± SDs; n = 3 in each group. NS: No significant difference; ^{a}P < 0.05, ^{b}P < 0.01, ^{c}P < 0.005, ^{d}P < 0.001. AS: Ankylosing spondylitis; HD: Healthy donors; si-NC: Small interfering RNA of negative control; TRAP: Tartrate resistant acid phosphatase; NFATc1: Nuclear factor of activated T cells 1; CTSK: Cathepsin K; OE-NC: Overexpression of negative control; OE-NORAD: Overexpression of Non-coding RNA activated by DNA damage.

differences in osteoclast differentiation marker expression between AS-MSCs and HD-MSCs (Figure 4D and E). To validate the impact of lnc NORAD on MSCs, we employed lentiviral vectors to increase the expression of lnc NORAD. TRAP, F-actin staining, and western blotting revealed that the overexpression of NORAD in MSCs resulted in decreased osteoclast formation (Figure 4F-H). These findings collectively suggest that the lncRNA NORAD in MSCs facilitates MSC-mediated osteoclast formation, indicating a potential regulatory role for the lncRNA NORAD in modulating osteoclast differentiation processes.

FTO in MSCs inhibits osteoclastogenesis through the lnc NORAD/miR-4284 axis

To further verify the effect of the FTO/lnc NORAD interaction in MSCs on osteoclast differentiation, we used siRNAs and lentiviruses to silence FTO while overexpressing NORAD in MSCs. The results of TRAP, F-actin staining, and western blotting demonstrated that overexpressing NORAD significantly attenuated the increased osteoclastogenesis induced by FTO knockdown (Figure 5A-D). Additionally, by downregulating NORAD and inhibiting miR-4284 in MSCs, we observed a marked reduction in osteoclastogenesis resulting from NORAD knockdown, as demonstrated by TRAP assays, F-actin staining, and western blotting (Figure 5E-H). Taken together, these results suggest that FTO positively regulates osteoclast differentiation in MSCs through the NORAD/miR-4284 pathway.

Targeting FTO alleviates enthesitis-related new bone formation in AS animal models

To assess the effect of FTO knockdown *in vivo*, we established an AS animal model by administering 3 mg of curdlan *via* intraperitoneal injection to SKG mice to induce AS features. We subsequently administered Av-shFTO *via* intravenous tail vein injection. Our findings revealed that the suppression of FTO markedly reduced the degree of enthesopathy, as well as the size and thickness of inflamed ankles. These results suggest that FTO could be a potential target for the treatment of AS (Figure 6A).

DISCUSSION

In this study, we revealed notable upregulation of FTO in AS-MSCs compared with HD-MSCs. Inhibiting FTO diminished the suppressive effects of AS-MSCs on osteoclastogenesis by influencing the stability of the lncRNA NORAD, which subsequently targeted miR-4284 (Figure 6B). This investigation examined the FTO/lnc NORAD/miR-4284 axis to understand the pathological osteogenesis associated with AS.

Pathologic osteogenesis is a significant concern in AS, as it can lead to the development of spinal ankylosis in severe cases, posing a serious threat to their lives[15]. The balance between osteoblasts (bone-forming cells) and osteoclasts (bone-resorbing cells) is crucial for bone homeostasis and remodelling. Dysfunction or abnormal regulation of these cell types can contribute to various bone diseases, potentially leading to abnormal osteogenesis in conditions such as AS[16].

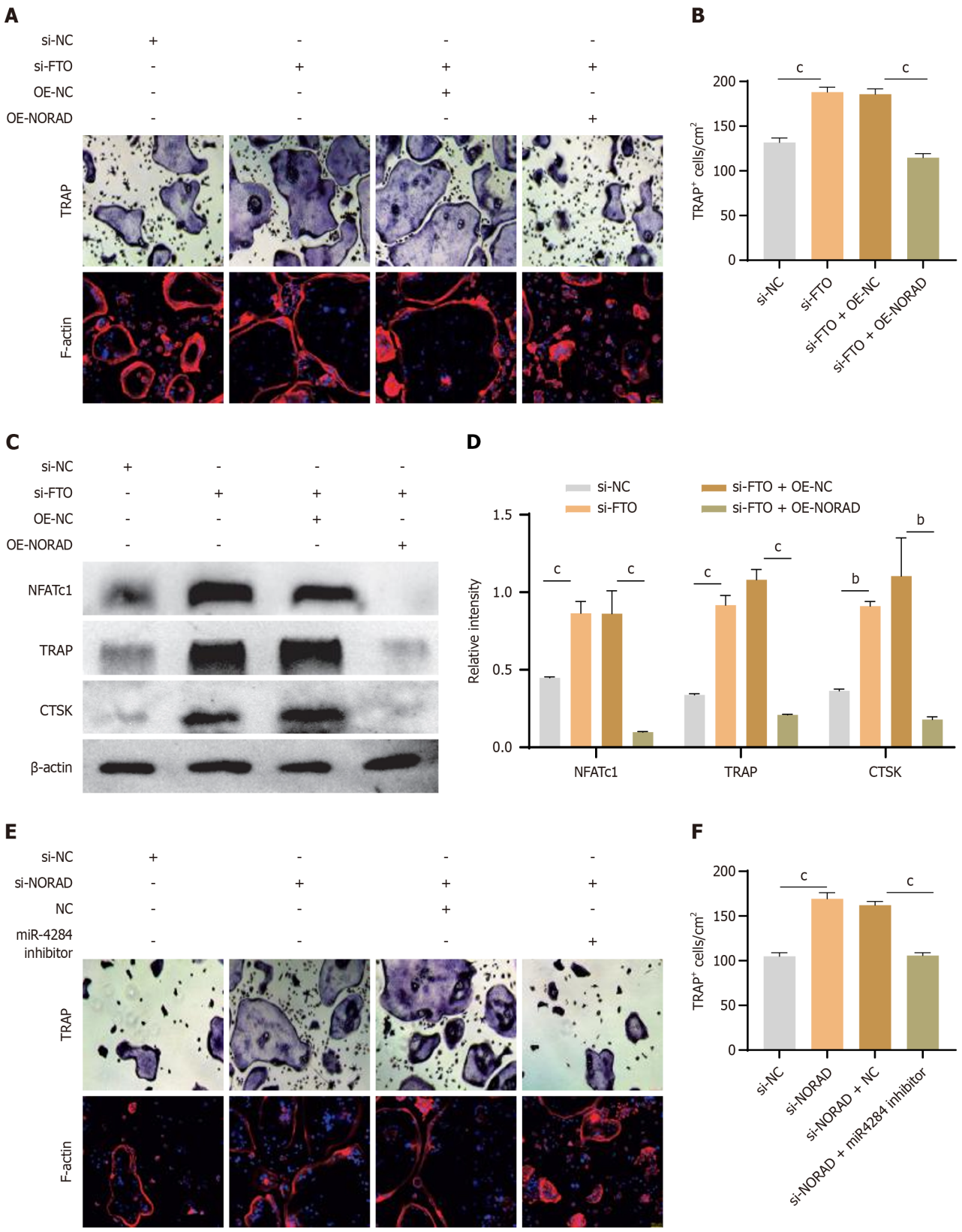
A
si-NC
si-FTO
OE-NC
OE-NORAD
TRAP
F-actin
B
TRAP+ cells/cm2
si-NC
si-FTO
si-FTO + OE-NC
si-FTO + OE-NORAD
C
NFATc1
TRAP
CTSK
β-actin
D
Relative intensity
NFATc1
TRAP
CTSK
E
si-NORAD
NC
miR-4284 inhibitor
F
si-NORAD + NC
si-NORAD + miR4284 inhibitor

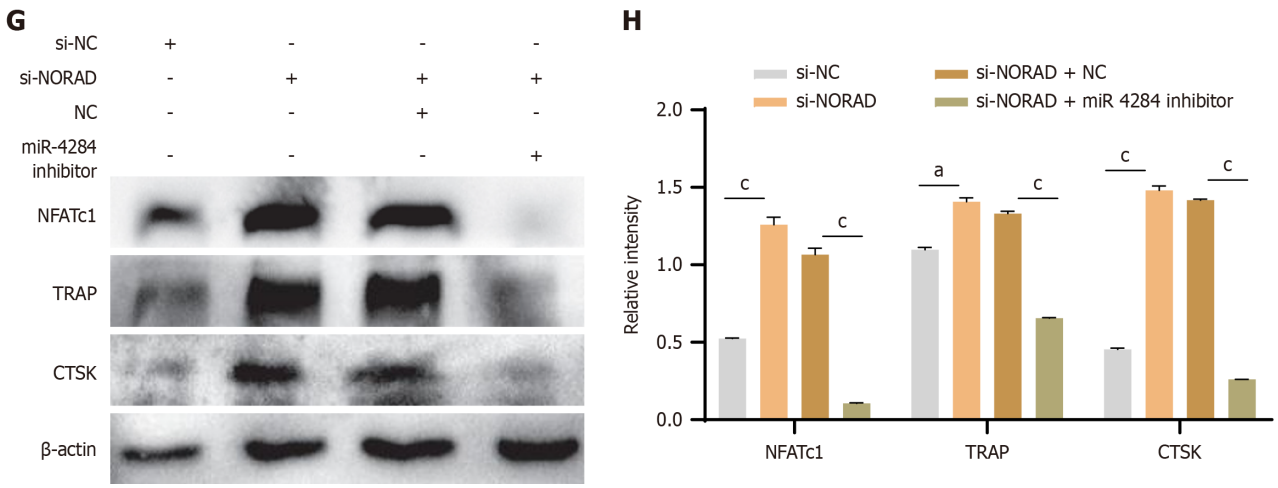

Figure 5 Fat mass and obesity-associated in mesenchymal stem cells inhibits osteoclastogenesis through the long non-coding RNA activated by DNA damage/miR-4284 axis. A: Representative images of tartrate resistant acid phosphatase (TRAP) staining (× 100) and F-actin assays (× 200); B: Quantitative data of TRAP⁺ osteoclasts number in each well is shown; C: Western blot analysis was performed to detect protein levels of nuclear factor of activated T cells 1 (NFATc1), TRAP, and cathepsin K (CTSK); D: Quantitative data for NFATc1, TRAP, and CTSK protein levels determined by western blot analyses are shown; E: Representative images of TRAP staining (× 100) and F-actin assays (× 200); F: Quantitative data of TRAP⁺ osteoclasts number in each well is shown; G: Western blot analysis was performed to detect protein levels of NFATc1, TRAP, and CTSK; H: Quantitative data for NFATc1, TRAP, and CTSK protein levels determined by western blot analyses are shown. The statistical data are presented as the means ± SDs; n = 3 in each group. $^{a}P < 0.05$, $^{b}P < 0.01$, $^{c}P < 0.005$, $^{d}P < 0.001$. si-NC: Small interfering RNA of negative control; si-FTO: Small interfering RNA targeting fat mass and obesity-associated; OE-NC: Overexpression of negative control; OE-FTO: Overexpression of fat mass and obesity-associated; TRAP: Tartrate resistant acid phosphatase; NFATc1: Nuclear factor of activated T cells 1; CTSK: Cathepsin K; NORAD: Non-coding RNA activated by DNA damage.

Previous research has indicated that, compared with HD-MSCs, AS-MSCs exhibit a greater capacity for osteogenic differentiation[5]. Additionally, AS-MSCs have been shown to more effectively inhibit osteoclastogenesis[6]. These findings suggest that AS-MSCs may play a crucial role in the pathologic osteogenesis observed in AS. By demonstrating the enhanced osteogenic potential and regulatory effects on osteoclastogenesis of AS-MSCs, this research provides valuable insights into the mechanisms underlying pathologic osteogenesis in AS. Understanding the unique properties of AS-MSCs in bone metabolism may offer new avenues for developing targeted therapies to address abnormal osteogenesis and associated complications in AS patients.

m6A methylation is a crucial RNA modification that impacts the stability, splicing, and translation of RNA molecules, playing a significant role in various biological processes such as cell differentiation, immune responses, and tumor development[17,18]. Studies have shown that m6A modification can influence the biological functions of MSCs. Research by Wu *et al*[19] revealed that conditional knockout of methyltransferase 3, an m6A methyltransferase, in MSCs could accelerate bone loss and modulate the differentiation potential of MSCs. Similarly, other m6A-related enzymes such as the demethylases FTO have been found to be essential for osteogenesis[20]. These findings underscore the importance of m6A modification in regulating MSC function. In this study, we found that the expression of FTO was elevated in AS-MSCs. Furthermore, silencing FTO in both HD-MSCs and AS-MSCs promoted osteoclastogenesis *in vitro* when MSCs were co-cultured with monocytes. These results suggest that the upregulation of FTO in AS-MSCs may contribute to the abnormal osteogenesis observed in AS. However, further research is needed to fully understand the role of FTO in AS-MSCs, particularly in an *in vivo* setting.

The interaction between lncRNAs and microRNAs, which act as molecular sponges is a well-established mechanism for regulating gene expression[21]. Building upon previous research that identified miR-4284 as a key molecule enhancing the ability of AS-MSCs to inhibit osteoclastogenesis, this study aimed to explore the potential role of lncRNAs in mediating the relationship between FTO, miR-4284, and osteoclastogenesis. In this study, global profiling of lncRNA expression in FTO-silenced MSCs revealed lnc NORAD as a crucial link connecting FTO and miR-4284. Further investigations demonstrated that FTO could stabilize lnc NORAD by removing m6A methylation, and in turn, lnc NORAD acted as a sponge to negatively regulate the activity of miR-4284. Importantly, interference with lnc NORAD was found to increase osteoclastogenesis in coculture assays, suggesting that lnc NORAD may contribute to the inhibited osteoclastogenesis exhibited by AS-MSCs. These findings shed light on a potential regulatory axis involving FTO, lnc NORAD, miR-4284, and osteoclastogenesis in the context of AS-MSCs. By elucidating the intricate interplay between these molecules, this study provides valuable insights into the molecular mechanisms underlying the altered osteoclastogenesis observed in AS. Targeting this regulatory network involving lncRNAs, microRNAs, and m6A-modifying enzymes like FTO may offer novel therapeutic strategies for managing bone-related complications in AS.

Indeed, lnc NORAD, which was originally identified as a regulator of genome integrity in response to DNA damage [22-24], has been implicated in various human cancers as an oncogene[25,26]. It has been shown to play a role in manipulating cancer cell development[27,28]. Interestingly, NORAD has also been found to undergo m6A modification, and Li *et al*[14] reported that the m6A modification of NORAD by WTAP negatively regulates its stability, which aligns with our findings. While recent studies have primarily focused on the role of NORAD as a competitive endogenous RNA that

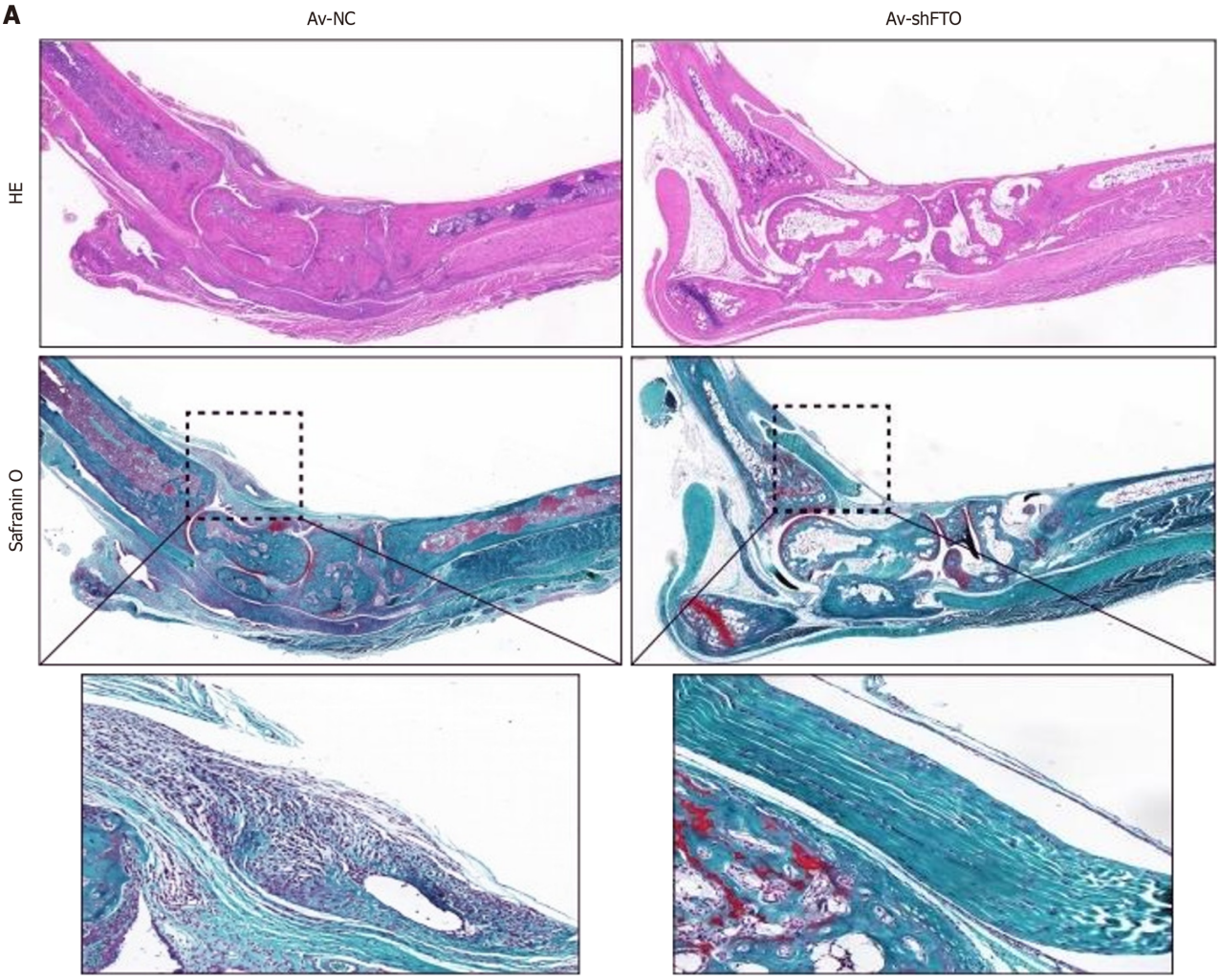

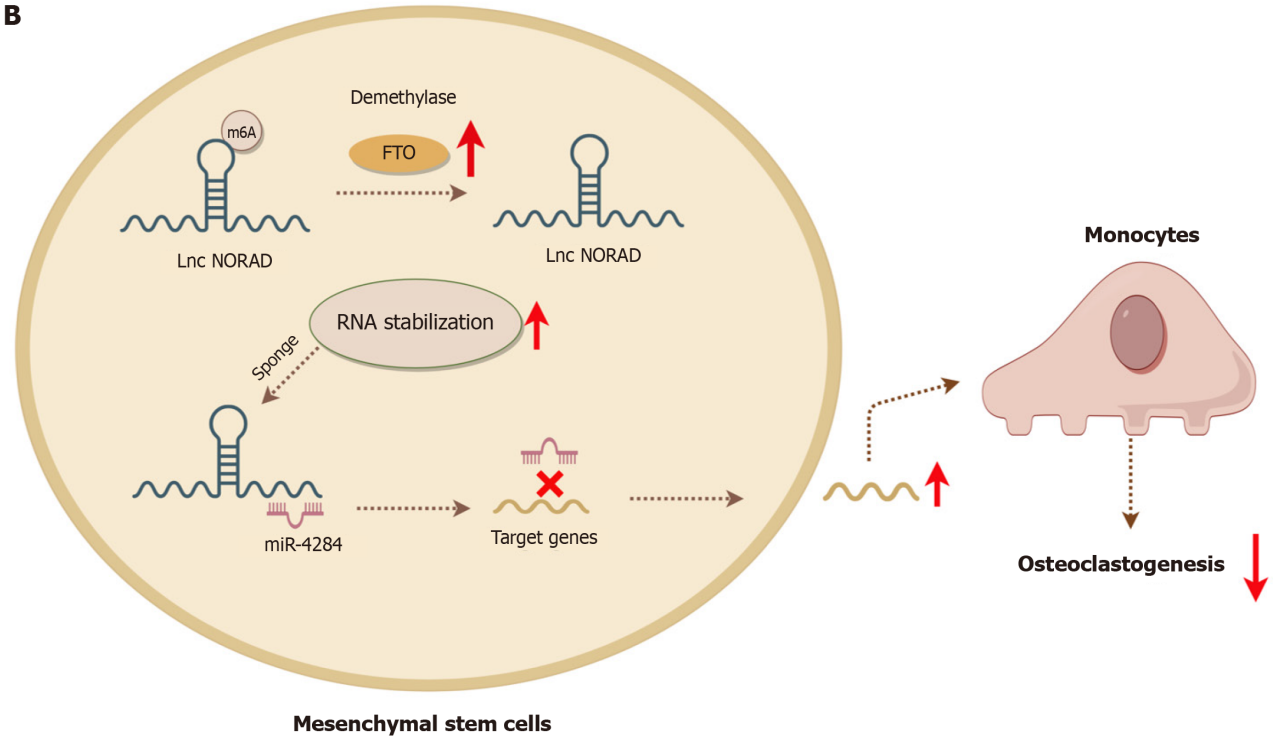

Figure 6 Targeting fat mass and obesity-associated alleviates enthesitis-related new bone formation in ankylosing spondylitis animal models. A: Histological analysis of bone formation in the enthesis was performed using hematoxylin and eosin (HE) staining and Safranin O. Scale bar = 500 μm

(upper) or 250 μm (lower) (n = 5); B: The proposed model shows upregulation of fat mass and obesity-associated in mesenchymal stem cells leads to defects in osteoclastogenesis in ankylosing spondylitis *via* the long non-coding RNA activated by DNA damage/miR-4284 axis. HE: Hematoxylin and eosin; FTO: Fat mass and obesity-associated; Av-NC: Adeno-associated virus of negative control; Av-shFTO: Adeno-associated virus of short hairpin RNA targeting fat mass and obesity-associated; NORAD: Non-coding RNA activated by DNA damage.

regulates downstream microRNA and mRNA expression[29-31], the specific mechanism through which NORAD targets miR-4284 in the context of AS-MSCs remains unclear in this study. However, whether other target molecular of NORAD mediate the function of FTO-NORAD axis in AS-MSCs remains unknown and broader insights into this process should be further investigated.

CONCLUSION

In this work, we focused on the role of m6A modification in the enhanced inhibition of osteoclastogenesis by AS-MSCs. Our results revealed that FTO regulated the function of AS-MSCs through the NORAD/miR-4284 axis, which may contribute to elucidating the mechanism of pathological osteogenesis and provide potential treatment targets for AS.

FOOTNOTES

Author contributions: Liu WJ and Wang JX conducted the experiments and investigation and contributed equally to this work as co-first authors. Liu WJ, Wang JX, and Li QF contributed to the conceptualization and methodology of this study; Ji PF, Jin JH, Zhang YB, and Yuan ZH were involved in the data curation and analysis of this manuscript; Liu WJ and Li QF wrote the original draft; Zhang YH and Feng P participated in the writing - review & editing; Wu YF, Shen HY, and Wang P were involved in the resources and supervision and funding acquisition. Shen HY and Wang P designed the research and approved the final version of the manuscript as co-corresponding authors of this manuscript.

Supported by Guangdong Provincial Clinical Research Center for Orthopedic Diseases, No. 2023B110001; the Excellent Medical Innovation Talent Program of the Eighth Affiliated Hospital of Sun Yat-sen University, No. YXYXCXRC202101; the National Natural Science Foundation of China, No. 82172349, No. 82372372, No. 22105229, No. 32170708, No. 82102530, No. 82102541, No. 82103098, No. 82103909, No. 82104182, No. 82104350, No. 82170427, No. 82171291, No. 82172215, No. 82172385, and No. 82302661; Guangdong Natural Science Foundation, No. 2023A1515010568 and No. 2021A1515111057; Shenzhen Science and Technology Program, No. JCYJ20220530144201004 and No. RCBS20210609104445097; and Futian Healthcare Research Project, No. FTWS2022022, No. FTWS2021013, No. FTWS2023072, and No. FTWS2022047.

Institutional review board statement: The collection of human specimens and the experiments with human specimens were approved by the Ethics Committee of the Eighth Affiliated Hospital, Sun Yat-sen University. The approval numbers for handling human subjects were 2021r171.

Institutional animal care and use committee statement: The animal experimentation protocols received approval from the Ethics Committee of the Eighth Affiliated Hospital, Sun Yat-Sen University. The assigned approval number for the experiments was SYSU-IACUC-2022-001060.

Conflict-of-interest statement: All the authors report no relevant conflicts of interest for this article.

Data sharing statement: All data findings are provided in this study, and raw data can be requested from the corresponding author upon reasonable request.

ARRIVE guidelines statement: The authors have read the ARRIVE guidelines, and the manuscript was prepared and revised according to the ARRIVE guidelines.

Country of origin: China

ORCID number: Yan-Feng Wu 0000-0001-8563-3795; Hui-Yong Shen 0000-0002-4317-3468; Peng Wang 0000-0003-2807-3909.

S-Editor: Wang JJ
L-Editor: A
P-Editor: Zheng XM

REFERENCES

1 **Sieper J**, Poddubnyy D. Axial spondyloarthritis. *Lancet* 2017; **390**: 73-84 [PMID: 28110981 DOI: 10.1016/S0140-6736(16)31591-4]

2 **Ritchlin C**, Adamopoulos IE. Axial spondyloarthritis: new advances in diagnosis and management. *BMJ* 2021; **372**: m4447 [PMID: 33397652 DOI: 10.1136/bmj.m4447]

3 **Sieper J**. How to define remission in ankylosing spondylitis? *Ann Rheum Dis* 2012; **71** Suppl 2: i93-i95 [PMID: 22460148 DOI: 10.1136/annrheumdis-2011-200798]

4 **Yue R**, Zhou BO, Shimada IS, Zhao Z, Morrison SJ. Leptin Receptor Promotes Adipogenesis and Reduces Osteogenesis by Regulating Mesenchymal Stromal Cells in Adult Bone Marrow. *Cell Stem Cell* 2016; **18**: 782-796 [PMID: 27053299 DOI: 10.1016/j.stem.2016.02.015]

5 **Xie Z**, Wang P, Li Y, Deng W, Zhang X, Su H, Li D, Wu Y, Shen H. Imbalance Between Bone Morphogenetic Protein 2 and Noggin Induces Abnormal Osteogenic Differentiation of Mesenchymal Stem Cells in Ankylosing Spondylitis. *Arthritis Rheumatol* 2016; **68**: 430-440 [PMID: 26413886 DOI: 10.1002/art.39433]

6 **Liu W**, Wang P, Xie Z, Wang S, Ma M, Li J, Li M, Cen S, Tang S, Zheng G, Ye G, Wu X, Wu Y, Shen H. Abnormal inhibition of osteoclastogenesis by mesenchymal stem cells through the miR-4284/CXCL5 axis in ankylosing spondylitis. *Cell Death Dis* 2019; **10**: 188 [PMID: 30804325 DOI: 10.1038/s41419-019-1448-x]

7 **Huang H**, Weng H, Chen J. The Biogenesis and Precise Control of RNA m(6)A Methylation. *Trends Genet* 2020; **36**: 44-52 [PMID: 31810533 DOI: 10.1016/j.tig.2019.10.011]

8 **Chen X**, Hua W, Huang X, Chen Y, Zhang J, Li G. Regulatory Role of RNA N(6)-Methyladenosine Modification in Bone Biology and Osteoporosis. *Front Endocrinol (Lausanne)* 2019; **10**: 911 [PMID: 31998240 DOI: 10.3389/fendo.2019.00911]

9 **Xie Z**, Yu W, Zheng G, Li J, Cen S, Ye G, Li Z, Liu W, Li M, Lin J, Su Z, Che Y, Ye F, Wang P, Wu Y, Shen H. TNF-α-mediated m(6)A modification of ELMO1 triggers directional migration of mesenchymal stem cell in ankylosing spondylitis. *Nat Commun* 2021; **12**: 5373 [PMID: 34508078 DOI: 10.1038/s41467-021-25710-4]

10 **Kopp F**, Mendell JT. Functional Classification and Experimental Dissection of Long Noncoding RNAs. *Cell* 2018; **172**: 393-407 [PMID: 29373828 DOI: 10.1016/j.cell.2018.01.011]

11 **Iyer MK**, Niknafs YS, Malik R, Singhal U, Sahu A, Hosono Y, Barrette TR, Prensner JR, Evans JR, Zhao S, Poliakov A, Cao X, Dhanasekaran SM, Wu YM, Robinson DR, Beer DG, Feng FY, Iyer HK, Chinnaiyan AM. The landscape of long noncoding RNAs in the human transcriptome. *Nat Genet* 2015; **47**: 199-208 [PMID: 25599403 DOI: 10.1038/ng.3192]

12 **Beermann J**, Piccoli MT, Viereck J, Thum T. Non-coding RNAs in Development and Disease: Background, Mechanisms, and Therapeutic Approaches. *Physiol Rev* 2016; **96**: 1297-1325 [PMID: 27535639 DOI: 10.1152/physrev.00041.2015]

13 **Sun R**, Wang X, Sun X, Zhao B, Zhang X, Gong X, Wong SH, Chan MTV, Wu WKK. Emerging Roles of Long Non-Coding RNAs in Ankylosing Spondylitis. *Front Immunol* 2022; **13**: 790924 [PMID: 35222376 DOI: 10.3389/fimmu.2022.790924]

14 **Li G**, Ma L, He S, Luo R, Wang B, Zhang W, Song Y, Liao Z, Ke W, Xiang Q, Feng X, Wu X, Zhang Y, Wang K, Yang C. WTAP-mediated m(6)A modification of lncRNA NORAD promotes intervertebral disc degeneration. *Nat Commun* 2022; **13**: 1469 [PMID: 35304463 DOI: 10.1038/s41467-022-28990-6]

15 **Braun J**, Sieper J. Ankylosing spondylitis. *Lancet* 2007; **369**: 1379-1390 [PMID: 17448825 DOI: 10.1016/S0140-6736(07)60635-7]

16 **Rosen CJ**. Bone remodeling, energy metabolism, and the molecular clock. *Cell Metab* 2008; **7**: 7-10 [PMID: 18177720 DOI: 10.1016/j.cmet.2007.12.004]

17 **Oerum S**, Meynier V, Catala M, Tisné C. A comprehensive review of m6A/m6Am RNA methyltransferase structures. *Nucleic Acids Res* 2021; **49**: 7239-7255 [PMID: 34023900 DOI: 10.1093/nar/gkab378]

18 **Sendinc E**, Shi Y. RNA m6A methylation across the transcriptome. *Mol Cell* 2023; **83**: 428-441 [PMID: 36736310 DOI: 10.1016/j.molcel.2023.01.006]

19 **Wu Y**, Xie L, Wang M, Xiong Q, Guo Y, Liang Y, Li J, Sheng R, Deng P, Wang Y, Zheng R, Jiang Y, Ye L, Chen Q, Zhou X, Lin S, Yuan Q. Mettl3-mediated m(6)A RNA methylation regulates the fate of bone marrow mesenchymal stem cells and osteoporosis. *Nat Commun* 2018; **9**: 4772 [PMID: 30429466 DOI: 10.1038/s41467-018-06898-4]

20 **Zhang Q**, Riddle RC, Yang Q, Rosen CR, Guttridge DC, Dirckx N, Faugere MC, Farber CR, Clemens TL. The RNA demethylase FTO is required for maintenance of bone mass and functions to protect osteoblasts from genotoxic damage. *Proc Natl Acad Sci U S A* 2019; **116**: 17980-17989 [PMID: 31434789 DOI: 10.1073/pnas.1905489116]

21 **Ghafouri-Fard S**, Abak A, Tavakkoli Avval S, Rahmani S, Shoorei H, Taheri M, Samadian M. Contribution of miRNAs and lncRNAs in osteogenesis and related disorders. *Biomed Pharmacother* 2021; **142**: 111942 [PMID: 34311172 DOI: 10.1016/j.biopha.2021.111942]

22 **Lee S**, Kopp F, Chang TC, Sataluri A, Chen B, Sivakumar S, Yu H, Xie Y, Mendell JT. Noncoding RNA NORAD Regulates Genomic Stability by Sequestering PUMILIO Proteins. *Cell* 2016; **164**: 69-80 [PMID: 26724866 DOI: 10.1016/j.cell.2015.12.017]

23 **Munschauer M**, Nguyen CT, Sirokman K, Hartigan CR, Hogstrom L, Engreitz JM, Ulirsch JC, Fulco CP, Subramanian V, Chen J, Schenone M, Guttman M, Carr SA, Lander ES. The NORAD lncRNA assembles a topoisomerase complex critical for genome stability. *Nature* 2018; **561**: 132-136 [PMID: 30150775 DOI: 10.1038/s41586-018-0453-z]

24 **Ventura A**. NORAD: Defender of the Genome. *Trends Genet* 2016; **32**: 390-392 [PMID: 27157388 DOI: 10.1016/j.tig.2016.04.002]

25 **Soghli N**, Yousefi T, Abolghasemi M, Qujeq D. NORAD, a critical long non-coding RNA in human cancers. *Life Sci* 2021; **264**: 118665 [PMID: 33127516 DOI: 10.1016/j.lfs.2020.118665]

26 **Yang Z**, Zhao Y, Lin G, Zhou X, Jiang X, Zhao H. Noncoding RNA activated by DNA damage (NORAD): Biologic function and mechanisms in human cancers. *Clin Chim Acta* 2019; **489**: 5-9 [PMID: 30468715 DOI: 10.1016/j.cca.2018.11.025]

27 **Han T**, Wu Y, Hu X, Chen Y, Jia W, He Q, Bian Y, Wang M, Guo X, Kang J, Wan X. NORAD orchestrates endometrial cancer progression by sequestering FUBP1 nuclear localization to promote cell apoptosis. *Cell Death Dis* 2020; **11**: 473 [PMID: 32555178 DOI: 10.1038/s41419-020-2674-y]

28 **Sun Y**, Wang J, Ma Y, Li J, Sun X, Zhao X, Shi X, Hu Y, Qu F, Zhang X. Radiation induces NORAD expression to promote ESCC radiotherapy resistance *via* EEPD1/ATR/Chk1 signalling and by inhibiting pri-miR-199a1 processing and the exosomal transfer of miR-199a-5p. *J Exp Clin Cancer Res* 2021; **40**: 306 [PMID: 34587992 DOI: 10.1186/s13046-021-02084-5]

29 **Jia Y**, Tian C, Wang H, Yu F, Lv W, Duan Y, Cheng Z, Wang X, Wang Y, Liu T, Wang J, Liu L. Long non-coding RNA NORAD/miR-224-3p/MTDH axis contributes to CDDP resistance of esophageal squamous cell carcinoma by promoting nuclear accumulation of β-catenin. *Mol Cancer* 2021; **20**: 162 [PMID: 34893064 DOI: 10.1186/s12943-021-01455-y]

30 **Argoetti A**, Shalev D, Polyak G, Shima N, Biran H, Lahav T, Hashimshony T, Mandel-Gutfreund Y. lncRNA NORAD modulates STAT3/STAT1 balance and innate immune responses in human cells *via* interaction with STAT3. *Nat Commun* 2025; **16**: 571 [PMID: 39794357 DOI: 10.1038/s41467-025-55822-0]

31 **Zhang X**, Chen T, Li Z, Wan L, Zhou Z, Xu Y, Yan D, Zhao W, Chen H. NORAD exacerbates metabolic dysfunction-associated steatotic liver disease development *via* the miR-511-3p/Rock2 axis and inhibits ubiquitin-mediated degradation of ROCK2. *Metabolism* 2025; **164**: 156111 [PMID: 39710000 DOI: 10.1016/j.metabol.2024.156111]

World Journal of Stem Cells

Submit a Manuscript: https://www.f6publishing.com

World J Stem Cells 2025 March 26; 17(3): 99472

DOI: 10.4252/wjsc.v17.i3.99472

ISSN 1948-0210 (online)

ORIGINAL ARTICLE

Basic Study

DNA methyltransferase 1/miR-342-3p/Forkhead box M1 signaling axis promotes self-renewal in cervical cancer stem-like cells *in vitro* and nude mice models

Xiao-Zheng Cao, Yao-Feng Zhang, Yu-Wei Song, Lei Yuan, Hui-Li Tang, Jin-Yuan Li, Ye-Bei Qiu, Jia-Zhi Lin, Ying-Xia Ning, Xiao-Yu Wang, Yong Xu, Shao-Qiang Lin

Specialty type: Cell and tissue engineering

Provenance and peer review: Unsolicited article; Externally peer reviewed.

Peer-review model: Single blind

Peer-review report's classification
Scientific Quality: Grade B, Grade C
Novelty: Grade B
Creativity or Innovation: Grade B
Scientific Significance: Grade A

P-Reviewer: Li SC; Tamizh Selvan G

Received: July 29, 2024
Revised: October 24, 2024
Accepted: January 2, 2025
Published online: March 26, 2025
Processing time: 234 Days and 22.8 Hours

Xiao-Zheng Cao, Lei Yuan, Shao-Qiang Lin, Guangdong Provincial Engineering Research Center for Esophageal Cancer Precise Therapy, The First Affiliated Hospital of Guangdong Pharmaceutical University, Guangzhou 510062, Guangdong Province, China

Xiao-Zheng Cao, Yong Xu, Institute of Drug Discovery, Guangzhou Institutes of Biomedicine and Health, Chinese Academy of Sciences, Guangzhou 510530, Guangdong Province, China

Yao-Feng Zhang, School of Pharmacy, Guangdong Pharmaceutical University, Guangzhou 510006, Guangdong Province, China

Yu-Wei Song, Central Laboratory, The First Affiliated Hospital of Jinan University, Guangzhou 510630, Guangdong Province, China

Hui-Li Tang, Xiao-Yu Wang, Shao-Qiang Lin, Central Laboratory, The Affiliated Shunde Hospital of Jinan University, Foshan 528000, Guangdong Province, China

Jin-Yuan Li, Department of Pelvic Radiotherapy, Meizhou People's Hospital, Meizhou 514030, Guangdong Province, China

Ye-Bei Qiu, Department of Oncology, The First Affiliated Hospital of Jinan University, Guangzhou 510630, Guangdong Province, China

Jia-Zhi Lin, Ying-Xia Ning, Department of Gynaecology and Obstetrics, The First Affiliated Hospital of Guangzhou Medical University, Guangzhou 510000, Guangdong Province, China

Co-corresponding authors: Yong Xu and Shao-Qiang Lin.

Corresponding author: Shao-Qiang Lin, MD, PhD, Guangdong Provincial Engineering Research Center for Esophageal Cancer Precise Therapy, The First Affiliated Hospital of Guangdong Pharmaceutical University, No. 19 Nonglinxia Road, Guangzhou 510062, Guangdong Province, China. sqlin123@163.com

Abstract

BACKGROUND

Cervical cancer (CC) stem cell-like cells (CCSLCs), defined by the capacity of

differentiation and self-renewal and proliferation, play a significant role in the progression of CC. However, the molecular mechanisms regulating their self-renewal are poorly understood. Therefore, elucidation of the epigenetic mechanisms that drive cancer stem cell self-renewal will enhance our ability to improve the effectiveness of targeted therapies for cancer stem cells.

AIM

To explore how DNA methyltransferase 1 (DNMT1)/miR-342-3p/Forkhead box M1 (FoxM1), which have been shown to have abnormal expression in CCSLCs, and their signaling pathways could stimulate self-renewal-related stemness in CCSLCs.

METHODS

Sphere-forming cells derived from CC cell lines HeLa, SiHa and CaSki served as CCSLCs. Self-renewal-related stemness was identified by determining sphere and colony formation efficiency, CD133 and CD49f protein level, and SRY-box transcription factor 2 and octamer-binding transcription factor 4 mRNA level. The microRNA expression profiles between HeLa cells and HeLa-derived CCSLCs or mRNA expression profiles that HeLa-derived CCSLCs were transfected with or without miR-342-3p mimic were compared using quantitative PCR analysis. The expression levels of *DNMT1* mRNA, miR-342-3p, and FoxM1 protein were examined by quantitative real-time PCR and western blotting. *In vivo* carcinogenicity was assessed using a mouse xenograft model. The functional effects of the DNMT1/miR-342-3p/FoxM1 axis were examined by *in vivo* and *in vitro* gain-of-activity and loss-of-activity assessments. Interplay among DNMT1, miR-342-3p, and FoxM1 was tested by methylation-specific PCR and a respective luciferase reporter assay.

RESULTS

CCSLCs derived from the established HeLa cell lines displayed higher self-renewal-related stemness, including enhanced sphere and colony formation efficiency, increased CD133 and CD49f protein level, and heightened transcriptional quantity of stemness-related factors SRY-box transcription factor 2 and octamer-binding transcription factor 4 *in vitro* as well as a stronger tumorigenic potential *in vivo* compared to their parental cells. Moreover, quantitative PCR showed that the *miR-342-3p* level was downregulated in HeLa-derived CCSLCs compared to HeLa cells. Its mimic significantly decreased *DNMT1* and *FoxM1* mRNA expression levels in CCSLCs. Knockdown of *DNMT1* or *miR-342-3p* mimic transfection suppressed *DNMT1* expression, increased *miR-342-3p* quantity by promoter demethylation, and inhibited CCSLC self-renewal. Inhibition of FoxM1 by shRNA transfection also resulted in the attenuation of CCSLC self-renewal but had little effect on the DNMT1 activity and miR-342-3p expression. Furthermore, the loss of CCSLC self-renewal exerted by miR-342-3p mimic was inverted by the overexpression of DNMT1 or FoxM1. Furthermore, DNMT1 and FoxM1 were recognized as straight targets by miR-342-3p in HeLa-derived CCSLCs.

CONCLUSION

Our findings suggested that a novel DNMT1/miR-342-3p/FoxM1 signal axis promotes CCSLC self-renewal and presented a potential target for the treatment of CC through suppression of CCSLC self-renewal. However, this pathway has been previously implicated in CC, as evidenced by prior studies showing miR-342-3p-mediated downregulation of FoxM1 in cervical cancer cells. Additionally, research on liver cancer further supports the involvement of miR-342-3p in suppressing FoxM1 expression. While our study contributed to this body of knowledge, we did not present a completely novel axis but reinforced the therapeutic potential of targeting the DNMT1/miR-342-3p/FoxM1 axis to suppress CCSLC self-renewal in CC treatment.

Key Words: DNA methyltransferase 1; Cancer stem cell; Cervical cancer; MiR-342-3p; Forkhead box M1

Core Tip: The study revealed a novel DNA methyltransferase 1 (DNMT1)/miR-342-3p/Forkhead box M1 (FoxM1) signaling axis that enhances self-renewal of cervical cancer stem cell-like cells (CCSLCs). Knockdown of DNMT1 or miR-342-3p elevation inhibits CCSLC self-renewal, while FoxM1 suppression also attenuates this process. Overexpression of DNMT1 or FoxM1 reverses the effects of miR-342-3p mimic. This signaling pathway presents a potential therapeutic target for inhibiting CCSLC self-renewal in cervical cancer, offering new insights for targeted treatment strategies.

Citation: Cao XZ, Zhang YF, Song YW, Yuan L, Tang HL, Li JY, Qiu YB, Lin JZ, Ning YX, Wang XY, Xu Y, Lin SQ. DNA methyltransferase 1/miR-342-3p/Forkhead box M1 signaling axis promotes self-renewal in cervical cancer stem-like cells *in vitro* and nude mice models. *World J Stem Cells* 2025; 17(3): 99472
URL: https://www.wjgnet.com/1948-0210/full/v17/i3/99472.htm
DOI: https://dx.doi.org/10.4252/wjsc.v17.i3.99472

INTRODUCTION

Cervical cancer (CC) is the fourth most common cancer in the world, representing a severe burden for females in underdeveloped nations[1,2]. Individuals with developed CC are frequently deprived of an operation choice and show poor outcomes after radiation treatment and chemotherapy. In this context, the 5-year survival rate for those with far-off metastasis reaches only 17.1%[3]. In the last decades, much attention has been paid to the cancer stem cell (CSC) hypothesis, which claims that an uncommon type of stem cell-like tumor cell is accountable for tumor progression, resistance, and recurrence[4]. According to this hypothesis, cancer stem-like cells derived from CC (CCSLCs) are a major cause of poor prognosis due to their high potential for inducing tumor formation and progression[5,6]. However, the mechanism that drives the initiation and progression of human CC is not fully understood.

Endogenous noncoding single-stranded RNAs, known as microRNAs (miRNAs), control 30% of the human genes through their union to the 3′-untranslated regions (3′-UTRs) of the miRNAs of interest[7]. In fact, some of the miRNA-based cancer therapeutic strategies have shown promising results even in early-phase human clinical trials[8]. In particular, abnormal miR-342-3p expression has significant associations with progression, proliferation, invasion, and even metastasis in a variety of tumors[9,10]. On the other hand, miR-342-3p reduces the proliferative, migratory, and invasive features of CC cells[11]. In this regard, Tao *et al*[12] demonstrated that determining the miR-342-3p expression profile might improve disease prognosis and help in decision-making during treatments for colon cancer. However, whether miR-342-3p promotes and maintains CCSLC self-renewal is still unclear.

Epigenetic regulation can promote oncogenes and/or suppress genes that prevent tumor growth, which have an important part in carcinogenesis, progress, invasion, and metastasis[13]. The epigenetic mechanism mainly includes DNA methylation, histone DNA methylation and deacetylation, non-coding RNA regulation, and crosstalk[14]. The main function of DNA methyltransferase 1 (DNMT1) is methylation of DNA[15]. Many reports have indicated that DNMT1 is deeply connected to the incidence and expansion of a variety of tumors. For instance, DNMT1 is crucial for the conservation of breast stem/progenitor cells and their CSCs[16]. The transactivation mechanism of the DNMT1 promoter reprograms the transcription factors octamer-binding transcription factor 4 (OCT4) and SRY-box transcription factor 2 (SOX2) to promote self-renewal of glioblastoma cells and leads to total DNA methylation and DNMT-dependent miRNAs downregulation[17].

Lee *et al*[18] found that suppressing DNMT1 expression had a relevant role in prostate cancer cells reversing the epithelial-mesenchymal transition and CSC phenotypes. Furthermore, Wang *et al*[19] showed that DNMT1 was inhibited by miR-342-3p, which signifies stronger proliferation and invasion in colorectal cancer cells. Nonetheless, further work is necessary to understand whether irregular DNMT1 expression leads to the downregulation of miR-342-3p and subsequent induction of CCSLC self-renewal *in vitro* and *in vivo*.

Forkhead box M1 (FoxM1) is necessary not only for cellular cycle advancement but also for apoptosis, angiogenesis, and DNA repair[20]. FoxM1 is significantly upregulated in several cancers, such as CC[21-23]. More importantly, FoxM1 has an important part in maintaining the CSC characteristics. Luo *et al*[23] found that in nasopharyngeal carcinoma tissues FoxM1 is associated with CSC-related clinicopathological characteristics (late clinical stage, tumor recurrence, and distant metastasis), and the expression of FoxM1 is also closely related to higher levels of the CSC markers Nanog, OCT4, and SOX2. It was also found that FoxM1 stimulates the proliferative, invasive, and stem cell characteristics of nasopharyngeal carcinoma cells[23].

However, more research is needed to evaluate how low miR-342-3p expression and subsequent FoxM1 overexpression in the context of the epigenetic regulation involved in DNMT1 could contribute to enriching CCSLCs and inducing CCSLC self-renewal in CC. In the present study, our objective was to evaluate the possibility that mutual adverse regulation between DNMT1 and miR-342-3p could induce CCSLC self-renewal by upregulating FoxM1 expression in CC cells.

MATERIALS AND METHODS

Cell culture

The cell types for the cultures were HeLa, SiHa, and CaSki, together with the control cervical epithelial cell line HcerEpiC from the Cell Bank of Chinese Academy of Sciences (Shanghai, China). For every culture, the medium of choice was Dulbecco's Modified Eagle's Medium (DMEM; Gibco, CA, United States), which included fetal bovine serum (10%; Gibco), in conditions of 37 °C, humidity, and 5% CO_2. To obtain sphere-forming cells (SFCs) of CC, DMEM/F12 including 2% B27, basic fibroblast growth factor (20 ng/mL), epidermal growth factor (20 ng/mL), insulin (4 μg/mL), penicillin G (100 IU/mL), and streptomycin (100 μg/mL) was used as described previously[24]. HeLa cell-derived SFCs were then analyzed as CCSLCs. The SFCs derived from SiHa and CaSki were considered as CCSLCs. All medium reagents were

obtained from Invitrogen (United States) except for the insulin (Sigma-Aldrich).

Real-time quantitative PCR

Trizol (Tiangen Biotech, China) was utilized to obtain total RNA from HeLa (1×10^6) or CCSLCs (1×10^6) cells. To extract total miRNA, we worked with the miRcute miRNA isolation Kit (Tiangen Biotech, China). For mRNA quantitation, transcription was performed on total RNA (2 μg) *via* the SureScript™ First-Strand cDNA Synthesis Kit (GeneCopoeia Inc., MD, United States). cDNA was replicated using the primers shown in Supplementary Table 1. The reaction entailed: Amplification at 95 °C (10 minutes); and 40 cycles at 95 °C (30 seconds), 55 °C (30 seconds), and 70 °C (30 seconds). To quantify miRNA, total miRNA (2 μg) underwent transcription and amplification through the All-in-One™ miRNA quantitative real-time PCR (qPCR) Detection Kit and the TaqMan MicroRNA Assay (Applied Biosystems, CA, United States), as suggested by the provider (GeneCopoeia Inc., MD, United States). U6 was considered the reference. For data analysis, the $2^{-\Delta\Delta Ct}$ method was conducted.

A qPCR array (including 29 miRNAs that changed by flavonoids reported and 3 internal label genes) was used to detect miRNA expression profiles in HeLa-derived CCSLCs and HeLa cells according to the manufacturer's protocol (Wcgene Biotech, Shanghai, China). Subsequently, the qPCR array (including 92 target genes associated with regulation of stem cell signaling that predicted using miRWalk network) was performed to compare in HeLa-derived CCSLCs transfected with miR-342-3p mimic or with miR-negative control (NC) according to the manufacturer's protocol (Wcgene Biotech, Shanghai, China). The data underwent analysis utilizing Wcgene Biotech software. MiRNAs or genes displaying fold changes greater than or less than 2.0 were considered to hold biological significance.

Methylation-specific PCR

DNA from HeLa (1×10^6) or CCSLCs (1×10^6) cells was obtained using the DNA-EZ Reagents V All-DNA-Out (Sangon Biotech, China). The incubation of genomic DNA was conducted with the Methylamp One-Step DNA Modification Kit (Epigentek), as recommended by the manufacturer. For PCR, the HotStar Taq Polymerase (Qiagen, Germany) was applied, together with methylated and unmethylated PCR primers targeting the miR-342-3p promoter (Sangon Biotech; Supplementary Table 2). For imaging of the methylation-specific PCR products, 2.0% agarose gel electrophoresis was used.

Western blot

HeLa (1×10^6) or SFCs (1×10^6) cells were lysed using cold RIPA buffer (Beyotime Biotechnology, China). Proteins (20 μg) were first quantified with the Bradford assay (Bio-Rad, CA, United States). Then, proteins were separated on a 10% sodium-dodecyl sulfate gel electrophoresis and electrotransferred onto polyvinylidene fluoride membranes (Millipore, MA, United States). The membranes were blocked (2 h, room temperature, 5% BSA in Tris-buffered saline with tween) before overnight incubation with primary antibodies against DNMT1 (1:1000), FOXM1 (1:1000), CD44 (1:1000), and β-actin (1:2000) at 4 °C. Cell Signaling (United States) provided all antibodies. Suitable HRP-conjugated secondary antibodies (Beyotime Biotechnology, China) were included in a further incubation of the membranes (1 h). For detection, the enhanced chemiluminescence kit (Amersham, TN, United States) was implemented.

Spheroid formation assay

HeLa, CaSki, and SiHa cells (1×10^3) or their CCSLCs (1×10^3) underwent a sphere generation culture for 6 days. To determine the sphere formation efficiency, we considered the number of spheres generated/cells seeded (1000 cells per well in a 24-well plate) × 100%. Independent triplicates were included.

Clonogenic assay

DMEM (0.8% agarose; Invitrogen, CA, United States) was first placed into 24-well plates (500 μL). Second, HeLa and SiHa cells and their CCSLCs (100 cells/well) were seeded in 24-well plates with CSC-M with 0.4% agarose (top layer) for a 3-week incubation. For colony counting, we employed an IX53 inverted microscope (Olympus, Japan). To know the colony formation efficiency (CFE), we considered the number of colonies generated/cells seeded (100 cells per well in a 24-well plate) × 100%. Independent triplicates were conducted.

Transfection

HeLa cells (1×10^5) or CCSLCs (1×10^5) were infected for 48 h with lentiviruses bearing DNMT1 shRNA or cDNA or RFP setups in a 6 μg/mL polybrene-complemented medium; afterwards, a second 48 h-culture was carried out. Puromycin (4 μg/mL) was used for the selection assay during the first 7 days, and additional cell supply was conducted with 1 μg/mL puromycin. Transfection of 50 nM micrON™ miR-342 mimic and 100 nM micrOFF™ miR-342 suppressor into HeLa or CCSCs cells was performed using the iboFECT™ CP Reagent, as instructed by the provider (RiboBio, Guangzhou, China). In parallel, the NC of miR-342-3p suppressor (anti-NC) and miR-342-3p mimic (miR-NC) were transfected as well. Cell incubation with small RNA complexes was carried out for 2 h prior to changing the medium. shRNA control (sh-NC) and FOXM1 (shFOXM1) were acquired from Santa Cruz Biotechnology. The respective sequences were shown in Supplementary material. In addition, pcDNA3.1 both control (pcDNA) and FOXM1 (pcDNA-FOXM1) were acquired from Invitrogen. For cell transfection, the opti-MEM Lipofectamine™ 2000 (Invitrogen, CA, United States) was employed as recommended by the provider.

Luciferase analysis

The 3′UTR target sequence of DNMT1 and FOXM1 [wildtype (WT)] that encompassed the ham-miR-342-3p binding spot was introduced into the pGL3 Luciferase vector (Ambion, TX, United States), as recommended by the provider. The control sample was a DNMT1 and FOXM1 3′UTR sequence with a mutation. The transfection of those arrangements (0.2 μg) into HeLa-derived CCSLCs was performed in 24-well microplates together with miR-342-3p or miR-NC using Lipofectamine 2000 (48 h). Finally, the dual luciferase reporter procedure (Promega) was conducted as recommended by the provider.

In vivo tumorigenicity assay

Nude mice of 4-5 weeks and 12-14 g (female, nude) were acquired from the Hunan SJA Laboratory Animal Co., Ltd. (certificate No: 43004700050992, China). The mice underwent adaptation for 1 week before assay initiation. Subcutaneous injections with HeLa cells (1×10^3, 1×10^4, 1×10^5) and HeLa-derived CCSLCs cells (1×10^2, 1×10^3, 1×10^4) were administered into the left flank and the right flank of the mice (n = 5/group) for the *in vivo* tumorigenicity assessment. The animals underwent sacrifice 1 month after the injection, and the weight of the xenografts was determined. Limiting dilutions were calculated using the Extreme Limiting Dilution Analysis software (http://bioinf.wehi.edu.au/software/elda/). The Ethics Committee of Hunan Normal University together with the Committee of Experimental Animal Feeding and Management approved all research assays (Permit No: 2020041).

To assess the *in vivo* functional impact of *DNMT1* and *FOXM1* genes on the xenograft expansion of CCSCs, the mice received subcutaneous inoculations (100 μL). HeLa-derived CCSLCs (1×10^5) were transduced with sh-NC, sh-DNMT1, or sh-FOXM1 in DMEM/F12 medium with no serum and matrigel (1:1; BD Biosciences). There were four mice in each group. To evaluate the impact of miR-342-3p on the xenograft expansion of CCSCs *in vivo*, the mice received subcutaneous inoculations (100 μL) with HeLa-derived CCSCs (1×10^5) in DMEM/F12 medium in the absence of matrigel and serum (1:1; BD Biosciences). When the xenografts extended to 50 mm^3, the agomiR-342 block received an intratumoral inoculation of micrON™ agomiR-342 (1 nmol) (RiboBio Co., China) in 10 μL of phosphate buffered saline one day a week in triplicate. Additionally, micrON™ agomir-NC served as control. In total, four mice were inoculated per group. Following sacrifice *via* CO_2 inhalation, the xenografts were acquired, measured, and snap-frozen using liquid nitrogen or fixed (10% formalin) for later experiments.

Immunohistochemistry

Immunohistochemistry was achieved through conventional procedures[24]. Target slides were incubated (4 °C, overnight) using the antibodies anti-DNMT1, FoxM1, and CD133 (all 1:200; Cell Signaling). As a NC, phosphate buffered saline replaced primary antibodies.

Cy3-miR-342-3p fluorescent in situ hybridization

The fluorescent *in situ* hybridization kit (Gene-Pharma, Shanghai, China) was implemented for the fluorescent *in situ* hybridization experiment as recommended by the provider. The hybridization was executed by means of Cy3-labeled *miR-342-3p* probes (Gene-Pharma; Supplementary Table 3), and subsequent analysis was performed *via* an upright fluorescence microscope (ECLIPSE E600, Nikon, Japan).

Statistical analysis

Measurement data were manifested as mean ± SD, and three or more independent assays were performed. Data analysis employed SPSS 20.0 (SPSS, United States). Additionally, two-tailed Student's *t*-tests were carried out for comparisons to control groups. For multiple group comparisons, we applied one-way analysis of variance plus the post-hoc Dunnett's analysis. Statistical significance was recognized when $P < 0.05$.

RESULTS

HeLa-derived SFCs possessed self-renewal related stemness and displayed stronger tumorigenesis in vivo

SFCs derived from the HeLa cell line were cultured and characterized for subsequent experiments. These SFCs had stronger self-renewal-related stemness *in vitro*, involving stronger spheres and CFE (Figure 1A and B), higher CD133 and CD49f protein levels (Figure 1C), and elevated mRNA expression of stemness-related factors *SOX2* and *OCT4* (Figure 1D). Importantly, SFCs exhibited stronger tumorigenesis *in vivo* (Figure 1E) and higher protein levels of DNMT1, FoxM1, and CD133 as well as lower miR-342-3p *in vivo* (Figure 1F). The above indicated that HeLa-derived SFCs had self-renewal-related stemness *in vitro* and displayed stronger tumorigenesis *in vivo*.

DNMT1/miR-342-3p/FoxM1 signal axis in HeLa-derived CCSLCs

MiRNAs have a critical role in regulating CSCs including their stemness characteristics. To prioritize miRNAs with the greatest difference in expression between CCSLCs and HeLa cells (control), the mRNA level was compared using a qPCR array. The results demonstrated that hsa-miR-342-3p, hsa-miR-199a-3p, hsa-miR-148a-3p, hsa-miR-34a-5p, and hsa-miR-200a-3p were significantly lower in CCSLCs compared with HeLa cells (Figure 2A; Supplementary Table 4).

To further explore the molecular mechanism by which miR-342-3p inhibited self-renewal-related stemness in CCSLCs, we used a qPCR array to compare the differential expression profiles of gene mRNAs in CCSLCs transfected with miR-342-3p mimic (miR-342) and miR-342-3p mimic-NC oligonucleotide (miR-NC). Transfection with miR-342-3p mimics was

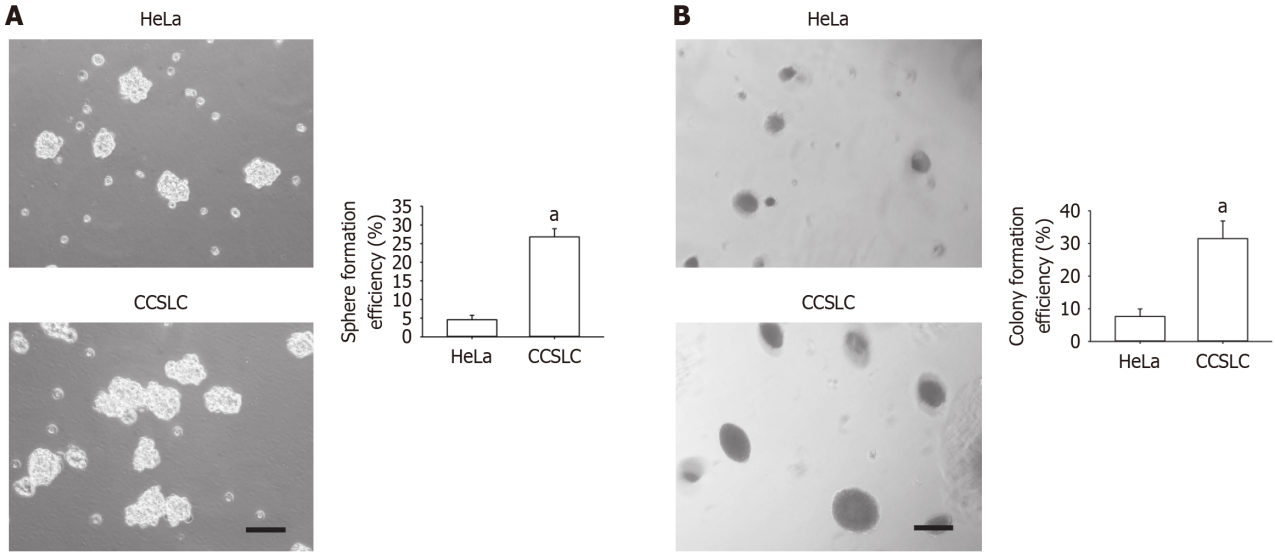

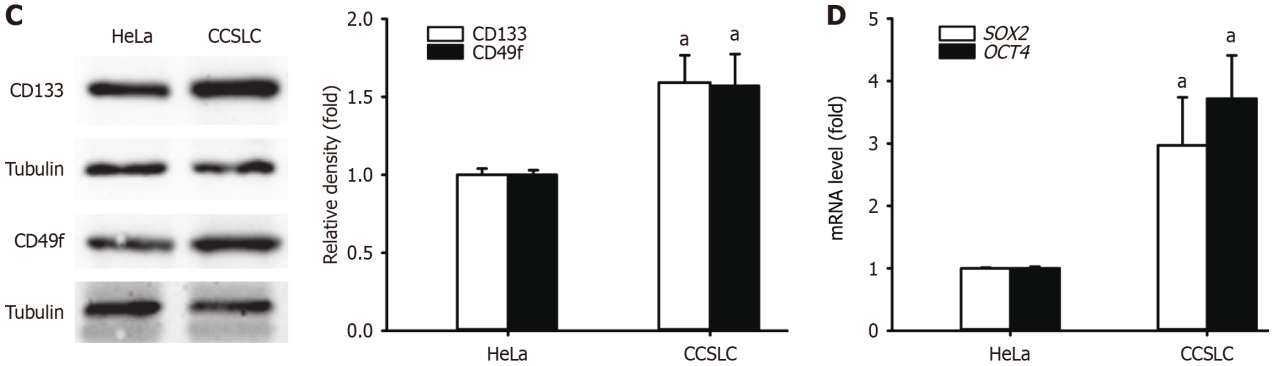

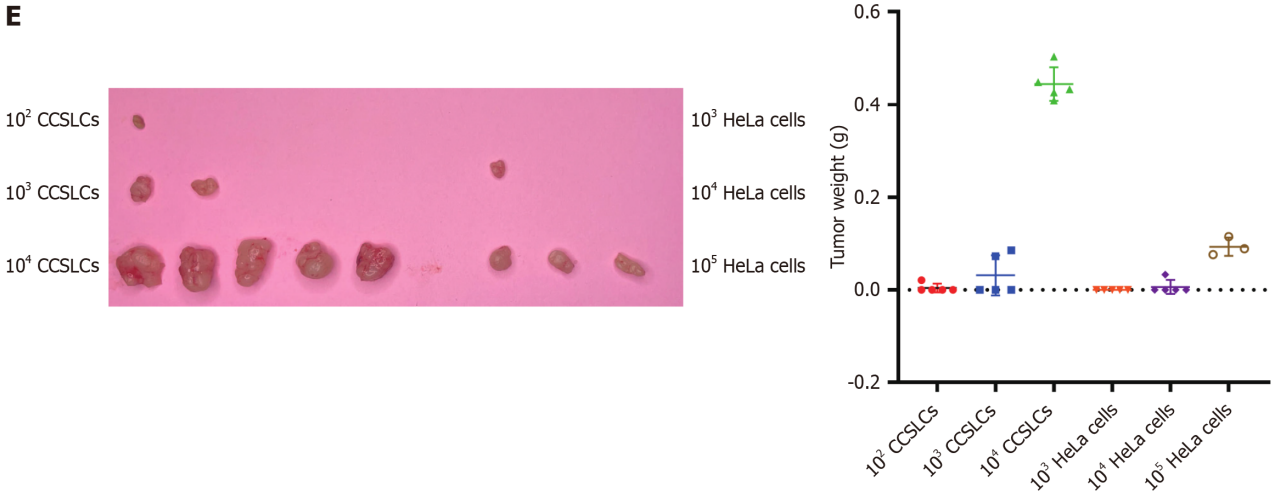

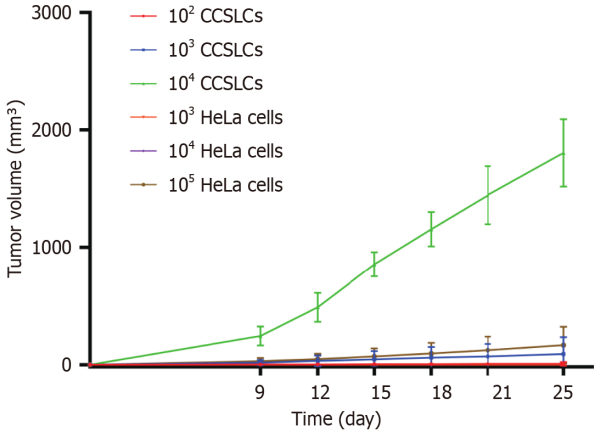

CCSLC	No. of tumor (injection sites)	HeLa cells	No. of tumor (injection sites)
100	1 (5)	1000	0 (5)
1000	2 (5)	10000	1 (5)
10000	5 (5)	100000	3 (5)
TICf	1430	TICf	93412
TIC/10^4	6.99	TIC/10^4	0.11
P	$1.76E^{-8}$		

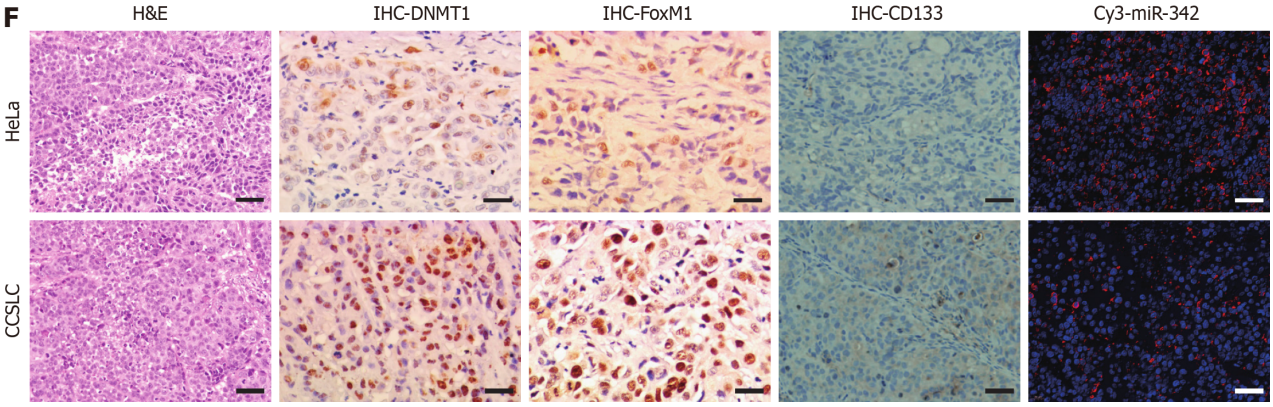

Figure 1 Comparing the self-renewal related stemness between HeLa cells and corresponding cervical cancer stem cell-like cells. A and B: Representative images of spheres (A) and colonies (B) (left) (scale bars = 100 μm); sphere formation efficiency and colony formation efficiency (right) in HeLa cells and their cervical cancer stem cell-like cells (CCSLCs); C: Expression levels of CD133 and CD49f in HeLa cells and their CCSLCs; D: SRY-box transcription factor 2 (*SOX2*) and octamer-binding transcription factor 4 (*OCT4*) mRNA levels in HeLa cells and their CCSLCs; E: *In vivo* carcinogenicity between HeLa cells and their CCSLCs in the nude mice xenograft model, including the weight of xenograft tumors harvested from nude mice (upper right), growth curves of tumor xenografts (bottom left), and tumor initiated cell frequency (bottom right); F: Histology, expression of DNA methyltransferase 1 (DNMT1), forkhead box M1 (FOXM1), and CD133 proteins and microRNA (miR)-342-3p (scale bars = 50 μm). Data were obtained from xenografts at 5 inoculation sites (n = 5) per group. $^{a}P < 0.05$ *vs* HeLa cells (n = 3). TICf: Tumor initiated cell frequency; H&E: Hematoxylin and eosin; IHC: Immunohistochemistry.

found to downregulate the mRNA expression of seven target genes, including *DNMT1*, *FOXM1*, and insulin-like growth factor-1 receptor *etc.* (Figure 2B; Supplementary Table 5).

Notably, the methylation level of the miR-342-3p promoter was higher in the HeLa-derived CCSLCs *vs* the HeLa cells (Figure 2C). The luciferase reporter assay showed that the luciferase activity was repressed or stimulated after cotransfection with the miR-342-3p mimic or inhibitor and DNMT1-3′-UTR-WT (Figure 2D). Nevertheless, this outcome was not replicated after cotransfection with miR-342-3p mimic or suppressor and DNMT1-3′-UTR-Mutation (Figure 2D). Our findings indicated that DNMT1 was a plain target of miR-342-3p in HeLa-derived CCSLCs.

High FoxM1 levels and downregulation of miR-342-3p altogether hold a relevant role in CC advancement[11]. Moreover, previous reports, including ours, have indicated that FoxM1 is a crucial modulator of CSLC characteristics in a variety of cancer cells[11,21-23]. We found the luciferase activity was repressed or raised after cotransfection with miR-342-3p mimic or suppressor and FOXM1-3′-UTR-WT (Figure 2E). Nevertheless, this outcome was not present after cotransfection with miR-342-3p mimic or suppressor and FOXM1-3′-UTR-Mutation (Figure 2E).

We next determined whether SFCs from HeLa cells were considered HeLa-derived CCSLCs with the phenotypes of DNMT1 and FoxM1 upregulation as well as low miR-342-3p levels. As expected, CCSLCs from HeLa cells shared the expression pattern of the above three for DNMT1, FoxM1, and miR-342-3p (Figure 2F-H). Accordingly, the aforementioned results suggested that constitutive activation of DNMT1 silences miR-342-3p expression by its promoter methylation. Low expression of miR-342-3p activates DNMT1 by ceasing inhibition. This reciprocal negative feedback regulation leads to higher expression of DNMT1 and lower expression of miR-342-3p. Lower expression of miR-342-3p caused FoxM1 upregulation by ceasing inhibition and subsequently promoted and maintained the CCSLC self-renewal in CC (Figure 2I).

MiR-342-3p overexpression repressed self-renewal-related stemness in HeLa-derived CCSLCs

To study the *in vitro* impact of miR-342-3p on self-renewal-related stemness, HeLa-derived CCSLCs were transfected using miR-342-3p mimic (miR-342) or miR-NC. Compared to the miR-NC transfection group, *DNMT1* mRNA level in CCSLCs was markedly decreased in CCSLCs transfection with miR-342-3p mimic (Figure 3A), and miR-342-3p was higher in CCSLCs after transfecting with miR-342-3p mimic (Figure 3B). In addition, FoxM1 protein amounts in CCSLCs were remarkably decreased (Figure 3C). Furthermore, the miR-342-3p mimic transfection attenuated sphere and CFE in CCSLCs *vs* the miR-NC transfection block or the non-transfected cells (Figure 3D and E). Moreover, the levels of CD133 and CD49f protein (Figure 3F) and *SOX2* and *OCT4* mRNA (Figure 3G) diminished after transfection of CCSLCs with miR-342-3p mimic.

Next, we tested the effects of agomir-342 (a miR-342-3p mimic) in xenografts of nude mice. The result showed that agomir-342 efficiently decreased the volume and weight of the tumor (Figure 3H). Most importantly, agomir-342 effectively inhibited tumor growth and appeared to downregulate DNMT1, FoxM1, and CD133 protein expression and elevated miR-342-3p levels in individuals bearing HeLa-derived CCSLCs (Figure 3I). Our results imply that miR-342-3p could reduce DNMT1 and FoxM1 expression to attenuate self-renewal-related stemness, suggesting that mutual negative regulation between DNMT1 and miR-342-3p leading to the regulation of FoxM1 might be involved in the maintenance and promotion of self-renewal-related stemness.

Knockdown of DNMT1 suppressed self-renewal-related stemness in HeLa-derived CCSLCs

To evaluate the increased function of DNMT1 in preserving CSLC characteristics, DNMT1 shRNA was implemented for the knockdown of DNMT1 in HeLa-derived CCSLCs (sh-DNMT1). *DNMT1* mRNA level were remarkably reduced in the

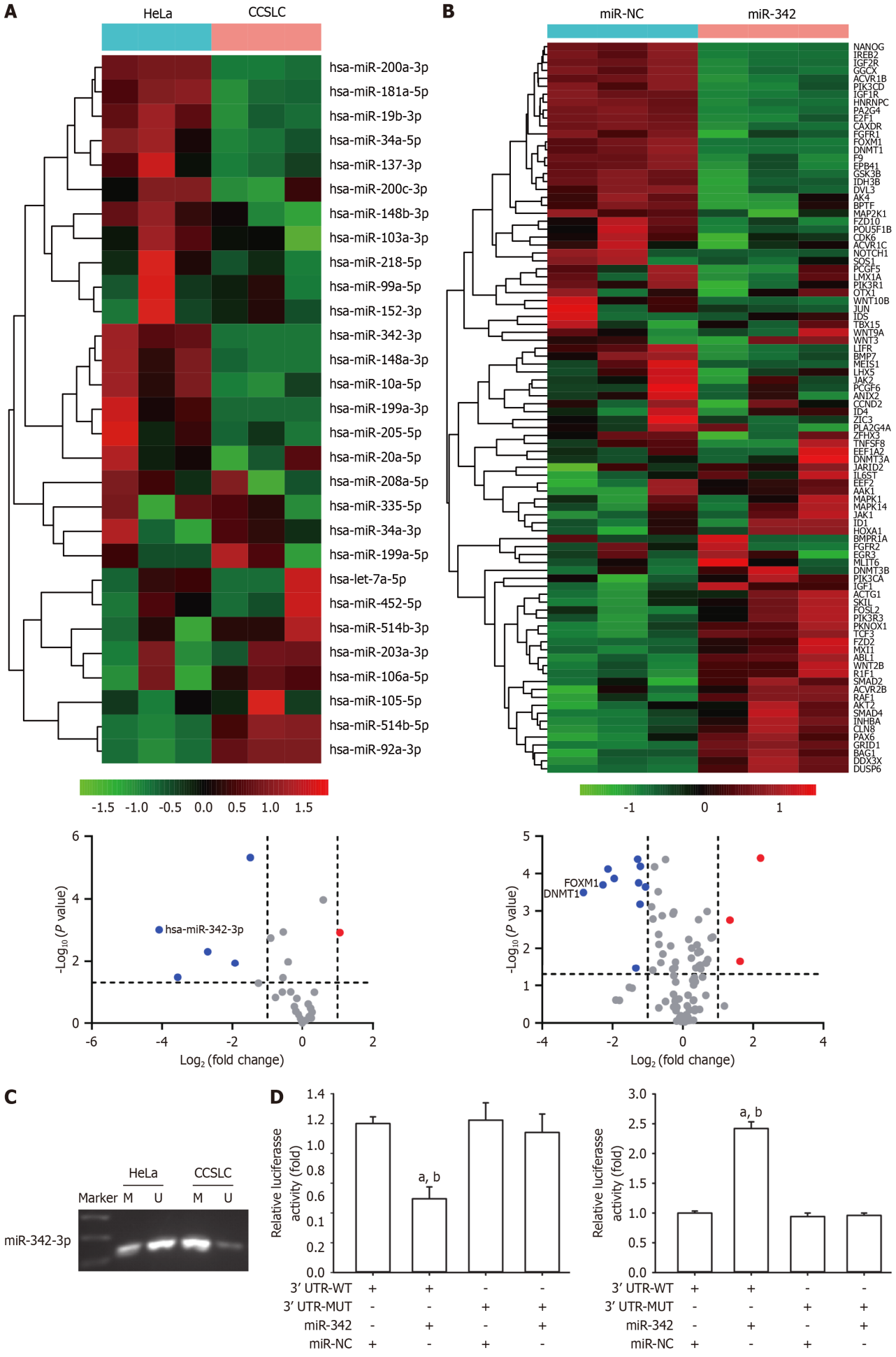
A
HeLa
CCSLC
hsa-miR-200a-3p
hsa-miR-181a-5p
hsa-miR-19b-3p
hsa-miR-34a-5p
hsa-miR-137-3p
hsa-miR-200c-3p
hsa-miR-148b-3p
hsa-miR-103a-3p
hsa-miR-218-5p
hsa-miR-99a-5p
hsa-miR-152-3p
hsa-miR-342-3p
hsa-miR-148a-3p
hsa-miR-10a-5p
hsa-miR-199a-3p
hsa-miR-205-5p
hsa-miR-20a-5p
hsa-miR-208a-5p
hsa-miR-335-5p
hsa-miR-34a-3p
hsa-miR-199a-5p
hsa-let-7a-5p
hsa-miR-452-5p
hsa-miR-514b-3p
hsa-miR-203a-3p
hsa-miR-106a-5p
hsa-miR-105-5p
hsa-miR-514b-5p
hsa-miR-92a-3p
-1.5 -1.0 -0.5 0.0 0.5 1.0 1.5
B
miR-NC
miR-342
-1 0 1
hsa-miR-342-3p
-Log10 (P value)
Log2 (fold change)
FOXM1
DNMT1
C
Marker M U M U
HeLa
CCSLC
miR-342-3p
D
Relative luciferasse activity (fold)
a, b
3′ UTR-WT
3′ UTR-MUT
miR-342
miR-NC

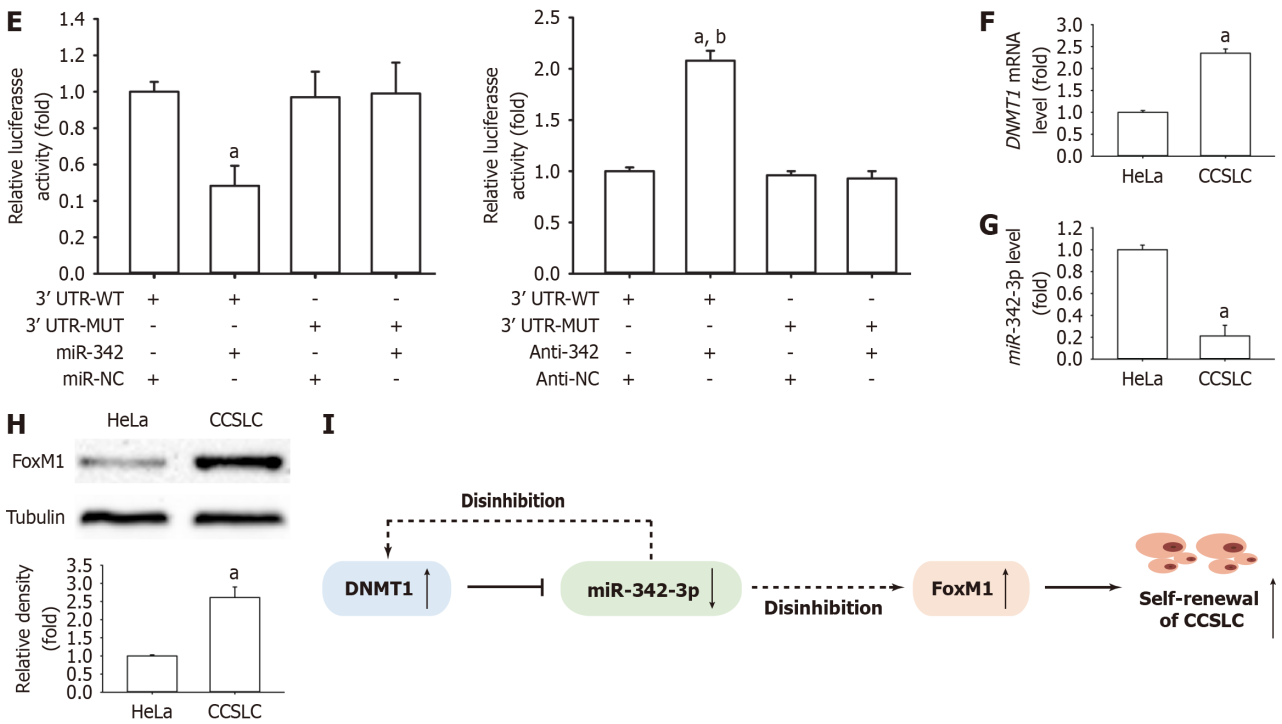

Figure 2 DNA methyltransferase 1 and forkhead box M1 as the direct targets of miR-342-3p in HeLa-derived cervical cancer stem cell-like cells. A: Heatmaps depict the relative expression levels of all 29 tumor microRNAs (miRNAs) in HeLa cells and their responding cervical cancer stem cell-like cells (CCSLCs). The color scale represents the expression levels of miRNA as upregulation (red), downregulation (green), or middle expression (light color) across all samples. Lower volcano plot analysis showed differentially expressed ($P < 0.005$, student's *t*-test, $\log_2$ fold change > 2) miRNA in HeLa cells and their responding CCSLCs; B: Visual representation displaying the expression levels of all 92 genes investigated in this study through heatmap analysis. Scale: Relative expression levels were normalized for internal control. Lower volcano plot showing the differentially expressed mRNAs ($P < 0.005$, student's *t*-test, $\log_2$ fold change > 2) in HeLa-derived CCSLCs treated with miRNA (miR)-negative control or miR-342 ($n = 3$); C: MiR-342-3p promoter methylation in HeLa cells and their CCSLCs; D: The relative luciferase activity in HeLa-derived CCSLCs was determined after the DNA methyltransferase 1 (DNMT1) 3'-untranslated regions (3'-UTRs) or mutant (MUT) plasmids were cotransfected with miR-342-3p mimics or inhibitors or negative control; E: The relative luciferase activity in HeLa-derived CCSLCs was determined after the forkhead box M1 (FOXM1) 3' UTR or mutant plasmids were cotransfected with miR-342-3p mimics or inhibitors or the negative control; F: *DNMT1* mRNA level in HeLa cells and its corresponding CCSLCs; G: MiR-342-3p level in HeLa cells and its corresponding CCSLCs; H: FoxM1 protein amounts in HeLa cells and its corresponding CCSLCs, with α-tubulin as a loading control; I: Schematic representation of the pathomechanism by which DNMT1/miR-342-3p/FOXM1 axis promotes self-renewal-related stemness in CCSLCs. $^aP < 0.05$ *vs* HeLa-derived cervical cancer stem cell-like cells cotransfected with DNMT1 3'-UTR with miR-negative; $^bP < 0.05$ *vs* HeLa-derived cervical cancer stem cell-like cells cotransfected of mutant plasmid in the presence or absence of miR-342 mimics ($n = 3$). WT: Wildtype; M: Methylated; U: Unmethylated.

knocked-down DNMT1 CCSLCs (Figure 4A). Meanwhile, miR-342-3p was higher and had lower miR-342-3p promoter methylation *vs* the sh-NC control cells (Figure 4B and C). FoxM1 protein levels in CCSLCs were remarkably reduced (Figure 4D). Among CCSLCs, DNMT1 knockdown decreased spheres and CFE (Figure 4E and F). Additionally, the CD133 and CD49f protein quantities decreased in CCSLCs bearing DNMT1 shRNA (Figure 4G). Moreover, *SOX2* and *OCT4* gene expression in CCSLCs bearing DNMT1 shRNA were lower *vs* the HeLa-derived CCSCs transfected with sh-NC (Figure 4H). The knockdown of DNMT1 blocked tumor growth (Figure 4I) and appeared to reduce DNMT1, FoxM1, and CD133 protein expression as well as elevated miR-342-3p levels in our xenograft samples (Figure 4J). These findings suggest that the knockdown of DNMT1 repressed self-renewal-related stemness in HeLa-derived CCSLCs, probably by upregulation of miR-342-3p after its promoter hypomethylation.

Overexpression of DNMT1 rescued the inhibitory effects of miR-342 on self-renewal-related stemness in HeLa cells

DNMT1 is responsible for self-renewal-related stemness in a variety of cancers and may be subject to miRNA regulation [15,25,26]. To investigate the interplay between miR-342-3p and DNMT1, we constructed DNMT1 expression plasmids to perform a rescue experiment. Among our results, overexpression of DNMT1 reestablished the *DNMT1* mRNA level that had been diminished by miR-342-3p and that had been increased by miR-342-3p mimics (Figure 5A and B). Additionally, restoration of DNMT1 abrogated effects of miR-342-3p mimic on the FoxM1 protein expression, the spheres, CFE, and the CD133 and CD49f protein levels (Figure 5C-F). The *SOX2* and *OCT4* mRNA amounts were lower in miR-342-3p mimics (Figure 5G). The above suggested that DNMT1 might be a straight functional target gene of miR-342-3p. Moreover, miR-342-3p operated as a tumor suppressor *via* the mutual adverse modulation between miR-342-3p and DNMT1.

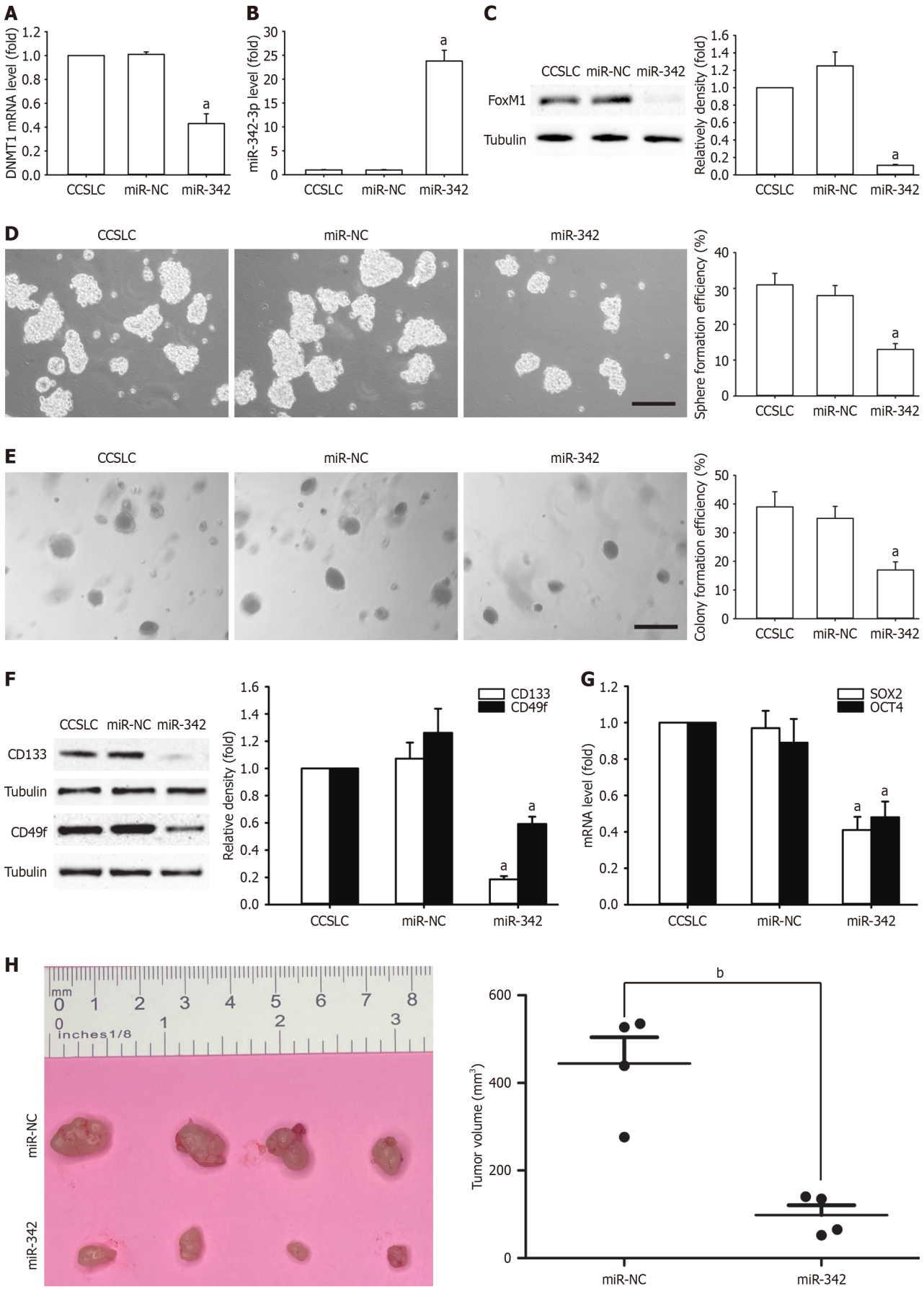
A
DNMT1 mRNA level (fold)
CCSLC
miR-NC
miR-342
B
miR-342-3p level (fold)
C
CCSLC miR-NC miR-342
FoxM1
Tubulin
Relatively density (fold)
D
Sphere formation efficiency (%)
E
Colony formation efficiency (%)
F
CD133
Tubulin
CD49f
Relative density (fold)
G
SOX2
OCT4
mRNA level (fold)
H
miR-NC
miR-342
Tumor volume (mm3)
b

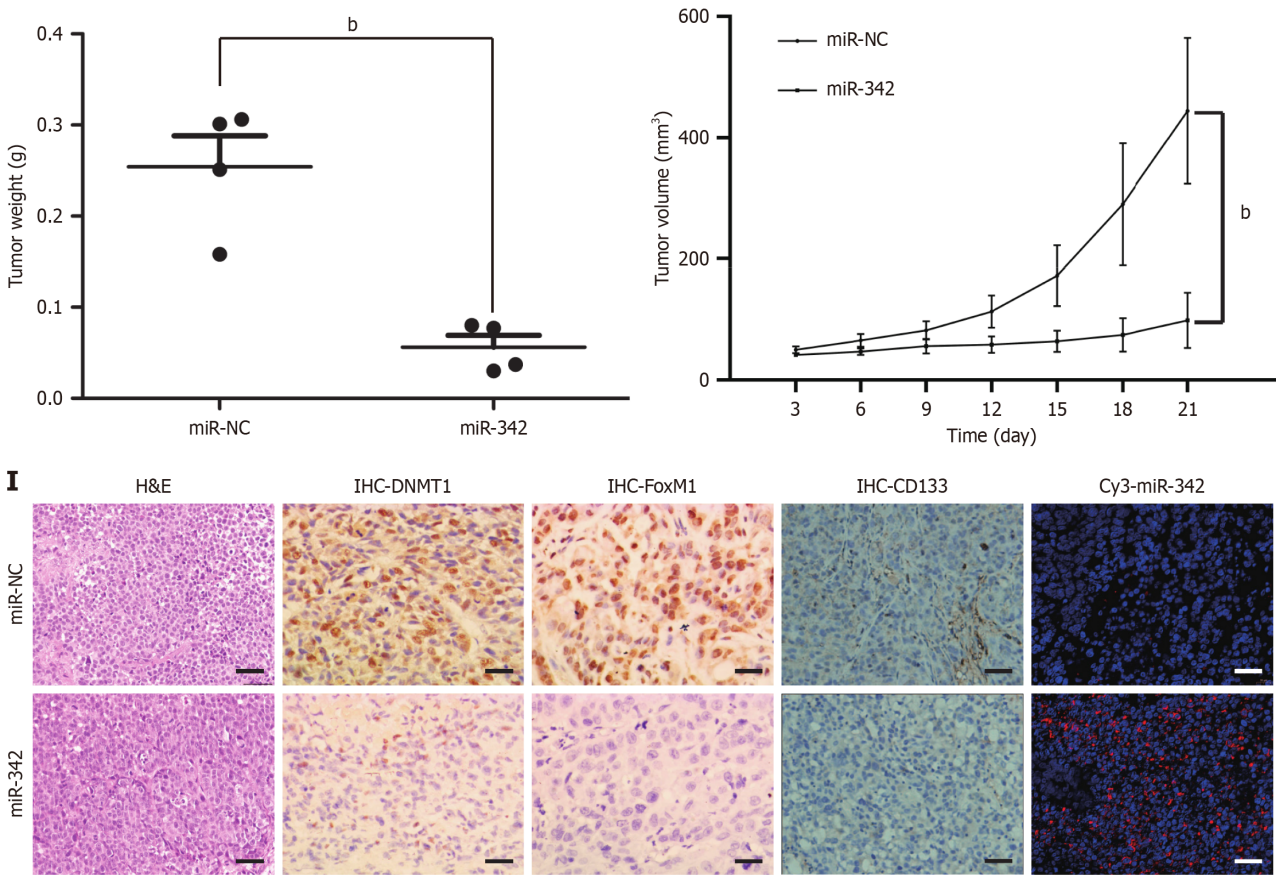

Figure 3 Effect of miR-342-3p mimic on self-renewal-related stemness of HeLa-derived cervical cancer stem cell-like cells. A-C: DNA methyltransferase 1 (*DNMT1*) mRNA level (A), microRNA (miR)-342-3p level (B), forkhead box M1 (FoxM1) protein amounts in cervical cancer stem cell-like cells (CCSLCs) transfected with miR-342-3p mimic (C); D and E: Representative images of spheres and colonies (left) (scale bars = 100 μm); sphere formation efficiency and colony formation efficiency (right) in CCSLCs transfected with miR-342-3p mimic; F: CD133 and CD49f protein amount; G: SRY-box transcription factor 2 (*SOX2*) and octamer-binding transcription factor 4 (*OCT4*) mRNA amounts in CCSLCs transfected with miR-342-3p mimic; H: Subcutaneous xenografts of HeLa-derived CCSLCs (1×10^5) treated with miR-negative control (miR-NC) or miR-342-3p mimic (miR-342) (left); the comparison of tumor volume (middle left), tumor weight (middle right), and growth curves of tumor xenografts (right) between CCSLCs treated with miR-NC or miR-342; I: Micrographs of hematoxylin and eosin staining and immunohistochemistry to detect the expression of DNMT1, FoxM1, and CD133 proteins as well as *in situ* immunofluorescent hybridization for miR-342-3p (scale bars = 50 μm). Data were obtained from xenografts with four mice per group (n = 4). $^aP < 0.05$ *vs* cervical cancer stem cell-like cells transfected with miR-NC (n = 4); $^bP < 0.01$ *vs* cervical cancer stem cell-like cells treated with miR-NC. H&E: Hematoxylin and eosin; IHC: Immunohistochemistry.

Knockdown of FoxM1 inhibited self-renewal-related stemness in HeLa-derived CCSCs, with no impact on DNMT1 function and expression of miR-342-3p

To understand how FoxM1 maintained self-renewal-related stemness in CCSLCs, FOXM1 was downregulated using shRNA in HeLa-derived CCSLCs (shFOXM1). The resulting FoxM1 protein amounts were markedly decreased (Figure 6A). However, *DNMT1* mRNA and miR-342-3p levels were not significantly altered in comparison to the non-transduced cells and the sh-NC control block (Figure 6B and C). In CCSLCs, FOXM1 knockdown diminished spheres and CFE (Figure 6D and E). In CCSLCs bearing FOXM1 shRNA, the CD133 and CD49f protein levels were decreased (Figure 6F). On the other hand, in CCSCs bearing FOXM1 shRNA, *SOX2* and *OCT4* gene expression levels were lower to those transfected with sh-NC (Figure 6G). Moreover, knockdown of FOXM1 inhibited tumor expansion (Figure 6H) and appeared to downregulate FoxM1 and CD133 protein expressions but did not affect DNMT1 and miR-342-3p expression in our xenograft model (Figure 6I). These findings suggest that knockdown of FOXM1 inhibited self-renewal-related stemness, mimicked the impact of miR-342-3p upregulation, and indicated that the reciprocal regulation of DNMT1 and miR-342-3p was upstream of FoxM1.

Overexpression of FoxM1 rescued the inhibitory effects of miR-342 on self-renewal-related stemness in HeLa cells

FoxM1 has a pivotal function in the generation of self-renewal-related stemness, and it may be subject to miRNA regulation[22,27,28]. To explore whether miR-342-3p plays an inhibitory role in self-renewal-related stemness in CCSLCs *via* FoxM1, we created FOXM1 plasmids to perform a rescue experiment. As a result, overexpression of FOXM1 did not change *DNMT1* mRNA and miR-342-3p by miR-342-3p mimics (Figure 7A and B). Furthermore, restoration of FOXM1 abrogated the inhibitory effects of miR-342-3p mimics on FoxM1 protein levels, spheres, CFE, and CD133 and CD49f protein (Figure 7C-F). The *SOX2* and *OCT4* mRNA quantities decreased by miR-342-3p mimics, and these effects were rescued by restoration of FOXM1 (Figure 7G). The above suggested that FoxM1 might be a straight functional target gene of *miR-342-3p*. Moreover, miR-342-3p operated as a tumor suppressor *via* FoxM1.

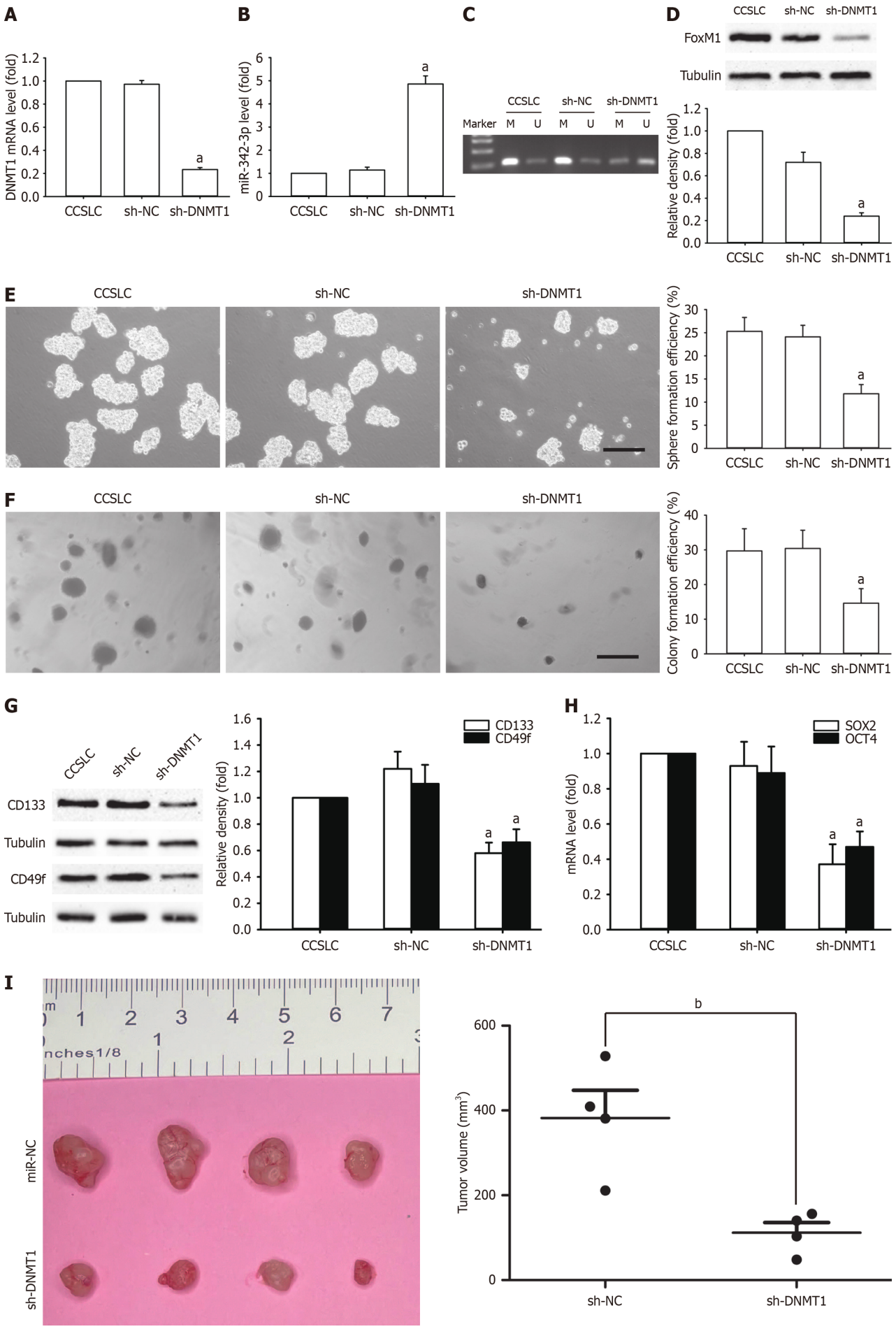
A
DNMT1 mRNA level (fold)
CCSLC
sh-NC
sh-DNMT1
B
miR-342-3p level (fold)
C
Marker
M
U
D
FoxM1
Tubulin
Relative density (fold)
E
Sphere formation efficiency (%)
F
Colony formation efficiency (%)
G
CD133
CD49f
H
SOX2
OCT4
mRNA level (fold)
I
miR-NC
Tumor volume (mm3)

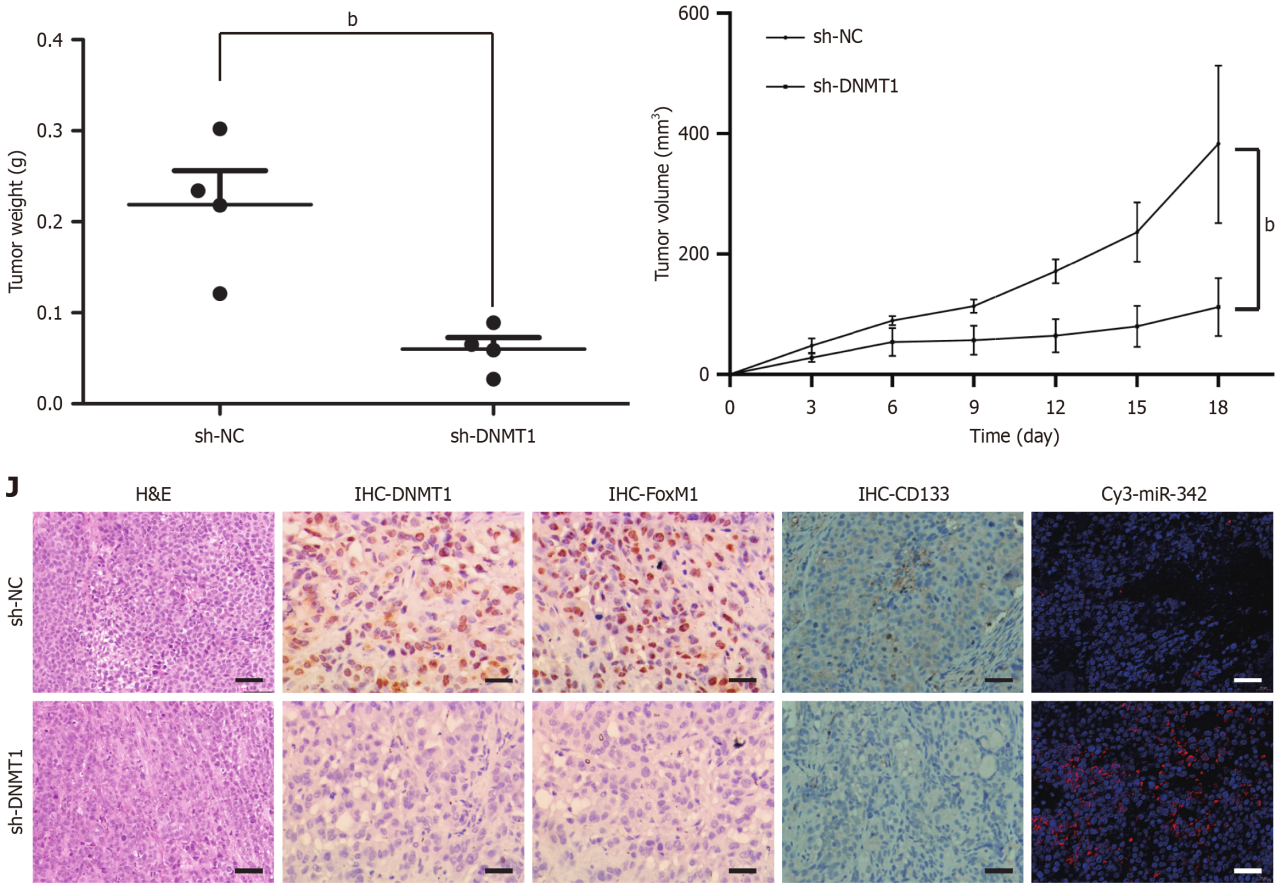

Figure 4 Effect of DNA methyltransferase 1 shRNA on cervical cancer stem cell-like cell characteristics in HeLa-derived cervical cancer stem cell-like cells. A: DNA methyltransferase 1 (*DNMT1*) mRNA level in cervical cancer stem cell-like cells (CCSLCs) transfected with DNMT1 shRNA; B: MicroRNA (miR)-342-3p levels in CCSLCs transfected with DNMT1 shRNA; C: MiR-342-3p promoter methylation in CCSLCs transfected with DNMT1 shRNA; D: Forkhead box M1 (FoxM1) protein amounts in CCSLCs transfected with DNMT1 shRNA, with α-tubulin as a loading control; E and F: Representative images of spheres (E) and colonies (F) (left) (scale bars = 100 μm). Sphere formation efficiency and colony formation efficiency in CCSLCs transfected with DNMT1 shRNA (right); G: CD133 and CD49f protein amount in CCSLCs transfected with DNMT1 shRNA, with α-tubulin as a loading control; H: SRY-box transcription factor 2 (*SOX2*) and octamer-binding transcription factor 4 (*OCT4*) mRNA amounts in CCSLCs transfected with DNMT1 shRNA; I: Subcutaneous xenografts of CCSLCs (1×10^5) treated with sh-negative control (sh-NC) or sh-DNMT1 (left); the comparison of tumor volume (middle left), tumor weight (middle right), and growth curves of tumor xenografts (right) between CCSLCs treated with sh-NC and sh-DNMT1; J: Micrographs of hematoxylin and eosin (H&E) staining and immunohistochemistry (IHC) to detect the expression of DNMT1, FoxM1, and CD133 proteins as well as *in situ* immunofluorescence hybridization for miR-342-3p (scale bars = 50 μm). Data were obtained from xenografts with four mice per group. $^aP < 0.05$ *vs* CCSLCs transfected with sh-NC ($n = 4$); $^bP < 0.001$ *vs* CCSLCs treated with sh-NC. M: Methylated; U: Unmethylated.

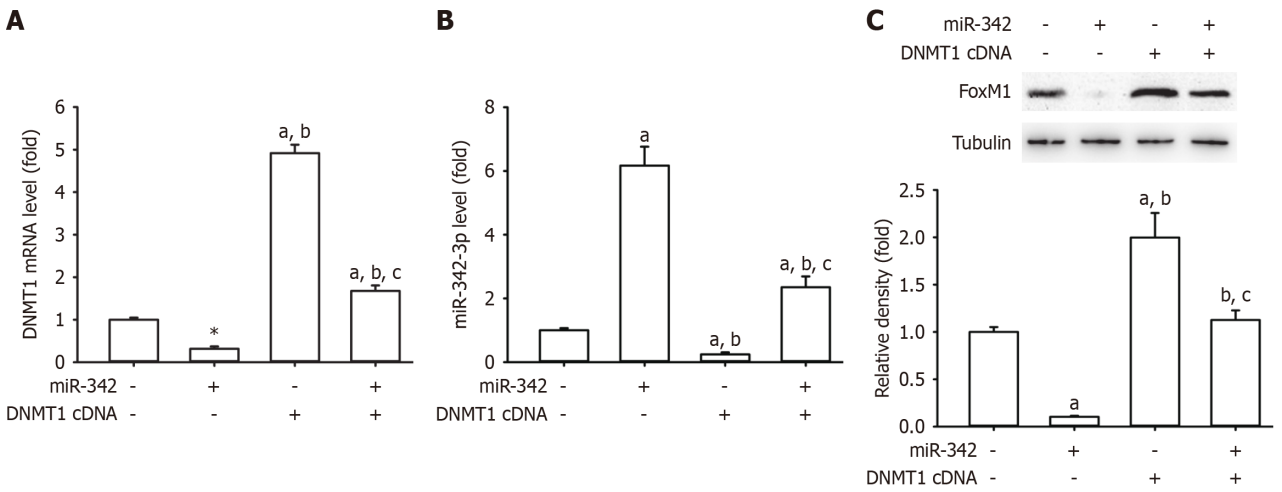

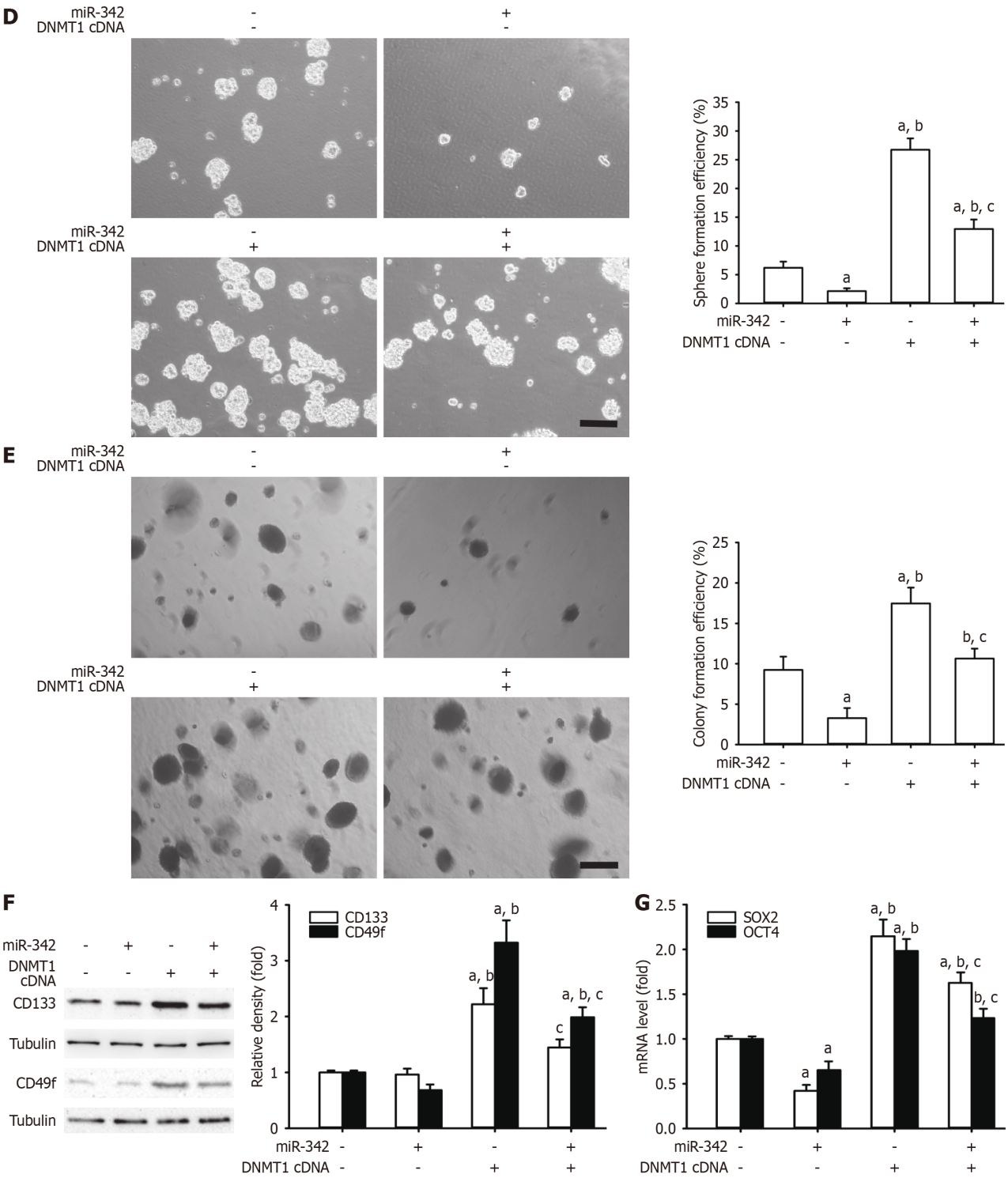

Figure 5 Overexpression of DNA methyltransferase 1 reversed the inhibitory effects of microRNA-342 on cervical cancer stem cell-like cell self-renewal in HeLa cells. A and B: Restoration of DNA methyltransferase 1 (DNMT1) could reverse its mRNA level inhibition (A) and upregulation of microRNA (miR)-342-3p expression (B); C-E: Downregulation of forkhead box M1 (FoxM1) protein expression with α-tubulin as a loading control led to attenuation of cervical cancer stem cell-like cell self-renewal characteristics, including sphere formation efficiency and colony formation efficiency (D and E); F and G: CD133 and CD49f protein expressions with α-tubulin as a loading control and SRY-box transcription factor 2 (*SOX2*) (G) and octamer-binding transcription factor 4 (*OCT4*) mRNA expression caused by miR-342-3p mimics in HeLa cells. $^{a}P < 0.05$ *vs* HeLa cells; $^{b}P < 0.05$ *vs* HeLa cells transfected with miR-342-3p mimic alone; $^{c}P < 0.05$ *vs* HeLa cells transfected with DNA methyltransferase 1 cDNA alone ($n = 3$).

DNMT1/miR-342-3p/FoxM1 axis as a novel target of self-renewal-related stemness in CCSLCs

Two additional CC cell lines, CasKi and SiHa cells, were chosen to contrast the level of *DNMT1* mRNA, miR-342-3p, and FoxM1, and self-renewal-related stemness. The comparison was performed between the cellular monolayer and the respective SFCs. As a result, *DNMT1* mRNA level increased (Figure 8A), while miR-342-3p levels were significantly decreased (Figure 8B). In addition, FoxM1 protein expression (Figure 8C), spheres, and CFE (Figure 8D and E) were

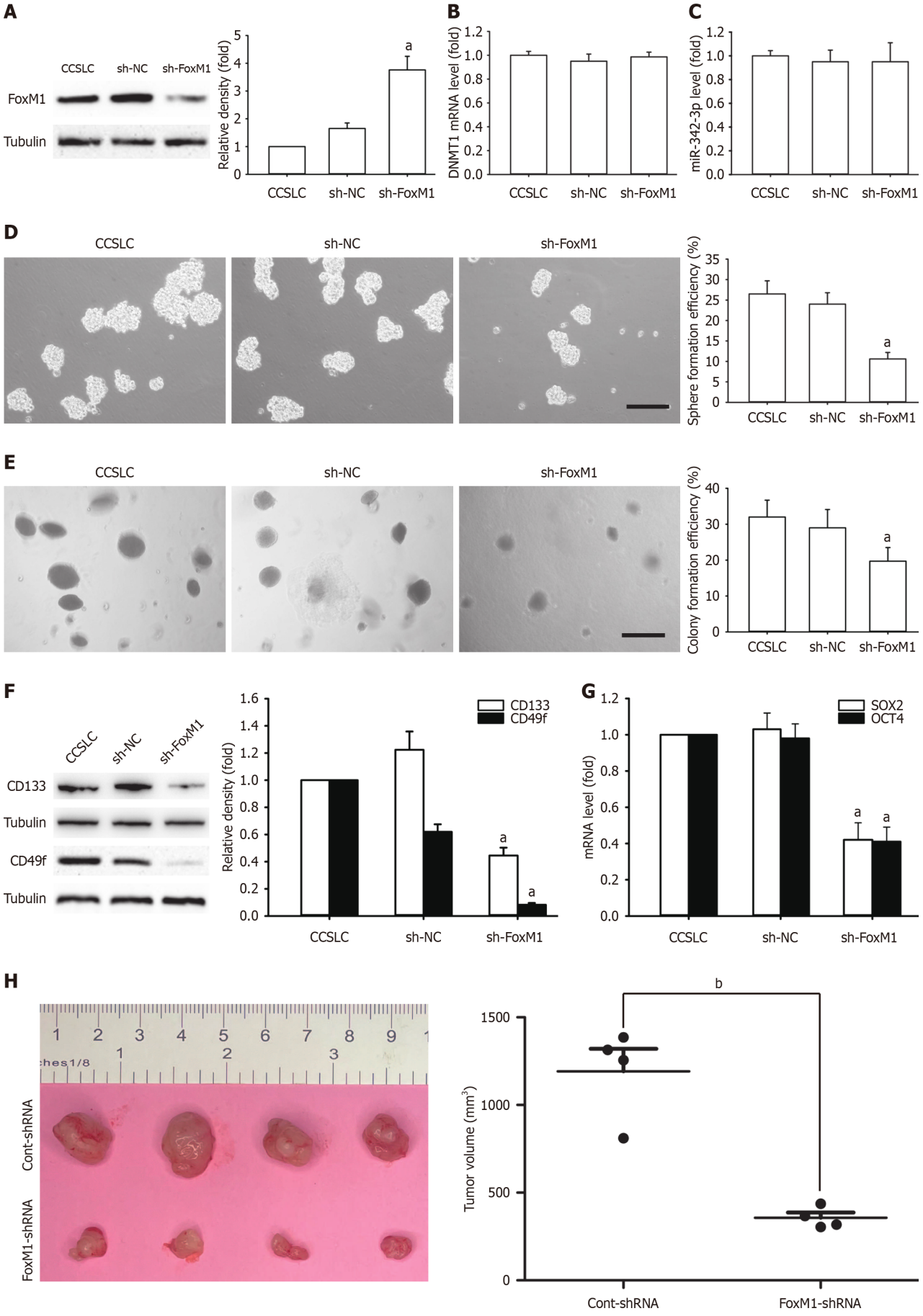
A
CCSLC
sh-NC
sh-FoxM1
FoxM1
Tubulin
Relative density (fold)
a
B
DNMT1 mRNA level (fold)
C
miR-342-3p level (fold)
D
Sphere formation efficiency (%)
E
Colony formation efficiency (%)
F
CD133
CD49f
Relative density (fold)
G
SOX2
OCT4
mRNA level (fold)
H
Cont-shRNA
FoxM1-shRNA
Tumor volume (mm³)
b

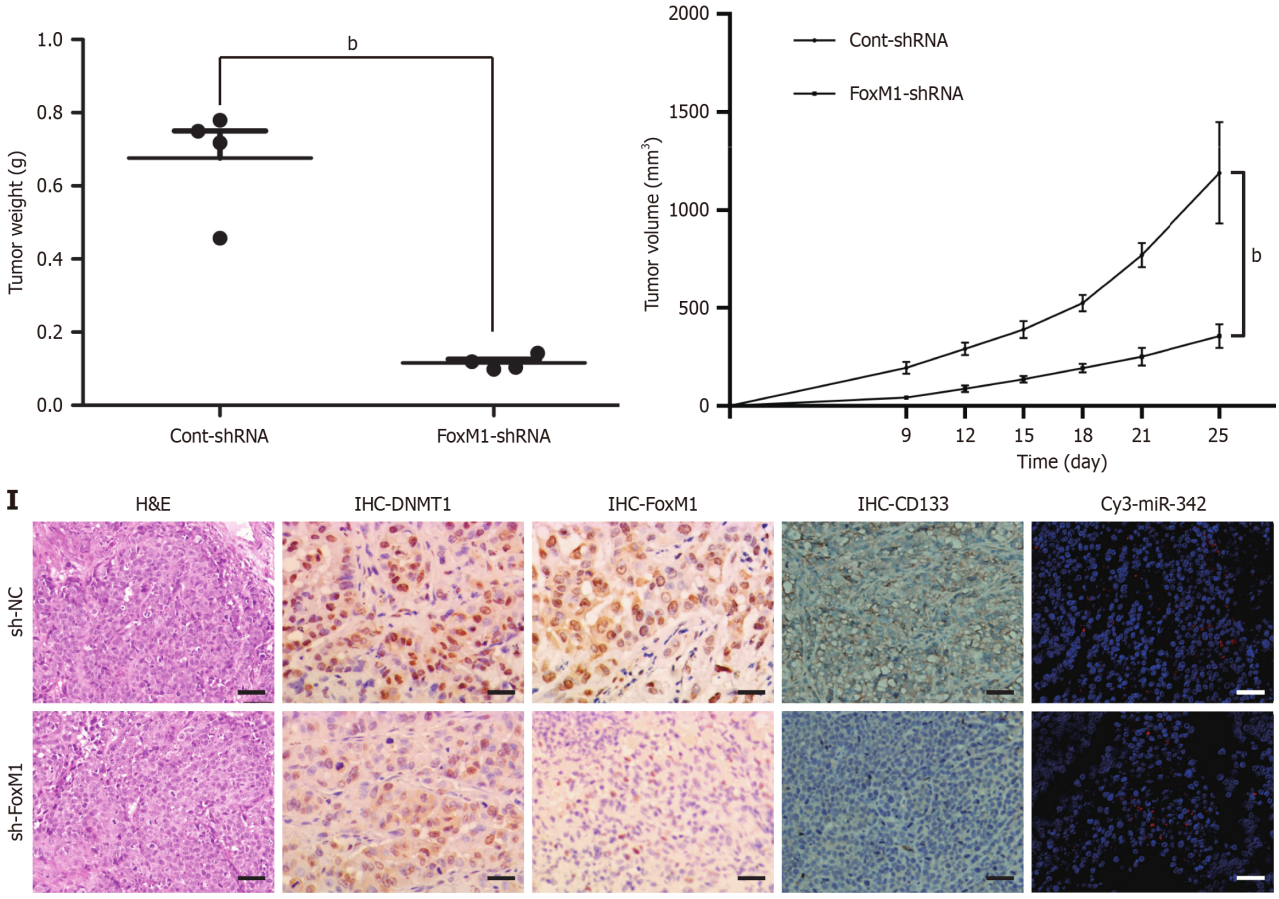

Figure 6 Effects of forkhead box M1 shRNA on cervical cancer stem cell-like cell self-renewal of HeLa derived cervical cancer stem cell-like cells. A: Forkhead box M1 (FoxM1) protein in cervical cancer stem cell-like cells (CCSLCs) transfected with FoxM1 shRNA, with α-tubulin as a loading control; B: DNA methyltransferase 1 (*DNMT1*) mRNA level in CCSLCs transfected with FoxM1 shRNA; C: MicroRNA (miR)-342-3p levels in CCSLCs transfected with FoxM1 shRNA; D and E: Representative images of spheres and colonies (left) (scale bars = 100 μm); sphere formation efficiency and colony formation efficiency (right) in CCSLCs transfected with FoxM1 shRNA; F: CD133 and CD49f protein amount in CCSLCs transfected with DNMT1 shRNA with α-tubulin as a loading control; G: SRY-box transcription factor 2 (*SOX2*) and octamer-binding transcription factor 4 (*OCT4*) mRNA amounts in CCSLCs transfected with FOXM1 shRNA; H: Subcutaneous xenografts of HeLa-derived CCSLCs (1×10^5) treated with sh-negative control (sh-NC) or sh-FOXM1 (left); comparison of tumor volume (middle left), tumor weight (middle right), and growth curves of tumor xenografts (right) between CCSLCs treated with sh-NC or sh-FOXM1; I: Micrographs of hematoxylin and eosin (H&E) staining and immunohistochemistry (IHC) to detect the expression of DNMT1, FoxM1, and CD133 proteins as well as in situ immunofluorescent hybridization for miR-342-3p (scale bars = 50 μm). Data were obtained from xenografts with four mice per group ($n = 4$). $^aP < 0.05$ *vs* CCSLCs transfected with sh-NC; $^bP < 0.001$ *vs* CCSLCs treated with sh-NC. Cont: Control.

considerably amplified in the respective CCSLCs. We also assessed CD133 and CD49f levels in CasKi and SiHa cells in relation to the respective CCSLCs, with increasing results (Figure 8F). The *SOX2* and *OCT4* mRNA quantities were enhanced as well (Figure 8G). The present outcome indicated that the DNMT1/miR-342-3p/FoxM1 axis might promote self-renewal-related stemness in CasKi and SiHa cell lines. Finally, the DNMT1/miR-342-3p/FoxM1 axis could be a new target to mimic self-renewal-related stemness in CCSLCs for CC treatment.

DISCUSSION

We aimed to study the functional linkage between DNMT1, miR-342-3p, and FoxM1, which regulates CCSLC self-renewal in CC. As far as we know, this is the first time that the CCSLC self-renewal in CC *in vitro* and *in vivo* was enhanced by the mutual negative regulation between DNMT1 and miR-342-3p, with the subsequent increase in FoxM1 levels by reactivation *via* miR-342-3p silencing. These results seem important not only because they describe the links among DNMT1, miR-342-3p, and FoxM1 in a cell subpopulation with CCSLC self-renewal but also because they might provide ideas for the development of novel therapies against CCSLCs, which are causal cells in CC.

In recent years, much attention has been paid to silencing tumor suppressors or miRNAs inhibitors in precancerous cells *via* epigenetic regulation[29]. DNMT1 is unusually triggered in tumors and CSC, which catalyze DNA methylation [30-32]. Moreover, DNMT1 is essential to keep CSLC characteristics[16]. In breast cancer, epigenetic altering factors, including 5-azacytidine, can significantly shrink the CSC subgroup[33]. Based on the GEO analyses, *DNMT1* and *FOXM1* transcript levels were increased in CC tissues compared with paracarcinoma tissues. With respect to the positive correlation between the expression levels of DNMT1 and FOXM1 in CC progression, we hypothesized that DNMT1 (an

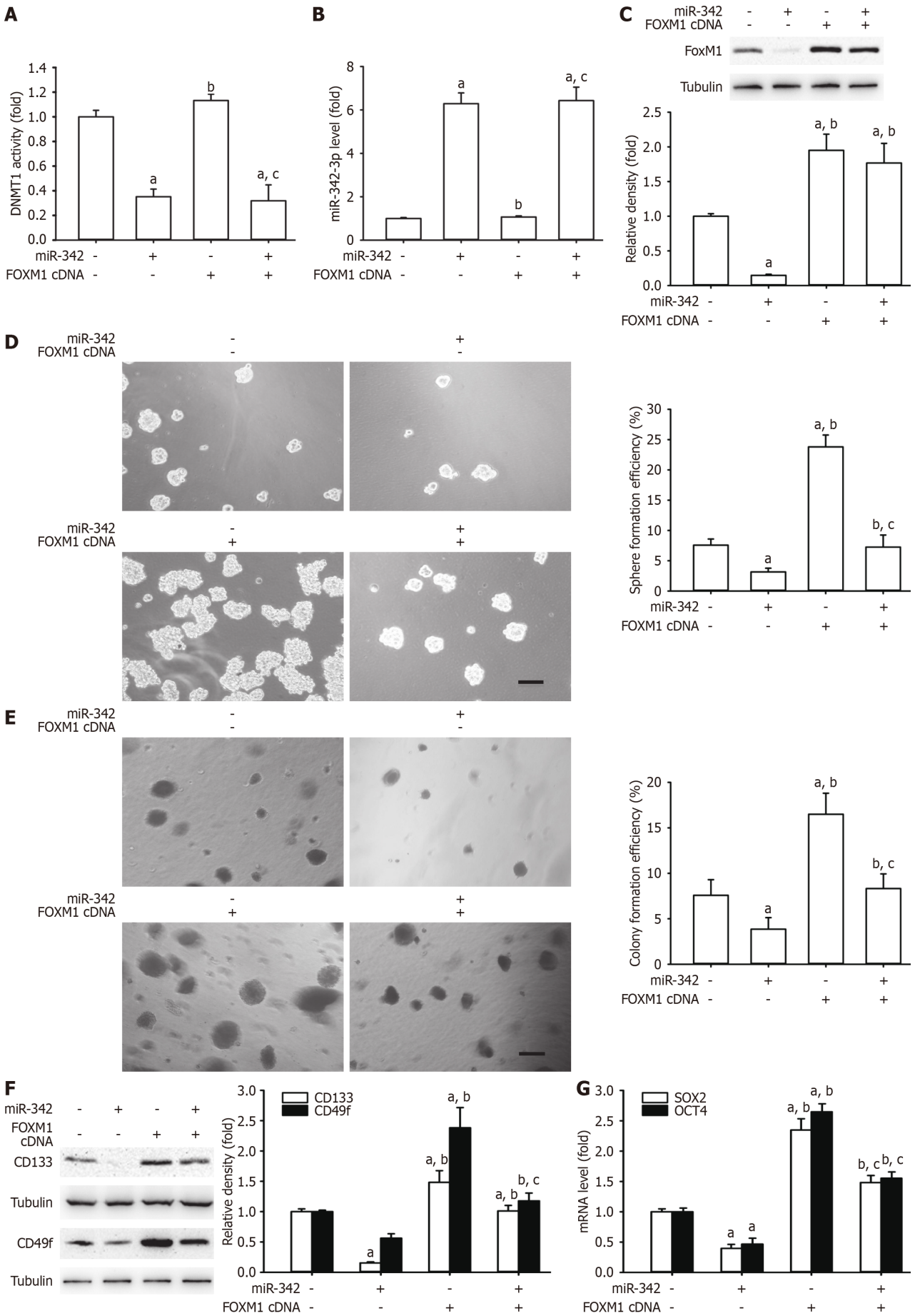

Figure 7 Overexpression of forkhead box M1 reversed the inhibitory effect of microRNA-342 on cervical cancer stem cell-like cell self-

renewal in HeLa cells. A-C: Restoration of forkhead box M1 (FOXM1) did not alter DNA methyltransferase 1 (DNMT1) (A) and microRNA (miR)-342-3p expression (B) but could reverse FOXM1 protein downregulation with α-tubulin as a loading control (C); D and E: Attenuation of cervical cancer stem cell-like cell characteristics, including sphere formation efficiency and colony formation efficiency; F: CD133 and CD49f protein expression with α-tubulin as a loading control; G: SRY-box transcription factor 2 (*SOX2*) and octamer-binding transcription factor 4 (*OCT4*) mRNA levels caused by miR-342-3p mimics in HeLa cells. [a]$P < 0.05$ *vs* HeLa cells; [b]$P < 0.05$ *vs* HeLa cells transfected with miR-342-3p mimic alone; [c]$P < 0.05$ *vs* HeLa cells transfected with FOXM1 cDNA alone ($n = 3$).

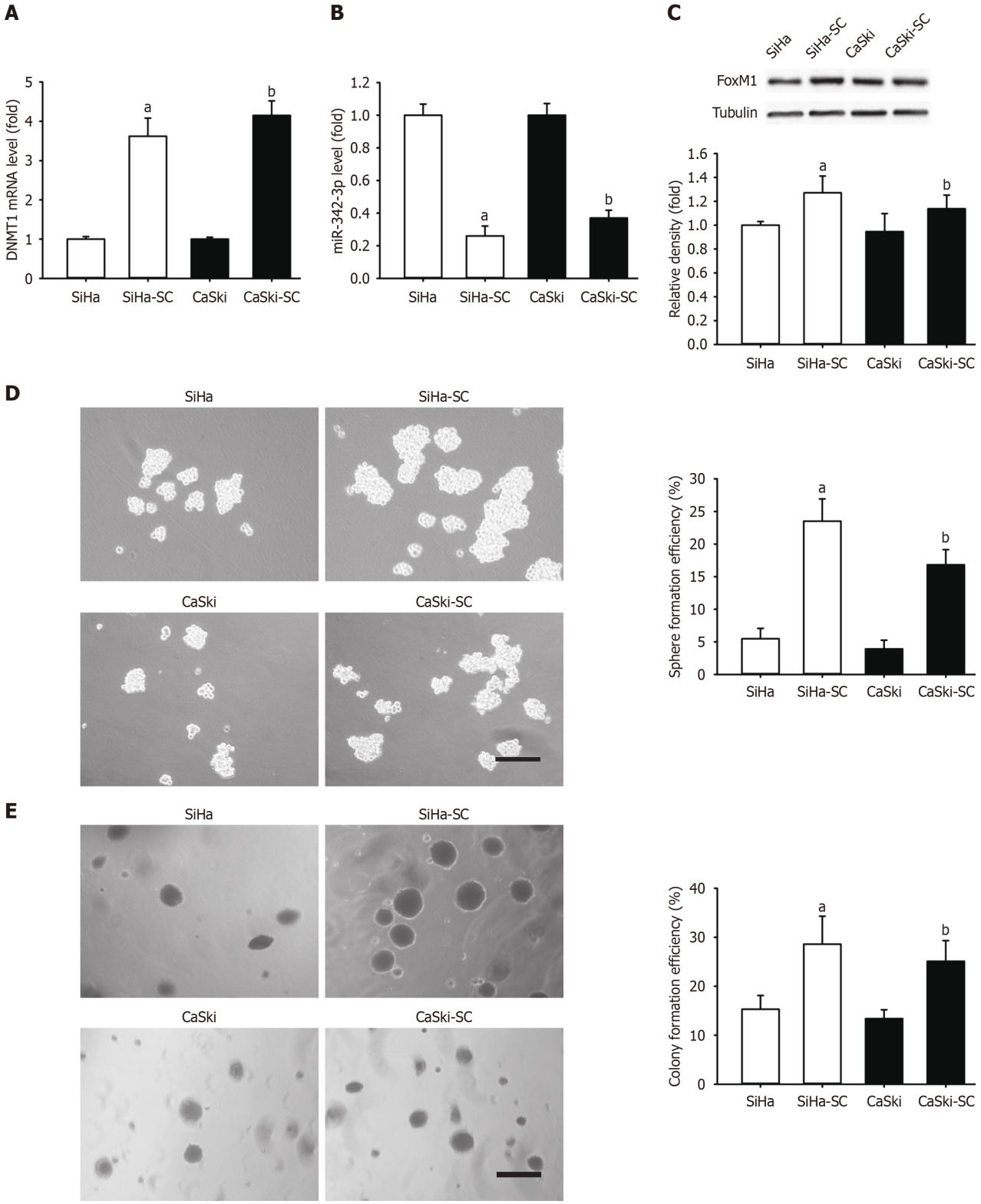

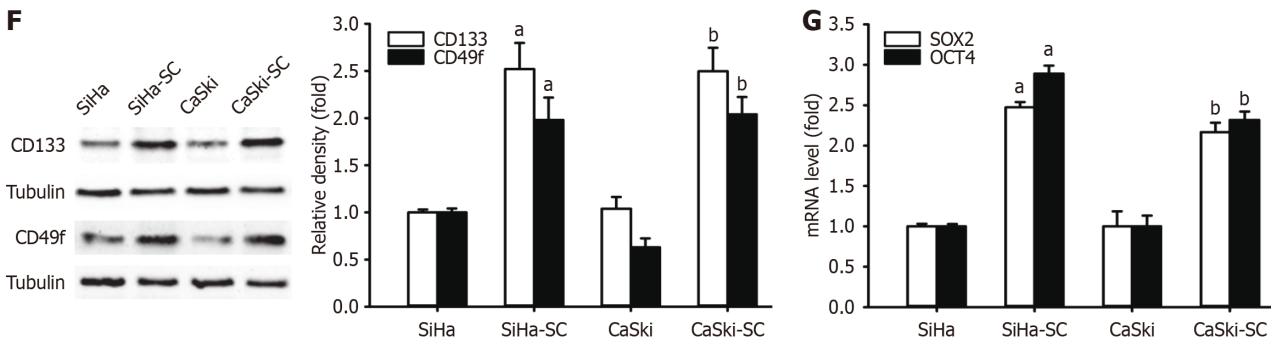

Figure 8 Comparing self-renewal related stemness between SiHa or CaSki cells and the corresponding cervical cancer stem cell-like cells. A: DNA methyltransferase 1 (*DNMT1*) mRNA level in SiHa and CaSki cells and their corresponding cervical cancer stem cell-like cells (CCSLCs); B: MicroRNA (miR)-342-3p level in SiHa and CaSki cells and their corresponding CCSLCs; C: Forkhead box M1 (FOXM1) protein expression level SiHa and CaSki cells and their corresponding CCSLCs with α-tubulin as a loading control; D and E: Representative images of spheres and colonies (left) (scale bars = 100 μm); sphere formation efficiency and colony formation efficiency (right) in SiHa and CaSki cells and their corresponding CCSLCs; F: CD133 and CD49f protein amount with α-tubulin as a loading control; G: SRY-box transcription factor 2 (*SOX2*) and octamer-binding transcription factor 4 (*OCT4*) mRNA levels in SiHa and CaSki cells and their corresponding CCSLCs. $^{a}P < 0.05$ *vs* SiHa cells; $^{b}P < 0.05$ *vs* CaSki cells ($n = 3$). SC: Stem cell.

epigenetic modification enzyme) activates FoxM1 in an epigenetic regulatory event, which simultaneously affects DNMT1 and FoxM1. The above seems to play a relevant role in CC progression, particularly by promoting the CCSLC self-renewal in CC.

Increasing evidence shows that miRNAs are implicated in abnormal machinery of DNA hypermethylation *via* DNMT regulation. In particular, miR-342-3p works as a tumor inhibitor and has low levels in various cancers, such as human acute myeloid leukemia and CC[10,11,19,34]. Interestingly, it has been suggested that miR-342-3p is modulated by DNMT1 *via* promoter methylation in cancerous cells or CSLCs[19,35]. Our study provided evidence that the mutual negative interplay between DNMT1 and miR-342-3p stimulated the emergence of CCSLC self-renewal and carcinogenicity in CCSLCs. Knockdown of DNMT1 elevated miR-342-3p levels and decreased CCSLC self-renewal and carcinogenicity. MiR-342-3p mimic transfection repressed both the transcriptional and posttranscriptional expression of DNMT1. More notably, the overexpression of DNMT1 reversed the blocking impact of overexpressing miR-342-3p on CCSLC self-renewal and carcinogenicity in HeLa cell lines. Furthermore, the luciferase assay showed *DNMT1* as a target gene of miR-342-3p, which would signify that miR-342-3p is particularly implicated in the modulation of DNMT1. These findings suggest that the mutual negative modulation between DNMT1 and miR-342-3p could become a prospective therapeutic approach for treatment through CCSLCs targeting. The above could assist in the search for a demethylating agent in the field of epigenetic cancer therapy.

FoxM1 is a well-known cancerogenic transcription element that plays a role in numerous biological routes, including the generation of CSLC characteristics[21-23]. However, in CCSLCs, the FoxM1-linked upstream modulatory processes remain unclear. This study is consistent with this hypothesis since we observed that knockdown of FOXM1 can replicate the inhibitory impact of miR-342-3p on CCSLC self-renewal. Importantly, increased expression of FOXM1 reversed the suppressive effects of overexpressing miR-342-3p on CCSLC self-renewal and carcinogenicity but did not affect DNMT1 and miR-342-3p expression in HeLa cells. However, one limitation should be noted. Differential self-renewal capability between the CC cell lines HeLa, SiHa, and CasKi used in our study were observed, and the reason was unclear. This may be attributed to the different sensitivities of the cell lines and their differentially expressed genes[36,37].

CONCLUSION

Our results in this work provided a rationale for FoxM1 promoting CCSLC self-renewal by miR-342-3p downregulation, which functioned through the mutual negative modulation between DNMT1 and miR-342-3p in CC. Interestingly, we also demonstrated that overexpression of FOXM1 is able to reverse the suppressive impact of miR-342-3p over CCSLC self-renewal without influencing the expression of miR-342-3p and DNMT1. As far as we know, this is the first report to demonstrate miR-342-3p downregulation *via* upregulation of FOXM1 by DNMT1 activation in promoting CCSLC self-renewal of CC.

ACKNOWLEDGEMENTS

The authors would like to acknowledge Prof. Jian-Guo Cao (Hunan Normal University, Changsha, Hunan) for his enthusiastic support and strong guidance and Prof. Ying-Jun Chen (Guangdong Pharmaceutical University, Guangzhou, Guangdong) for her professional review of the statistical methods of this study.

FOOTNOTES

Author contributions: Cao XZ conducted the experiments and drafted the manuscript; Zhang YF and Yuan L assisted in the study design and data analysis; Song YW and Li JY performed the immunohistochemistry and western blotting of cell and tumor tissue; Tang HL, Qiu YB, and Lin JZ performed the date collection; Ning YX and Wang XY consulted the literature and contributed to revision; Xu Y and Lin SQ contributed equally as co-corresponding authors, whereby Xu Y led the study design, data interpretation, and manuscript preparation, and Lin SQ co-led the experimental design, data analysis, and manuscript editing; All authors approved the final version of the article.

Supported by Guangzhou Basic and Applied Basic Research Foundation, No. 202201010121; Medical Joint Fund of Jinan University, No. YXZY2024014 and No. YXJC2022001; Hospital Achievement Transformation and Cultivation Project, No. ZH201911; the Key Discipline Project of Guangdong Province, No. 2019-GDXK-0016; and the Medical Science and Technology Research Foundation of Guangdong Province, No. B2021145.

Institutional animal care and use committee statement: The study was reviewed and approved by the Committee of Experimental Animal Feeding and Management approved all research assays (Permit No. D2020041).

Conflict-of-interest statement: All the authors report no relevant conflicts of interest for this article.

Data sharing statement: The datasets used and/or analyzed during the current study are available from the corresponding author on reasonable request.

ARRIVE guidelines statement: The authors have read the ARRIVE guidelines, and the manuscript was prepared and revised according to the ARRIVE guidelines.

Country of origin: China

ORCID number: Xiao-Zheng Cao 0000-0003-4259-9317; Ye-Bei Qiu 0000-0001-5322-3310; Shao-Qiang Lin 0000-0002-2931-7648.

S-Editor: Wang JJ
L-Editor: Filipodia
P-Editor: Zhang L

REFERENCES

1 **Liu Y**, Shi W, Mubarik S, Wang F. Assessment of secular trends of three major gynecologic cancers burden and attributable risk factors from 1990 to 2019: an age period cohort analysis. *BMC Public Health* 2024; **24**: 1349 [PMID: 38764017 DOI: 10.1186/s12889-024-18858-3]
2 **Siegel RL**, Giaquinto AN, Jemal A. Cancer statistics, 2024. *CA Cancer J Clin* 2024; **74**: 12-49 [PMID: 38230766 DOI: 10.3322/caac.21820]
3 **Cohen PA**, Jhingran A, Oaknin A, Denny L. Cervical cancer. *Lancet* 2019; **393**: 169-182 [PMID: 30638582 DOI: 10.1016/S0140-6736(18)32470-X]
4 **Pardal R**, Clarke MF, Morrison SJ. Applying the principles of stem-cell biology to cancer. *Nat Rev Cancer* 2003; **3**: 895-902 [PMID: 14737120 DOI: 10.1038/nrc1232]
5 **Beck B**, Blanpain C. Unravelling cancer stem cell potential. *Nat Rev Cancer* 2013; **13**: 727-738 [PMID: 24060864 DOI: 10.1038/nrc3597]
6 **Di Fiore R**, Suleiman S, Drago-Ferrante R, Subbannayya Y, Pentimalli F, Giordano A, Calleja-Agius J. Cancer Stem Cells and Their Possible Implications in Cervical Cancer: A Short Review. *Int J Mol Sci* 2022; **23** [PMID: 35563557 DOI: 10.3390/ijms23095167]
7 **Shang R**, Lee S, Senavirathne G, Lai EC. microRNAs in action: biogenesis, function and regulation. *Nat Rev Genet* 2023; **24**: 816-833 [PMID: 37380761 DOI: 10.1038/s41576-023-00611-y]
8 **Toden S**, Zumwalt TJ, Goel A. Non-coding RNAs and potential therapeutic targeting in cancer. *Biochim Biophys Acta Rev Cancer* 2021; **1875**: 188491 [PMID: 33316377 DOI: 10.1016/j.bbcan.2020.188491]
9 **Xu C**, Sun W, Liu J, Pu H, Li Y. MiR-342-3p inhibits LCSC oncogenicity and cell stemness through HDAC7/PTEN axis. *Inflamm Res* 2022; **71**: 107-117 [PMID: 34842937 DOI: 10.1007/s00011-021-01521-7]
10 **Komoll RM**, Hu Q, Olarewaju O, von Döhlen L, Yuan Q, Xie Y, Tsay HC, Daon J, Qin R, Manns MP, Sharma AD, Goga A, Ott M, Balakrishnan A. MicroRNA-342-3p is a potent tumour suppressor in hepatocellular carcinoma. *J Hepatol* 2021; **74**: 122-134 [PMID: 32738449 DOI: 10.1016/j.jhep.2020.07.039]
11 **Li XR**, Chu HJ, Lv T, Wang L, Kong SF, Dai SZ. miR-342-3p suppresses proliferation, migration and invasion by targeting FOXM1 in human cervical cancer. *FEBS Lett* 2014; **588**: 3298-3307 [PMID: 25066298 DOI: 10.1016/j.febslet.2014.07.020]
12 **Tao K**, Yang J, Guo Z, Hu Y, Sheng H, Gao H, Yu H. Prognostic value of miR-221-3p, miR-342-3p and miR-491-5p expression in colon cancer. *Am J Transl Res* 2014; **6**: 391-401 [PMID: 25075256]
13 **Sun L**, Zhang H, Gao P. Metabolic reprogramming and epigenetic modifications on the path to cancer. *Protein Cell* 2022; **13**: 877-919 [PMID: 34050894 DOI: 10.1007/s13238-021-00846-7]
14 **Zhou S**, Feng S, Qin W, Wang X, Tang Y, Yuan S. Epigenetic Regulation of Spermatogonial Stem Cell Homeostasis: From DNA Methylation

to Histone Modification. *Stem Cell Rev Rep* 2021; **17**: 562-580 [PMID: 32939648 DOI: 10.1007/s12015-020-10044-3]

15 **Wong KK**. DNMT1: A key drug target in triple-negative breast cancer. *Semin Cancer Biol* 2021; **72**: 198-213 [PMID: 32461152 DOI: 10.1016/j.semcancer.2020.05.010]

16 **Pathania R**, Ramachandran S, Elangovan S, Padia R, Yang P, Cinghu S, Veeranan-Karmegam R, Arjunan P, Gnana-Prakasam JP, Sadanand F, Pei L, Chang CS, Choi JH, Shi H, Manicassamy S, Prasad PD, Sharma S, Ganapathy V, Jothi R, Thangaraju M. DNMT1 is essential for mammary and cancer stem cell maintenance and tumorigenesis. *Nat Commun* 2015; **6**: 6910 [PMID: 25908435 DOI: 10.1038/ncomms7910]

17 **Lopez-Bertoni H**, Lal B, Li A, Caplan M, Guerrero-Cázares H, Eberhart CG, Quiñones-Hinojosa A, Glas M, Scheffler B, Laterra J, Li Y. DNMT-dependent suppression of microRNA regulates the induction of GBM tumor-propagating phenotype by Oct4 and Sox2. *Oncogene* 2015; **34**: 3994-4004 [PMID: 25328136 DOI: 10.1038/onc.2014.334]

18 **Lee E**, Wang J, Yumoto K, Jung Y, Cackowski FC, Decker AM, Li Y, Franceschi RT, Pienta KJ, Taichman RS. DNMT1 Regulates Epithelial-Mesenchymal Transition and Cancer Stem Cells, Which Promotes Prostate Cancer Metastasis. *Neoplasia* 2016; **18**: 553-566 [PMID: 27659015 DOI: 10.1016/j.neo.2016.07.007]

19 **Wang H**, Wu J, Meng X, Ying X, Zuo Y, Liu R, Pan Z, Kang T, Huang W. MicroRNA-342 inhibits colorectal cancer cell proliferation and invasion by directly targeting DNA methyltransferase 1. *Carcinogenesis* 2011; **32**: 1033-1042 [PMID: 21565830 DOI: 10.1093/carcin/bgr081]

20 **Gu L**, Liu HM. Forkhead box M1 transcription factor: a novel target for pulmonary arterial hypertension therapy. *World J Pediatr* 2020; **16**: 113-119 [PMID: 31190319 DOI: 10.1007/s12519-019-00271-1]

21 **Kopanja D**, Pandey A, Kiefer M, Wang Z, Chandan N, Carr JR, Franks R, Yu DY, Guzman G, Maker A, Raychaudhuri P. Essential roles of FoxM1 in Ras-induced liver cancer progression and in cancer cells with stem cell features. *J Hepatol* 2015; **63**: 429-436 [PMID: 25828473 DOI: 10.1016/j.jhep.2015.03.023]

22 **Alimardan Z**, Abbasi M, Hasanzadeh F, Aghaei M, Khodarahmi G, Kashfi K. Heat shock proteins and cancer: The FoxM1 connection. *Biochem Pharmacol* 2023; **211**: 115505 [PMID: 36931349 DOI: 10.1016/j.bcp.2023.115505]

23 **Luo W**, Gao F, Li S, Liu L. FoxM1 Promotes Cell Proliferation, Invasion, and Stem Cell Properties in Nasopharyngeal Carcinoma. *Front Oncol* 2018; **8**: 483 [PMID: 30416986 DOI: 10.3389/fonc.2018.00483]

24 **Wang XL**, Cao XZ, Wang DY, Qiu YB, Deng KY, Cao JG, Lin SQ, Xu Y, Ren KQ. Casticin Attenuates Stemness in Cervical Cancer Stem-Like Cells by Regulating Activity and Expression of DNMT1. *Chin J Integr Med* 2023; **29**: 224-232 [PMID: 35809177 DOI: 10.1007/s11655-022-3469-z]

25 **Xu P**, Wang L, Liu Q, Gao P, Hu F, Xie X, Jiang L, Bi R, Ding F, Yang Q, Xiao H. The abnormal expression of circ-ARAP2 promotes ESCC progression through regulating miR-761/FOXM1 axis-mediated stemness and the endothelial-mesenchymal transition. *J Transl Med* 2022; **20**: 318 [PMID: 35842667 DOI: 10.1186/s12967-022-03507-3]

26 **Wang Q**, Liang N, Yang T, Li Y, Li J, Huang Q, Wu C, Sun L, Zhou X, Cheng X, Zhao L, Wang G, Chen Z, He X, Liu C. DNMT1-mediated methylation of BEX1 regulates stemness and tumorigenicity in liver cancer. *J Hepatol* 2021; **75**: 1142-1153 [PMID: 34217777 DOI: 10.1016/j.jhep.2021.06.025]

27 **Sheng Y**, Yu C, Liu Y, Hu C, Ma R, Lu X, Ji P, Chen J, Mizukawa B, Huang Y, Licht JD, Qian Z. FOXM1 regulates leukemia stem cell quiescence and survival in MLL-rearranged AML. *Nat Commun* 2020; **11**: 928 [PMID: 32066721 DOI: 10.1038/s41467-020-14590-9]

28 **Weng W**, Okugawa Y, Toden S, Toiyama Y, Kusunoki M, Goel A. FOXM1 and FOXQ1 Are Promising Prognostic Biomarkers and Novel Targets of Tumor-Suppressive miR-342 in Human Colorectal Cancer. *Clin Cancer Res* 2016; **22**: 4947-4957 [PMID: 27162244 DOI: 10.1158/1078-0432.CCR-16-0360]

29 **Hamurcu Z**, Sener EF, Taheri S, Nalbantoglu U, Kokcu ND, Tahtasakal R, Cınar V, Guler A, Ozkul Y, Dönmez-Altuntas H, Ozpolat B. MicroRNA profiling identifies Forkhead box transcription factor M1 (FOXM1) regulated miR-186 and miR-200b alterations in triple negative breast cancer. *Cell Signal* 2021; **83**: 109979 [PMID: 33744419 DOI: 10.1016/j.cellsig.2021.109979]

30 **Liu H**, Song Y, Qiu H, Liu Y, Luo K, Yi Y, Jiang G, Lu M, Zhang Z, Yin J, Zeng S, Chen X, Deng M, Jia X, Gu Y, Chen D, Zheng G, He Z. Downregulation of FOXO3a by DNMT1 promotes breast cancer stem cell properties and tumorigenesis. *Cell Death Differ* 2020; **27**: 966-983 [PMID: 31296961 DOI: 10.1038/s41418-019-0389-3]

31 **Gao X**, Sheng Y, Yang J, Wang C, Zhang R, Zhu Y, Zhang Z, Zhang K, Yan S, Sun H, Wei J, Wang X, Yu X, Zhang Y, Luo Q, Zheng Y, Qiao P, Zhao Y, Dong Q, Qin L. Osteopontin alters DNA methylation through up-regulating DNMT1 and sensitizes CD133+/CD44+ cancer stem cells to 5 azacytidine in hepatocellular carcinoma. *J Exp Clin Cancer Res* 2018; **37**: 179 [PMID: 30064482 DOI: 10.1186/s13046-018-0832-1]

32 **Zhang MY**, Calin GA, Yuen KS, Jin DY, Chim CS. Epigenetic silencing of miR-342-3p in B cell lymphoma and its impact on autophagy. *Clin Epigenetics* 2020; **12**: 150 [PMID: 33076962 DOI: 10.1186/s13148-020-00926-1]

33 **Chang HW**, Wang HC, Chen CY, Hung TW, Hou MF, Yuan SS, Huang CJ, Tseng CN. 5-azacytidine induces anoikis, inhibits mammosphere formation and reduces metalloproteinase 9 activity in MCF-7 human breast cancer cells. *Molecules* 2014; **19**: 3149-3159 [PMID: 24633350 DOI: 10.3390/molecules19033149]

34 **Wang Y**, Guo X, Wang L, Xing L, Zhang X, Ren J. miR-342-3p Inhibits Acute Myeloid Leukemia Progression by Targeting SOX12. *Oxid Med Cell Longev* 2022; **2022**: 1275141 [PMID: 36120594 DOI: 10.1155/2022/1275141]

35 **Xiong X**, Yang M, Yu H, Hu Y, Yang L, Zhu Y, Fei X, Pan B, Xiong Y, Fu W, Li J. MicroRNA-342-3p regulates yak oocyte meiotic maturation by targeting DNA methyltransferase 1. *Reprod Domest Anim* 2022; **57**: 761-770 [PMID: 35352412 DOI: 10.1111/rda.14119]

36 **Tamizh Selvan G**, Venkatachalam P. Ataxia Telengectesia Protein Influences Bleomycin-Induced DNA Damage in Human Fibroblast Cells. *Cell Biochem Biophys* 2024; **82**: 1235-1242 [PMID: 38696104 DOI: 10.1007/s12013-024-01275-z]

37 **Selvan TG**, Gollapalli P, Kumar SHS, Ghate SD. Early diagnostic and prognostic biomarkers for gastric cancer: systems-level molecular basis of subsequent alterations in gastric mucosa from chronic atrophic gastritis to gastric cancer. *J Genet Eng Biotechnol* 2023; **21**: 86 [PMID: 37594635 DOI: 10.1186/s43141-023-00539-0]

World Journal of Stem Cells

Submit a Manuscript: https://www.f6publishing.com

World J Stem Cells 2025 March 26; 17(3): 100079

DOI: 10.4252/wjsc.v17.i3.100079

ISSN 1948-0210 (online)

ORIGINAL ARTICLE

Basic Study

Regulation of lncRNA-ENST on Myc-mediated mitochondrial apoptosis in mesenchymal stem cells: *In vitro* evidence implicated for acute lung injury therapeutic potential

Ye-Zhou Shen, Guang-Ping Yang, Qi-Min Ma, Yu-Song Wang, Xin Wang

Specialty type: Cell and tissue engineering

Provenance and peer review: Unsolicited article; Externally peer reviewed.

Peer-review model: Single blind

Peer-review report's classification
Scientific Quality: Grade B, Grade C, Grade D, Grade D
Novelty: Grade A, Grade B, Grade C
Creativity or Innovation: Grade A, Grade C, Grade C
Scientific Significance: Grade B, Grade C, Grade C

P-Reviewer: Li SC; Merlin JPJ; Wang G

Received: August 6, 2024
Revised: December 4, 2024
Accepted: February 5, 2025
Published online: March 26, 2025
Processing time: 226 Days and 16.7 Hours

Ye-Zhou Shen, Qi-Min Ma, Yu-Song Wang, Department of Critical Care Medicine, Shanghai East Hospital, Tongji University, Shanghai 200120, China

Guang-Ping Yang, Xin Wang, Medical Center of Burn Plastic and Wound Repair, The First Affiliated Hospital of Nanchang University, Nanchang 330006, Jiangxi Province, China

Co-first authors: Ye-Zhou Shen and Guang-Ping Yang.

Corresponding author: Xin Wang, Medical Center of Burn Plastic and Wound Repair, The First Affiliated Hospital of Nanchang University, No. 17 Yongwai Zhengjie, Donghu District, Nanchang 330006, Jiangxi Province, China. 18772407841@163.com

Abstract

BACKGROUND

Acute lung injury (ALI) is a fatal and heterogeneous disease. While bone marrow mesenchymal stem cells (BMSCs) have shown promise in ALI repair, their efficacy is compromised by a high apoptotic percentage. Preliminary findings have indicated that long noncoding RNA (lncRNA)-ENST expression is markedly downregulated in MSCs under ischemic and hypoxic conditions, establishing a rationale for *in vitro* exploration.

AIM

To elucidate the role of lncRNA-ENST00000517482 (lncRNA-ENST) in modulating MSC apoptosis.

METHODS

Founded on ALI in BEAS-2B cells with lipopolysaccharide, this study employed a transwell co-culture system to study BMSC tropism. BMSCs were genetically modified to overexpress or knockdown lncRNA-ENST. After analyzing the effects on autophagy, apoptosis and cell viability, the lncRNA-ENST/miR-539/c-MYC interaction was confirmed by dual-luciferase assays.

RESULTS

These findings have revealed a strong correlation between lncRNA-ENST levels and the apoptotic and autophagic status of BMSCs. On the one hand, the over-expression of lncRNA-ENST, as determined by Cell Counting Kit-8 assays,

increased the expression of autophagy markers LC3B, ATG7, and ATG5. On the other hand, it reduced apoptosis and boosted BMSC viability. In co-cultures with BEAS-2B cells, lncRNA-ENST overexpression also improved cell vitality. Additionally, by downregulating miR-539 and upregulating c-MYC, lncRNA-ENST was found to influence mitochondrial membrane potential, enhance BMSC autophagy, mitigate apoptosis and lower the secretion of pro-inflammatory cytokines interleukin-6 and interleukin-1β. Collectively, within the *in vitro* framework, these results have highlighted the therapeutic potential of BMSCs in ALI and the pivotal regulatory role of lncRNA-ENST in miR-539 and apoptosis in lipopolysaccharide-stimulated BEAS-2B cells.

CONCLUSION

Our *in vitro* results show that enhanced lncRNA ENST expression can promote BMSC proliferation and viability by modulating the miR-539/c-MYC axis, reduce apoptosis and induce autophagy, which has suggested its therapeutic potential in the treatment of ALI.

Key Words: Long noncoding RNA; Mesenchymal stem cell; Mitochondrial; Apoptosis; Autophagy; Acute lung injury

Core Tip: In this research, we established an acute lung injury (ALI) model and manipulated long noncoding RNA (lncRNA)-ENST levels in bone marrow mesenchymal stem cells (BMSCs) using a lentiviral system. We discovered that lncRNA-ENST00000517482 is a pivotal regulator of BMSC apoptosis and autophagy in ALI. Modulating lncRNA-ENST00000517482 not only reduces apoptosis and induces autophagy in BMSCs but also enhances their viability, offering a novel approach to enhance ALI treatment efficacy *via* the miR-539/c-MYC axis.

Citation: Shen YZ, Yang GP, Ma QM, Wang YS, Wang X. Regulation of lncRNA-ENST on Myc-mediated mitochondrial apoptosis in mesenchymal stem cells: *In vitro* evidence implicated for acute lung injury therapeutic potential. *World J Stem Cells* 2025; 17(3): 100079

URL: https://www.wjgnet.com/1948-0210/full/v17/i3/100079.htm

DOI: https://dx.doi.org/10.4252/wjsc.v17.i3.100079

INTRODUCTION

The typical symptoms of acute lung injury (ALI) include acute respiratory failure with tachypnea, refractory cyanosis, decreased lung compliance, and diffuse pulmonary alveolar infiltrates on chest X-ray[1]. Recently, in addition to the better understanding of the pathophysiology of ALI, there has also been some progress in clinical treatment[2-4]. For example, some treatment concepts and methods, such as lung-protective ventilation, fluid management and extracorporeal membrane oxygenation, have been applied widely. However, the overall clinical mortality rate has not significantly decreased[5,6]. Since the 1990s, mesenchymal stem cells (MSCs) have worked in ALI/acute respiratory distress syndrome and inflammatory lung diseases (chronic obstructive pulmonary disease, asthma, *etc.*)[3,7,8]. Bone marrow derived MSCs (BMSCs) can significantly improve the local and systemic inflammatory response in the lung caused by smoke inhalation injury[9,10].

Extracellular vesicles derived from BMSCs can effectively alleviate pulmonary edema, extensive alveolar hemorrhage, inflammatory cell infiltration, and reduce lung injury scores[9]. Notwithstanding, after injecting a large number of BMSCs into the animals' bodies, most of the BMSCs underwent apoptosis or were lost for unknown reasons within a few days after being transferred to the damaged lung tissue. Ultimately, the number of cells that differentiated into the corresponding functional cells was very limited, which greatly affected the therapeutic efficacy[11]. Chen *et al*[7] confirmed that MSCs transplanted into the lungs exhibited significant apoptosis in ALI caused by ischemia-reperfusion. Autophagy, the primary mechanism for delivering various cellular components to lysosomes for degradation and recycling, plays a crucial protective role in a variety of diseases[12,13]. It was concluded that reducing MSCs apoptosis and improving their transplantation rate and survival rate were key to enhancing the therapeutic efficacy of MSCs.

Mitochondrial apoptosis control is regulated by multiple signaling molecules, including long noncoding RNA (lncRNA). There is growing evidence that lncRNAs are closely associated with the occurrence and progression of various diseases, such as myocardial infarction[14] and cancer[15,16]. In previous experiments, MSCs under hypoxic-ischemic conditions were cultured. Furthermore, a gene chip (Arraystar LncRNA V3.0 Microarray, United States) was employed to screen six significantly downregulated lncRNAs, including lncRNA-ENST00000517482 (lncRNA-ENST). According to small interfering RNA, it was found that MSC apoptosis could be greatly enhanced by interference with lncRNA-ENST, which was not b achieved by interference with the other five lncRNAs. Therefore, lncRNA-ENST was selected as the target gene for further experiments. ENST can promote the progression of papillary thyroid carcinoma by activating the phosphatidylinositol 3-kinase/protein kinase B signaling pathway[17] and inhibit the progression of renal cancer through the Wnt/β-catenin signaling pathway[18].

In mRNA-related studies, microRNAs (miRNAs) are generally considered to be downstream targets of lncRNAs, which can regulate the expression of target mRNAs by competitively binding with miRNAs. By virtue of the RNA22 prediction software, the potential binding sites between lncRNA ENST and miR-539 were identified, which may have regulatory effects on mitochondrial-related proteins. This mechanism of indirectly regulating target mRNAs is known as the competing endogenous RNA (ceRNA) network[19,20].

There is a close relationship between *C-MYC* gene and lncRNA, which can participate in the regulation of cell proliferation and apoptosis through the mitochondrial apoptosis channel[21,22]. Therefore, it can be assumed that when stem cells are subjected to apoptotic stimuli such as ischemia and hypoxia, the expression of lncRNA-ENST in the cell nucleus may be downregulated, leading to changes in mitochondrial outer membrane potential. The formation of permeability transition pores in the mitochondrial outer membrane can then result in increased permeability. Soluble proteins in the intermembrane space and pro-apoptotic factors that enter the cytoplasm, such as cytochrome C, further accelerate the opening of the mitochondrial permeability transition pore and induce stem cell apoptosis. This study aimed to validate the apoptotic regulatory pathway of stem cells involving "lncRNA-miRNA-MYC-mitochondrial apoptosis".

MATERIALS AND METHODS

Cell culture and treatment

BMSCs obtained from Thermo Fisher Scientific (Catalog Number: HUM-iCell-s011) were cultured using the Non-Serum Culture System of Primary Mesenchymal Stem Cells of iCell. The obtained BMSCs were placed in complete culture medium at 37°C with 5% CO_2. Our *in vitro* stem cell study, devoid of animal testing or human samples, complied with scientific and safety protocols, utilizing only commercially available, de-identified cell lines without ethical or privacy concerns.

BMSCs lentivirus transfection

The infection solution was added to the BMSCs culture dish and an appropriate amount of virus was also added based on the cell's multiplicity of infection value. After 18-20 hours of infection, the freshly-prepared medium replaced the ready-prepared medium. After 72 hours, microscopy was employed to observe the fluorescence and infection efficiency.

RNA extraction

According to the manufacturer's instructions, Trizol (Sigma) and an ND-1000 spectrophotometer were utilized to extract the total RNA from cell samples and determine the RNA concentration and purity, respectively. Only samples with an absorbance ratio of 260 nm/280 nm around 2.0 and a ratio of 260 nm/230 nm between 1.9 and 2.2 were considered for further study.

Quantitative reverse transcriptase polymerase chain reaction

SYBR Green Real-Time PCR Master Mix (Thermo Fisher Scientific) was adopted to quantify mRNA levels found using the quantitative reverse transcriptase polymerase chain reaction (PCR) method. The relative levels of the target gene were determined by the -ΔΔCt method. TaqMan miRNA RT-Real Time PCR was employed to detect the levels of miR-539. The TaqMan MicroRNA Reverse Transcription Kit (Vazyme Scientific) was utilized to synthesize single-stranded cDNA, followed by amplification using TaqMan Universal PCR Master Mix (Thermo Fisher Scientific). U6 snRNA was used for normalization. The relative levels of miRNA were determined by means of the -ΔΔCt method.

The primer sequences are as follows: Forward 5′-TGACTTCAACAGCGACACCCA-3′ and reverse 5′-CACCCTGTTGCTGTAGCCAAA-3′ for human GAPDH, forward 5′-TGCTCCCAGAACTGTTTCTCCTGA-3′ and reverse 5′-CTTGGTTGCTGCTCCTGTGTCTT-3′ for human ENST0000051748, forward 5′-GCGGAGAAATTATCCTTG-3′ and reverse 5′-GTGCAGGGTCCGAGGT-3′ for human miR-539, forward 5′-GGCTCCTGGCAAAAGGTCA-3′ and reverse 5′-CTGCGTAGTTGTGCTGATGT-3′ for human MYC.

Cell Counting Kit-8

The cell viability of BMSCs after different interventions was determined using a Cell Counting Kit-8 (CCK-8, LabLead, CK001-5000T). Cells in suspension, counted using a hemocytometer, were plated to form a gradient of cell concentrations. Determined after 2 to 4 hours of cell incubation after seeding, the optical density values were measured, followed by the addition of CCK-8 reagent.

Flow cytometry

After collecting cells treated with different interventions, they were incubated with annexin V-APC and propidium iodide. According to the detection of apoptotic cells by flow cytometry, the results were analyzed using FlowJo software (v10.4.1) (Tree Star, Inc., Ashland, OR, United States).

Western blot

A lysis buffer [(RIPA lysis buffer):(proteinase inhibitor) = 99:1] was employed to perform the protein extraction in the BMSCs culture. After determining protein concentration by the BCA method, electrophoresis, wet transfer, blocking and antibody incubation were carried out. Following color development, the gel was photographed and the expression level of the target protein was analyzed using a gel imaging system. The antibodies used in the study were as follows: LC3B

(Abcam, #ab48394, 1:3000), ATG7 (CST, #8558, 1:1000), GAPDH (Proteintech, #60004-1-Ig, 1:30000), goat anti-rabbit (Beyotime, #A0208, 1:3000), and goat anti-mouse (Beyotime, #A0216, 1:3000).

Cell migration

Cell migration experiments were performed using the Transwell system (Corning, NY, United States) to evaluate the migratory capacity of BMSCs in an indirect co-culture system. BMSCs were seeded in the upper chamber of a Transwell, which was coated with Matrigel. The lower chamber contained BEAS-2B lung epithelial cells treated with lipopolysaccharide (LPS) (10 μg/mL) for 12 hours to simulate an ALI-like inflammatory environment. The biological conditions of ALI were simulated by stimulating lung epithelial cells or macrophages with LPS. This setup allowed for indirect interaction between BMSCs and BEAS-2B cells through soluble factors in the shared medium, without direct cell-to-cell contact. The migration of BMSCs was assessed after a 12-hour incubation period by staining the cells that migrated to the lower surface of the membrane, which was then quantified using a cell counting method.

Enzyme-linked immunosorbent assay

The concentrations of inflammatory cytokines in the culture medium, including interleukin (IL)-6 enzyme-linked immunosorbent assay (ELISA) Kit (ML002293) and IL-1β ELISA Kit (SEKM-0002), were determined by an ELISA assay kit.

The luciferase reporter experiment

DMEM (10 μL) was thoroughly mixed with the desired plasmid (lncRNA-ENST or c-MYC)-3′ untranslated region (0.16 μg) and the hsa-miR-539-5p or negative control (NC) (5 pmol). Then, 10 μL of DMEM and 0.3 μL of transfection reagent were added to the mixture, which was transfected into 293T cells. After 48 hours of transfection, the dual-luciferase® reporter gene detection system was employed to perform a dual luciferase assay of the cells following the manufacturer's instructions.

Statistical analysis

For each sample in every group, three parallel experiments were set up and each experiment was independently repeated three times. The data from the experiments in each group conformed to normal distribution and homogeneity of variance, which are represented as the mean ± SD. GraphPad Prism software version 7.0 was used to analyze the data. Additionally, either an independent samples *t*-test or analysis of variance (ANOVA) was employed to assess differences between the groups. A P value of ≤ 0.05 was considered to indicate statistically significant differences.

RESULTS

Screening and identification of lncRNA ENST

In the preliminary study, we established a BMSC apoptosis model by simulating pulmonary epithelial cells, and screened and identified ischemia and hypoxia related lncRNA-ENST. We obtained the clustering analysis chart (Figure 1A) and the normalized lncRNA expression values (Figure 1B), as well as the volcano plot (Figure 1C). Additionally, through gene chip screening (Arraystar LncRNA V3.0 Microarray, United States) in MSCs cultured under ischemia and hypoxia conditions, we found that the expression of lncRNA-ENST and five other lncRNAs was significantly reduced, suggesting that they may be associated with ischemia and hypoxia-induced apoptosis, while the expression of six other lncRNAs was significantly increased (Figure 1D)

LncRNA-ENST affects the apoptosis and autophagy levels of BMSCs

As shown in Figure 2, observations under an inverted fluorescence microscope demonstrated high transfection efficiency of lentiviral transduction. Knockdown BMSC was constructed by packaging lncRNA-ENST with lentivirus, and quantitative PCR was used to detect the knockdown efficiency of lncRNA-ENST. The results showed that compared to the sh-NC group, the expression efficiency of lncRNA-ENST was significantly reduced in the shlncRNA-ENST group (Figure 3A). Similarly, overexpressed BMSC was constructed by packaging lncRNA-ENST with lentivirus, and quantitative PCR was used to detect the overexpression efficiency of lncRNA-ENST. The results showed that compared to the NC group, the overexpression efficiency of lncRNA-ENST in the lncRNA-ENST-OE group was 343.09 (P < 0.001) (Figure 3B). BMSCs were treated with 10 mmol/L 3-MA, an autophagy inhibitor, and the CCK-8 assay was used to assess cell viability and evaluate cell damage, while flow cytometry was used to detect apoptosis. The results showed that compared to the sh-NC group, the cell viability of the shlncRNA-ENST group was significantly reduced, with an increase in apoptosis levels; and compared to the lncRNA-ENST-OE group, the cell viability of the lncRNA-ENST-OE-3MA group was significantly increased (Figure 3C), with reduced apoptosis and the apoptosis levels and statistical chart are shown in Figure 3D. In addition, the expression of autophagy-related proteins LC3B, ATG7, and ATG5 was upregulated in the silenced group, while the expression in the lncRNA-ENST-OE-3MA group was lower compared to the NC-3MA group (Figure 3E).

BMSCs promote the viability and migration of lung epithelial cells BEAS-2B

A transwell chamber was used to construct an *in vitro* indirect co-culture model. After treating lung epithelial cells BEAS-2B with LPS for 12 hours to induce ALI, the migration level of BMSCs in the ENST knockdown group was decreased, and

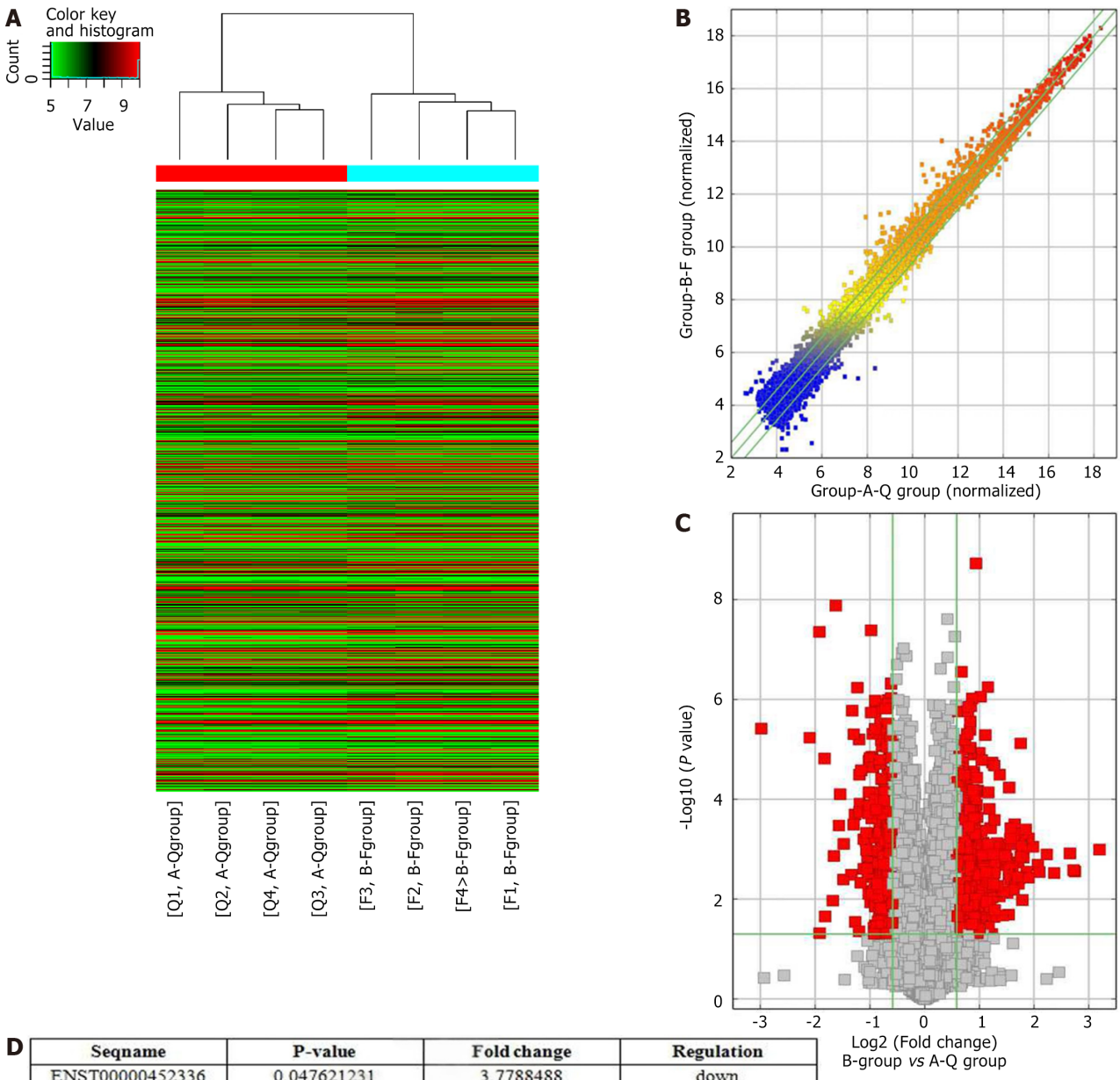

D

Seqname	P-value	Fold change	Regulation
ENST00000452336	0.047621231	3.7788488	down
ENST00000415237	1.50487E-05	3.5532828	down
ENST00000517482	1.65358E-06	2.5000627	down
ENST00000455081	0.000318203	2.4604451	down
ENST00000581442	6.24881E-06	2.2934846	down
ENST00000475331	7.15689E-05	2.0285119	down
ENST00000453348	0.001010134	9.149845	up
ENST00000416124	0.002602645	6.5702061	up
ENST00000434859	0.002969832	5.1535587	up
ENST00000555250	0.002816394	4.2674811	up
ENST00000422831	0.00060091	3.7332966	up
ENST00000422366	0.002795976	3.6307133	up

ENST00000517482 Ensembl Transcript chromosome:GRCh38:8:1:145138636:1
TTCCATTACCGGCCAGCTACATTTAAGGGGCCATTCAACAGTGGCAGGGAGGGAAGAGCC
ACAGCTCTGGAGAGCACTCTTTTCTTCTGGTCCATTATTTTCCCTGAAGAGACCCCTGAC
GCCTAAAGAGACGGTATCGCTCTGCTGCCCAGGCTGCAGTGCAGTGGCACAATCACAGCT
GACGGCAGACTTGACCCCCCCAGGCTCAAGCGATCCTCCCACCTCAGCCTCCAGAGTAGC
TTGGACTACAGCCCTGTCTCAGTGTGGCCTGCTCCCAGAACTGTTTCTCCTGACTTCTCA
TTTCACCAAGAAGACATGGACTCAGAAAAATGAAGAGAGAAACACAAAGACACAGGAGCA
GCAACCAAGCCCCTCTTCTCCAGGCAATCATCTGACTTCAATTGGCATAGACCCCTTAGG
GGTGTGGACACTGTCTGAAAGTATCTGGAGAGACCAAGTTTCAGCAGCCACTAAGCTGTC
AAGGCTCTTTAAAAATCTGATTCCTGGCCAGGCACGGGGGCGCACGCCTGTCACCCCAGT
ACTTTGGGAGGCT

Figure 1 Screening and identification of ischemia, hypoxia, and oxidative stress-related long noncoding RNAs in lung injury. A: Heatmap of differentially expressed long noncoding RNAs (lncRNAs) between lung injury groups and controls; B: Based on the normalized lncRNA expression levels in lung injury

and control groups; C: Volcano plot of differentially expressed lncRNAs between lung injury and control groups; D: Sequences of lncRNAs and lncRNA-ENST screened by gene chip.

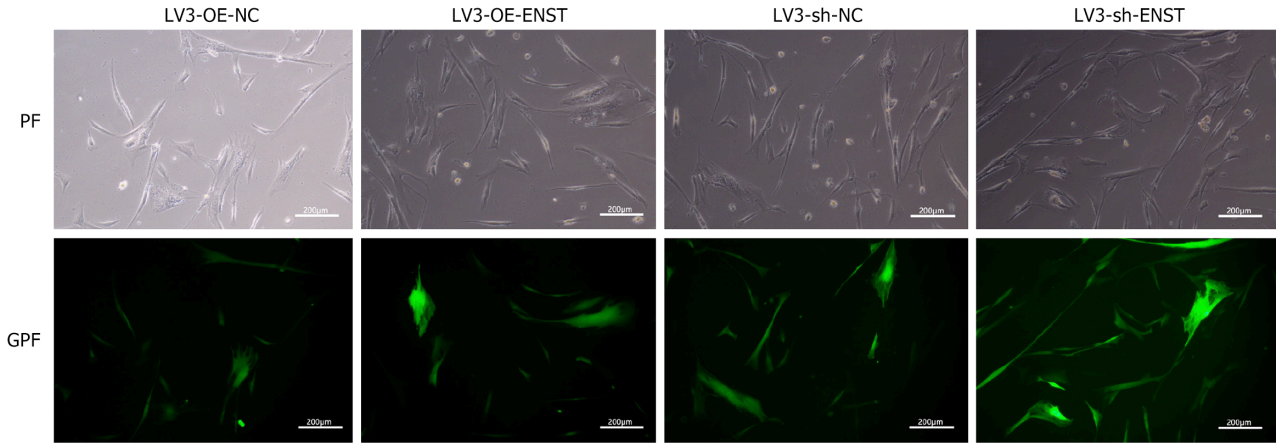

Figure 2 Inverted fluorescence microscopy was used to observe the cell lentiviral transfection efficiency. "Transfection efficiency" was qualitatively evaluated based on green photo fluorescence, with cells exhibiting green photo fluorescence expression considered successfully transfected. "Quantitative analysis" was performed by flow cytometry, where the percentage of green photo fluorescence-positive cells was determined. The transfection efficiency was calculated to be "greater than 80%" based on flow cytometry results. NC: Negative control; PF: Photo fluorescence; GPF: Green photo fluorescence; OE: Overexpression.

the viability of BEAS-2B cells was reduced. In contrast, the migration level of BMSCs in the ENST overexpression group was increased, and the viability of BEAS-2B cells was enhanced (Figure 4A and B). At the same time, ELISA experiments observed that the overexpression of ENST significantly decreased the expression levels of related factors IL-1β and IL-6 (Figure 4C).

LncRNA ENST binds to miR-539-5p

In preliminary work, we used the RNA22 prediction software to identify potential binding sites between lncRNA-ENST and miR-539. Through luciferase assays, we found that the mimic of miR-539-5p significantly inhibited the luciferase activity of the wild-type ENST reporter gene but had no significant effect on the luciferase activity of the mutant ENST reporter gene. Additionally, the level of ENST was overexpressed or silenced in BMSCs (Figure 5A).

MiR-539-5p binds to c-MYC

Similarly, the luciferase reporter assay revealed the presence of miR-539 binding sites in the 3′ untranslated region of c-MYC. The luciferase activity of the wild-type c-MYC reporter gene was inhibited by the mimic of miR-539-5p, while no significant change was observed in the luciferase activity of the mutant c-MYC reporter gene (Figure 5B).

LncRNA ENST is involved in regulation through the miR-539-5p/c-MYC axis

Through luciferase reporter assays, we validated the binding sites between lncRNA ENST and miR-539-5P, as well as the binding sites between miR-539-5P and c-MYC. As shown in Figure 6, observations under an inverted fluorescence microscope demonstrated high transfection efficiency of lentiviral transduction. Using lentivirus packaging, we constructed plasmids for the overexpression of lncRNA ENST and the knockdown of c-MYC. Through quantitative reverse transcriptase PCR, we found that successful overexpression of ENST resulted in downregulation of miR-539-5P expression and upregulation of c-MYC expression. After functionally silencing c-MYC, we also observed the same effects: Silencing c-MYC led to downregulation of lncRNA-ENST expression and upregulation of c-MYC expression. By combining the binding sites among the three genes, we discovered that lncRNA-ENST is involved in regulation through the miR-539-5P/c-MYC axis (Figure 7).

LncRNA ENST regulates autophagy and apoptosis of BMSCs through the miR-539-5p/c-MYC axis

After identifying the ceRNA regulatory relationship among the three genes, we detected apoptosis and autophagy of BMSCs. Flow cytometry analysis revealed that the apoptosis level of the OE-lncRNA-ENST + NC (KD) group was significantly decreased, while the apoptosis level of the sh-cMYC + NC (OE) group was significantly increased, and the apoptosis levels and statistical chart are shown in Figure 8A. Western blot analysis of autophagy-related proteins indicated that the expression of autophagy-related proteins LC3B, ATG7, and ATG5 was significantly upregulated in the OE-lncRNA-ENST + NC (KD) group, whereas the expression levels of autophagy-related proteins were significantly downregulated in the sh-cMYC + NC (OE) group (Figure 8B). This suggests that lncRNA-ENST induces autophagy in BMSCs through the miR-539-5p/c-MYC axis, reducing their apoptosis level.

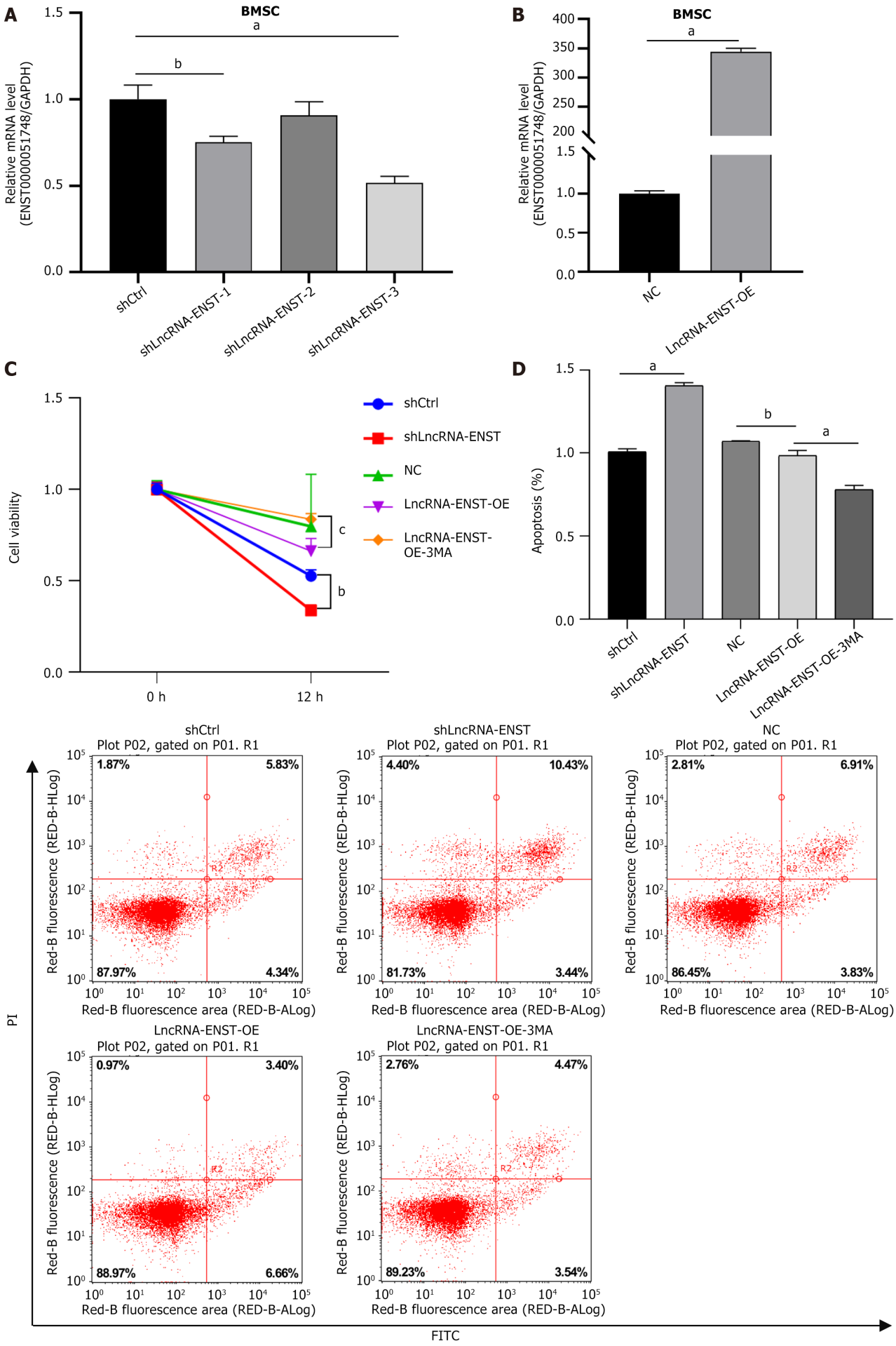
A
BMSC
Relative mRNA level (ENST00000051748/GAPDH)
shCtrl
shLncRNA-ENST-1
shLncRNA-ENST-2
shLncRNA-ENST-3
B
BMSC
Relative mRNA level (ENST00000051748/GAPDH)
NC
LncRNA-ENST-OE
C
Cell viability
0 h
12 h
shCtrl
shLncRNA-ENST
NC
LncRNA-ENST-OE
LncRNA-ENST-OE-3MA
D
Apoptosis (%)
shCtrl
shLncRNA-ENST
NC
LncRNA-ENST-OE
LncRNA-ENST-OE-3MA
shCtrl
Plot P02, gated on P01. R1
1.87%
5.83%
87.97%
4.34%
shLncRNA-ENST
Plot P02, gated on P01. R1
4.40%
10.43%
81.73%
3.44%
NC
Plot P02, gated on P01. R1
2.81%
6.91%
86.45%
3.83%
LncRNA-ENST-OE
Plot P02, gated on P01. R1
0.97%
3.40%
88.97%
6.66%
LncRNA-ENST-OE-3MA
Plot P02, gated on P01. R1
2.76%
4.47%
89.23%
3.54%
Red-B fluorescence (RED-B-HLog)
Red-B fluorescence area (RED-B-ALog)
PI
FITC

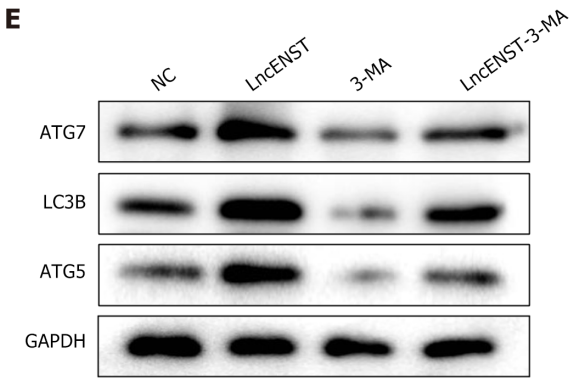

Figure 3 Long noncoding RNA-ENST affects the apoptosis and autophagy levels of bone marrow mesenchymal stem cells. A: The quantitative polymerase chain reaction analysis revealed the knockdown efficiency of long noncoding RNA (lncRNA)-ENST (n = 3); B: The quantitative polymerase chain reaction analysis showed the overexpression efficiency of lncRNA-ENST (n = 3); C: The Cell Counting Kit-8 assay was used to evaluate cell viability and assess cell damage (n = 3); D: Flow cytometry dual staining was conducted to detect cell apoptosis (apoptosis level statistics chart and flow cytometry chart) (n = 3); E: Western blot analysis was performed to detect the expression of LC3B, ATG7, and ATG5 after knocking down lncRNA-ENST (n = 3). $^{a}P < 0.001$, $^{b}P < 0.01$, $^{c}P < 0.05$. BMSC: Bone marrow mesenchymal stem cell; LncRNA: Long noncoding RNA; NC: Negative control; OE: Overexpression.

LncRNA ENST regulates the cell viability and mitochondrial membrane potential of BMSCs through the miR-539-5p/c-MYC axis

We constructed overexpression plasmids for LncRNA-ENST and knockdown plasmids for c-MYC, packaged lentivirus, and infected BMSCs. We assessed cell damage using the CCK-8 assay to detect BMSC viability. The results showed that cell viability in the OE-lncRNA-ENST + NC (KD) group was significantly increased ($P < 0.001$), while cell viability in the sh-cMYC + NC (OE) group was significantly decreased (Figure 9A). In the JC-1 staining experiments to detect mitochondrial membrane potential, it was observed that the overexpression of ENST resulted in a significant increase in mitochondrial membrane potential, while c-MYC knockdown led to a significant decrease in mitochondrial membrane potential (Figure 9B).

DISCUSSION

Autophagy and apoptosis are two interrelated mechanisms that occur in response to cellular stress. However, the molecular interactions between these two mechanisms have not been fully understood. It is well known that autophagy serves as a cellular protective mechanism under physiological conditions, which encompasses the negative regulation of cell apoptosis, and *vice versa*. Recent research has confirmed the cross-talk between autophagy and apoptosis, which was manifested through the regulation of shared pathways and genes. These regulated genes consisted of p53, Atg5, Bcl-2 and others. Stimulation leading to the activation or inhibition of these genes would have effects on the cellular fate through specific pathways[23].

As a hot topic of research, lncRNA ENST has played a significant role in numerous biological processes, such as epigenetic regulation, cell cycle control, regulation of apoptosis and senescence, cell differentiation, transcription and post-transcriptional regulation[24-26]. *MYC* is an important regulatory gene in the process of tumorigenesis[27]. The encoded protein by c-*MYC* gene, which is a vital intracellular transcription factor as a proto-oncogene, mediates the transfer of biological signals from extracellular to intracellular to the nucleus. Moreover, it is involved in the regulation of cell proliferation, metabolism and apoptosis. The normal c-*MYC* gene maintains cell division and proliferation. Notwithstanding, if the external signal changes or the cell genetic genes are damaged, the c-*MYC* gene will induce cell apoptosis [28,29].

This study has demonstrated that the lncRNA-miR-539-c-MYC axis selectively regulates the apoptosis and autophagy of BMSCs and may potentially serve as a novel pathway to enhance the survival rate of BMSCs and ALI. Through small interfering RNA interference, it was found that the interference with lncRNA-ENST led to a significant increase in MSCs apoptosis, while the interference with the other 5 lncRNAs had little effects on MSCs apoptosis. Furthermore, the luciferase reporter assay demonstrated the binding sites between lncRNA ENST and miR539, as well as between miR539 and c-MYC. Therefore, the scientific hypothesis has been proposed that when stem cells are stimulated by apoptotic signals such as ischemia or hypoxia, the downregulation of nuclear lncRNA-ENST, in cooperation with MYC, induces conformational changes in the pro-apoptotic protein BAX/BAK, located in the cytoplasm. These changes bring about the translocation to the outer mitochondrial membrane and help the formation of pores for release, thus enhancing mitochondrial membrane permeability. Furthermore, by allowing the soluble proteins in the intermembrane space and pro-apoptotic factors such as cytochrome C to enter the cytoplasm, apoptosis in stem cells is ultimately triggered (Figure 10).

This study has determined the effects of lncRNA-ENST on the apoptosis of BMSCs under conditions of ischemia and hypoxia. The experimental studies of knockdown and overexpression have demonstrated that lncRNA expression within a certain range can enhance the autophagy of MSCs and reduce the apoptosis rate. Under conditions such as ischemia

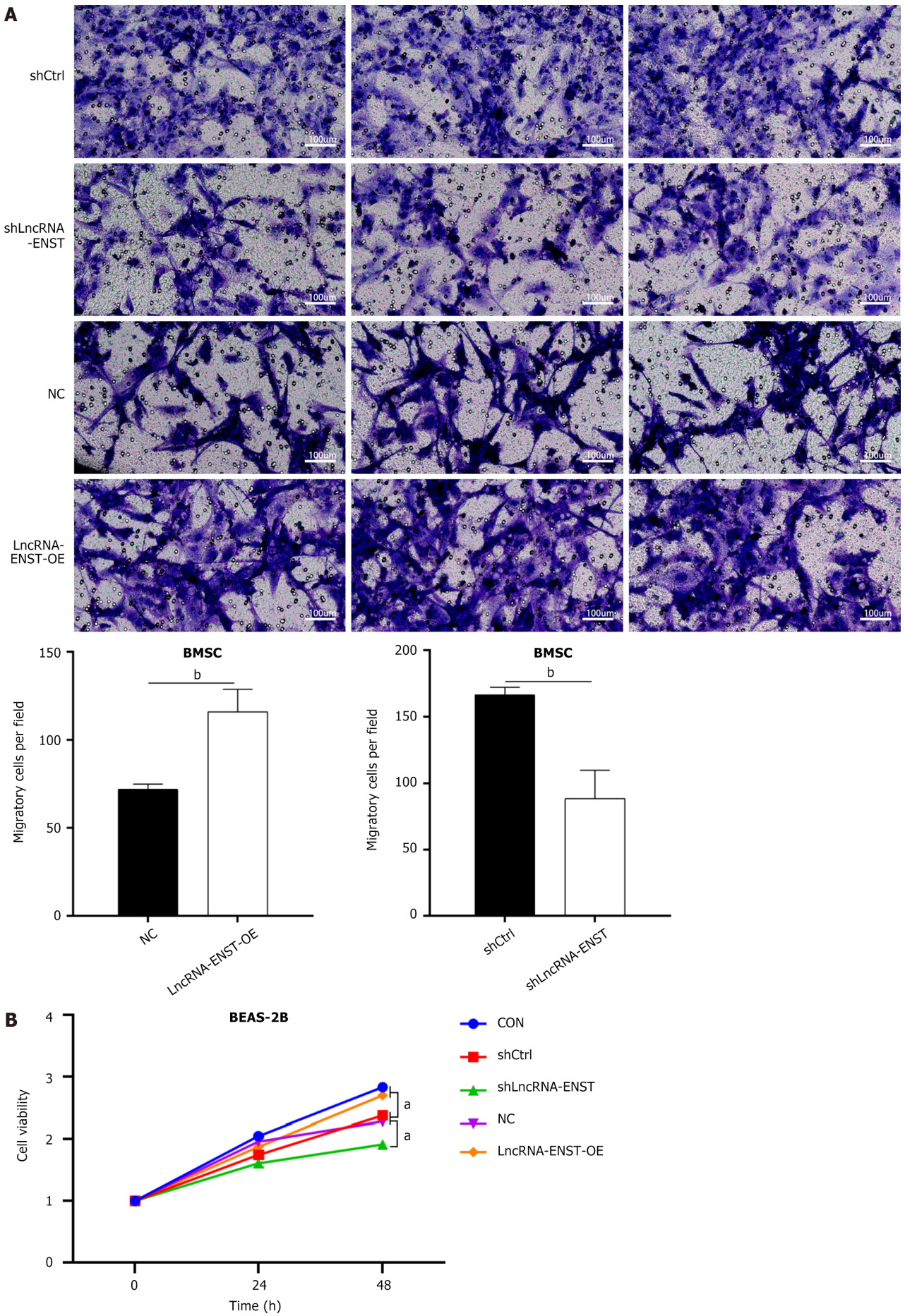
A
shCtrl
shLncRNA -ENST
NC
LncRNA-ENST-OE
100um
BMSC
b
Migratory cells per field
150
100
50
0
NC
LncRNA-ENST-OE
BMSC
b
Migratory cells per field
200
150
100
50
0
shCtrl
shLncRNA-ENST
B
BEAS-2B
Cell viability
4
3
2
1
0
0
24
48
Time (h)
a
a
CON
shCtrl
shLncRNA-ENST
NC
LncRNA-ENST-OE

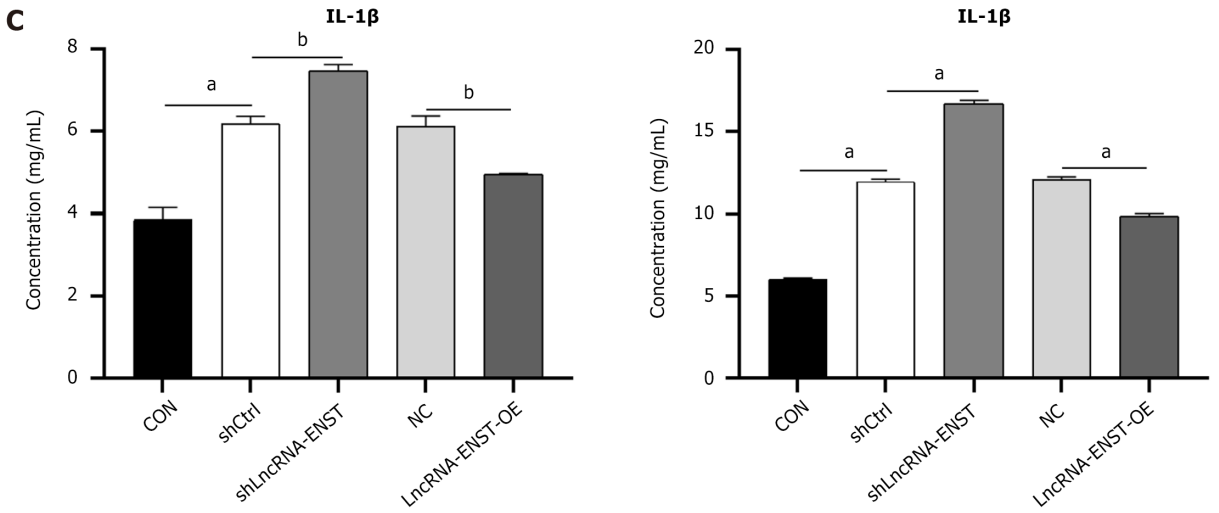

Figure 4 Bone marrow mesenchymal stem cells influence the migration of lung epithelial cells BEAS-2B in an indirect co-culture system. A: Transwell assay was employed to evaluate the migration ability of bone marrow mesenchymal stem cells (n = 3); B: Cell Counting Kit-8 assay was performed to assess the viability of BEAS-2B cells (n = 3); C: Enzyme-linked immunosorbent assay was used to detect the expression of interleukin-1β and interleukin-6 (n = 3). ^{a}P < 0.001, ^{b}P < 0.01. BMSC: Bone marrow mesenchymal stem cell; LncRNA: Long noncoding RNA; NC: Negative control; OE: Overexpression; IL: Interleukin.

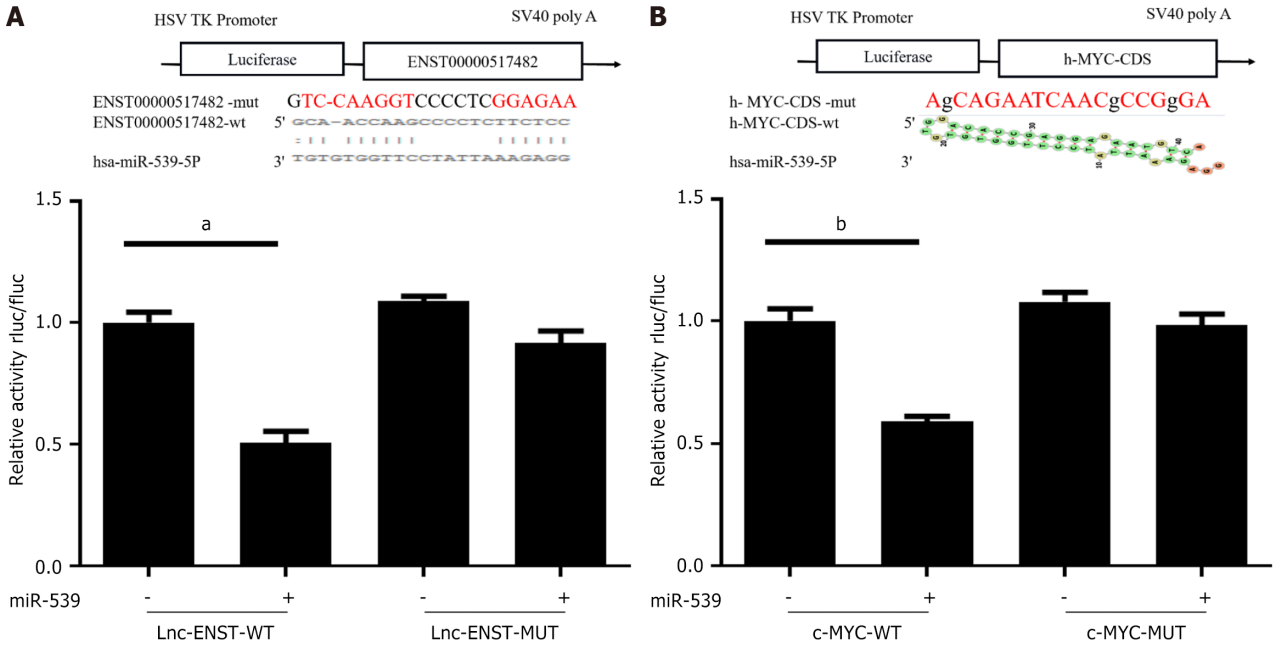

Figure 5 Dual-luciferase reporter assay was performed to investigate both the binding affinity and transcriptional regulation between lncRNA-ENST and miR-539. A: The assay assessed the binding affinity between lncRNA-ENST and miR-539-5p; B: The same assay was performed to assess the interaction between c-MYC and miR-539-5p and its impact on luciferase activity. ^{a}P < 0.001, ^{b}P < 0.01.

and hypoxia, the apoptosis of MSCs was regulated by various aspects of lncRNA. First, the expression of lncRNA-ENST can enhance autophagy by increasing the expression of autophagy-related proteins, and make full use of intracellular injurious substances to improve the stress ability of cells and lower cell apoptosis. Moreover, inhibition of its expression will lead to a further increase in cell apoptosis. However, it has found that when autophagy inhibitors were added to overexpressed lncRNA-ENTS, the apoptosis level of cells was significantly decreased. It can be assumed that cells can reduce apoptosis by raising autophagy to a certain extent, but when the autophagy level is too high, apoptosis will increase. At the same time, the expression of ENST can also reduce cell apoptosis by enhancing the migration ability of BMSCs, increasing cell activity and reducing the expression of inflammation-related factors IL-6 and IL-1β. The mechanism may be related to the down-regulation of miRNA-539 and its synergistic effect with *c-MYC* gene and the decreased expression of apoptosis-related proteins.

Through the dual luciferase system, the binding sites between lncRNA and mirNA-539 and the binding sites between miRNA and *c-MYC* gene, even encompassing the interaction through binding sites, were verified. Previous studies have confirmed that lncRNA and miRNA can interact with each other through binding, lncRNA can regulate miRNA

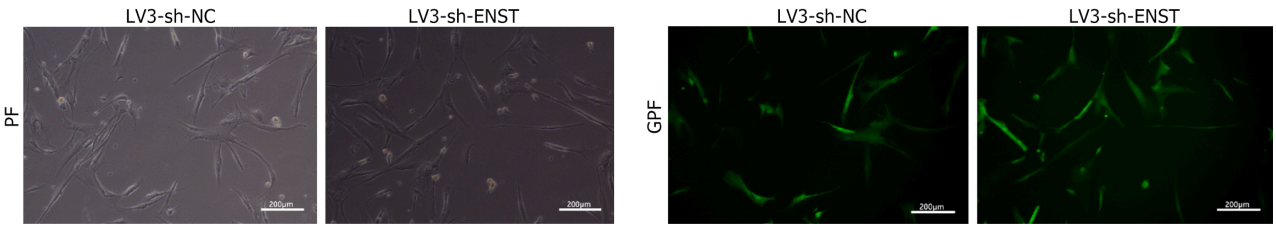

Figure 6 Inverted fluorescence microscopy was used to assess lentiviral transfection efficiency. The percentage of green photo fluorescence-positive cells was calculated using flow cytometry (n = 3). A transfection efficiency of "greater than 80%" was considered high, based on green photo fluorescence. Flow cytometry analysis confirmed the high transfection efficiency in both bone marrow mesenchymal stem cells and 293T cells. NC: Negative control; PF: Photo fluorescence; GPF: Green photo fluorescence.

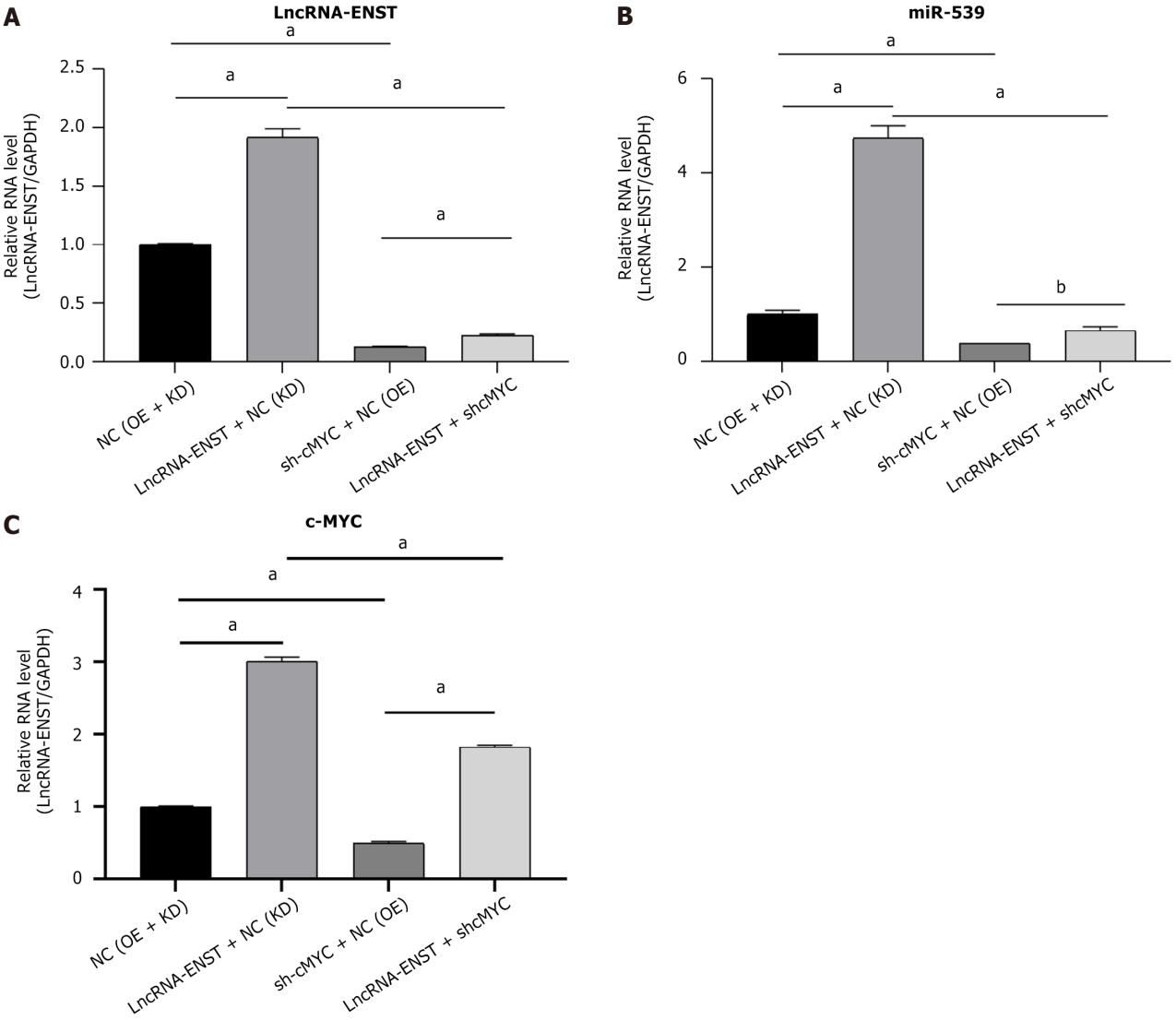

Figure 7 Long noncoding RNA ENST is involved in regulation through the miR-539-5p/c-MYC axis. A: Quantitative polymerase chain reaction was conducted to measure the expression levels of long noncoding RNA-ENST and sh-cMYC (n = 3); B: Quantitative polymerase chain reaction was used to detect the expression levels of *miR539* gene (n = 3); C: Quantitative polymerase chain reaction was conducted to measure the expression levels of *c-MYC* gene (n = 3). ^{a}P < 0.001, ^{b}P < 0.01. LncRNA: Long noncoding RNA; NC: Negative control; KD: Knockdown; OE: Overexpression.

expression through competitive binding and miRNA can influence its activity after binding with lncRNA[30,31]. For example, during the occurrence of colorectal cancer, lncRNA can reduce the expression of miRNA through its binding with miRNA, thus affecting the biological behavior of tumor cells[32]. In addition, the genetic analysis of leukemia cells has shown that when miRNA-155 is overexpressed in leukemia cell lines, the expression level of target lncRNA is significantly decreased; conversely, the opposite is also true[33]. This study found that the expression of lncRNA was negatively correlated with that of miRNA, that is, the overexpressed lncRNA could reduce the apoptosis of MSCs by inhibiting the expression of miRNA. At present, the role of miRNAs is mainly based on the hypothesis of the competitive

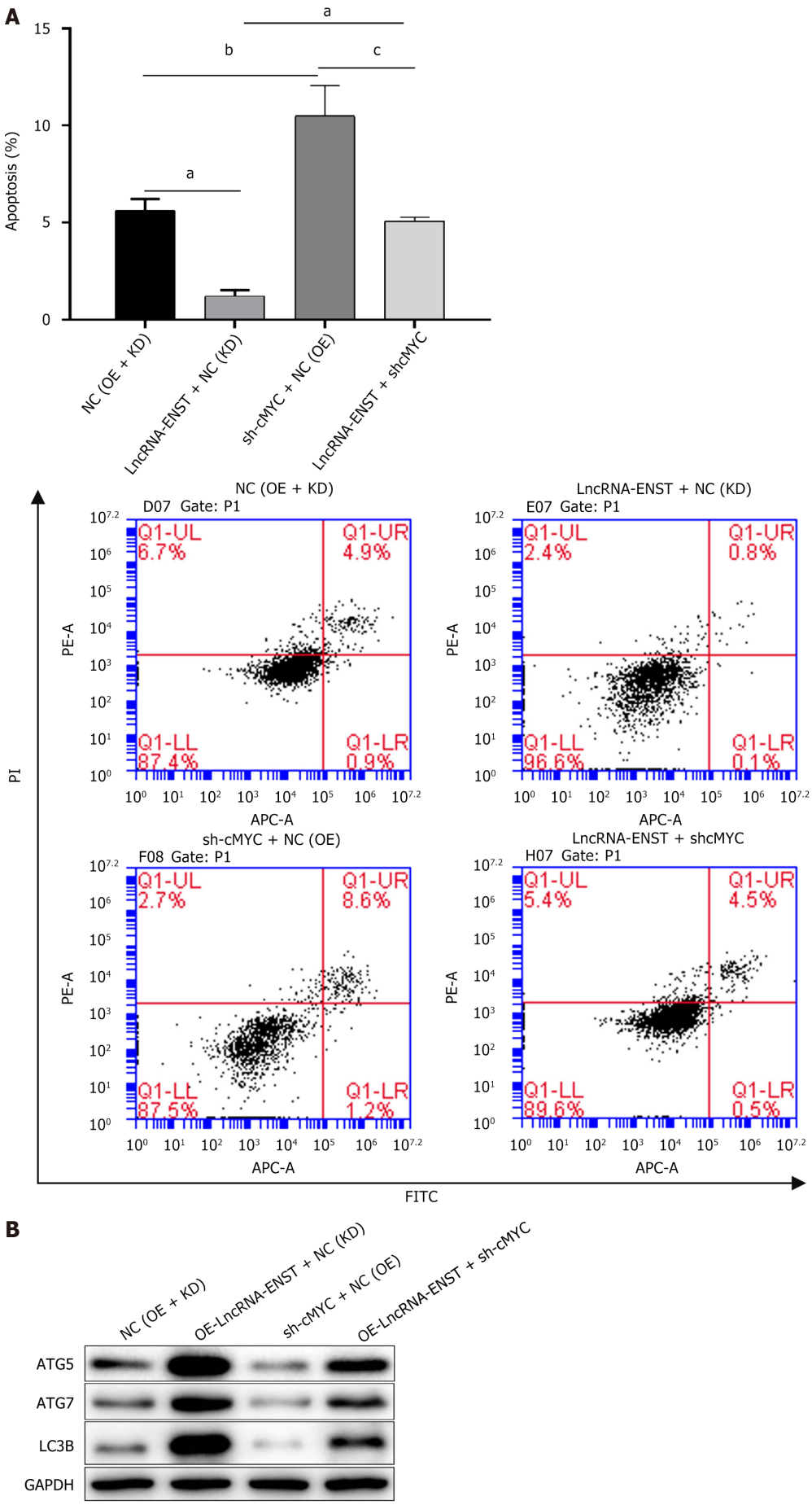

Figure 8 Long noncoding RNA ENST regulates autophagy and apoptosis of bone marrow mesenchymal stem cells through the miR-539-

5p/c-MYC axis. A: Flow cytometry was used to detect cell apoptosis (apoptosis level statistics chart and flow cytometry chart) (n = 3); B: Western blot was used to detect the protein expression of autophagy-related proteins LC3B, ATG7, and ATG5 (n = 3). $^{a}P < 0.001$, $^{b}P < 0.01$, $^{c}P < 0.05$. LncRNA: Long noncoding RNA; NC: Negative control; KD: Knockdown; OE: Overexpression; PI: Propidium iodide.

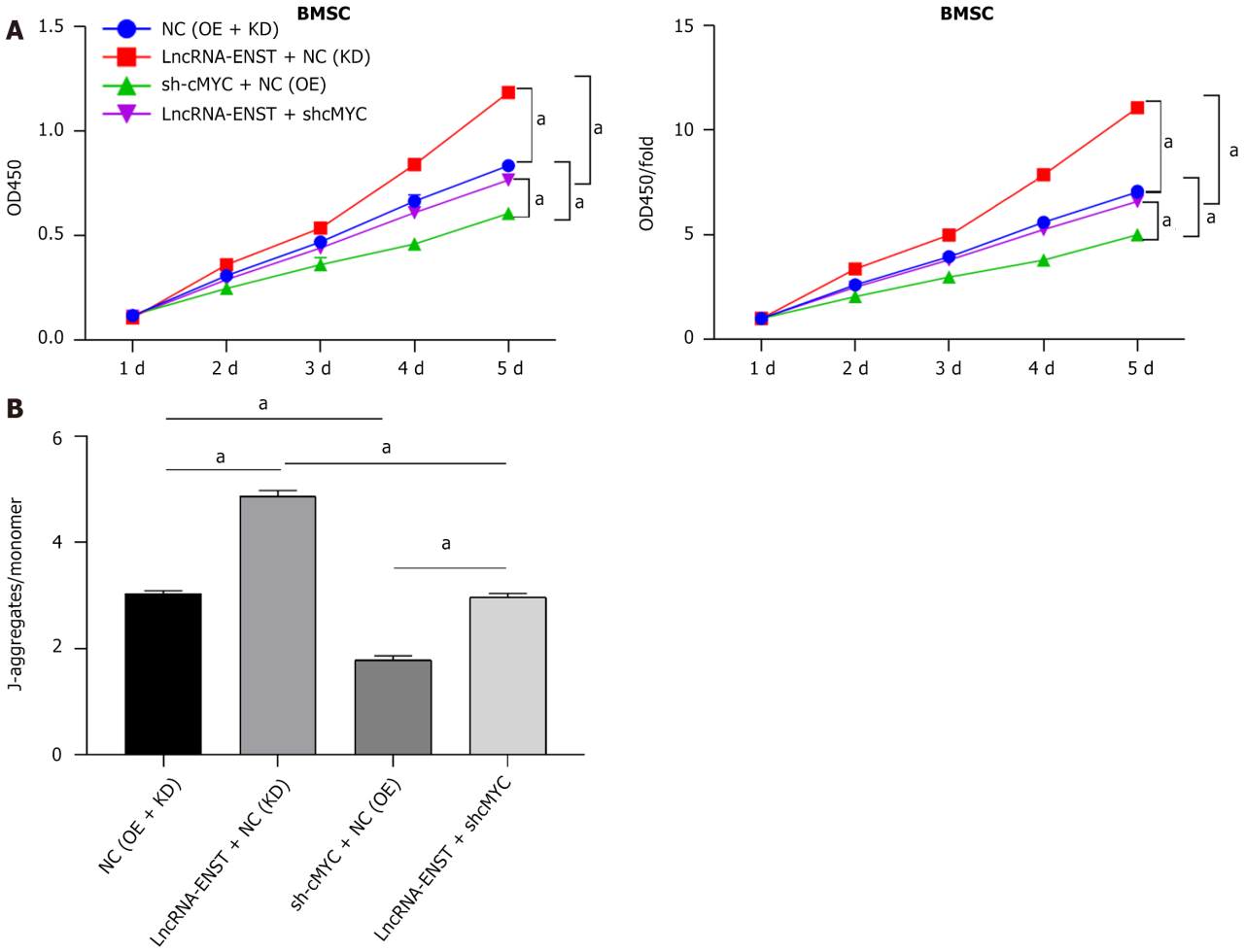

Figure 9 Long noncoding RNA ENST regulates the cell viability and mitochondrial membrane potential of bone marrow mesenchymal stem cells through the miR-539-5p/c-MYC axis. A: Cell Counting Kit-8 assay was performed to measure the viability of bone marrow mesenchymal stem cells (n = 3); B: JC-1 staining was performed to detect mitochondrial membrane potential (n = 3). $^{a}P < 0.001$. BMSC: Bone marrow mesenchymal stem cell; LncRNA: Long noncoding RNA; NC: Negative control; KD: Knockdown; OE: Overexpression.

internal RNA (ceRNA) network, that is, miRNAs can affect the expression of target mRNA through the competitive role of lncRNA. In this experiment, the effect of miRNA-539 on the expression of *c-MYC* gene is through direct binding, but whether it also has an effect on the expression of *c-MYC* gene through indirect influence on lncRNA expression requires further study. In the validation experiments of the lncRNA-miRNA-c-MYC axis, it has found that lncRNA overexpression promoted the expression of *c-MYC* gene. In the case of lncRNA overexpression, knocking down *c-MYC* gene could lead to a decrease in lncRNA expression, while in the case of normal lncRNA expression, lncRNA could reduce the expression of *c-MYC* gene. Knockdown of *c-MYC* gene led to increased lncRNA expression.

A possible explanation for this is that the influence of the *c-MYC* gene on lncRNA is associated with the expression status of the lncRNA itself. Through detection of the *miR539* gene, it was found that overexpression of lncRNA can reduce miR539 expression, while knockdown of the *c-MYC* gene can increase miR539 expression. The results of protein detection related to cell activity, apoptosis and autophagy are consistent with those of the lncRNA knockdown/overexpression experiments. Therefore, it is reasonable that the lncRNA-miRNA-c-MYC axis can induce changes in autophagy, cell activity and inflammatory factors in BMSCs, thereby exerting an influence on the level of cell apoptosis.

As important organelles in MSCs, mitochondria not only provide ATP in MSCs, but also transmit extracellular and intracellular signals when MSCs are subjected to environmental stress or injury. Persistent mitochondrial dysfunction can lead to hypoxia-induced MSCs injury, thus causing reduced stem cell therapy efficacy after MSCs apoptosis and inhalation injury[34,35]. BAX/BAK is an important protein that influences mitochondrial fate by regulating mitochondrial permeability and further regulates mitochondrial transport by influencing mitochondrial permeability transition pores[36-38]. The detection of mitochondrial membrane potential by JC-1 staining has shown that lncRNA

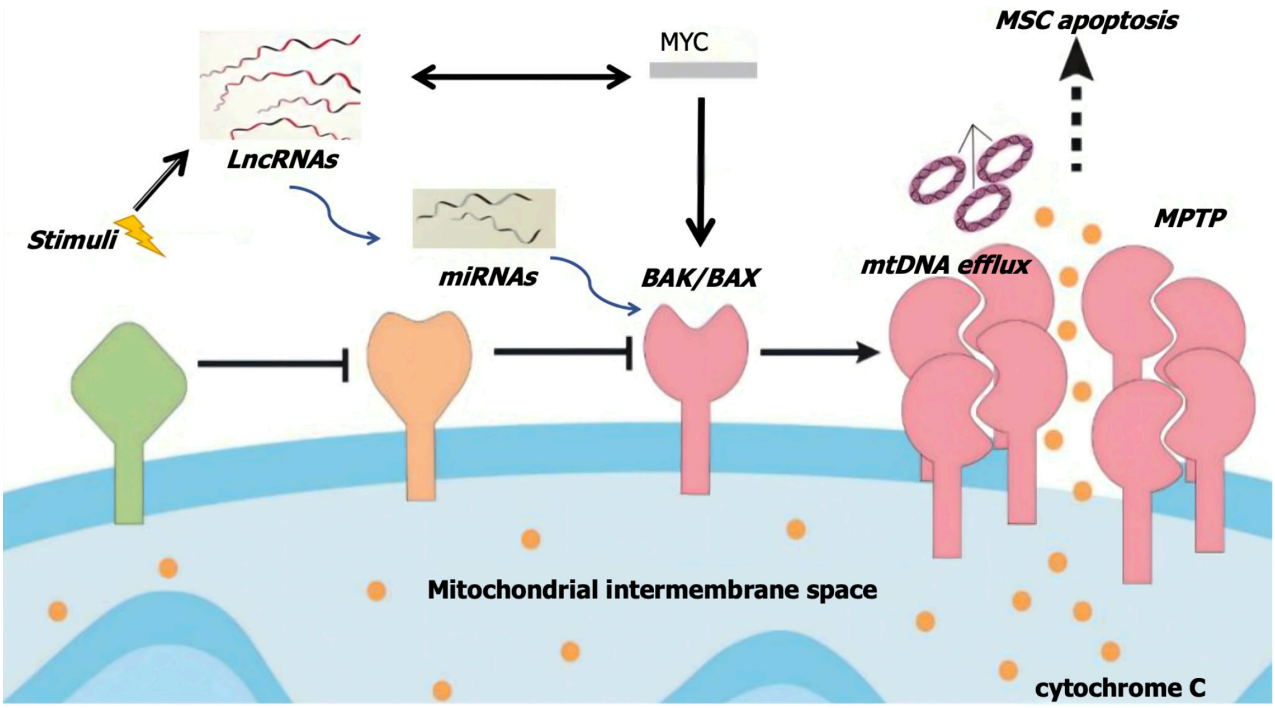

Figure 10 Schematic diagram of long noncoding RNA-microRNA-MYC-BAX/BAK-mitochondrial permeability transition pore apoptosis pathway. LncRNAs: Long noncoding RNAs; miRNAs: MicroRNAs; MSC: Mesenchymal stem cell; MPTP: Mitochondrial permeability transition pore.

overexpression can result in a significant increase in mitochondrial membrane potential, while knockdown of *c-MYC* gene can lead to a significant reduction in mitochondrial membrane potential. These results revealed that the lncRNA-miRNA-c-MYC axis can change mitochondrial membrane potential. Specifically, the membrane potential is impacted by the change in relevant proteins on the mitochondrial membrane, which then leads to changes in mitochondrial permeability. In addition, it has also been indirectly verified that the lncRNA-miRNA-c-MYC axis can change the permeability of the mitochondrial membrane by regulating BAX/BAK, thus affecting the apoptosis level of cells.

At present, there is a lot of evidence that lncRNA can control mitochondrial function and change disease prognosis by regulating the dynamics of mitochondrial-related proteins and mitochondrial channel proteins[39]. However, even outside the field of stem cell research, there are no studies to demonstrate the specific association and mechanism of action between lncRNA and c-MYC. This study has revealed that the regulation of BMSCs apoptosis may be realized through a synergistic effect between the two. Whether *lncRNA* and *c-MYC* gene interact with each other through direct binding or through miR539 as an intermediate to achieve mutual influence, and whether miR539 affects *c-MYC* gene indirectly through lncRNA, requires further investigation.

It should be noted that this research also has limitations. Specifically, the reliance on *in vitro* experiments and an LPS-induced ALI model may not fully represent the intricacies of the human disease. While these *in vitro* experiments have suggested that lncRNA-ENST has therapeutic potential for ALI, this study has emphasized that these findings are preliminary and require validation with *in vivo* models to confirm their clinical translational potential. Future research must bridge this gap by extending the investigation to *in vivo* environments, ensuring that our understanding of the role of lncRNA-ENST in ALI is both comprehensive and clinically relevant.

CONCLUSION

This study has proved that lncRNA-ENST can reduce pulmonary epithelial cell apoptosis in the treatment of ALI, thereby enhancing the therapeutic effects. Furthermore, it has revealed the potential of the lncRNA-ENST-miR539-c-MYC axis in treating ALI by elucidating its regulatory mechanism. However, these results are based on *in vitro* experiments, and further *in vivo* studies are required to validate the therapeutic potential of lncRNA-ENST in ALI treatment.

ACKNOWLEDGEMENTS

The authors express their gratitude to the individuals who participated in this study.

FOOTNOTES

Author contributions: Shen YZ and Yang GY contributed equally to the study design, data analysis, and manuscript preparation and are co-first authors of this manuscript; Shen YZ and Wang X were involved in the study design; Shen YZ and Yang GP mainly conducted the experiments and the statistical analyses, and wrote the manuscript; Ma QM and Wang YS assisted in data analysis. All authors have read the final manuscript and approved the submitted version.

Supported by the Peak Supporting Clinical Discipline of Shanghai Health Bureau, No. 2023ZDFC0104; and the National Key R&D Program of China, No. 2019YFA0110601.

Institutional review board statement: The study described in this manuscript involved the use of stem cell-derived extracellular vesicles (exosomes) *in vitro*, without the involvement of any human or animal subjects. As such, it did not require ethical review or approval from an Institutional Review Board or Institutional Ethics Committee. The research was conducted in compliance with all relevant guidelines and regulations for *in vitro* research, and no ethical concerns were raised in the context of this study.

Conflict-of-interest statement: All the authors report no relevant conflicts of interest for this article.

Data sharing statement: Technical appendix, statistical code, and dataset available upon reasonable request from the corresponding author at 18772407841@163.com.

Country of origin: China

ORCID number: Ye-Zhou Shen 0009-0002-9253-3842; Xin Wang 0009-0006-5331-8778.

S-Editor: Wang JJ
L-Editor: Webster JR
P-Editor: Zhang XD

REFERENCES

1 **Mokrá D**. Acute lung injury - from pathophysiology to treatment. *Physiol Res* 2020; **69**: S353-S366 [PMID: 33464919 DOI: 10.33549/physiolres.934602]
2 **Curley GF**, McAuley DF. Stem cells for respiratory failure. *Curr Opin Crit Care* 2015; **21**: 42-49 [PMID: 25486575 DOI: 10.1097/MCC.0000000000000171]
3 **Ho MS**, Mei SH, Stewart DJ. The Immunomodulatory and Therapeutic Effects of Mesenchymal Stromal Cells for Acute Lung Injury and Sepsis. *J Cell Physiol* 2015; **230**: 2606-2617 [PMID: 25913273 DOI: 10.1002/jcp.25028]
4 **Zhou Z**, Hua Y, Ding Y, Hou Y, Yu T, Cui Y, Nie H. Conditioned Medium of Bone Marrow Mesenchymal Stem Cells Involved in Acute Lung Injury by Regulating Epithelial Sodium Channels *via* miR-34c. *Front Bioeng Biotechnol* 2021; **9**: 640116 [PMID: 34368091 DOI: 10.3389/fbioe.2021.640116]
5 **Bos LDJ**, Ware LB. Acute respiratory distress syndrome: causes, pathophysiology, and phenotypes. *Lancet* 2022; **400**: 1145-1156 [PMID: 36070787 DOI: 10.1016/S0140-6736(22)01485-4]
6 **Li M**, Yang J, Wu Y, Ma X. miR-186-5p improves alveolar epithelial barrier function by targeting the wnt5a/β-catenin signaling pathway in sepsis-acute lung injury. *Int Immunopharmacol* 2024; **131**: 111864 [PMID: 38484663 DOI: 10.1016/j.intimp.2024.111864]
7 **Chen S**, Chen L, Wu X, Lin J, Fang J, Chen X, Wei S, Xu J, Gao Q, Kang M. Ischemia postconditioning and mesenchymal stem cells engraftment synergistically attenuate ischemia reperfusion-induced lung injury in rats. *J Surg Res* 2012; **178**: 81-91 [PMID: 22520057 DOI: 10.1016/j.jss.2012.01.039]
8 **Zhao R**, Wang L, Wang T, Xian P, Wang H, Long Q. Inhalation of MSC-EVs is a noninvasive strategy for ameliorating acute lung injury. *J Control Release* 2022; **345**: 214-230 [PMID: 35307508 DOI: 10.1016/j.jconrel.2022.03.025]
9 **Xu B**, Gan CX, Chen SS, Li JQ, Liu MZ, Guo GH. BMSC-derived exosomes alleviate smoke inhalation lung injury through blockade of the HMGB1/NF-κB pathway. *Life Sci* 2020; **257**: 118042 [PMID: 32621926 DOI: 10.1016/j.lfs.2020.118042]
10 **Liang Y**, Yin C, Lu X, Jiang H, Jin F. Bone marrow mesenchymal stem cells protect lungs from smoke inhalation injury by differentiating into alveolar epithelial cells *via* Notch signaling. *J Biosci* 2019; **44**: 2 [DOI: 10.1007/s12038-018-9824-8]
11 **Li F**, Zhang F, Wang T, Xie Z, Luo H, Dong W, Zhang J, Ren C, Peng W. A self-amplifying loop of TP53INP1 and P53 drives oxidative stress-induced apoptosis of bone marrow mesenchymal stem cells. *Apoptosis* 2024; **29**: 882-897 [PMID: 38491252 DOI: 10.1007/s10495-023-01934-1]
12 **Debnath J**, Gammoh N, Ryan KM. Autophagy and autophagy-related pathways in cancer. *Nat Rev Mol Cell Biol* 2023; **24**: 560-575 [PMID: 36864290 DOI: 10.1038/s41580-023-00585-z]
13 **Vargas JNS**, Hamasaki M, Kawabata T, Youle RJ, Yoshimori T. The mechanisms and roles of selective autophagy in mammals. *Nat Rev Mol Cell Biol* 2023; **24**: 167-185 [PMID: 36302887 DOI: 10.1038/s41580-022-00542-2]
14 **Chen Y**, Li S, Zhang Y, Wang M, Li X, Liu S, Xu D, Bao Y, Jia P, Wu N, Lu Y, Jia D. The lncRNA Malat1 regulates microvascular function after myocardial infarction in mice *via* miR-26b-5p/Mfn1 axis-mediated mitochondrial dynamics. *Redox Biol* 2021; **41**: 101910 [PMID:

33667993 DOI: 10.1016/j.redox.2021.101910]
15 **Park EG**, Pyo SJ, Cui Y, Yoon SH, Nam JW. Tumor immune microenvironment lncRNAs. *Brief Bioinform* 2022; **23**: bbab504 [PMID: 34891154 DOI: 10.1093/bib/bbab504]
16 **Ashrafizadeh M**, Rabiee N, Kumar AP, Sethi G, Zarrabi A, Wang Y. Long noncoding RNAs (lncRNAs) in pancreatic cancer progression. *Drug Discov Today* 2022; **27**: 2181-2198 [PMID: 35589014 DOI: 10.1016/j.drudis.2022.05.012]
17 **Zuo Z**, Liu L, Song B, Tan J, Ding D, Lu Y. Silencing of Long Non-coding RNA ENST00000606790.1 Inhibits the Malignant Behaviors of Papillary Thyroid Carcinoma through the PI3K/AKT Pathway. *Endocr Res* 2021; **46**: 1-9 [PMID: 32791924 DOI: 10.1080/07435800.2020.1804928]
18 **Luo NQ**, Ma DR, Yang XC, Liu Y, Zhou P, Guo LJ, Huang XD. Long non-coding RNA ENST00000434223 inhibits the progression of renal cancer through Wnt/hygro-catenin signaling pathway. *Eur Rev Med Pharmacol Sci* 2019; **23**: 6868-6877 [PMID: 31486486 DOI: 10.26355/eurrev_201908_18726]
19 **Salmena L**, Poliseno L, Tay Y, Kats L, Pandolfi PP. A ceRNA hypothesis: the Rosetta Stone of a hidden RNA language? *Cell* 2011; **146**: 353-358 [PMID: 21802130 DOI: 10.1016/j.cell.2011.07.014]
20 **Orso F**, Virga F, Dettori D, Dalmasso A, Paradzik M, Savino A, Pomatto MAC, Quirico L, Cucinelli S, Coco M, Mareschi K, Fagioli F, Salmena L, Camussi G, Provero P, Poli V, Mazzone M, Pandolfi PP, Taverna D. Stroma-derived miR-214 coordinates tumor dissemination. *J Exp Clin Cancer Res* 2023; **42**: 20 [PMID: 36639824 DOI: 10.1186/s13046-022-02553-5]
21 **Winkle M**, van den Berg A, Tayari M, Sietzema J, Terpstra M, Kortman G, de Jong D, Visser L, Diepstra A, Kok K, Kluiver J. Long noncoding RNAs as a novel component of the Myc transcriptional network. *FASEB J* 2015; **29**: 2338-2346 [PMID: 25690653 DOI: 10.1096/fj.14-263889]
22 **Zeng C**, Liu S, Lu S, Yu X, Lai J, Wu Y, Chen S, Wang L, Yu Z, Luo G, Li Y. The c-Myc-regulated lncRNA NEAT1 and paraspeckles modulate imatinib-induced apoptosis in CML cells. *Mol Cancer* 2018; **17**: 130 [PMID: 30153828 DOI: 10.1186/s12943-018-0884-z]
23 **Wang K**. Autophagy and apoptosis in liver injury. *Cell Cycle* 2015; **14**: 1631-1642 [PMID: 25927598 DOI: 10.1080/15384101.2015.1038685]
24 **Bridges MC**, Daulagala AC, Kourtidis A. LNCcation: lncRNA localization and function. *J Cell Biol* 2021; **220**: e202009045 [PMID: 33464299 DOI: 10.1083/jcb.202009045]
25 **Herman AB**, Tsitsipatis D, Gorospe M. Integrated lncRNA function upon genomic and epigenomic regulation. *Mol Cell* 2022; **82**: 2252-2266 [PMID: 35714586 DOI: 10.1016/j.molcel.2022.05.027]
26 **Nojima T**, Proudfoot NJ. Mechanisms of lncRNA biogenesis as revealed by nascent transcriptomics. *Nat Rev Mol Cell Biol* 2022; **23**: 389-406 [PMID: 35079163 DOI: 10.1038/s41580-021-00447-6]
27 **Ye M**, Fang Y, Chen L, Song Z, Bao Q, Wang F, Huang H, Xu J, Wang Z, Xiao R, Han M, Gao S, Liu H, Jiang B, Qing G. Therapeutic targeting nudix hydrolase 1 creates a MYC-driven metabolic vulnerability. *Nat Commun* 2024; **15**: 2377 [PMID: 38493213 DOI: 10.1038/s41467-024-46572-6]
28 **Zhang X**, Li S, Malik I, Do MH, Ji L, Chou C, Shi W, Capistrano KJ, Zhang J, Hsu TW, Nixon BG, Xu K, Wang X, Ballabio A, Schmidt LS, Linehan WM, Li MO. Reprogramming tumour-associated macrophages to outcompete cancer cells. *Nature* 2023; **619**: 616-623 [PMID: 37380769 DOI: 10.1038/s41586-023-06256-5]
29 **Casey SC**, Baylot V, Felsher DW. The MYC oncogene is a global regulator of the immune response. *Blood* 2018; **131**: 2007-2015 [PMID: 29514782 DOI: 10.1182/blood-2017-11-742577]
30 **Karreth FA**, Tay Y, Perna D, Ala U, Tan SM, Rust AG, DeNicola G, Webster KA, Weiss D, Perez-Mancera PA, Krauthammer M, Halaban R, Provero P, Adams DJ, Tuveson DA, Pandolfi PP. In vivo identification of tumor- suppressive PTEN ceRNAs in an oncogenic BRAF-induced mouse model of melanoma. *Cell* 2011; **147**: 382-395 [PMID: 22000016 DOI: 10.1016/j.cell.2011.09.032]
31 **Tay Y**, Kats L, Salmena L, Weiss D, Tan SM, Ala U, Karreth F, Poliseno L, Provero P, Di Cunto F, Lieberman J, Rigoutsos I, Pandolfi PP. Coding-independent regulation of the tumor suppressor PTEN by competing endogenous mRNAs. *Cell* 2011; **147**: 344-357 [PMID: 22000013 DOI: 10.1016/j.cell.2011.09.029]
32 **Wang L**, Cho KB, Li Y, Tao G, Xie Z, Guo B. Long Noncoding RNA (lncRNA)-Mediated Competing Endogenous RNA Networks Provide Novel Potential Biomarkers and Therapeutic Targets for Colorectal Cancer. *Int J Mol Sci* 2019; **20**: 5758 [PMID: 31744051 DOI: 10.3390/ijms20225758]
33 **di Iasio MG**, Norcio A, Melloni E, Zauli G. SOCS1 is significantly up-regulated in Nutlin-3-treated p53wild-type B chronic lymphocytic leukemia (B-CLL) samples and shows an inverse correlation with miR-155. *Invest New Drugs* 2012; **30**: 2403-2406 [PMID: 22238073 DOI: 10.1007/s10637-011-9786-2]
34 **Piao L**, Huang Z, Inoue A, Kuzuya M, Cheng XW. Human umbilical cord-derived mesenchymal stromal cells ameliorate aging-associated skeletal muscle atrophy and dysfunction by modulating apoptosis and mitochondrial damage in SAMP10 mice. *Stem Cell Res Ther* 2022; **13**: 226 [PMID: 35659361 DOI: 10.1186/s13287-022-02895-z]
35 **Yang M**, Cui Y, Song J, Cui C, Wang L, Liang K, Wang C, Sha S, He Q, Hu H, Guo X, Zang N, Sun L, Chen L. Mesenchymal stem cell-conditioned medium improved mitochondrial function and alleviated inflammation and apoptosis in non-alcoholic fatty liver disease by regulating SIRT1. *Biochem Biophys Res Commun* 2021; **546**: 74-82 [PMID: 33578292 DOI: 10.1016/j.bbrc.2021.01.098]
36 **Peña-Blanco A**, García-Sáez AJ. Bax, Bak and beyond - mitochondrial performance in apoptosis. *FEBS J* 2018; **285**: 416-431 [PMID: 28755482 DOI: 10.1111/febs.14186]
37 **Karch J**, Kwong JQ, Burr AR, Sargent MA, Elrod JW, Peixoto PM, Martinez-Caballero S, Osinska H, Cheng EH, Robbins J, Kinnally KW, Molkentin JD. Bax and Bak function as the outer membrane component of the mitochondrial permeability pore in regulating necrotic cell death in mice. *Elife* 2013; **2**: e00772 [PMID: 23991283 DOI: 10.7554/eLife.00772]
38 **Victorelli S**, Salmonowicz H, Chapman J, Martini H, Vizioli MG, Riley JS, Cloix C, Hall-Younger E, Machado Espindola-Netto J, Jurk D, Lagnado AB, Sales Gomez L, Farr JN, Saul D, Reed R, Kelly G, Eppard M, Greaves LC, Dou Z, Pirius N, Szczepanowska K, Porritt RA, Huang H, Huang TY, Mann DA, Masuda CA, Khosla S, Dai H, Kaufmann SH, Zacharioudakis E, Gavathiotis E, LeBrasseur NK, Lei X, Sainz AG, Korolchuk VI, Adams PD, Shadel GS, Tait SWG, Passos JF. Apoptotic stress causes mtDNA release during senescence and drives the SASP. *Nature* 2023; **622**: 627-636 [PMID: 37821702 DOI: 10.1038/s41586-023-06621-4]
39 **Chen Y**, Zhang Y, Li N, Jiang Z, Li X. Role of mitochondrial stress and the NLRP3 inflammasome in lung diseases. *Inflamm Res* 2023; **72**: 829-846 [PMID: 36905430 DOI: 10.1007/s00011-023-01712-4]

World Journal of Stem Cells

Submit a Manuscript: https://www.f6publishing.com

World J Stem Cells 2025 March 26; 17(3): 101454

DOI: 10.4252/wjsc.v17.i3.101454

ISSN 1948-0210 (online)

ORIGINAL ARTICLE

Basic Study

MiR-21-5p-enriched exosomes from hiPSC-derived cardiomyocytes exhibit superior cardiac repair efficacy compared to hiPSC-derived exosomes in a murine MI model

Jing-Jun Jin, Rong-Hua Liu, Jin-Yan Chen, Kun Wang, Jun-Yong Han, Dao-Shun Nie, Yu-Qing Gong, Bin Lin, Guo-Xing Weng

Specialty type: Cell and tissue engineering

Provenance and peer review: Unsolicited article; Externally peer reviewed.

Peer-review model: Single blind

Peer-review report's classification

Scientific Quality: Grade B, Grade B, Grade B, Grade C

Novelty: Grade B, Grade B, Grade B

Creativity or Innovation: Grade B, Grade B, Grade C

Scientific Significance: Grade B, Grade C, Grade C

P-Reviewer: Corrales FJ; Li SC; Wu CN

Received: September 15, 2024

Revised: October 15, 2024

Accepted: January 15, 2025

Published online: March 26, 2025

Processing time: 187 Days and 3.3 Hours

Jing-Jun Jin, Rong-Hua Liu, Jin-Yan Chen, Kun Wang, Jun-Yong Han, Fujian Key Laboratory of Medical Analysis, Fujian Academy of Medical Sciences, Fuzhou 350001, Fujian Province, China

Dao-Shun Nie, Yu-Qing Gong, Bin Lin, Guo-Xing Weng, Shengli Clinical Medical College, Fujian Medical University, Fuzhou 350001, Fujian Province, China

Co-corresponding authors: Jing-Jun Jin and Guo-Xing Weng.

Corresponding author: Jing-Jun Jin, Fujian Key Laboratory of Medical Analysis, Fujian Academy of Medical Sciences, No. 7 Wusi Road, Fuzhou 350001, Fujian Province, China. yolanda_jin19@hotmail.com

Abstract

BACKGROUND

Heart disease remains a leading cause of mortality worldwide, with existing treatments often failing to effectively restore damaged myocardium. Human-induced pluripotent stem cells (hiPSCs) and their derivatives offer promising therapeutic options; however, challenges such as low retention, engraftment issues, and tumorigenic risks hinder their clinical utility. Recent focus has shifted to exosomes (exos) - nanoscale vesicles that facilitate intercellular communication - as a safer and more versatile alternative. Understanding the specific mechanisms and comparative efficacy of exos from hiPSCs *vs* hiPSC-derived cardiomyocytes (hiPSC-CMs) is crucial for advancing cardiac repair therapies.

AIM

To evaluate and compare the therapeutic efficacy of exos secreted by hiPSCs and hiPSC-CMs in cardiac repair, and to elucidate the role of microRNA 21-5p (miR-21-5p) in the observed effects.

METHODS

We differentiated hiPSCs into CMs using small molecule methods and characterized the cells and their exos.

RESULTS
Our findings indicate that hiPSC-CMs and their exos enhanced cardiac function, reduced infarct size, and decreased myocardial fibrosis in a murine myocardial infarction model. Notably, hiPSC-CM exos outperformed hiPSC-CM cell therapy, showing improved ejection fraction and reduced apoptosis. We identified miR-21-5p, a microRNA in hiPSC-CM exos, as crucial for CM survival. Exos with miR-21-5p were absorbed by AC16 cells, suggesting a mechanism for their cytoprotective effects.

CONCLUSION
Overall, hiPSC-CM exos could serve as a potent therapeutic agent for myocardial repair, laying the groundwork for future research into exos as a treatment for ischemic heart disease.

Key Words: Human-induced pluripotent stem cells; Human-induced pluripotent stem cell-derived cardiomyocytes; Myocardial infarction; Exosomes; MicroRNA 21-5p; Apoptosis

Core Tip: This study explored human-induced pluripotent stem cell-derived cardiomyocytes (hiPSC-CMs) and their exosomes (exos) for myocardial infarction (MI) repair. Despite issues with hiPSC-CMs, exos are promising due to low immunogenicity. By differentiating hiPSCs and characterizing, it was found that they improved cardiac function in a murine MI model. hiPSC-CMs exos are superior, with microRNA 21-5p being key. Thus, they may be a strong agent for myocardial repair and inspire further research on exo treatment for heart disease.

Citation: Jin JJ, Liu RH, Chen JY, Wang K, Han JY, Nie DS, Gong YQ, Lin B, Weng GX. MiR-21-5p-enriched exosomes from hiPSC-derived cardiomyocytes exhibit superior cardiac repair efficacy compared to hiPSC-derived exosomes in a murine MI model. *World J Stem Cells* 2025; 17(3): 101454
URL: https://www.wjgnet.com/1948-0210/full/v17/i3/101454.htm
DOI: https://dx.doi.org/10.4252/wjsc.v17.i3.101454

INTRODUCTION

Myocardial infarction (MI), more commonly referred to as a heart attack, occurs when blood flow to a section of the heart is severely curtailed or obstructed, leading to damage or death of the heart muscle cells. It stands as a primary cause of morbidity and mortality worldwide and imposes a considerable healthcare burden due to its profound effects on the quality of life and the economic costs associated with treatment and recovery[1]. Current therapies for heart diseases primarily slow progression, yet they fall short of repairing damaged myocardium. Human pluripotent stem cells (SCs) exhibit immense potential as a cellular source for cardiac repair due to their boundless self-renewal capacity and their potential to differentiate into cardiomyocytes (CMs)[2,3]. However, challenges such as low cell retention and engraftment rates, along with the risks of tumorigenesis and ventricular arrhythmia, impede their clinical application[4]. Studies have shown that human-induced pluripotent SC (hiPSC)-derived CMs (hiPSC-CMs) can booster myocardial function, mitigate ventricular remodeling, and curtail mortality in rats with MI. Transplanted hiPSC-CMs not only achieve electromechanical integration with the host tissue[5-8] but also secrete cytokines that foster angiogenesis and survival of the injured muscle[9]. These improvements in cardiac function have largely been attributed to paracrine factors[10,11].

Exosomes (exos) are vital mediators of intercellular communication, characterized as small membrane vesicles that carry a variety of biomolecules[12]. Studies have indicated that exos can modulate the survival, proliferation, and apoptosis of CMs, as well as participate in inflammatory responses and angiogenesis[13,14]. In the pathology of MI, exos play a pivotal role. Particularly after MI, exos released by damaged CMs may carry signaling molecules that are beneficial to myocardial repair and regeneration. For example, Sun *et al*[15] documented that exos with overexpressed hypoxia-inducible factor 1 alpha (HIF-1α) can rescue the impaired angiogenic potential, migratory capacity, and proliferative activity of hypoxia-damaged human umbilical vein endothelial cells. Furthermore, cardiosphere-derived SCs have been shown to produce exos that stimulate myocardial regeneration by delivering microRNAs (miRNAs) to the heart tissue, thereby facilitating the therapeutic potential of these vesicles for the treatment of MI[14,16].

MiR-21-5p is an miRNA that is upregulated in various cardiovascular diseases and has a particularly prominent role in MI[17,18]. In MI, miR-21-5p is involved in processes such as apoptosis, fibrosis, and angiogenesis of CMs by regulating multiple target genes. For instance, miR-21-5p can suppress the expression of certain anti-apoptotic genes, thereby promoting the death of CMs[19,20]. Furthermore, miR-21-5p is involved in the regulation of the expression of angiogenesis-related factors, affecting vascular regeneration after MI[21]. Therefore, miR-21 has potential clinical application value in the treatment of MI. By modulating the expression levels of miR-21, it may provide new strategies for the treatment of MI.

In this study, we explored the therapeutic potential of hiPSC-CM exos in a murine model of MI.

MATERIALS AND METHODS

Differentiation of hiPSCs into cardiac cells

HiPSCs were obtained from Nuwacell Biotechnologies Co., Ltd. (Anhui, China) and were genetically labeled with green fluorescent protein (Luc-GFP). HiPSCs were cultured in an incubator with 5% CO_2 at 37 °C in ncEpic (Nuwacell) iPSC medium (Nuwacell), and prepared using serum-free basal medium mixed with additives in a ratio of 1:125. The complete culture medium was stored at 4 °C and could be used for up to 4 weeks, ensuring that it was equilibrated to room temperature before use.

HiPSCs were induced to CMs by selective modulation of the Wnt pathway in a monolayer culture using the CardioEasy Kit (Cellapy Biotechnology, Beijing, China) as previously reported[22]. In brief, the medium was changed to Induction Medium I when the hiPSCs reached about 80% confluency. After 48 hours, hiPSCs were cultured in Induction Medium II for another 48 hours and then in Induction Medium III, with the media changed every other day. On days 7-9, the cells began to contract. Then hiPSC-CMs were glucose-starved for 3 days by CardioEasy purification. Afterward, the media were replaced with a maintenance medium for human myocardial cells (Cellapy) and were changed every other day. HiPSC-CMs were identified by immunofluorescence staining. For cell recovery, a 10 μM culture medium was prepared by mixing the complete culture medium with Nuwacell™ blebbistatin at a ratio of 4000:1. The culture medium for the first day of cell recovery and passaging was supplemented with 10 μM blebbistatin to support cell viability and proliferation.

The myocardial differentiation additives were stored at -20 °C and thawed at 4 °C before use. After thawing, the additives were briefly centrifuged to ensure homogeneity. The differentiation reagents were prepared by mixing the myocardial differentiation additives with the basal medium at a ratio of 1:49. To avoid repeated freeze-thaw cycles, the thawed additives were aliquoted according to usage and stored at -20 °C. The prepared differentiation reagents could be stored at 4 °C and used within 1 month.

Immunofluorescence staining

Immunofluorescence staining was performed in a confocal dish, with hiPSC-CMs fixed in 4% paraformaldehyde for 10 minutes. The fixed cells were washed with Tris-buffered saline with Tween-20 (TBST), and then the samples were permeabilized with 0.1% Triton X-100 for 10 minutes at room temperature and blocked in 10% goat serum to reduce nonspecific binding. The cells were incubated overnight at 4 °C with cardiac troponin T (cTNT, 1:100; R&D Systems, Minnesota, MN, United States), 2v isoform of myosin light chain (1:100; ProteinTech, Chicago, IL, United States), and NK2 homeobox 5 (1:200; Abcam, United Kingdom) monoclonal antibodies and then incubated with the appropriate anti-mouse secondary antibodies (1:100; Santa Cruz Biotechnology, Santa Cruz, TX, United States) conjugated to Alexa Flour 647. The above-mentioned secondary antibodies were incubated at room temperature for 1 hour in the dark. The nuclei were counterstained with DAPI staining solution and incubated at room temperature for 5 minutes. The cells were visualized using the inverted Leica DMi8 microscope (Leica, Wetzlar, Germany).

Confocal and high-content imaging as well as microelectrode array of hiPSC-CMs

Confocal imaging (TCSP8; Leica) and high-content imaging (ImageXpress Micro Confocal; Molecular Devices, San Jose, CA, United States) were used to investigate the morphology of hiPSC-CMs and assess their contractile function. The microelectrode array platform was utilized to evaluate the cardiac electrophysiological function of hiPSC-CMs.

Extraction and identification of exos

Purified exos secreted by hiPSC- and hiPSC-CM-derived cells were isolated using an exo isolation kit (Umibio, Shanghai, China) in accordance with the manufacturer's protocol. The exo pellet was resuspended in Dulbecco's Phosphate-Buffered Saline (DPBS) with the volume indexed to the number of cells from which the exos/microvesicles were derived (100 μL DPBS/5 × 10^5 cells). The protein content of exos was assessed using the BCA protein assay kit (Beyotime, Shanghai, China), and western blotting was used to evaluate the expression of exo-specific markers (cluster of differentiation 63 [CD63] and tumor susceptibility gene 101 [TSG101]). The concentration and size of exos were measured using nanoparticle tracking analysis (Zetaview-PMX120-Z; Particle Metrix, Inning am Ammersee, Germany), and the morphology of the exos was assessed by transmission electron microscopy (JEM1400; JEOL Ltd., Tokyo, Japan).

Western blotting

The purified exos were mixed with the lysate in equal volumes, incubated on ice for 30 minutes, and then centrifuged at 12000 rpm for 15 minutes at 4 °C. The supernatant was transferred to a new Eppendorf (EP) tube, and the protein concentration was determined using the BCA method. Subsequently, 5 × loading buffer was added to the supernatant, mixed well, and boiled at 100 °C for 5 minutes. The samples were separated on a 5% stacking gel and 12% resolving gel, and then the proteins were electrotransferred to polyvinylidene fluoride membranes at 300 mA for 50 minutes on ice. The polyvinylidene fluoride membrane was blocked in a solution containing 5% skim milk in poly(butylene succinate-butylene terephthalate) (PBST) at room temperature for 1 hour. Primary antibodies including β-actin (1:2000), B-cell lymphoma 2 (Bcl-2) (1:2000), Bcl-2-associated X protein (Bax) (1:2000), HIF-1α (1:2000), CD63 (1:1000), and TSG101 (1:1000) were added and incubated at 4 °C overnight. After washing three times with PBST, horseradish peroxidase-

labeled secondary antibody (diluted 1:10000) was added and incubated at room temperature for 1 hour. Finally, after washing three times with PBST, enhanced chemiluminescence reagent was applied and images were captured using the ChemiDoc MP Imaging System (Bio-Rad, Hercules, CA, United States).

Induction of MI model and grouping

The acute MI model was developed as previously described[23-26]. In brief, adult male Sprague-Dawley rats (about 250 g) were initially anesthetized with chloral hydrate (300 mg/kg) and maintained under 2.0% lidocaine anesthesia. The rats were connected to a rodent ventilator *via* tracheal intubation. The left anterior descending coronary artery was permanently ligated, and complete ligation was confirmed by the rapid change in color, pallor, and ST elevation observed with continuous electrocardiogram monitoring during the procedure. Thirty minutes after establishment of the MI model, intramyocardial injections were performed at four sites surrounding the rat MI area. All rats were randomly assigned to the following groups (n = 10/group): (1) PBS group; (2) iPSC group, injection of 5×10^5 iPSCs and Matrigel at a ratio of 1:1 to 60 μL mixture; (3) hiPSC-CM-group, injection of 5×10^5 hiPSC-CMs and Matrigel at a ratio of 1:1 to 60 μL mixture; (4) iPSC-exo group, injection of 40 μg exos extracted from iPSCs and Matrigel at a ratio of 1:1 to 60 μL mixture; and (5) Exos derived from hiPSC-CMs (hiPSC-CM-exo) group, injection of 40 μg exos extracted from hiPSC-CMs and Matrigel at a ratio of 1:1 to 60 μL mixture. The chest was closed, and animals were extubated and removed from anesthesia following restoration of spontaneous respiration.

M-mode echocardiography

Post-MI, M-mode echocardiography was administered at 3, 7, 14, and 28 days by an investigator unaware of the experimental protocols. Standard M-mode parameters, including left ventricular internal diameter in end-diastole and end-systole internal diameters, were meticulously measured to calculate the left ventricular ejection fraction (LVEF) and left ventricular fractional shortening (LVFS) in accordance with the guidelines set by the American Society of Echocardiography recommendations[27]. All parameters were presented as the average of three beats.

Bioluminescence imaging (in vitro and in vivo)

In evaluating the presence of iPSC-Luc-GFP and hiPSC-CM-Luc-GFP in rats, bioluminescence detection was performed using the IVIS Lumina II detector (PerkinElmer, Hopkinton, MA, United States) on days 0, 3, and 7 post-surgery. Rats were administered an intraperitoneal injection of 3% pentobarbital sodium for anesthesia (0.1 mL/100 g), followed by imaging using the IVIS Lumina X5 detector after injection of D-luciferin (150 mg/kg).

Immunohistochemistry and transferase dUTP nick-end labeling staining

In quantifying apoptotic CMs in a rat model of MI, the hearts of three rats were harvested 3 days post-MI. The rats were anesthetized with intraperitoneal injection of 3% pentobarbital sodium (0.1 mL/100 g) for heart extraction. The hearts were fixed in 4% polyformaldehyde and embedded in paraffin. Subsequently, paraffin blocks were sectioned into 5 μm slides for terminal deoxynucleotidyl transferase dUTP nick-end labeling (TUNEL) assay. The TUNEL assay was performed using a fluorescein (FITC) TUNEL Cell Apoptosis Detection Kit (Servicebio, Wuhan, China) following the manufacturer's protocol. DAPI was used for nuclear counterstaining. Under the Leica DMi8 microscope, five positive view fields were photographed for each section. ImageJ was used for image analysis. On the 28th day post-model establishment, four rats from each group were selected randomly. The hearts were fixed in paraformaldehyde and embedded in paraffin. Subsequently, paraffin blocks were sectioned into 5 μm slides. After slicing, the heart tissue sections were deparaffinized and dehydrated, followed by staining. The pathological changes of myocardial tissues were evaluated by immunohistochemical analysis.

Masson trichrome staining

Paraffin-embedded sections were deparaffinized with xylene and graded alcohols, followed by PBS rinses. After overnight soaking in Masson A solution, sections were treated with Masson B and C mixtures, hydrochloric acid ethanol, and Masson D and E solutions, and then differentiated in glacial acetic acid and dehydrated in ethanol and xylene. Finally, sections were neutral gum sealed, observed under a microscope, and the degree of fibrosis was quantified using ImageJ software (https://imagej.net/software/imagej/) based on histological analysis.

Infarct size assessment (2,3,5-triphenyl-tetrazoliumchloride staining)

On the 28th day following model establishment, three rats from each group were randomly selected. The rats were anesthetized using intraperitoneal injection of 3% pentobarbital sodium (0.1 mL/100 g) to facilitate heart extraction. PBS was used to wash away blood stains. The heart was dried with gauze and then frozen at -80 °C in a refrigerator for 15 minutes. Subsequently, the heart was sliced into serial sections along with a surgical ligature and then immersed in 1% 2,3,5-triphenyltetrazoliumchloride solution (Sigma Aldrich, Milwaukee, WI, United States). The sections were incubated in a water bath at 37 °C for 20 minutes. After staining, photographs were taken. The brick red coloration denoted a normal area, whereas the gray-white color represented the MI area. ImageJ was utilized to calculate the infarction size. The infarction percentage (%) was determined by dividing the infarction area by the total area of the heart's cutting surface and multiplying by 100%.

High-throughput sequencing

The supernatants of hiPSC and hiPSC-CM cells were collected to extract extracellular vesicles, and sent to Shu Pu (Shanghai, China) Biotechnologies LLC (DBA Aksomics) for miRNA sequencing. Sequencing of miRNAs in extracellular

vesicles was performed using the Illumina NextSeq500 sequencer.

Exo RNA extraction and real-time reverse transcription polymerase chain reaction

HiPSC and hiPSC-CM cell supernatants were collected, and exo suspensions were isolated by ultracentrifugation. Then 1 mL TRIzol reagent was added to the exo pellet in an EP tube and exos were lysed by repeated pipetting on ice for 10 minutes. After lysis, 200 μL chloroform was added and mixed thoroughly by vigorous inversion. The mixture was incubated on ice for 5 minutes before centrifuging at 12000 rpm for 15 minutes. Next, the top aqueous layer was carefully transferred to a new EP tube, followed by the addition of an equal volume of isopropanol. Then the tube was inverted 10 times and incubated on ice for 10 minutes, followed by centrifugation at 12000 rpm for 10 minutes. The supernatant was discarded, the RNA pellet was washed with 75% ethanol, and centrifuged again at 7500 rpm for 10 minutes. The liquid was discarded, and the pellet was air dried. The RNA was resuspended in 30 μL DEPC-treated water. miRNA reverse transcription was conducted using the PrimeScript™ RT Reagent Kit (Takara Bio Inc., Shiga, Japan) according to the manufacturer's protocol. Quantitative PCR (qPCR) was conducted using the Novo Start SYBR qPCR SuperMix Plus (E096-01B; Novoprotein, Scientific Inc., Shanghai, China) on the CFX96 Real-Time PCR Detection System (Bio-Rad). Beta-actin served as an endogenous control for normalizing the expression levels of the target genes. The primers utilized in this study are detailed in Supplementary Table 1.

Transfection with miR-21-5p mimic or inhibitor

A total of 2×10^5 cells were seeded in each well of a 6-well plate with antibiotic-free medium 1 day prior to transfection, ensuring 50% confluence at transfection time and preventing cell clumping. A total of 10 μL miR-21-5p mimic or inhibitor was diluted in 250 μL Opti-MEM, and 6 μL Lipofectamine 3000 was diluted in another 250 μL Opti-MEM. The solution was mixed gently and incubated at room temperature for 5 minutes. The diluted miRNA and transfection reagent were combined, mixed, and incubated for 20 minutes. The medium was replaced with 1.5 mL antibiotic-free complete medium, and 500 μL transfection complex was added to each well, followed by incubation at 37 °C with 5% CO_2 for 24-48 hours. Then the medium was replaced with complete medium after 4-6 hours if needed.

Flow cytometry

AC16 CMs were plated at a density of 3×10^5 cells per well in a 6-well plate with antibiotic-free complete medium. Transfection was performed when cells reached about 50% confluence. The medium was replaced with fresh antibiotic-free complete medium 6 hours post-transfection, and then switched to glucose-free Dulbecco's Eagle Modified Medium with 500 μM cobalt chloride ($CoCl_2$) after 48 hours for an additional 24 hours. After this incubation period, the cells were harvested by trypsinization without EDTA, centrifuged at 1000 *g* for 5 minutes, and washed with PBS, after which a working solution of 1 × binding buffer was prepared. Detach cells with trypsin, stop the digestion with culture medium, transfer to a centrifuge tube, and wash with pre-chilled PBS. The cell pellet was resuspended in 1 × binding buffer to a concentration of 1×10^6 cells/mL, and then 100 μL of this suspension was transferred to a new tube, followed by the addition of 5 μL Annexin V-FITC and 5 μL PI. The solution was mixed gently, and incubated in the dark for 15 minutes. Finally, 400 μL of 1 × binding buffer was added to each tube for flow cytometry analysis.

Statistical analyses

The data were meticulously analyzed and visualized using SPSS 26.0 (SPSS Inc., Chicago, IL, United States). All data are presented as the mean ± SD. Statistical significance was determined using the Student's *t*-test for comparisons between two groups and one-way analysis of variance for assessments involving more than two groups. The significance levels were $^aP < 0.05$ and $^bP < 0.01$.

Ethical approval

The study was approved by the Ethics Committee of Fujian Academy of Medical Sciences (Approval No. DL2021-09; Fuzhou, China).

Statement of animal rights

All animal protocols were performed in accordance with the Guidelines for Animal Experiments of Fujian Academy of Medical Sciences (Approval No. DL2021-09).

RESULTS

HiPSC-CM differentiation and identification

To obtain highly pure and relatively mature CMs, we employed small molecule-based methods for myocardial differentiation provided by Nuwacell Biotechnologies Co., Ltd. These cells were genetically labeled with GFP. During the initial stages of differentiation (days 0-2), the agglomerated hiPSC colonies displayed a typical morphology characterized by a high nuclear-cytoplasmic ratio (Supplementary Figure 1A). By days 8-9, a notable subset of cells had begun to exhibit rhythmic beating motions, reminiscent of wave-like patterns (Video 1). Following a 2-day purification process on day 14, the CMs demonstrated enhanced contractions compared to the earlier stages (Video 2). The purified, differentiated CMs presented distinct morphological features associated with these cells, including a large cell volume, irregular shape, and less pronounced nucleocytoplasmic ratio (Supplementary Figure 1B). Confocal microscopy disclosed interconnected

clusters of CMs displaying synchronized beating, a testament to their robust contractile function (Supplementary Figure 1C, Video 3). High-content imaging revealed a monolayer growth pattern, with individual cells contracting centripetally at an average frequency of 90 beats per minute (Supplementary Figure 1D, Video 4). The microelectrode array technology detected robust and regular baseline beating signals (Supplementary Figure 1E and F), with the detailed parameters outlined in Table 1. To further authenticate the differentiated CMs, immunofluorescence detection was conducted using specific CM makers, including cTNT, NK2 homeobox 5, and 2v isoform of myosin light chain. The cells showed positive staining for all three markers (Supplementary Figure 2A-C). These results confirmed the successful differentiation of hiPSCs into CMs with functional attributes.

Characterization of hiPSCs and hiPSC-CM exos

Exos were isolated from the culture media of hiPSCs and hiPSC-CMs. Utilizing nanoparticle tracking analysis analysis, we discovered that the exos derived from hiPSCs (hiPSC-exo) had an average diameter of approximately 165 nm. By contrast, hiPSC-CM-exo had an average diameter of approximately 108 nm (Figure 1A and B). Further examination by transmission electron microscopy substantiated the presence of characteristic bilayered membranes within these isolated exos, confirming their structural integrity (Figure 1C and D). The quantity of these exos/microvesicles was determined using the Bradford assay - a reputable and widely adopted method for protein quantification. Western blot analysis was employed to assess the presence of specific exo markers. Our results confirmed the expression of CD63 and TSG101 in both hiPSC-exos and hiPSC-CM-exos (Figure 1E). This molecular characterization is crucial for verifying the identity and potential functionality of these exos in subsequent therapeutic applications.

HiPSC-CM exos improve cardiac function in a murine MI model

We evaluated the protective effects of iPSCs, hiPSC-CMs, hiPSC-exo, and hiPSC-CM-exo on cardiac function following MI in rats. MI was surgically induced by occluding the distal left anterior descending coronary artery (Figure 2A and B). Of 54 rats that underwent the procedure, 50 survived and were evenly divided into five groups. The rats in the iPSC group were injected with 0.5 million hiPSCs, whereas those in the hiPSC-CMs group were injected with 0.5 million hiPSC-CMs at four sites surrounding the MI area in the rats. The iPSC-exo group and hiPSC-CMs-exo group were injected with 40 μg exos derived from hiPSCs and hiPSC-CMs, respectively. By contrast, the PBS group was injected with PBS only. To assess the retention of cells post-injection, luciferase activity was measured on days 0, 3, and 7 following MI. The bioluminescence signal was most intense on day 0, diminished by day 3, and was nearly undetectable by day 7 post-MI (Figure 2C). Cardiac function was evaluated using M-mode echocardiography at four distinct time points: 3, 7, 14, and 28 days post-MI. LVEF and LVFS were notably enhanced in the animals treated with hiPSC-CMs-exo compared to those that received PBS alone, particularly at the 4-week mark. Furthermore, the hiPSC-CMs-exo group demonstrated a significant improvement in LVEF and LVFS when juxtaposed with the iPSC-exo group and iPSC group in week 4 (Figure 2D-F). The hiPSC-CM-exo exhibited a trend toward a more pronounced amelioration of cardiac function compared to the other treatment groups, suggesting the potential therapeutic superiority of hiPSC-CM-exo in the context of myocardial repair.

HiPSC-CM exos reduce the infarction area and myocardial fibrosis

Next, we performed 2,3,5-triphenyltetrazoliumchloride staining to evaluate the myocardial infarct size 28 days after MI. The results showed that treatment with hiPSC-CM-exo significantly reduced the infarct size, indicating that these exos have the potential to alleviate cardiac damage post-MI (Figure 3). In alignment with the reduction in infarction area, Masson staining of the infarct site at the 4-week post-MI disclosed that the administration of hiPSC-CM-exo resulted in a markedly diminished level of fibrosis when compared to the other treatment groups (Figure 4). These results underscore the therapeutic impact of hiPSC-CM-exos in attenuating the fibrotic consequences of MI.

HiPSC-CM-exos reduce apoptosis when administered to infarcted rat hearts

In delving into the mechanisms behind the improved cardiac function with hiPSC-CM-exo treatment, we hypothesized that the mechanism might encompass the activation of cytoprotective pathways. To test this hypothesis, we quantified apoptotic cells in the hearts of animals euthanized 3 days post-MI (Figure 5 and Supplementary Figure 3). At the border zone of the infarction, a significantly reduced number of apoptotic cells, identified by TUNEL staining, were observed in the hiPSC-CM-exo group compared to other groups. This finding suggests that hiPSC-CM-exo may possess the capacity to suppress apoptosis induced by MI.

HiPSC-CM-exos promote CM survival, angiogenesis, and cell migration

Four weeks after MI, we conducted immunohistochemistry analyses to evaluate the expression levels of cTNT, CD31, and C-X-C chemokine receptor 4 (CXCR4). These markers are indicative of myocardial cell survival, angiogenesis[28,29], and cell migration[30], respectively. The group treated with hiPSC-CM-exo exhibited higher levels of cTNT, CD31, and CXCR4 compared to the other groups, with the most pronounced difference observed between the PBS and hiPSC-CM-exo groups (Figure 6). These results support the hypothesis that exos derived from hiPSC-CMs can enhance CM survival, stimulate angiogenesis, and promote cell migration. The results indicated that the transplantation of hiPSC-CM-exo may trigger paracrine mechanisms that encourage blood vessel growth, cell migration, survival, and intracellular communication, thereby contributing to the repair and regeneration of the heart tissue post-MI.

Table 1 Microelectrode array detailed parameters of human-induced pluripotent stem cell-derived cardiomyocytes

	Beat period (s)	FPD (ms)	FPDc (Fridericia ms)	Spike amplitude (mV)
HiPSC-CMs	1.6 ± 0.0	539 ± 59	460 ± 52	0.1 ± 0.0

FPD: Field potential duration; FPDc: Corrected field potential duration; HiPSC-CMs: Human-induced pluripotent stem cell-derived cardiomyocytes.

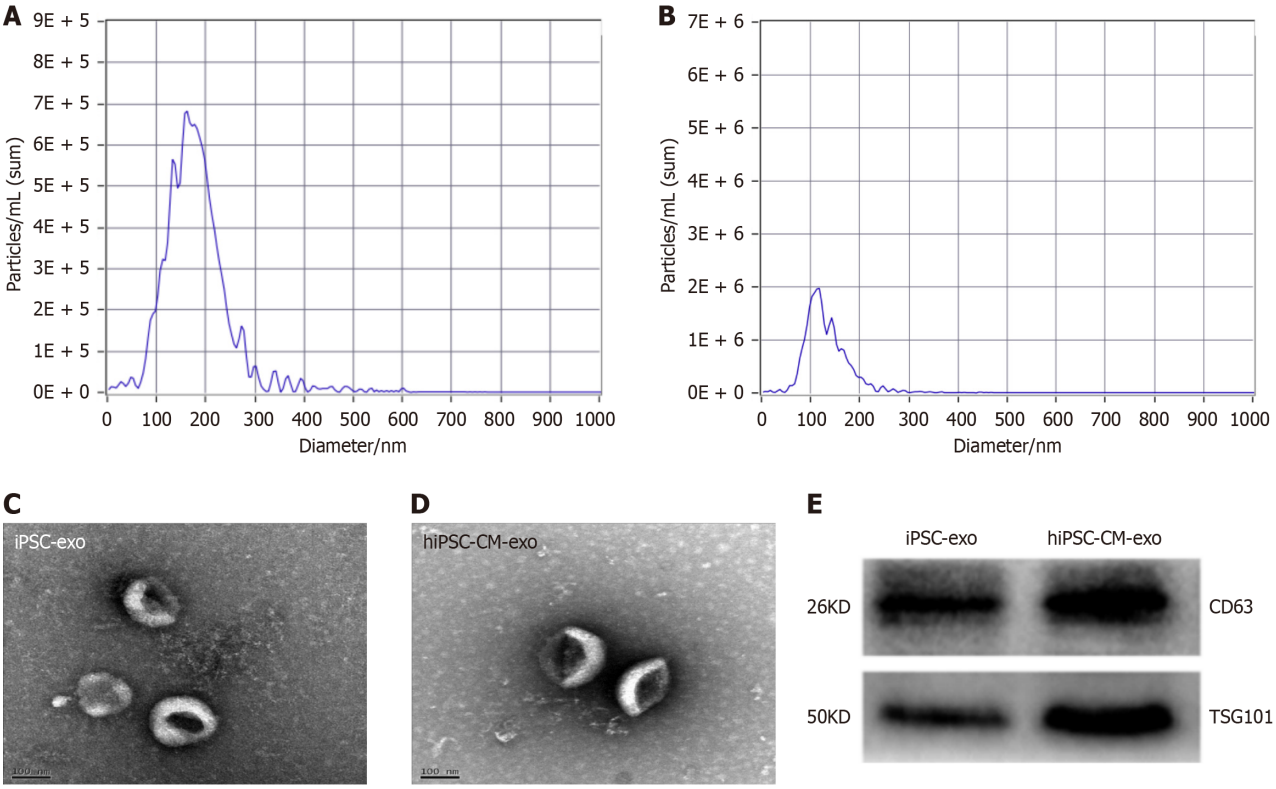

Figure 1 Characterization of human-induced pluripotent stem cells and human-induced pluripotent stem cell-derived cardiomyocyte exosomes. A and B: The size was assessed utilizing nanoparticle tracking analysis; C and D: Morphology of human-induced pluripotent stem cells (hiPSCs) and human-induced pluripotent SC-derived cardiomyocyte exosomes (hiPSC-CM-exos) was analyzed *via* electron microscopy; E: Western blot analysis confirmed the expression of cluster of differentiation 63 (CD63) and tumor susceptibility gene 101 in exos derived from hiPSCs and hiPSC-CMs. iPSC-exos: Induced pluripotent stem cell-derived exosomes.

Data analysis of sequencing miRNA

Screening for miRNAs with significantly increased expression levels in iPSC-exo compared to hiPSC-CM-exo, enrichment of target gene Gene Ontology (GO), and annotation of the possible pathways by which miRNAs with high iPSC-exo exert their effects in cells. The enrichment result of biological processes (BP) is GO:0050794 regulation of cellular processes; GO:0051171 regulation of nitrogen compound metabolic process; GO:0051173 Positive regulation of nitrogen compound metabolic process (Figure 7A). The enrichment results of cellular components are GO:0005737 cytoplasm, GO:0043227 membrane-bound organelle, and GO:0043231 intracellular membrane-bound organelle (Figure 7B). The molecular function enrichment results (as shown in Figure 7C) are GO:0005515 protein binding, GO:0003824 catalytic activity, and GO:0046872 metal ion binding. Four miRNAs, hsa-miR-148a-3p, hsa-miR-21-5p, hsa-miR-151a-3p, and hsa-miR-26a-5p, were obtained from the collection of highly expressed miRNAs in hiPSC-CMs-exo and iPSC-exo (Figure 7D). Additional, extract miRNAs from iPSCs-exo, hiPSC-CM-exo, and AC16, real-time reverse transcription polymerase chain reaction (RT-qPCR) showed that the miR-21-5p, miR-151a-3p, miR-26-5p, and miR-148a-3p were highly expressed in iPSCs-exo and hiPSC-CM-exo (Figure 7E).

Extracellular vesicles expressing miR-21-5p can be absorbed by AC16 cells

To visually observe whether the miR-21-5p-expressing exos can be absorbed by AC16 cells, we stained the AC16 cell membrane green (Dil) and labeled the extracellular vesicles red (Dio) with membrane dye. After co-culture of AC16 cells with extracellular vesicles, we found that the extracellular vesicles colocalized with AC16 cells (Figure 8A and B), indicating that the extracellular vesicles expressing miR-21-5p could be effectively absorbed by AC16 cells. Next, the expression of miR-21-5p in AC16 cells treated with extracellular vesicles was determined by RT-qPCR. Compared with the untreated group, hiPSC-exo and hiPSC-CM-exo treatments significantly increased the expression of miR-21-5p in

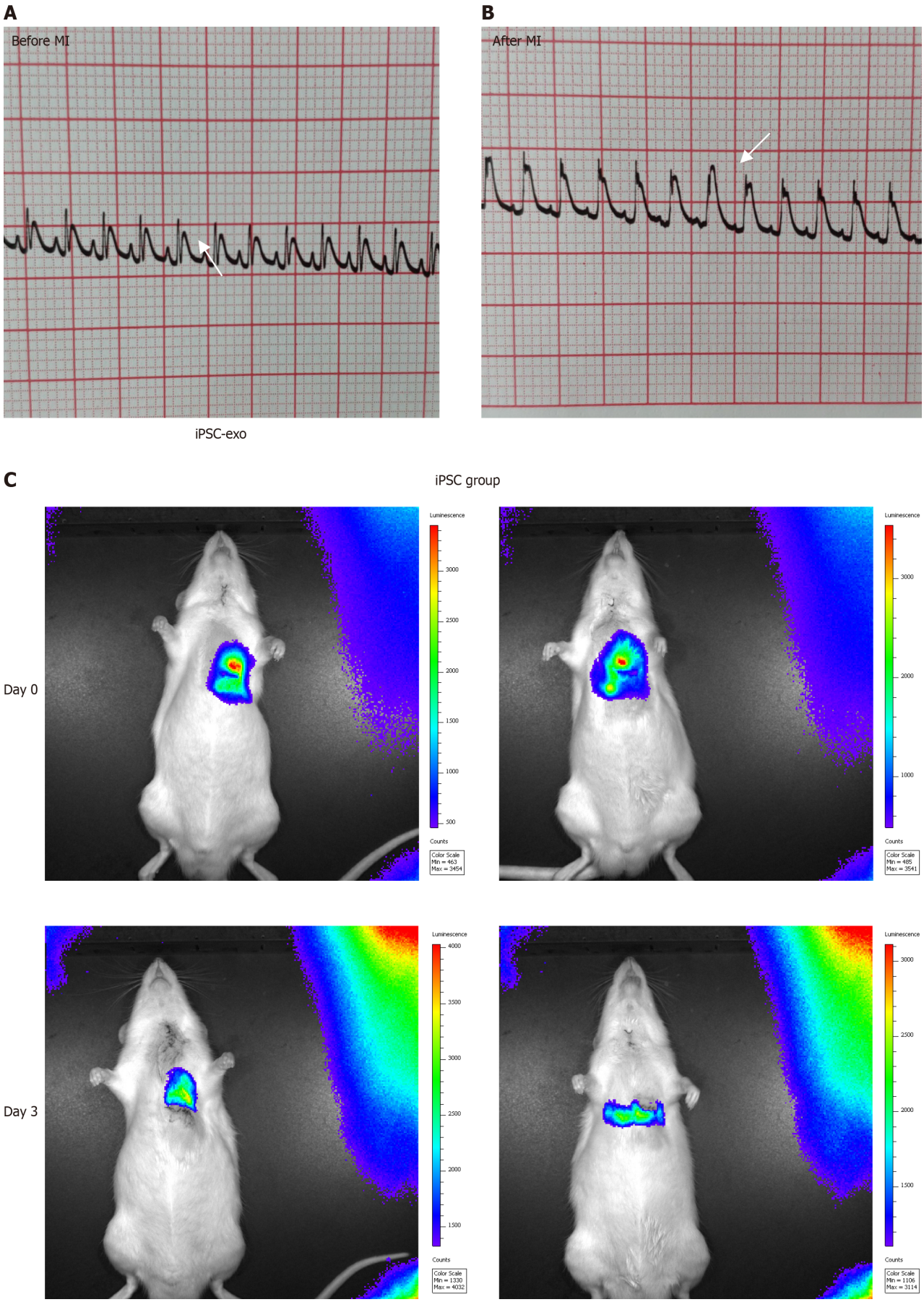
A
Before MI
B
After MI
iPSC-exo
C
iPSC group
Day 0
Day 3
Luminescence
Counts
Color Scale
Min = 463
Max = 3454
Color Scale
Min = 485
Max = 3541
Color Scale
Min = 1330
Max = 4032
Color Scale
Min = 1106
Max = 3114

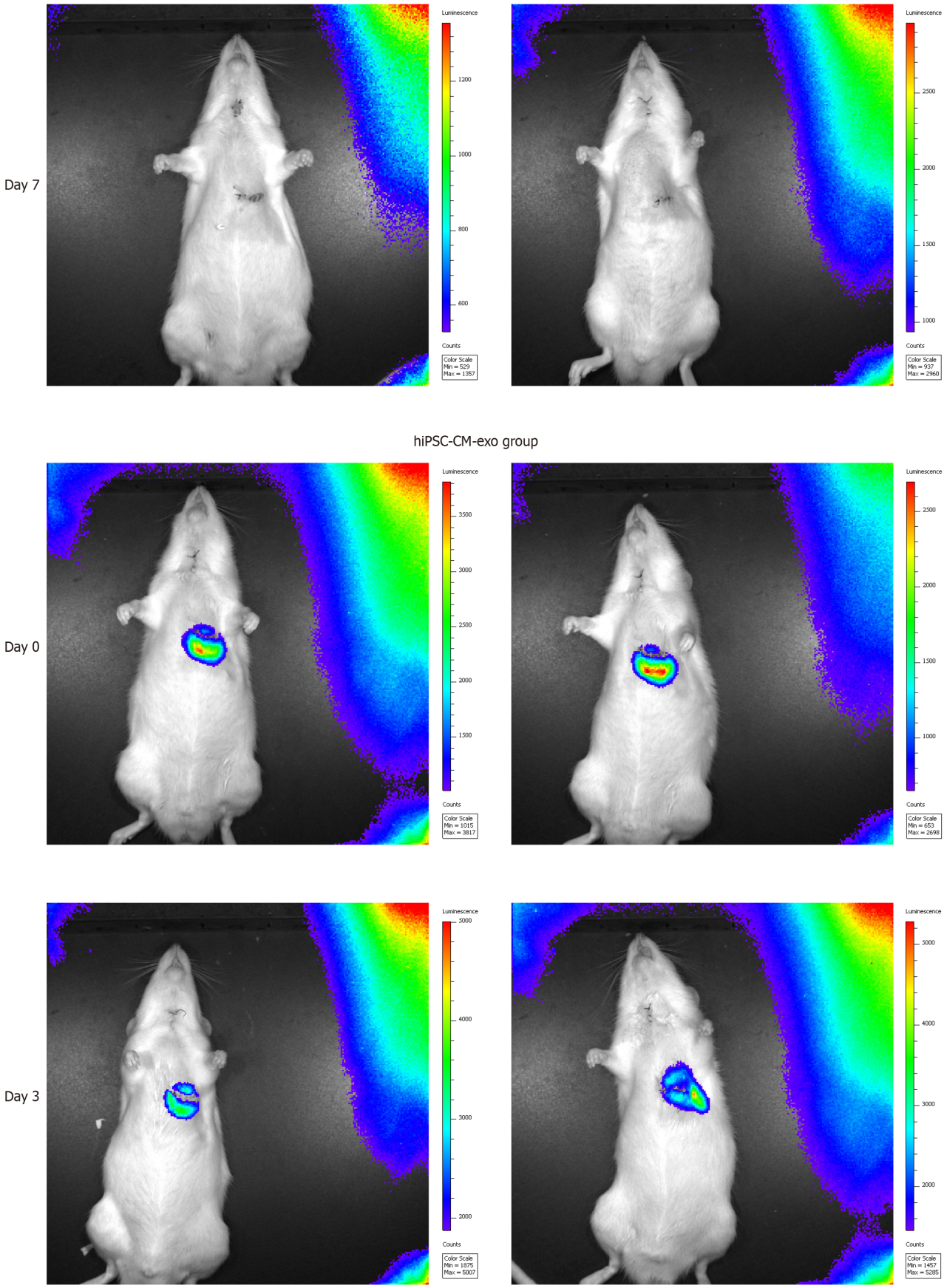
Day 7
Luminescence
1200
1000
800
600
Counts
Color Scale
Min = 529
Max = 1357
Luminescence
2500
2000
1500
1000
Counts
Color Scale
Min = 937
Max = 2960
hiPSC-CM-exo group
Day 0
Luminescence
3500
3000
2500
2000
1500
Counts
Color Scale
Min = 1015
Max = 3817
Luminescence
2500
2000
1500
1000
Counts
Color Scale
Min = 653
Max = 2698
Day 3
Luminescence
5000
4000
3000
2000
Counts
Color Scale
Min = 1875
Max = 5007
Luminescence
5000
4000
3000
2000
Counts
Color Scale
Min = 1457
Max = 5285

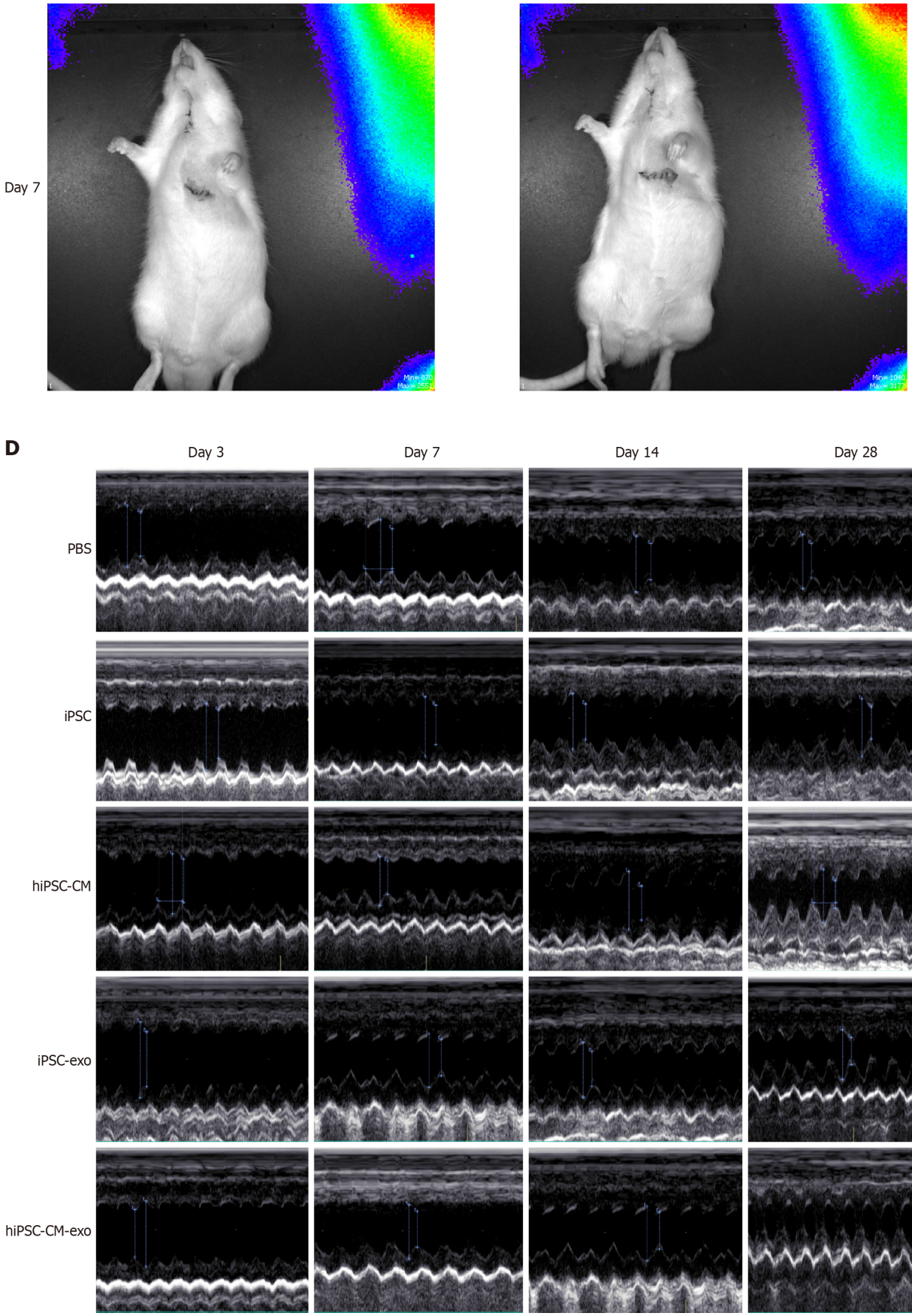
Day 7
D
Day 3
Day 7
Day 14
Day 28
PBS
iPSC
hiPSC-CM
iPSC-exo
hiPSC-CM-exo

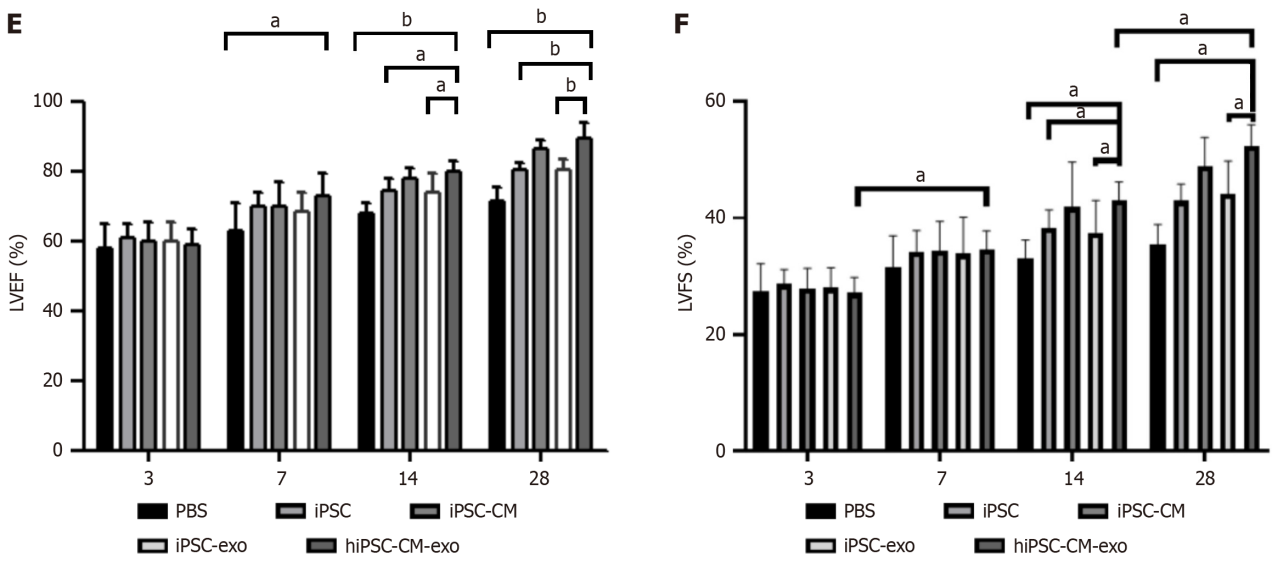

Figure 2 Human-induced pluripotent stem cell-derived cardiomyocyte exosomes improve cardiac function in a murine myocardial infarction model. A and B: Electrocardiogram changes after left anterior descending following left anterior descending ligation; all rats displayed ST segment elevations (indicated by the white arrow); C: Bioluminescence imaging of induced pluripotent stem cells (iPSCs) and human-induced pluripotent SC-derived cardiomyocytes (hiPSC-CMs) on days 0, 3, and 7 post-cell transplantation; D: Left ventricular ejection fractions (LVEFs) were assessed on days 3, 7, 14, and 28 post-myocardial infarction (MI) injury and treatment. Data are shown as the mean ± SD from n = 7 biologically independent samples across different groups; E and F: LVEF (E) and LVFS (F) were measured on days 3, 7, 14, and 28 post-MI injury and treatment. Data are shown as the mean ± SD from n = 7 biologically independent samples across different groups. $^{a}P < 0.05$, $^{b}P < 0.05$. hiPSC-CM-exos: Human-induced pluripotent stem cell-derived cardiomyocyte-derived exosomes; iPSC-CMs: Induced pluripotent stem cell-derived cardiomyocytes; iPSC-exos: Induced pluripotent stem cell-derived exosomes; PBS: Phosphate-buffered saline.

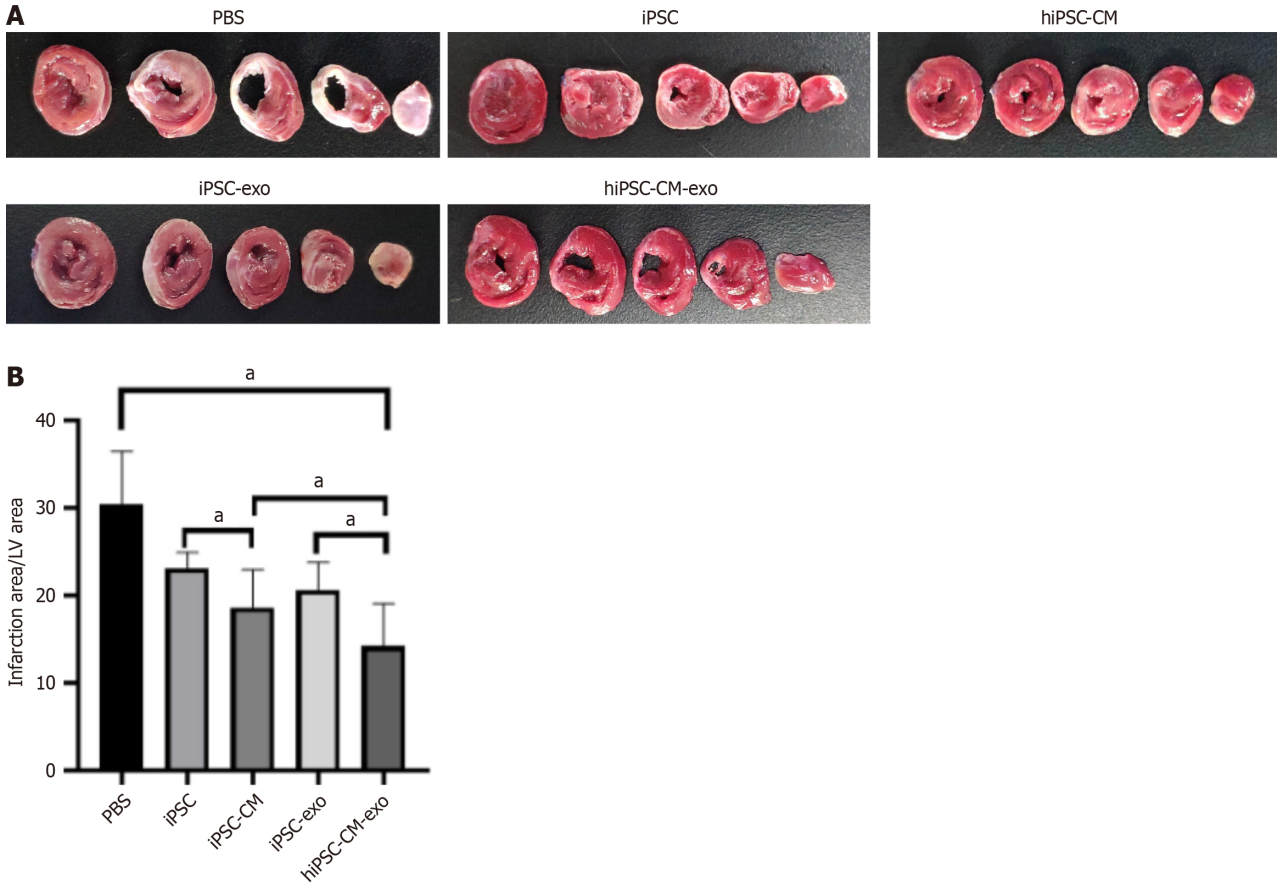

Figure 3 Human-induced pluripotent stem cell-derived cardiomyocyte exosomes reduce infarction area. A: Representative images of 2,3,5-triphenyltetrazoliumchloride staining across five continuous slices of the left ventricle from various group hearts; B: The infarct size, which is expressed as a percentage of the total left ventricle area, is depicted. Data are shown as the mean ± SD from n = 3 biologically independent samples among different groups. $^{a}P <$

0.05. hiPSC-CMs: Human-induced pluripotent stem cell-derived cardiomyocytes; hiPSC-CM-exos: Human-induced pluripotent stem cell-derived cardiomyocyte-derived exosomes; iPSCs: Induced pluripotent stem cells; iPSC-CMs: Induced pluripotent stem cell-derived cardiomyocytes; iPSC-exos: Induced pluripotent stem cell-derived exosomes; LV: Left ventricular; PBS: Phosphate-buffered saline.

AC16 cells (Figure 8C and D).

Construction of anoxic model of AC16 cells

After treating AC16 cells with 125, 250, and 500 μM $CoCl_2$ for 24 hours, the results of the Cell Counting Kit-8 assay showed that the viability of AC16 cells treated with 500 μM $CoCl_2$ for 24 hours decreased to about 50% (Supplementary Figure 4A). Western blot analysis and RT-qPCR results showed that the expression levels of HIF-1α protein and RNA were significantly increased in AC16 cells treated with 500 μM $CoCl_2$ for 24 hours (Supplementary Figures 4B and C), indicating that chemical hypoxia model of AC16 cells could be successfully constructed after treatment with 500 μM $CoCl_2$ for 24 hours and used for follow-up experiments.

MiR-21-5p inhibits apoptosis in AC16 cells

To further explore the role of miR-21-5p, we first transfected mimic or inhibitor into AC cells for miR-21-5p overexpression or knockdown. After transfection with the miR-21-5p mimic (mimic-21 group), compared with the normally cultured group (NC group), the miR-21-5p mimic significantly increased the expression of miR-21-5p (Supplementary Figure 5A), indicating that AC16 cells with high expression of miR-21-5p were successfully obtained. After transfection with the miR-21-5p inhibitor (inhibitor-21), compared with the NC group, the miR-21-5p inhibitor significantly reduced the expression of miR-21-5p (Supplementary Figure 5B), indicating that AC16 cells with low expression of miR-21-5p were successfully obtained.

To investigate the role of miR-21-5p in CMs, AC16 cells were transfected with mimic-21 and inhibitor-21. Then hypoxia was treated, and apoptosis was detected by the TUNEL method. The results showed that hypoxia and inhibitor-21 promoted apoptosis of AC16 cells, while the mimic significantly inhibited apoptosis (Supplementary Figure 5C and D). Furthermore, AC16 cells were transfected with mimic-21 and inhibitor-21. Then hypoxia was treated, and apoptosis was detected by flow cytometry. Consistent with the above results, in the hypoxia group compared to the NC group, cells showed a trend towards increased apoptosis, with an overall rate of apoptosis around 50%. Transfection with the mimic-21 could reduce the rate of apoptosis after hypoxia relative to the hypoxia group (Supplementary Figure 6A), while transfection with the inhibitor-21 could increase the rate of apoptosis after hypoxia relative to the hypoxia group (Supplementary Figure 6B).

MiR-21-5p regulates apoptosis-related gene expression in AC16 cells

To further explore the molecular mechanism of miR-21-5p's influence on CM apoptosis, we examined the effect of miR-21-5p on the expression of apoptosis-related genes. Western blot analysis showed that, compared with the hypoxia group, anti-apoptotic protein Bcl-2 was increased and pro-apoptotic protein Bax expression was decreased in AC16 CMs in the mimic-21 group (Supplementary Figure 6C). Meanwhile, RT-qPCR was used to detect the RNA expression of *Bcl-2* and *Bax* genes in AC16 cells. Relative to the hypoxia group, the mRNA expression of the anti-apoptotic gene Bcl-2 increased, whereas the mRNA expression of the pro-apoptotic gene *Bax* decreased in the mimic-21 group (Supplementary Figure 6D). This indicates that transfection with mimic-21 can regulate apoptosis-related genes to promote anti-apoptosis. Furthermore, we examined the effect of miR-21-5p knockdown on apoptosis-related gene expression. Western blotting showed that, compared with the hypoxia group, the levels of anti-apoptotic protein Bcl-2 decreased and pro-apoptotic protein Bax increased in AC16 cells after transfection with inhibitor-21 (Supplementary Figure 6E). RT-qPCR was used to detect the RNA expression of *Bcl-2* and *Bax* genes in AC16 cells. In cells in the inhibitor-21 group, relative to the hypoxia group, the expression of the anti-apoptotic *Bcl-2* gene was decreased and the expression of the pro-apoptotic *Bax* gene was increased (Supplementary Figure 6F). This suggests that transfection with the miR-21-5p inhibitor can regulate apoptosis-related genes to promote apoptosis.

DISCUSSION

The ongoing quest to treat heart disease has been marked by a significant shift towards regenerative medicine, with human pluripotent SCs emerging as a beacon of hope due to their unique properties of self-renewal and differentiation into CMs. The results of this study revealed that hiPSC-CM-exo significantly enhanced LVEF and LVFS in a murine MI model, indicative of improved cardiac function. This improvement was associated with a reduction in infarct size and myocardial fibrosis, suggesting a protective role of hiPSC-CM-exo in mitigating cardiac damage following MI. Furthermore, the study demonstrated that hiPSC-CM-exo can reduce apoptosis in infarcted rat hearts, potentially through the activation of cytoprotective pathways involving miR-21-5p. Furthermore, overexpression of miR-21-5p was found to significantly inhibit apoptosis in AC16 cells under hypoxic conditions, while its knockdown promoted apoptosis. This dual effect on apoptosis was confirmed by changes in the expression of apoptosis-related genes, with Bcl-2 (anti-apoptotic) increasing and Bax (pro-apoptotic) decreasing in the presence of miR-21-5p mimic, and vice versa with the inhibitor. This study underscores the significance of miR-21-5p in the context of hypoxia-induced apoptosis in AC16 myocardial cells, a finding that could have profound implications for myocardial repair strategies.

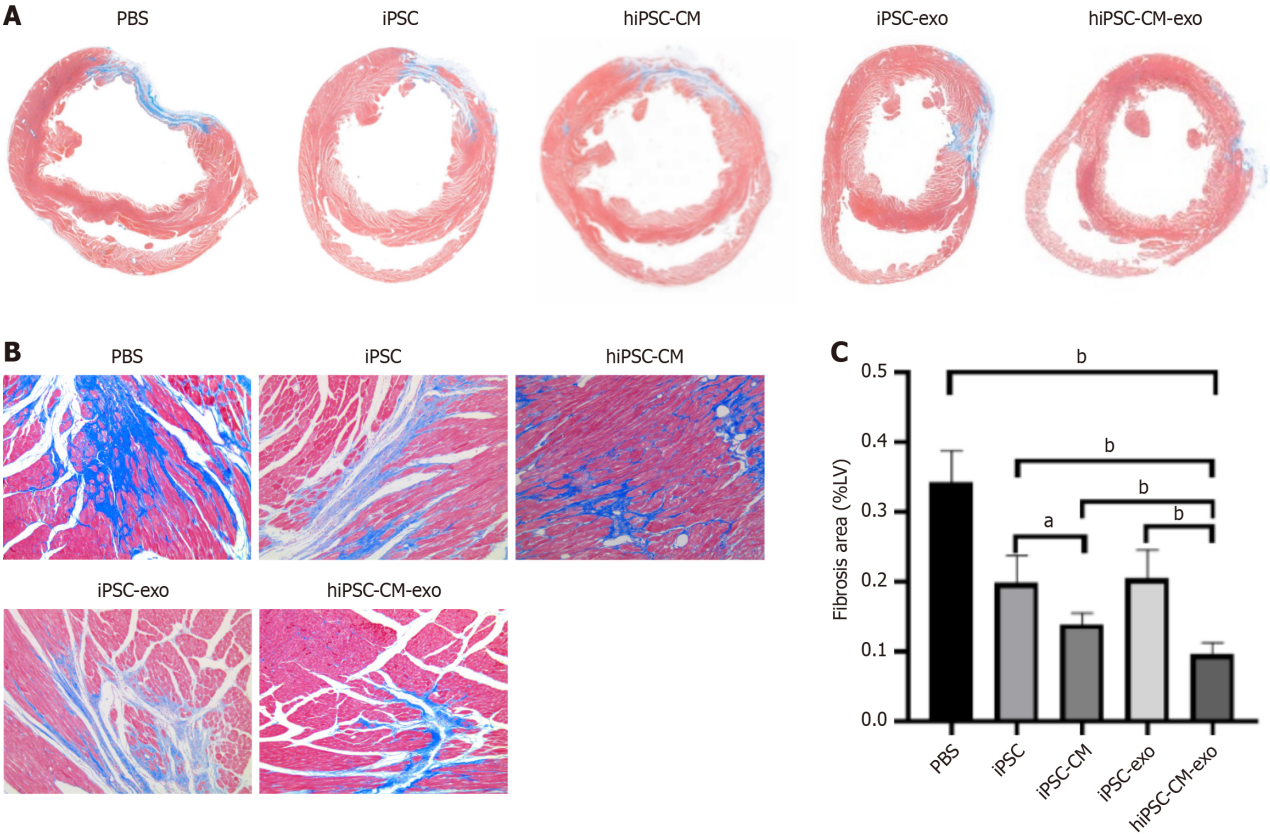

Figure 4 Human-induced pluripotent stem cell-derived cardiomyocytes exosomes reduce myocardial fibrosis. A: Representative images of Masson trichrome staining from various groups are presented in the upper panel, with a high magnification view shown in the lower panel (100 ×); B and C: The Masson average optical density per area was used as an indicator of the cardiac fibrosis level. Data are shown as the mean ± SD from n = 4 biologically independent samples across different groups. $^{a}P < 0.05$; $^{b}P < 0.01$. hiPSC-CMs: Human-induced pluripotent stem cell-derived cardiomyocytes; hiPSC-CM-exos: Human-induced pluripotent stem cell-derived cardiomyocyte-derived exosomes; iPSCs: Induced pluripotent stem cells; iPSC-CMs: Induced pluripotent stem cell-derived cardiomyocytes; iPSC-exos: Induced pluripotent stem cell-derived exosomes; LV: Left ventricular; PBS: Phosphate-buffered saline.

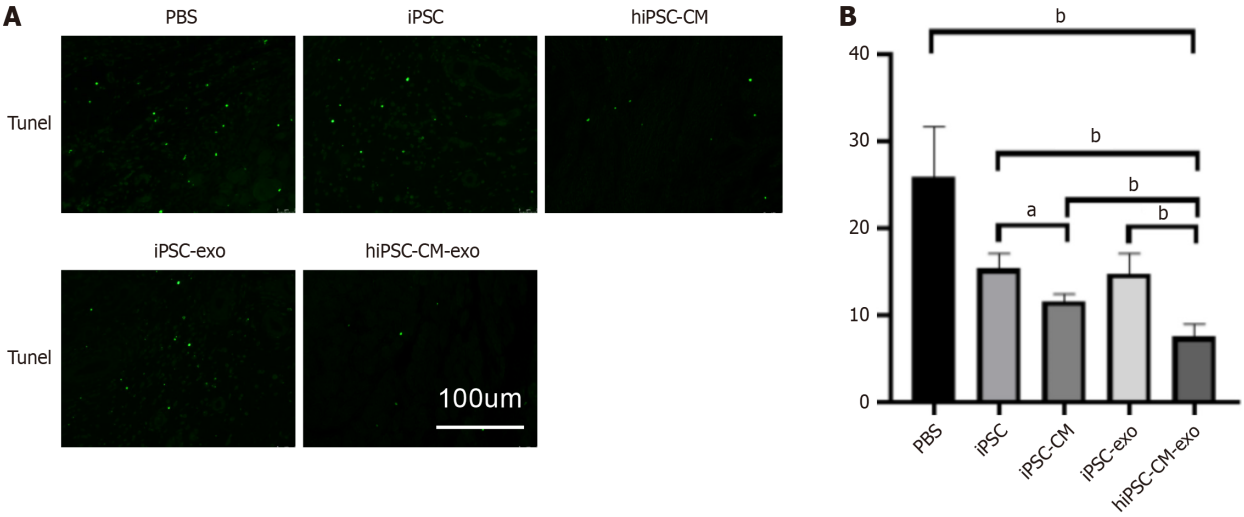

Figure 5 Human-induced pluripotent stem cell-derived cardiomyocyte exosomes reduce apoptosis when administered to infarcted rat hearts. A: Apoptotic cells were identified in sections from the border zone of infarcted hearts from animals across various groups using the transferase dUTP nick-end labeling assay; B: Apoptosis was quantified as the percentage of cells positive for transferase dUTP nick-end labeling staining. Data are shown as the mean ± SD from n = 3 biologically independent samples among different groups. $^{a}P < 0.05$, $^{b}P < 0.01$. hiPSC-CMs: Human-induced pluripotent stem cell-derived cardiomyocytes; hiPSC-CM-exos: Human-induced pluripotent stem cell-derived cardiomyocyte-derived exosomes; iPSCs: Induced pluripotent stem cells; iPSC-CMs: Induced pluripotent stem cell-derived cardiomyocytes; iPSC-exos: Induced pluripotent stem cell-derived exosomes; PBS: Phosphate-buffered saline; TUNEL: Transferase dUTP nick-end labeling.

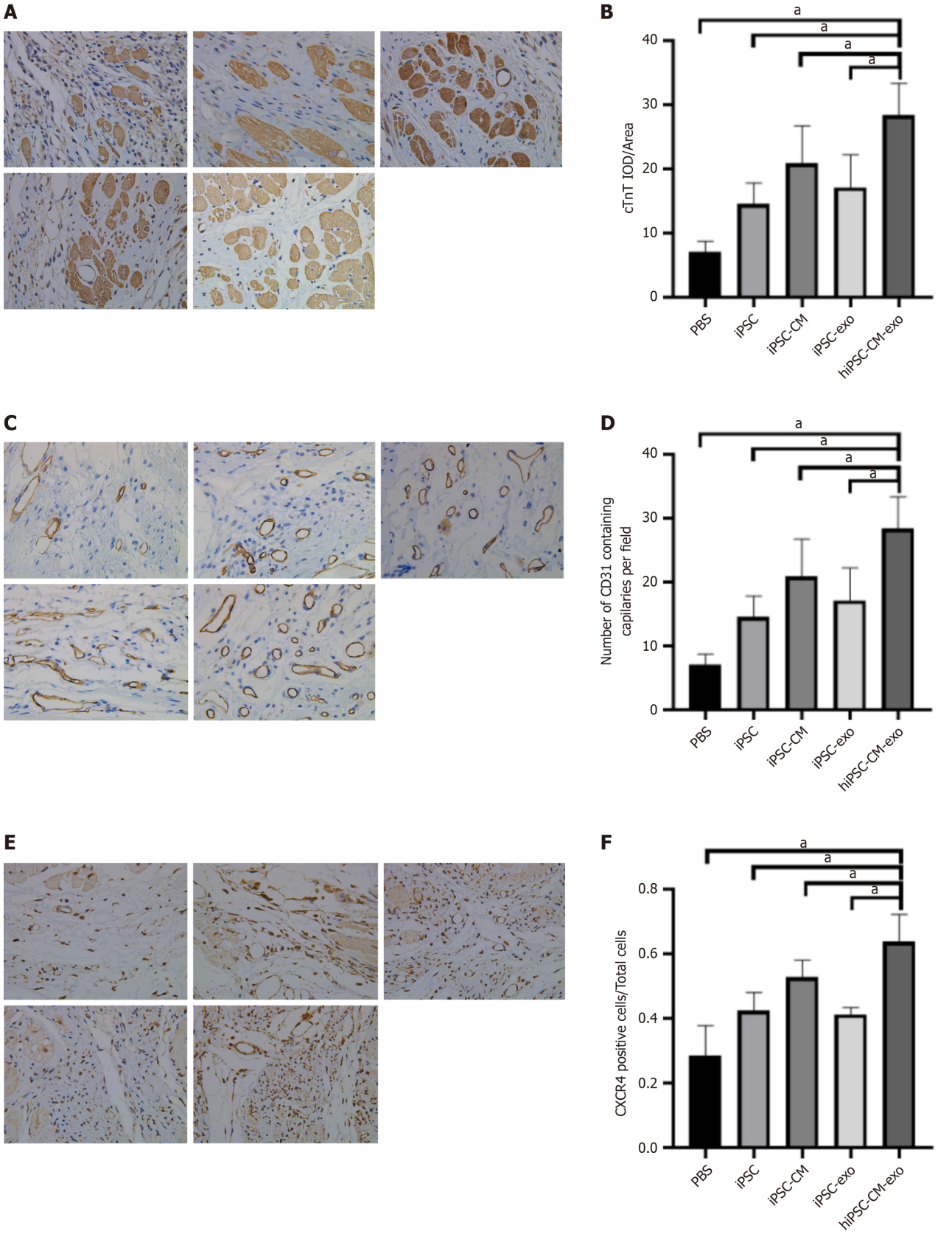

Figure 6 Administration of human-induced pluripotent stem cell-derived cardiomyocytes exosomes to infarcted rat hearts enhances the expression of cardiac troponin T, cluster of differentiation 31, and C-X-C chemokine receptor type 4. A: Post-myocardial infarction (MI) border zone sections were subjected to immunohistochemistry for cardiac troponin T (cTNT) expression. The black arrow indicates the cTNT-positive expression region; B: Average optical density value was used to represent the level of cTNT expression; C: Four weeks after MI, BZ sections were immunohistochemically stained for cluster of differentiation 31 (CD31). The black arrow indicates the CD31-positive expression region; D: Number of CD31-positive blood vessels serve as an indicator of angiogenesis at the myocardial infarction edge; E: BZ sections obtained 4 weeks after MI were immunohistochemically analyzed for C-X-C chemokine receptor 4

(CXCR4) expression. The black arrow indicated the CXCR4-positive expression region; F: Ratio of CXCR4-positive cells to total cells reflects the level of CXCR4 expression. Data are shown as the mean ± SD from n = 4 biologically independent samples across different groups. ^aP < 0.05. hiPSC-CM-exos: Human-induced pluripotent stem cell-derived cardiomyocyte-derived exosomes; iPSCs: Induced pluripotent stem cells; iPSC-CMs: Induced pluripotent stem cell-derived cardiomyocytes; iPSC-exos: Induced pluripotent stem cell-derived exosomes; PBS: Phosphate-buffered saline.

Although iPSCs, hiPSC-CMs, and exos have been utilized for cardiac repair, each possesses distinct advantages and disadvantages[31-34]. For the first time, we directly compared the cardiac reparative efficacy of iPSC-exos and hiPSC-CM-exos with that of iPSC and hiPSC-CM *in vivo* MI models. Our study results demonstrate the successful differentiation of hiPSC into hiPSC-CMs *in vitro*. The intensity of the cell imaging signal was positively correlated with cell number, enabling the tracking of cell survival in animals. exos secreted by hiPSC-CMs exhibited superior myocardial ischemia repair capabilities compared with hiPSC-CMs, iPSC, and iPSC exos through the promotion of angiogenesis and cell migration, anti-apoptosis, and the reduction of fibrosis. Consequently, exos derived from hiPSC-derived cardiac cells enhanced myocardial recovery, and thus may serve as a potential acellular therapeutic option for myocardial injury.

Many functional effects exerted by exos are mediated by exosomal miRNAs that are specific to the exos' cells of origin, although several miRNAs appear to be beneficial for myocardial recovery after MI[35]. As exos carry cargo representative of their origin cells, careful selection of the cell type is crucial when determining the therapeutic potential of secreted exos. HiPSC-CM exos effectively affect an injured heart through more CM-specific pathways, including pathological hypertrophy while being enriched with miRNAs that modulate cardiac-specific processes[35]. In investigating whether the miRNAs are associated with exo-mediated cardio protection, we will perform miRNA array analysis on iPSC-exos and hiPSC-CM-exos.

MiR-21-5p has been widely studied for its involvement in various BP, including cell survival, apoptosis, and angiogenesis[21,36,37] mic on apoptosis and the pro-apoptotic effect of its inhibitor, are in line with previous studies that have reported miR-21-5p as a negative regulator of apoptosis[19,38,39]. We found that the upregulation of miR-21-5p in our study led to an increase in Bcl-2, a known anti-apoptotic protein, and a decrease in Bax, a pro-apoptotic protein, suggesting that miR-21-5p may promote cell survival by shifting the balance between pro- and anti-apoptotic factors. Conversely, the knockdown of miR-21-5p resulted in decreased Bcl2 and increased Bax expression, which is consistent with the promotion of apoptosis under hypoxic conditions. This is consistent with the mechanism by which miR-21 inhibits apoptosis found in other cells[40]. Moreover, the cellular response to hypoxia is a complex process that involves multiple signaling pathways, including the HIF pathway[41]. It is plausible that miR-21-5p, through its target genes, may also influence the HIF pathway, which is critical for the adaptation of cells to low oxygen conditions. The activation of HIF can lead to the transcription of genes involved in angiogenesis, metabolism, and cell survival, among other processes [42]. Our study's observation of increased HIF-1α expression in response to $CoCl_2$ treatment further supports the role of hypoxia in modulating cellular responses and the potential interplay between miR-21-5p and HIF pathways in the context of apoptosis. These results not only corroborate previous findings on the anti-apoptotic role of miR-21-5p but also highlight the potential therapeutic applications of modulating miR-21-5p levels in the context of ischemic heart disease and other conditions involving hypoxia.

In this study, we screened miR-21-5p as a potential regulator of cardiac function through miRNA sequencing in exos. The Gene Ontology enrichment analysis showed that BP such as regulation of cellular processes and nitrogen compound metabolic process, aligns with the known roles of miR-21-5p in modulating cellular responses to stress and its potential involvement in metabolic pathways[43]. The experimental validation conducted in this study, which includes the use of mimics and inhibitors to modulate miR-21-5p expression, has provided direct evidence for its role in regulating apoptosis-related genes such as *Bcl-2* and *Bax*. The overexpression of miR-21-5p leading to decreased apoptosis and the knockdown resulting in increased apoptosis are consistent with the bioinformatics analysis that suggests miR-21-5p targets genes involved in cell survival and death. The combination of bioinformatics and experimental validation strengthens the causal relationship between miR-21-5p and the observed phenotype and is critical for understanding the complex regulatory network in which miR-21-5p operates and its role in regulating myocardial stress response.

Recent literature emphasizes the multifaceted role of miR-21-5p in cardiovascular health[39]. Its expression is linked to various cellular processes, including apoptosis, proliferation, and angiogenesis. One potential mechanism by which miR-21-5p exerts cardioprotective effects involves the regulation of the phosphatase and tensin homolog (PTEN)/Akt signaling pathway[44,45]. Inhibition of PTEN leads to increased Akt phosphorylation, promoting CM survival and anti-apoptotic signaling. Additionally, miR-21-5p/PTEN/Akt axis can enhance angiogenesis by regulating factors such as vascular endothelial growth factor[44,46]. Vascular endothelial growth factor is crucial for new vessel formation and tissue repair after ischemic injury. The involvement of the HIF pathway discussed in this study further highlights the potential of miR-21-5p to mediate hypoxic responses. This indicates that miR-21-5p plays a broader role in cardiac adaptation and recovery under stress conditions.

The differential effects observed between exos derived from hiPSC-CMs and those from iPSCs stem from their unique characteristics. Exos from different cell types exhibit distinct membrane compositions, surface markers, and cargo profiles [47-50]. HiPSC-CM-exos are specifically tailored for cardiac tissue. They preferentially interact with myocardial cells. This enhances their ability to promote angiogenesis and regulate apoptosis. In contrast, iPSC-exos may not possess these specialized attributes. As a result, they exhibit less effective therapeutic benefits in cardiac repair.

While our study provides compelling evidence for the therapeutic potential of hiPSC-CM-exos, particularly highlighting the role of miR-21-5p in modulating myocardial repair and apoptosis, it is important to acknowledge its limitations. One of the primary limitations is the use of a single cell line model, AC16, to investigate the effects of miR-21-5p. Although this model has been instrumental in elucidating the underlying mechanisms, the findings may not fully

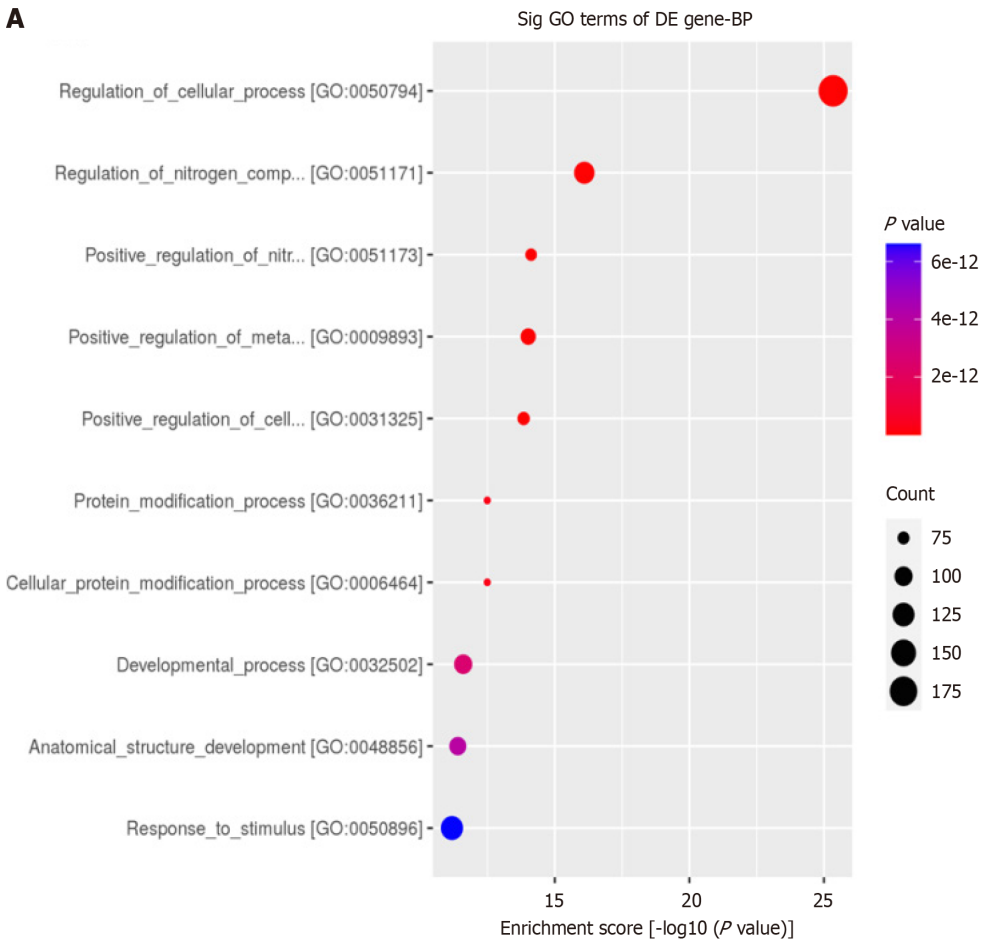
A
Sig GO terms of DE gene-BP
Regulation_of_cellular_process [GO:0050794]
Regulation_of_nitrogen_comp... [GO:0051171]
Positive_regulation_of_nitr... [GO:0051173]
Positive_regulation_of_meta... [GO:0009893]
Positive_regulation_of_cell... [GO:0031325]
Protein_modification_process [GO:0036211]
Cellular_protein_modification_process [GO:0006464]
Developmental_process [GO:0032502]
Anatomical_structure_development [GO:0048856]
Response_to_stimulus [GO:0050896]
15
20
25
Enrichment score [-log10 (P value)]
P value
6e-12
4e-12
2e-12
Count
75
100
125
150
175

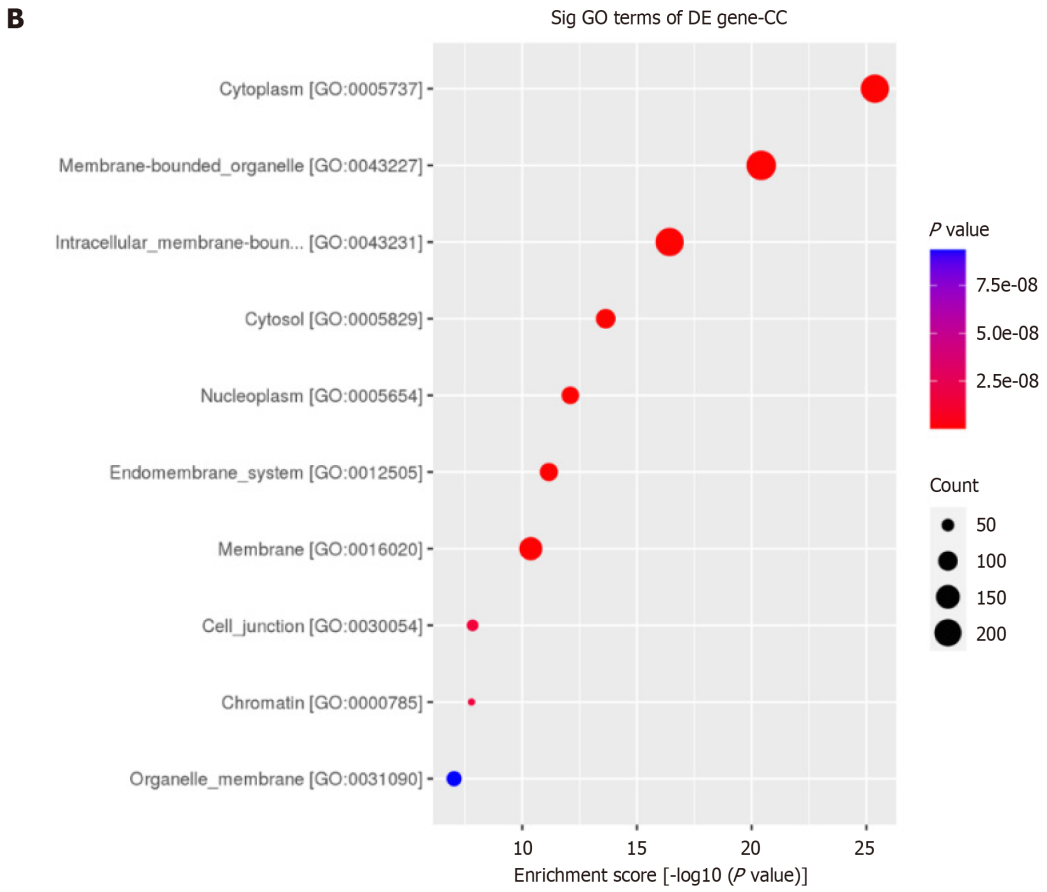
B
Sig GO terms of DE gene-CC
Cytoplasm [GO:0005737]
Membrane-bounded_organelle [GO:0043227]
Intracellular_membrane-boun... [GO:0043231]
Cytosol [GO:0005829]
Nucleoplasm [GO:0005654]
Endomembrane_system [GO:0012505]
Membrane [GO:0016020]
Cell_junction [GO:0030054]
Chromatin [GO:0000785]
Organelle_membrane [GO:0031090]
10
15
20
25
Enrichment score [-log10 (P value)]
P value
7.5e-08
5.0e-08
2.5e-08
Count
50
100
150
200

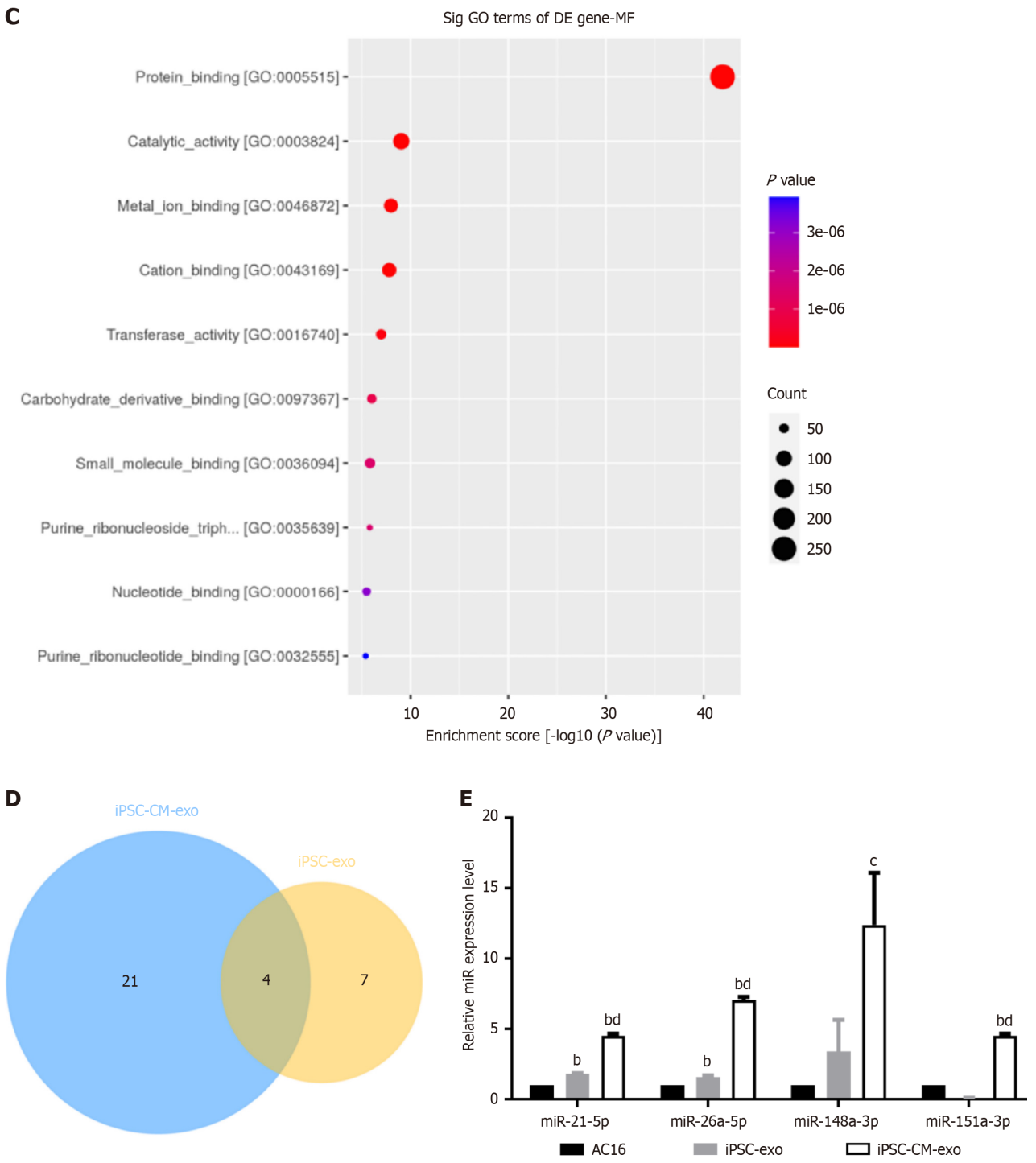

Figure 7 Data analysis of sequencing microRNA. A: Enrichment result of biological processes (BP) is Gene Ontology (GO): 0050794 regulation of cellular processes; GO: 0051171 regulation of nitrogen compound metabolic process; GO: 0051173 positive regulation of nitrogen compound metabolic process; B: Enrichment results of cellular components (CC) are GO: 0005737 cytoplasm, GO: 0043227 membrane bound organelle, GO: 0043231 intracellular membrane bound organelle; C: Molecular function (MF) enrichment results are GO: 0005515 protein binding, GO: 0003824 catalytic activity, and GO: 0046872 metal ion binding; D: Four miRNAs hsa-miR-148a-3p, hsa-miR-21-5p, hsa-miR-151a-3p and hsa-miR-26a-5p, were obtained from the collection of highly expressed microRNAs in human-induced pluripotent stem cell (hiPSC)-cardiomyocyte (CM)-exosome (exo) and iPSC exo; E: MicroRNA expression in AC16, hiPSC-exo, hiPSC-CM-exo, $^{b}P < 0.01$ comparison with AC16-exo, $^{c}P < 0.05$ comparison with hiPSC-exo, $^{d}P < 0.01$ comparison with hiPSC-exo.

represent the complexity of human myocardial tissue, which comprises a diverse array of cell types. Therefore, further studies using multiple cell lineages and *in vivo* models are necessary to confirm the observed effects and to explore the broader implications of miR-21-5p in cardiac repair. Additionally, the study did not delve into other potential regulatory mechanisms that may be influenced by miR-21-5p or other miRNAs present in the exos. Given the intricate regulatory networks within the heart, it is plausible that multiple miRNAs and their targets contribute to the observed phenotypes. Future research should aim to dissect these complex interactions to fully understand the spectrum of miRNA-mediated regulation in cardiac cells. Despite these limitations, the study's findings have significant clinical relevance. The identi-

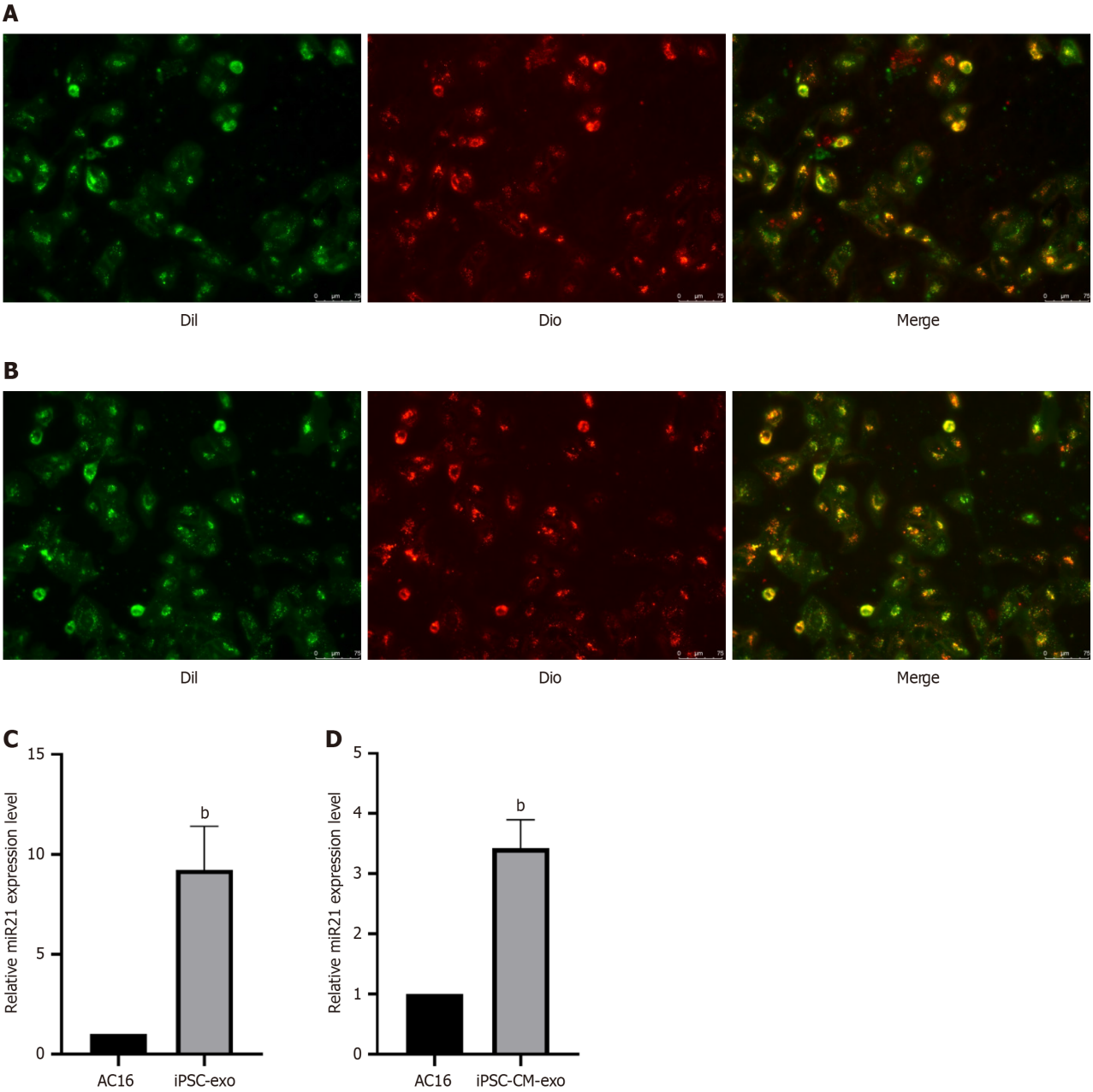

Figure 8 Effects of exosomes applied to AC16 cells on the expression level of microRNA 21. A: AC16 cells absorb human-induced pluripotent stem cell-exosomes (hiPSC-exos). Scale bar = 75 μm; B: AC16 cells absorb hiPSC-cardiomyocyte (CM)-exos Scale bar = 75 μm; C: Expression of miR-21 in AC16 cells after absorption of iPSC-exos; D: Expression of microRNA 21 in AC16 cells after absorption of hiPSC-CM-exos, $^{b}P < 0.01$.

fication of miR-21-5p as a key modulator of apoptosis in myocardial cells presents an opportunity to develop targeted therapies and diagnostic marker for ischemic heart disease.

CONCLUSION

Exos from hiPSC-CMs, enriched with miR-21-5p, demonstrated superior therapeutic efficacy over hiPSC-CM cell therapy by improving ejection fraction, reducing fibrosis, and preventing apoptosis, while their low immunogenicity and stability position them as promising candidates for off-the-shelf regenerative therapies.

FOOTNOTES

Author contributions: Jin JJ and Weng GX contributed to the conceptualization, writing-review, and editing of this manuscript, and they contributed equally to this article and as co-corresponding authors; Liu RH, Chen JY, Nie DS, Gong YQ, and Lin B participated in the methodology of this manuscript; Liu RH, Chen JY, Wang K, and Han JY took part in the formal analysis, investigation, and data

curation; Jin JJ and Liu RH contributed to the writing-original draft preparation; All authors have read and agreed to the published version of the manuscript.

Supported by the Nonprofit Research Institutes Foundation of Fujian Province, China, No. 2021R1012005 and No. 2021R1012003.

Institutional animal care and use committee statement: This study was carried out in accordance with the principles of the Basel Declaration. The study was approved by the Ethics Committee of Fujian Academy of Medical Sciences (Approval No. DL2021-09).

Conflict-of-interest statement: The authors have no conflicts of interest to declare.

Data sharing statement: No additional data are available.

ARRIVE guidelines statement: The authors have read the ARRIVE guidelines, and the manuscript was prepared and revised according to the ARRIVE guidelines.

Country of origin: China

ORCID number: Jing-Jun Jin 0000-0002-2823-4373.

S-Editor: Wang JJ
L-Editor: Filipodia
P-Editor: Zhao YQ

REFERENCES

1 **Liu X**, Wang L, Wang Y, Qiao X, Chen N, Liu F, Zhou X, Wang H, Shen H. Myocardial infarction complexity: A multi-omics approach. *Clin Chim Acta* 2024; **552**: 117680 [PMID: 38008153 DOI: 10.1016/j.cca.2023.117680]

2 **Cho S**, Discher DE, Leong KW, Vunjak-Novakovic G, Wu JC. Challenges and opportunities for the next generation of cardiovascular tissue engineering. *Nat Methods* 2022; **19**: 1064-1071 [PMID: 36064773 DOI: 10.1038/s41592-022-01591-3]

3 **Yan W**, Xia Y, Zhao H, Xu X, Ma X, Tao L. Stem cell-based therapy in cardiac repair after myocardial infarction: Promise, challenges, and future directions. *J Mol Cell Cardiol* 2024; **188**: 1-14 [PMID: 38246086 DOI: 10.1016/j.yjmcc.2023.12.009]

4 **Sayed N**, Liu C, Wu JC. Translation of Human-Induced Pluripotent Stem Cells: From Clinical Trial in a Dish to Precision Medicine. *J Am Coll Cardiol* 2016; **67**: 2161-2176 [PMID: 27151349 DOI: 10.1016/j.jacc.2016.01.083]

5 **Higuchi T**, Miyagawa S, Pearson JT, Fukushima S, Saito A, Tsuchimochi H, Sonobe T, Fujii Y, Yagi N, Astolfo A, Shirai M, Sawa Y. Functional and Electrical Integration of Induced Pluripotent Stem Cell-Derived Cardiomyocytes in a Myocardial Infarction Rat Heart. *Cell Transplant* 2015; **24**: 2479-2489 [PMID: 25606821 DOI: 10.3727/096368914X685799]

6 **Kawamura M**, Miyagawa S, Miki K, Saito A, Fukushima S, Higuchi T, Kawamura T, Kuratani T, Daimon T, Shimizu T, Okano T, Sawa Y. Feasibility, safety, and therapeutic efficacy of human induced pluripotent stem cell-derived cardiomyocyte sheets in a porcine ischemic cardiomyopathy model. *Circulation* 2012; **126**: S29-S37 [PMID: 22965990 DOI: 10.1161/CIRCULATIONAHA.111.084343]

7 **Ye L**, Chang YH, Xiong Q, Zhang P, Zhang L, Somasundaram P, Lepley M, Swingen C, Su L, Wendel JS, Guo J, Jang A, Rosenbush D, Greder L, Dutton JR, Zhang J, Kamp TJ, Kaufman DS, Ge Y, Zhang J. Cardiac repair in a porcine model of acute myocardial infarction with human induced pluripotent stem cell-derived cardiovascular cells. *Cell Stem Cell* 2014; **15**: 750-761 [PMID: 25479750 DOI: 10.1016/j.stem.2014.11.009]

8 **Shiba Y**, Gomibuchi T, Seto T, Wada Y, Ichimura H, Tanaka Y, Ogasawara T, Okada K, Shiba N, Sakamoto K, Ido D, Shiina T, Ohkura M, Nakai J, Uno N, Kazuki Y, Oshimura M, Minami I, Ikeda U. Allogeneic transplantation of iPS cell-derived cardiomyocytes regenerates primate hearts. *Nature* 2016; **538**: 388-391 [PMID: 27723741 DOI: 10.1038/nature19815]

9 **Tachibana A**, Santoso MR, Mahmoudi M, Shukla P, Wang L, Bennett M, Goldstone AB, Wang M, Fukushi M, Ebert AD, Woo YJ, Rulifson E, Yang PC. Paracrine Effects of the Pluripotent Stem Cell-Derived Cardiac Myocytes Salvage the Injured Myocardium. *Circ Res* 2017; **121**: e22-e36 [PMID: 28743804 DOI: 10.1161/CIRCRESAHA.117.310803]

10 **Ong SG**, Huber BC, Lee WH, Kodo K, Ebert AD, Ma Y, Nguyen PK, Diecke S, Chen WY, Wu JC. Microfluidic Single-Cell Analysis of Transplanted Human Induced Pluripotent Stem Cell-Derived Cardiomyocytes After Acute Myocardial Infarction. *Circulation* 2015; **132**: 762-771 [PMID: 26304668 DOI: 10.1161/CIRCULATIONAHA.114.015231]

11 **Kim PJ**, Mahmoudi M, Ge X, Matsuura Y, Toma I, Metzler S, Kooreman NG, Ramunas J, Holbrook C, McConnell MV, Blau H, Harnish P, Rulifson E, Yang PC. Direct evaluation of myocardial viability and stem cell engraftment demonstrates salvage of the injured myocardium. *Circ Res* 2015; **116**: e40-e50 [PMID: 25654979 DOI: 10.1161/CIRCRESAHA.116.304668]

12 **Colombo M**, Raposo G, Théry C. Biogenesis, secretion, and intercellular interactions of exosomes and other extracellular vesicles. *Annu Rev Cell Dev Biol* 2014; **30**: 255-289 [PMID: 25288114 DOI: 10.1146/annurev-cellbio-101512-122326]

13 **Zhu LP**, Tian T, Wang JY, He JN, Chen T, Pan M, Xu L, Zhang HX, Qiu XT, Li CC, Wang KK, Shen H, Zhang GG, Bai YP. Hypoxia-elicited mesenchymal stem cell-derived exosomes facilitates cardiac repair through miR-125b-mediated prevention of cell death in myocardial infarction. *Theranostics* 2018; **8**: 6163-6177 [PMID: 30613290 DOI: 10.7150/thno.28021]

14 **Valadi H**, Ekström K, Bossios A, Sjöstrand M, Lee JJ, Lötvall JO. Exosome-mediated transfer of mRNAs and microRNAs is a novel mechanism of genetic exchange between cells. *Nat Cell Biol* 2007; **9**: 654-659 [PMID: 17486113 DOI: 10.1038/ncb1596]

15 **Sun J**, Shen H, Shao L, Teng X, Chen Y, Liu X, Yang Z, Shen Z. HIF-1α overexpression in mesenchymal stem cell-derived exosomes mediates cardioprotection in myocardial infarction by enhanced angiogenesis. *Stem Cell Res Ther* 2020; **11**: 373 [PMID: 32859268 DOI: 10.1186/s13287-020-01881-7]

16 **Vandergriff A**, Huang K, Shen D, Hu S, Hensley MT, Caranasos TG, Qian L, Cheng K. Targeting regenerative exosomes to myocardial infarction using cardiac homing peptide. *Theranostics* 2018; **8**: 1869-1878 [PMID: 29556361 DOI: 10.7150/thno.20524]

17 **Hänninen M**, Jäntti T, Tolppanen H, Segersvärd H, Tarvasmäki T, Lassus J, Vausort M, Devaux Y, Sionis A, Tikkanen I, Harjola VP, Lakkisto P; For The CardShock Study Group. Association of miR-21-5p, miR-122-5p, and miR-320a-3p with 90-Day Mortality in Cardiogenic Shock. *Int J Mol Sci* 2020; **21**: 7925 [PMID: 33114482 DOI: 10.3390/ijms21217925]

18 **Mi XL**, Gao YP, Hao DJ, Zhang ZJ, Xu Z, Li T, Li XW. Prognostic value of circulating microRNA-21-5p and microRNA-126 in patients with acute myocardial infarction and infarct-related artery total occlusion. *Front Cardiovasc Med* 2022; **9**: 947721 [PMID: 36330017 DOI: 10.3389/fcvm.2022.947721]

19 **Raupach A**, Torregroza C, Niestegge J, Feige K, Klemm-Meyer S, Bauer I, Brandenburger T, Grievink H, Heinen A, Huhn R. MiR-21-5p but not miR-1-3p expression is modulated by preconditioning in a rat model of myocardial infarction. *Mol Biol Rep* 2020; **47**: 6669-6677 [PMID: 32789575 DOI: 10.1007/s11033-020-05721-y]

20 **Zhang J**, Lu Y, Mao Y, Yu Y, Wu T, Zhao W, Zhu Y, Zhao P, Zhang F. IFN-γ enhances the efficacy of mesenchymal stromal cell-derived exosomes *via* miR-21 in myocardial infarction rats. *Stem Cell Res Ther* 2022; **13**: 333 [PMID: 35870960 DOI: 10.1186/s13287-022-02984-z]

21 **Li Y**, Chen X, Jin R, Chen L, Dang M, Cao H, Dong Y, Cai B, Bai G, Gooding JJ, Liu S, Zou D, Zhang Z, Yang C. Injectable hydrogel with MSNs/microRNA-21-5p delivery enables both immunomodification and enhanced angiogenesis for myocardial infarction therapy in pigs. *Sci Adv* 2021; **7**: eabd6740 [PMID: 33627421 DOI: 10.1126/sciadv.abd6740]

22 **Lian X**, Zhang J, Azarin SM, Zhu K, Hazeltine LB, Bao X, Hsiao C, Kamp TJ, Palecek SP. Directed cardiomyocyte differentiation from human pluripotent stem cells by modulating Wnt/β-catenin signaling under fully defined conditions. *Nat Protoc* 2013; **8**: 162-175 [PMID: 23257984 DOI: 10.1038/nprot.2012.150]

23 **Tang J**, Shen D, Caranasos TG, Wang Z, Vandergriff AC, Allen TA, Hensley MT, Dinh PU, Cores J, Li TS, Zhang J, Kan Q, Cheng K. Therapeutic microparticles functionalized with biomimetic cardiac stem cell membranes and secretome. *Nat Commun* 2017; **8**: 13724 [PMID: 28045024 DOI: 10.1038/ncomms13724]

24 **Tang J**, Su T, Huang K, Dinh PU, Wang Z, Vandergriff A, Hensley MT, Cores J, Allen T, Li T, Sproul E, Mihalko E, Lobo LJ, Ruterbories L, Lynch A, Brown A, Caranasos TG, Shen D, Stouffer GA, Gu Z, Zhang J, Cheng K. Targeted repair of heart injury by stem cells fused with platelet nanovesicles. *Nat Biomed Eng* 2018; **2**: 17-26 [PMID: 29862136 DOI: 10.1038/s41551-017-0182-x]

25 **Tang J**, Cui X, Caranasos TG, Hensley MT, Vandergriff AC, Hartanto Y, Shen D, Zhang H, Zhang J, Cheng K. Heart Repair Using Nanogel-Encapsulated Human Cardiac Stem Cells in Mice and Pigs with Myocardial Infarction. *ACS Nano* 2017; **11**: 9738-9749 [PMID: 28929735 DOI: 10.1021/acsnano.7b01008]

26 **Luo L**, Tang J, Nishi K, Yan C, Dinh PU, Cores J, Kudo T, Zhang J, Li TS, Cheng K. Fabrication of Synthetic Mesenchymal Stem Cells for the Treatment of Acute Myocardial Infarction in Mice. *Circ Res* 2017; **120**: 1768-1775 [PMID: 28298296 DOI: 10.1161/CIRCRESAHA.116.310374]

27 **Sahn DJ**, DeMaria A, Kisslo J, Weyman A. Recommendations regarding quantitation in M-mode echocardiography: results of a survey of echocardiographic measurements. *Circulation* 1978; **58**: 1072-1083 [PMID: 709763 DOI: 10.1161/01.cir.58.6.1072]

28 **Majchrzak K**, Kaspera W, Szymaś J, Bobek-Billewicz B, Hebda A, Majchrzak H. Markers of angiogenesis (CD31, CD34, rCBV) and their prognostic value in low-grade gliomas. *Neurol Neurochir Pol* 2013; **47**: 325-331 [PMID: 23986422 DOI: 10.5114/ninp.2013.36757]

29 **Wang D**, Stockard CR, Harkins L, Lott P, Salih C, Yuan K, Buchsbaum D, Hashim A, Zayzafoon M, Hardy RW, Hameed O, Grizzle W, Siegal GP. Immunohistochemistry in the evaluation of neovascularization in tumor xenografts. *Biotech Histochem* 2008; **83**: 179-189 [PMID: 18846440 DOI: 10.1080/10520290802451085]

30 **Hu X**, Dai S, Wu WJ, Tan W, Zhu X, Mu J, Guo Y, Bolli R, Rokosh G. Stromal cell derived factor-1 alpha confers protection against myocardial ischemia/reperfusion injury: role of the cardiac stromal cell derived factor-1 alpha CXCR4 axis. *Circulation* 2007; **116**: 654-663 [PMID: 17646584 DOI: 10.1161/CIRCULATIONAHA.106.672451]

31 **Adamiak M**, Cheng G, Bobis-Wozowicz S, Zhao L, Kedracka-Krok S, Samanta A, Karnas E, Xuan YT, Skupien-Rabian B, Chen X, Jankowska U, Girgis M, Sekula M, Davani A, Lasota S, Vincent RJ, Sarna M, Newell KL, Wang OL, Dudley N, Madeja Z, Dawn B, Zuba-Surma EK. Induced Pluripotent Stem Cell (iPSC)-Derived Extracellular Vesicles Are Safer and More Effective for Cardiac Repair Than iPSCs. *Circ Res* 2018; **122**: 296-309 [PMID: 29118058 DOI: 10.1161/CIRCRESAHA.117.311769]

32 **Gallet R**, Dawkins J, Valle J, Simsolo E, de Couto G, Middleton R, Tseliou E, Luthringer D, Kreke M, Smith RR, Marbán L, Ghaleh B, Marbán E. Exosomes secreted by cardiosphere-derived cells reduce scarring, attenuate adverse remodelling, and improve function in acute and chronic porcine myocardial infarction. *Eur Heart J* 2017; **38**: 201-211 [PMID: 28158410 DOI: 10.1093/eurheartj/ehw240]

33 **Sanganalmath SK**, Bolli R. Cell therapy for heart failure: a comprehensive overview of experimental and clinical studies, current challenges, and future directions. *Circ Res* 2013; **113**: 810-834 [PMID: 23989721 DOI: 10.1161/CIRCRESAHA.113.300219]

34 **Jiang X**, Yang Z, Dong M. Cardiac repair in a murine model of myocardial infarction with human induced pluripotent stem cell-derived cardiomyocytes. *Stem Cell Res Ther* 2020; **11**: 297 [PMID: 32680540 DOI: 10.1186/s13287-020-01811-7]

35 **Gabisonia K**, Prosdocimo G, Aquaro GD, Carlucci L, Zentilin L, Secco I, Ali H, Braga L, Gorgodze N, Bernini F, Burchielli S, Collesi C, Zandonà L, Sinagra G, Piacenti M, Zacchigna S, Bussani R, Recchia FA, Giacca M. MicroRNA therapy stimulates uncontrolled cardiac repair after myocardial infarction in pigs. *Nature* 2019; **569**: 418-422 [PMID: 31068698 DOI: 10.1038/s41586-019-1191-6]

36 **Cong M**, Shen M, Wu X, Li Y, Wang L, He Q, Shi H, Ding F. Improvement of sensory neuron growth and survival *via* negatively regulating PTEN by miR-21-5p-contained small extracellular vesicles from skin precursor-derived Schwann cells. *Stem Cell Res Ther* 2021; **12**: 80 [PMID: 33494833 DOI: 10.1186/s13287-020-02125-4]

37 **Wang J**, Wang J, Wang Y, Ma R, Zhang S, Zheng J, Xue W, Ding X. Bone Marrow Mesenchymal Stem Cells-Derived miR-21-5p Protects Grafted Islets Against Apoptosis by Targeting PDCD4. *Stem Cells* 2023; **41**: 169-183 [PMID: 36512434 DOI: 10.1093/stmcls/sxac085]

38 **Cheng Y**, Zhu P, Yang J, Liu X, Dong S, Wang X, Chun B, Zhuang J, Zhang C. Ischaemic preconditioning-regulated miR-21 protects heart against ischaemia/reperfusion injury *via* anti-apoptosis through its target PDCD4. *Cardiovasc Res* 2010; **87**: 431-439 [PMID: 20219857 DOI: 10.1093/cvr/cvq082]

39 **Qiao L**, Hu S, Liu S, Zhang H, Ma H, Huang K, Li Z, Su T, Vandergriff A, Tang J, Allen T, Dinh PU, Cores J, Yin Q, Li Y, Cheng K. microRNA-21-5p dysregulation in exosomes derived from heart failure patients impairs regenerative potential. *J Clin Invest* 2019; **129**: 2237-2250 [PMID: 31033484 DOI: 10.1172/JCI123135]

40 **Gao X**, Huang X, Yang Q, Zhang S, Yan Z, Luo R, Wang P, Wang W, Xie K, Gun S. MicroRNA-21-5p targets PDCD4 to modulate apoptosis and inflammatory response to Clostridium perfringens beta2 toxin infection in IPEC-J2 cells. *Dev Comp Immunol* 2021; **114**: 103849 [PMID: 32888967 DOI: 10.1016/j.dci.2020.103849]

41 **Semenza GL**. Hypoxia-inducible factors in physiology and medicine. *Cell* 2012; **148**: 399-408 [PMID: 22304911 DOI: 10.1016/j.cell.2012.01.021]

42 **Semenza GL**. Targeting HIF-1 for cancer therapy. *Nat Rev Cancer* 2003; **3**: 721-732 [PMID: 13130303 DOI: 10.1038/nrc1187]

43 **Moghaddam AS**, Afshari JT, Esmaeili SA, Saburi E, Joneidi Z, Momtazi-Borojeni AA. Cardioprotective microRNAs: Lessons from stem cell-derived exosomal microRNAs to treat cardiovascular disease. *Atherosclerosis* 2019; **285**: 1-9 [PMID: 30939341 DOI: 10.1016/j.atherosclerosis.2019.03.016]

44 **Gao X**, Xiong Y, Li Q, Han M, Shan D, Yang G, Zhang S, Xin D, Zhao R, Wang Z, Xue H, Li G. Extracellular vesicle-mediated transfer of miR-21-5p from mesenchymal stromal cells to neurons alleviates early brain injury to improve cognitive function *via* the PTEN/Akt pathway after subarachnoid hemorrhage. *Cell Death Dis* 2020; **11**: 363 [PMID: 32404916 DOI: 10.1038/s41419-020-2530-0]

45 **Liu HY**, Zhang YY, Zhu BL, Feng FZ, Yan H, Zhang HY, Zhou B. miR-21 regulates the proliferation and apoptosis of ovarian cancer cells through PTEN/PI3K/AKT. *Eur Rev Med Pharmacol Sci* 2019; **23**: 4149-4155 [PMID: 31173285 DOI: 10.26355/eurrev_201905_17917]

46 **Dimmeler S**, Zeiher AM. Akt takes center stage in angiogenesis signaling. *Circ Res* 2000; **86**: 4-5 [PMID: 10625297 DOI: 10.1161/01.res.86.1.4]

47 **Li M**, Li S, Du C, Zhang Y, Li Y, Chu L, Han X, Galons H, Zhang Y, Sun H, Yu P. Exosomes from different cells: Characteristics, modifications, and therapeutic applications. *Eur J Med Chem* 2020; **207**: 112784 [PMID: 33007722 DOI: 10.1016/j.ejmech.2020.112784]

48 **Zhang M**, Hu S, Liu L, Dang P, Liu Y, Sun Z, Qiao B, Wang C. Engineered exosomes from different sources for cancer-targeted therapy. *Signal Transduct Target Ther* 2023; **8**: 124 [PMID: 36922504 DOI: 10.1038/s41392-023-01382-y]

49 **Phan J**, Kumar P, Hao D, Gao K, Farmer D, Wang A. Engineering mesenchymal stem cells to improve their exosome efficacy and yield for cell-free therapy. *J Extracell Vesicles* 2018; **7**: 1522236 [PMID: 30275938 DOI: 10.1080/20013078.2018.1522236]

50 **Zhu X**, Badawi M, Pomeroy S, Sutaria DS, Xie Z, Baek A, Jiang J, Elgamal OA, Mo X, Perle K, Chalmers J, Schmittgen TD, Phelps MA. Comprehensive toxicity and immunogenicity studies reveal minimal effects in mice following sustained dosing of extracellular vesicles derived from HEK293T cells. *J Extracell Vesicles* 2017; **6**: 1324730 [PMID: 28717420 DOI: 10.1080/20013078.2017.1324730]

World Journal of Stem Cells

Submit a Manuscript: https://www.f6publishing.com

World J Stem Cells 2025 March 26; 17(3): 102088

DOI: 10.4252/wjsc.v17.i3.102088

ISSN 1948-0210 (online)

ORIGINAL ARTICLE

Basic Study

Mesenchymal stem cell exosomes enhance the development of hair follicle to ameliorate androgenetic alopecia

Yu Fu, Yao-Ting Han, Jun-Ling Xie, Rong-Qi Liu, Bo Zhao, Xing-Liao Zhang, Jun Zhang, Jing Zhang

Specialty type: Cell and tissue engineering

Provenance and peer review: Unsolicited article; Externally peer reviewed.

Peer-review model: Single blind

Peer-review report's classification
Scientific Quality: Grade A, Grade B, Grade B, Grade B, Grade C
Novelty: Grade B, Grade B, Grade B, Grade C
Creativity or Innovation: Grade B, Grade B, Grade C, Grade C
Scientific Significance: Grade B, Grade B, Grade C, Grade C

P-Reviewer: Duan Y; Jafar Sameri M; Kim DK; Li SC

Received: October 9, 2024
Revised: January 21, 2025
Accepted: February 26, 2025
Published online: March 26, 2025
Processing time: 163 Days and 3.3 Hours

Yu Fu, Yao-Ting Han, Rong-Qi Liu, Bo Zhao, Jing Zhang, Research Center for Translational Medicine at East Hospital, School of Life Science and Technology, Tongji University, Shanghai 200092, China

Jun-Ling Xie, Xing-Liao Zhang, Research Center for Translational Medicine at East Hospital, School of Medicine, Tongji University, Shanghai 200092, China

Jun Zhang, Jing Zhang, Tongji Lifeng Institute of Regenerative Medicine, Tongji University, Shanghai 200092, China

Jun Zhang, Research Center for Translational Medicine at East Hospital, Shanghai Institute of Stem Cell Research and Clinical Translation, School of Medicine, Tongji University, Shanghai 200092, China

Co-first authors: Yu Fu and Yao-Ting Han.

Co-corresponding authors: Jun Zhang and Jing Zhang.

Corresponding author: Jing Zhang, PhD, Professor, Research Center for Translational Medicine at East Hospital, School of Life Science and Technology, Tongji University, No. 1239 Siping Road, Shanghai 200092, China. 96755@tongji.edu.cn

Abstract

BACKGROUND

Mesenchymal stem cells (MSCs) and their secretome have significant potential in promoting hair follicle development. However, the effects of MSC therapy have been reported to vary due to their heterogeneous characteristics. Different sources of MSCs or culture systems may cause heterogeneity of exosomes.

AIM

To define the potential of human adipose-derived MSC exosomes (hADSC-Exos) and human umbilical cord-derived MSC exosomes (hUCMSC-Exos) for improving dermal papillary cell proliferation in androgenetic alopecia.

METHODS

We conducted liquid chromatography-mass spectrometry proteomic analysis of hADSC-Exos and hUCMSC-Exos. Liquid chromatography-mass spectrometry suggested that hADSC-Exos were related to metabolism and immunity. Additionally, the hADSC-Exo proteins regulated the cell cycle and other 9

functional groups.

RESULTS
We verified that hADSC-Exos inhibited glycogen synthase kinase-3β expression by activating the Wnt/β-catenin signaling pathway *via* cell division cycle protein 42, and enhanced dermal papillary cell proliferation and migration. Excess dihydrotestosterone caused androgenetic alopecia by shortening the hair follicle growth phase, but hADSC-Exos reversed these effects.

CONCLUSION
This study indicated that hair development is influenced by hADSC-Exo-mediated cell-to-cell communication *via* the Wnt/β-catenin pathway.

Key Words: Mesenchymal stem cells; Exosome; Dermal papillary cells; Hair development; Liquid chromatography-mass spectrometry proteomic analysis

Core Tip: Liquid chromatography-mass spectrometry proteomic analysis was conducted to reveal the commonalities and heterogeneities across the human adipose-derived mesenchymal stem cell exosomes (hADSC-Exos) and human umbilical cord-derived mesenchymal stem cell exosomes. A total of 232 common proteins were found in hADSC-Exos and were categorized into 10 functional groups. We have confirmed that hADSC-Exos decrease glycogen synthase kinase-3β expression through the Wnt/β-catenin pathway, leading to increased proliferation and migration of dermal papillary cell. Excessive dihydrotestosterone can cause hair loss by shortening the hair growth phase, but hADSC-Exo treatment can reverse this effect. This study suggests that hADSC-Exo plays a role in hair regeneration through cell-to-cell communication *via* the Wnt/β-catenin pathway.

Citation: Fu Y, Han YT, Xie JL, Liu RQ, Zhao B, Zhang XL, Zhang J, Zhang J. Mesenchymal stem cell exosomes enhance the development of hair follicle to ameliorate androgenetic alopecia. *World J Stem Cells* 2025; 17(3): 102088
URL: https://www.wjgnet.com/1948-0210/full/v17/i3/102088.htm
DOI: https://dx.doi.org/10.4252/wjsc.v17.i3.102088

INTRODUCTION

Hair loss causes a greater financial burden[1]. The two basic categories of hair loss are scarring and nonscarring alopecia and the latter is more common. Nonscarring alopecia can be categorized into androgenetic alopecia (AGA) and non-AGA, such as alopecia areata and telogen effluvium[2]. AGA is the most common form of nonscarring alopecia, affecting up to 50% of women and 80% of men, and the prevalence of AGA increases with age[3]. It is estimated that 0.2%-2% of the world's population suffers from AGA, which affects 500000 men and 300000 women in the United States[4]. The causes of AGA are multifactorial, with genetic factors and androgens playing an important role in the development and progression of the disease. A recent United Kingdom biobank study showed a genealogical heritability of 0.62 and a single nucleotide polymorphism heritability of 0.39. A positive family history of AGA in Asian populations accounts for about 50% of cases[5]. AGA develops in 32.1%-63.3% of testosterone users[4]. By simple diffusion, testosterone enters the cell and is converted to dihydrotestosterone (DHT) by 5-a-reductase in the cytoplasm. When DHT binds to androgen receptors (ARs), it exerts transcriptional activity and contributes to the progression of AGA[6]. The dermal papillary cells (DPCs) of AGA patients have high levels of ARs, which makes them more sensitive to androgens[7]. Synthetic drugs, such as finasteride, used to treat hair loss, cause many side effects. Hence, it requires the development of new and efficient drugs to promote hair follicle development in AGA.

Mesenchymal stem cells (MSCs) and their secretomes show promise in promoting hair follicle regeneration. MSCs can be derived from a wide range of sources, such as umbilical cord, adipose tissue, amniotic fluid and bone marrow, which are named umbilical cord-derived MSCs (UCMSCs), adipose-derived MSCs (ADSCs) and bone marrow-derived MSCs, respectively[8,9]. Exosomes, 30-150 nm microvesicles, are actively released by viable cells and are composed of diverse proteins, encompassing signal proteins, noncoding RNAs and growth factors[10]. MSCs exert their therapeutic effect mainly through paracrine mechanisms, such as releasing exosomes[11]. Compared to MSCs, the exosomes derived from MSCs are cell-free and could be a promising therapy for AGA, with no major adverse effects[12]. However, various issues have restricted their clinical application.

MSCs exhibit heterogeneity at various levels, encompassing differences originating from subpopulations, donors, and different culture media[13,14]. With advances in sequencing techniques, liquid chromatography-mass spectrometry (LC-MS) proteome facilitates finding heterogeneity of MSCs. In previous studies, we obtained human adipose tissue from which human ADSCs (hADSCs) were isolated[15,16]. In this study, we obtained human UCMSCs (UCMSCs). We analyzed the protein composition of hADSC-exosomes (hADSC-Exos) and hUCMSC-Exos by LC-MS proteome analysis,

so that the heterogeneity of exosomes with different cell origins was revealed. hADSC-Exos were also tested from the same donor source, cultured through three different culture systems, and selected proteins that were common to each culture system. In hADSC-Exos, 232 proteins were stably expressed and categorized into 10 functional groups. Additionally, as the DPCs are unique mesenchymal cells, they regulate hair follicle stem cells (HFSCs) during hair follicle regeneration and development[17]. Researchers have shown that exosomes derived from DPCs stimulate hair follicle development; therefore, we examined if hADSC-Exos improved DPC proliferation in AGA. There was a significant increase in Wnt3a in DPC cocultured with hADSC-Exos[18]. hADSC-Exo-derived cell division cycle protein 42 (CDC42) promoted DPC proliferation *via* the Wnt/β-catenin pathway. These findings provide novel insights into improving hair development in AGA.

MATERIALS AND METHODS

Cell culture

After obtaining high purity hADSCs and hUCMSCs, both cells were cultured in minimal essential medium MEMα with no Phenol-Red (Gibco, NY, United States). + 10% fetal bovine serum (FBS; ScienCell, CA, United States) and incubated at 37 °C with 5% CO_2 for basal cell growth and proliferation. In subsequent analysis, hADSCs were cultured in three different culture systems, including basal culture medium (MEMα + 10% FBS), serum-free medium with phenol red (Cellartis® MSC Xeno-Free Culture Medium; Takara, Japan), and serum-free medium without phenol red (StemPro™ MSC SFM; Gibco, NY, United States) to explore the effect of different culture media on cellular exocytosis[19-21]. We purchased human hair DPCs (HHDPCs; ScienCell, CA, United States), which were obtained from a 58-year-old man. HHDPCs were cultured in MSC medium (ScienCell, CA, United States), containing 5% FBS, 1% MSC growth supplement (ScienCell, CA, United States) and 1% penicillin/streptomycin (ScienCell, CA, United States).

Exosome isolation

As described previously, the supernatant of hADSC/hUCMSC was obtained and subjected to centrifugation for eliminating suspended cells and cellular debris[22]. A 0.22-μm filter was used to filter the supernatant. Subsequently, the filtered supernatants were centrifuged using a Beckman Coulter ultra-high-speed centrifuge (Optima XPN-100 Ultracentrifuge; Beckman Coulter, Australia). Following centrifugation, Dulbecco phosphate buffer saline was introduced to cleanse the exosomes. Monitoring exosome uptake involves staining the exosomal membranes using fluorescent lipid membrane dye PKH26[23]. The hADSC-exos were processed using the PKH26 Red Fluorescent Cell Linker Kit (Sigma, St. Louis, MO, United States). Finally, a microscope (Nikon, Japan) was used to observe the PKH26-hADSC-exos location.

Transmission electron microscopy

Refer to the methods, a copper mesh was used for aspiration of exosomes obtained through ultracentrifuge[24]. Following about 1 minute of operation, the surplus liquid was removed by filter paper positioned at the periphery of the mesh. Subsequently, phosphotungstic acid was applied to the copper mesh, and after 30 seconds, the excess liquid was eliminated using filter paper at the edge of the mesh. The sample was subjected to baking for 1 minute, and electron micrograph images were captured, using an 80-kV transmission electron microscope (Hitachi H-7650, Japan). The exosomes were observed as cup-shaped membrane vesicles ranging in size from 30 to 150 nm.

Nanoparticle tracking analysis

After washing the cells with deionized water, they were calibrated with polystyrene microspheres (110 nm). This was followed by washing and dilution with phosphate buffered saline. ZetaView PMX 110 (Particle Metrix, Meerbusch, Germany) and NTA 3.0 software were used for nanoparticle tracking analysis (NTA)[25].

Western blotting

Total protein was extracted from the exosome samples using RIPA buffer, and the concentration was measured using the BCA protein assay. Western blotting with anti-CD9 and anti-CD81 was used to quantify total exosome proteins. Using rabbit anti-CD9 antibody (ab92726, 1:1000; Abcam, Cambridge, United Kingdom), rabbit anti-CD63 antibody (ab134045, 1:1000; Abcam, Cambridge, United Kingdom) for primary antibodies. Scanned images were acquired by Odyssey Infrared Imaging System (Licor, Lincoln, NE, United States).

Exosomal LC-MS proteome analysis

To commence the analysis, we introduced 30 μL of sample buffer (composed of acetonitrile, water, and formic acid in a ratio of 2:98:0.1) and agitated the mixture until the dried sample was fully dissolved. We subjected the sample to MS using an Easy-nLC 1000 system (Thermo Fisher Scientific, Bremen, Germany) equipped with a C18 reversed-phase column (PepMap100, C18 NanoViper, Thermofisher Dionex, CA, United States). The procedure involved a gradient from 2% to 40% of mobile phase B over a duration of 103 minutes. MS was conducted using a Q Exactive plus system (Thermo Scientific, CA, United States) featuring a nanoliter spray ESI ion source operating at a spray voltage of 1.6 kV. Three independent replicates from exosomes derived from control culture medium (FBS), phenol red culture medium (Takara, Japan), and phenol red free culture medium (Gibco, NY, United States) were analyzed for proteomics with Q Exactive plus (Thermo Fisher Scientific, Bremen, Germany). The different proteins in hADSC-Exo and hUCSMSC-Exo were listed in Supplementary Table 1.

Gene Ontology (GO) (https://geneontology.org) and Kyoto Encyclopedia of Genes and Genomes (KEGG) (https://genome.jp/kegg) were used for selected proteins pathway analysis. The bubble diagram was drawn according to the R language ggplot2 package. The differential proteins screened were imported into STRING (https://string-db.org/). The STRING protein query database was used to build a protein-protein functional interaction network in Cytoscape cluster plugin. The clusters within the network were identified using the MCODE clustering algorithm.

Mice

Male 6-week-old C57BL/6 mice weighing 18-22 g were used. The mice were divided into the control, negative control, positive control and experimental groups (n = 6 per group). To visualize the initial follicle morphogenesis in the skin, all mice were shaved of their back hair, and 2-3 cm were removed. There was a pink coloration in the depilated areas of all the mice treated with depilatory cream, which suggests the dorsal skin was induced into anagen[26]. The control mice were only depilated for observation of normal hair follicle recovery after hair loss. For the negative control, positive control and experimental mice, all mice were established as AGA models. Testosterone propionate (TP, 5 mg/kg) was subcutaneously injected into the back once daily for 4 weeks[27,28]. To evaluate the effect of TP on hair follicle growth and development, we left the negative control group untouched. The first day of injection was marked as day 1. The positive control group was treated with minoxidil, an Food and Drug Administration (FDA)-approved drug for AGA [29]. The experimental group was treated with hADSC-Exos. Minoxidil and hADSC-Exos were started simultaneously on day 1 of TP injection, and ended on day 21. Mice were anesthetized by inhalation of 2% isoflurane before treatment. Microneedle (Mefonol disposable skin prick needle, Suzhou, China) treatment was selected. The specification was 540 rolling needles, 0.22-0.5 mm. To absorb minoxidil, the microneedle treatment head was gently rolled back and forth against the skin. The positive control group received 0.2 mL 5% minoxidil tincture daily, and the hADSC-Exo group was injected daily with a roller needle, as described previously[30,31]. A previous study demonstrated the optimal concentration of ADSC-Exos that promoted DPC proliferation[32]. We selected 100 μg/mL ADSC-Exos per mouse in the assay. The hair growth was photographed in all mice on day 21.

Macroscopic measurement for hair growth

Referred to the previous research, we recorded the time when the skin color changed from pink to black, and we rated and photographed the result on days 7, 14, and 21[33]. The method has been optimized as described by Kwon *et al*[34]. A score of 0 indicated that there was no hair growth in the depilated area and the epidermis was flesh-colored; 1 indicated that the epidermis of the depilated area was gray; 2 indicated that the epidermis of the depilated area was black; and 3 indicated that there was hair growth in the depilated area and the epidermis was black. Referred to the previous research, hair follicles that formed in the new tissue at day 21 were counted on three randomly selected hematoxylin and eosin-stained sections per animal[35].

Cell proliferation

Enhanced cell counting kit-8 (CCK8, Sangon Biotech, China) was used to assess proliferation of DPCs. DPCs were seeded in 96-well plates that were incubated with CCK8 reagents (100 μL/well) for 1 hour and detected at 0, 24, and 48 hours. The results were quantitated using a 450 nm microplate reader.

Cell migration

Transwell assay was used to assess migration of DPCs by Corning TransWell Chamber (Corning, NY, United States). After trypsinization, counting and incubation in 100 μL medium without FBS, DPCs were collected in a 24-well plate (2×10^5 cells/well). In the lower chamber, 800 μL medium supplemented with 30% FBS was added. The migratory capacity of cells was assessed by fixing and staining with 4% formaldehyde and crystal violet solution (Biyuntian, China).

Quantitative polymerase chain reaction

Total RNA isolation was performed using QIAGEN miRNeasy Mini (Valencia, CA, United States). Reverse transcription was performed using a PrimeScript RT Master Mix (Takara, Shiga, Japan). Quantitative polymerase chain reaction was performed using an ABI7500 instrument (Oyster Bay, NY, United States).

RESULTS

Isolation and validation of hADSC-Exos and hUCMSC-Exos

To clarify the heterogeneity between MSCs from different cell sources, we cultured hADSCs and hUCMSCs. Microscopic images revealed that the hADSCs had a typical long spindle-shaped morphology, consistent with the morphological characterization of hUCMSCs (Figure 1A). hADSCs and hUCMSCs showed high levels of MSC marker expression, such as CD73, CD90, CD105, CD45, and HLA-DR (Figure 1B). hADSC-Exos and hUCMSC-Exos were extracted using ultra-high-speed centrifugation (Figure 1C). Transmission electron microscopy revealed a bowl-shaped structure of the hADSC-Exos and hUCMSC-Exos (Figure 1D). NTA demonstrated that the diameter of the hADSC-Exos was about 100 nm, falling within the size range criteria for exosomes (30-150 nm). NTA revealed that the average diameter of hUCMSC-Exos was 139 nm (Figure 1E). HADSC-Exos expressed the exosome markers CD9, CD63, and CD81 (Figure 1F). These results indicated that our exosomes met the morphological characteristics of hADSC-Exos and hUCMSC-Exos.

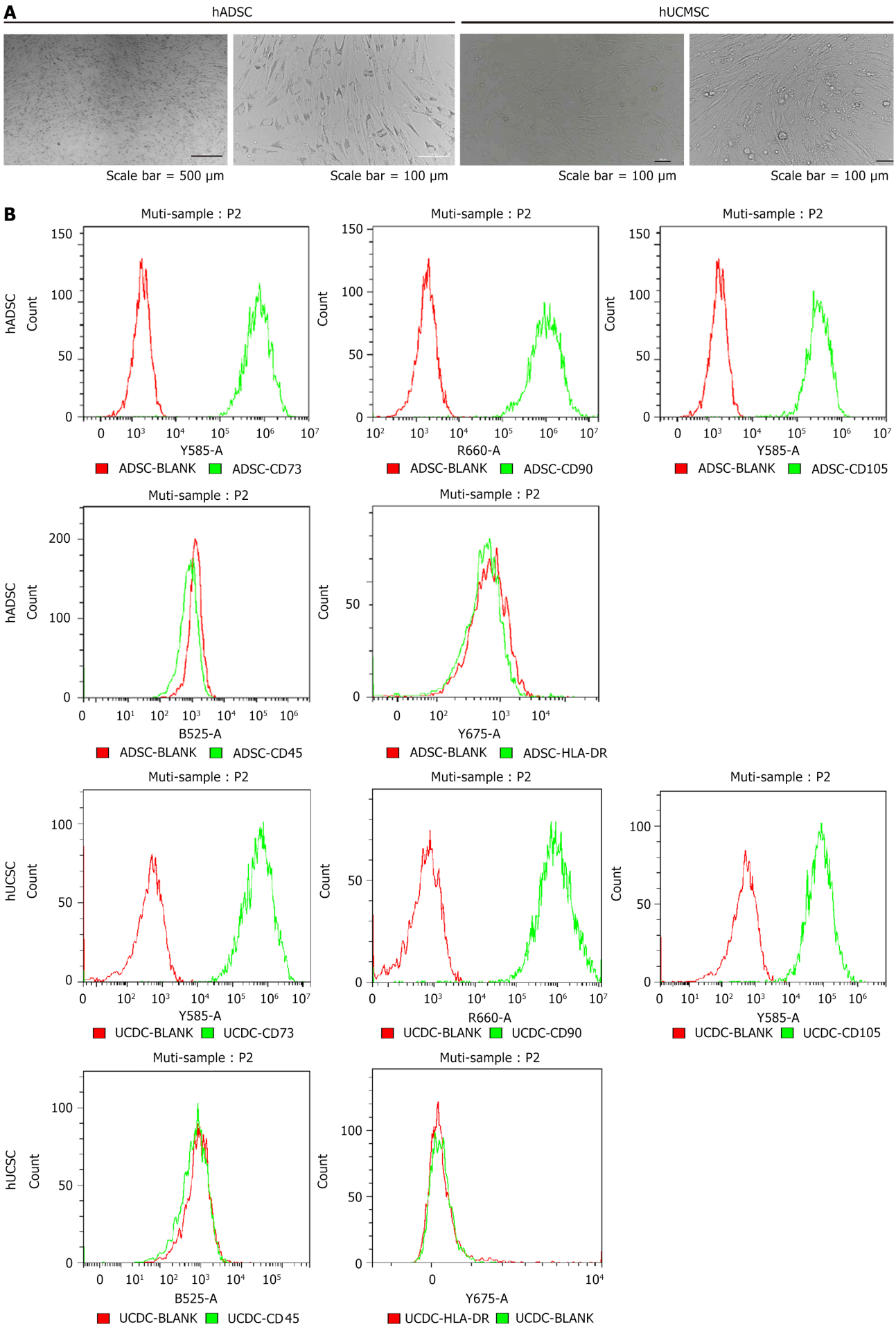
A
hADSC
hUCMSC
Scale bar = 500 μm
Scale bar = 100 μm
Scale bar = 100 μm
Scale bar = 100 μm
B
Muti-sample : P2
hADSC
Count
Y585-A
ADSC-BLANK
ADSC-CD73
R660-A
ADSC-CD90
ADSC-CD105
B525-A
ADSC-CD45
Y675-A
ADSC-HLA-DR
hUCSC
UCDC-BLANK
UCDC-CD73
UCDC-CD90
UCDC-CD105
UCDC-CD45
UCDC-HLA-DR

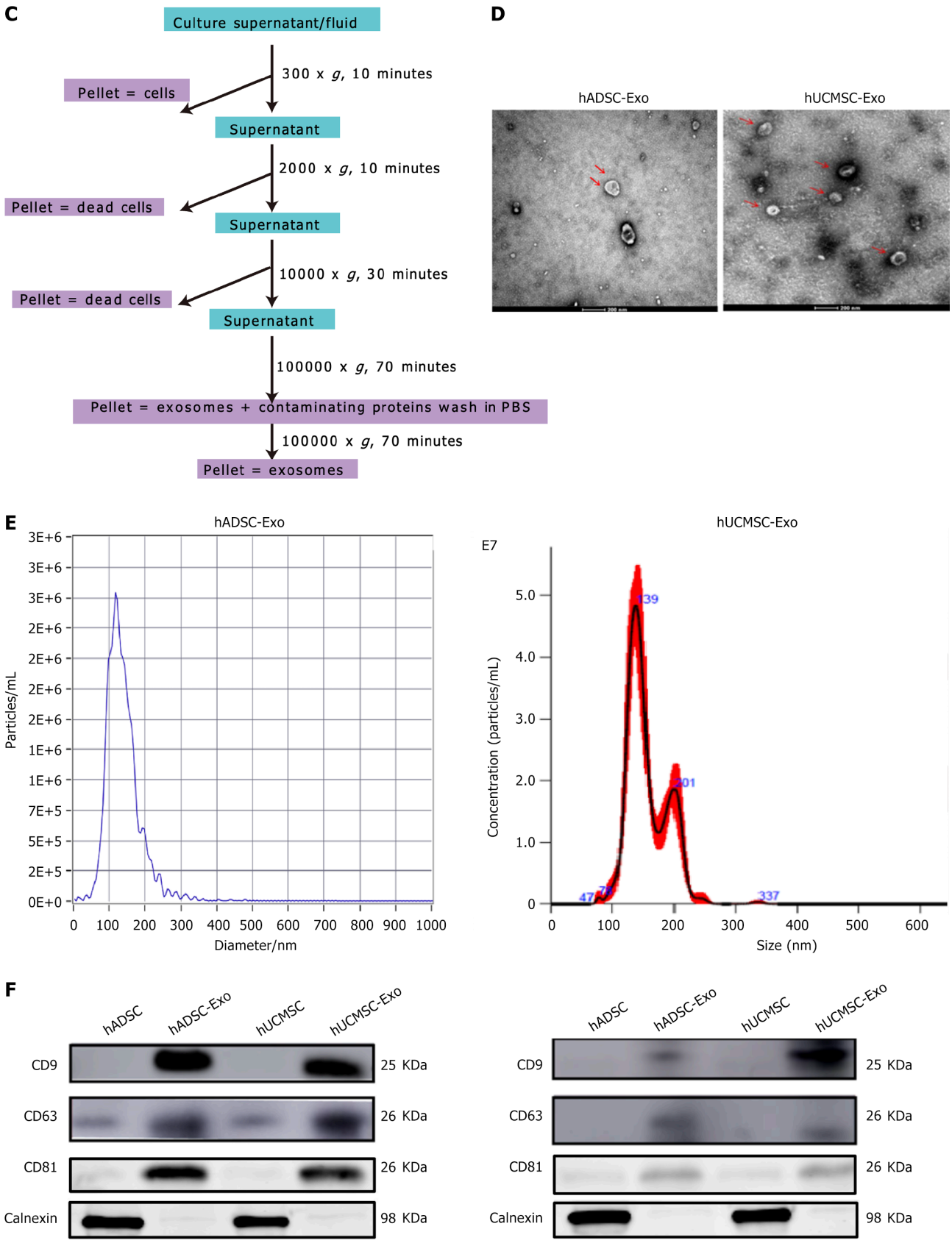

Figure 1 Identification of exosome from human adipose-derived mesenchymal stem cell and human umbilical cord-derived mesenchymal stem cell. A: Morphology of human adipose-derived mesenchymal stem cell (hADSC) and human umbilical cord-derived mesenchymal stem cell (hUCMSC); B: Analysis of surface markers on hADSCs and hUCMSCs showed high CD105, CD90, and CD73 expression, but negative HLA-DR and CD45 expression; C: Schematic presentation of exosome isolated from hADSC and hUCMSC by differential ultracentrifugation; D: By TEM, purified hADSC exosome (hADSC-Exo) and hUCMSC exosome (hUCMSC-Exo) exhibit cup-like morphologies; E: Nanoparticle analysis of hADSC-Exo and hUCMSC-Exo; F: hADSC-Exo and hUCMSC-Exo express CD63, CD9, CD81 and calnexin is not expressed. hADSC: Human adipose-derived mesenchymal stem cell; hUCMSC: Human umbilical cord-derived

mesenchymal stem cell; hADSC-Exo: Human adipose-derived mesenchymal stem cell exosome; hUCMSC-Exo: Human umbilical cord-derived mesenchymal stem cell exosome.

LC-MS proteome analysis to identify the common function of hADSC-Exos and hUCMSC-Exos

LC-MS proteome analysis was performed to explore the similarities and differences between hADSC-Exos and hUCMSC-Exos. hADSC-Exos included 724 proteins, while hUCMSC-Exos includes 1246. Six hundred and fifty overlapped proteins were obtained by investigating the intersection of the hADSC-Exos and hUCMSC-Exos (Figure 2A). The 650 overlapped proteins were used for GO term enrichment and KEGG pathway enrichment analysis to explore the common function of hADSC-Exos and hUCMSC-Exos. The GO biological process analysis revealed that the shared proteins were significantly associated with signal transduction, cell adhesion and cell-cell adhesion (Figure 2B). The GO cellular component analysis suggested that the common proteins were significantly associated with extracellular exosomes, cytosol and cytoplasm (Figure 2C). The GO molecular function analysis revealed that the common proteins were significantly associated with protein binding, poly(A) RNA binding and ATP binding (Figure 2D). KEGG pathway analysis showed that regulation of actin cytoskeleton, focal adhesion and phosphatidylinositol 3-kinase/protein kinase B signaling pathway were the main pathways (Figure 2E). These results illustrate potentially shared functional commonalities between hADSC-Exos and hUCMSC-Exos.

LC-MS proteome analysis of heterogeneous characteristics in hADSC-Exos and hUCMSC-Exos

Despite the functional commonalities between hADSC-Exos and hUCMSC-Exos, their specific functional differences have yet to be elucidated. The GO biological process analysis revealed that the specific proteins in hADSC-Exos were significantly associated with nucleosome assembly, blood coagulation and cell adhesion, while the specific proteins in hUCMSC-Exos were significantly associated with cell adhesion, cell-cell adhesion and proteolysis (Figure 3A and B). The GO cellular component analysis suggested that the specific proteins in hADSC-Exos and hUCMSC-Exos were related to extracellular exosomes and cytosol (Figure 3C and D). The GO molecular function analysis revealed that the specific proteins in hADSC-Exos were significantly associated with calcium ion binding, protein heterodimerization activity and nucleosomal DNA binding, while the specific proteins in hUCMSC-Exos were related to protein binding, RNA binding and ATP poly(A) binding (Figure 3E and F). The specific KEGG pathway in hADSC-Exos were metabolic pathways, systemic lupus erythematosus and alcoholism (Figure 3G). The specific KEGG pathway in hUCMSC-Exos were phosphatidylinositol 3-kinase/protein kinase B signaling, endocytosis and biosynthesis of antibiotics (Figure 3H). The LC-MS proteome analysis results were validated through quantitative real-time polymerase chain reaction (Figure 3I and J). hADSC-Exos mainly participated in blood coagulating, skin wound repair and inflammatory reaction. These findings suggest the beneficial role of hADSC-Exos in promoting skin repair. We then investigated whether hADSC-Exos affected the development of skin or hair follicles.

hADSC-Exos improved hair development in AGA mouse model

There are three phases of the hair follicle, anagen (active growth stage), catagen (regression of the hair follicle) and telogen (resting stage). There is a shorter anagen stage of hair follicles in the AGA patient's area of baldness, but a longer resting stage. Hair eventually fails to grow from the surface of the skin when the anagen period is too short[36]. The next step was to examine whether hADSC-Exos promoted hair growth in the AGA mouse model. Subcutaneous TP injections were administered daily in the dorsally depilated area to the androgen, positive control, and hADSC-Exos groups (Figure 4A). Immunofluorescence revealed that PKH26-labeled hADSC-Exos had the capability to enter the skin. Keratin K14, which highlights the epidermis and hair follicles, was the green counterstain (Figure 4B). To evaluate hair growth score and the number of follicles, skin samples were collected 21 days after depilation. Adult C57BL/6 mice with dorsal hair depilated had pink skin in the telogen phase after their dorsal hair was removed (Figure 4C). After 7 days, hair follicles re-entered anagen, resulting in dark grey skin[37]. The TP-treated mice still had pink backs, indicating that the hair follicles were still resting. Except for the TP-treated group, the hair of all mice at 14 days was mostly intact, suggesting that exosomes resisted androgens and promoted anagen hair growth. Hematoxylin and eosin staining of the hair shafts and photographs revealed the number of hair follicles (Figure 4D). The TP-treated hADSC-Exo group had significantly more hair development than the TP-treated group at 14 days (Figure 4E). The number of anagen hair follicles was similar between the positive control and hADSC-Exo groups after 21 days, and it significantly increased compared with the TP-treated group (Figure 4F). These findings suggested that hADSC-Exos played a beneficial role in promoting hair follicle development in an AGA mouse model *in vivo*.

Effective components of hADSC-Exos can modulate cell cycle

We performed LC-MS proteomic analysis on hADSC-Exos isolated from different ADSC culture media. A Venn diagram was drawn to find the common proteins of FBS-cultured hADSC-Exos, phenol red medium-cultured hADSC-Exos, and phenol red free medium-cultured hADSC-Exos. FBS-cultured hADSC-Exos included 621 proteins, phenol red medium-cultured hADSC-Exos 1026 proteins, and 302 proteins were found in phenol red free medium-cultured hADSC-Exos (Figure 5A). A total of 232 proteins were shared among the three different culture media, which were probably the main proteins in hADSC-Exos. The co-expressed proteins were analyzed by GO and KEGG pathway using the David database (https://david.ncifcrf.gov/) to further understand the biological functions of exosomes. The molecular functions of these co-detected proteins in hADSC-Exos were mainly protein heterodimerization activity, cell adhesion molecule binding, nucleosomal DNA binding, and GTP binding (Figure 5B). The cellular components involved in the exosomes were mainly

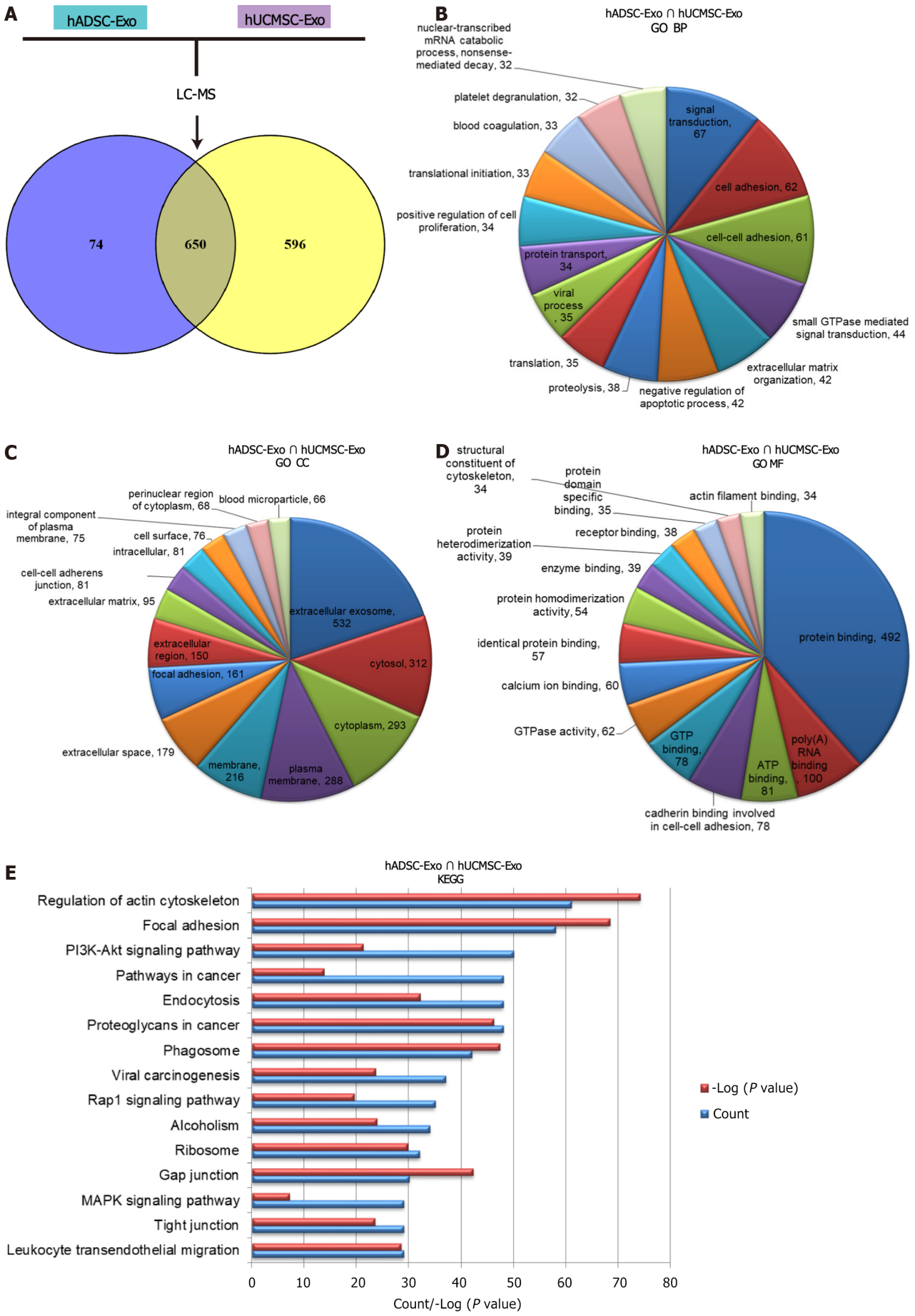

Figure 2 Gene Ontology and Kyoto Encyclopedia of Genes and Genomes analysis based on liquid chromatography-mass spectrometry

proteome analysis data of human adipose-derived mesenchymal stem cell exosome and human umbilical cord-derived mesenchymal stem cell exosome. A: Venn map showing the intersection proteins of human adipose-derived mesenchymal stem cell exosome (hADSC-Exo) and human umbilical cord-derived mesenchymal stem cell exosome (hUCMSC-Exo); B-D: Gene Ontology analysis of hADSC-Exo and hUCMSC-Exo liquid chromatography-mass spectrometry common proteins. A chart indicates biological process (B), cellular components (C) and molecular function (D); E: Kyoto Encyclopedia of Genes and Genomes pathway of hADSC-Exo and hUCMSC-Exo common proteins. hADSC-Exo: Human adipose-derived mesenchymal stem cell exosome; hUCMSC-Exo: Human umbilical cord-derived mesenchymal stem cell exosome; LC-MS: Liquid chromatography-mass spectrometry; GO: Gene Ontology; KEGG: Kyoto Encyclopedia of Genes and Genomes; BP: Biological process; CC: Cellular component; MF: Molecular function.

the nucleosome, DNA packaging complex and protein-DNA complex (Figure 5C). The biological processes involved in the exosomes were mainly chromatin silencing, nucleosome assembly, and negative regulation of epigenetic gene expression (Figure 5D). KEGG pathway enrichment analysis was performed on shared proteins, and the 15 pathways with the smallest *P* value were selected for bubble mapping, which indicated that the signaling pathways involved in exosomes were systemic lupus erythematosus, alcoholism and viral carcinogenesis. The 232 active proteins mentioned above were subjected to protein interactions network analysis using the String website, followed by annotation analysis of the proteins with GeneCards (https://www.genecards.org), and Ctyoscape software for analysis and mapping. These 232 active proteins were categorized into 10 groups according to their functions: Metabolism, complement and coagulation cascades, extracellular matrix (ECM), cell cycle, protein transport from cytoplasm to nucleus, post-translational modifications, nucleosome assembly, proteasome and exosome biogenesis (Figure 5E). We focused on the cell cycle group. Some cell cycle regulatory genes promoted cell growth, such as CDC42, RhoA, and Stratifin (SFN) (Figure 5F). The Rho GTPase family member CDC42 is essential for progression through G1[38]. Transient interactions between CDC42 and its downstream effector proteins are induced by various stimuli, and its deficiency might be associated with skin barrier damage or dysfunction[39,40]. Keratinocyte-specific deletion of RhoA promotes increased tumor growth, less differentiation and invasiveness in a mouse model of skin cancer[41]. SFN, also called 14-3-3σ protein, has been shown to be effective in treating UVB-induced skin disease. SFN regulates cellular activities such as cell cycle, cell growth, cell survival, and gene transcription[42]. These results suggest that hADSC-Exos play an essential role in maintaining the cell cycle.

hADSC-Exos improved hair development in AGA cell models

Increasing evidence indicates that DPCs stimulate hair regeneration. We investigated whether hADSC-Exos promoted hair regeneration by affecting HHDPCs. We analyzed HHDPCs in conventional culture at passage three. HHDPCs displayed long spindle□like shapes, formed colonies and reached confluency (Figure 6A). Referred to the previous research, we confirmed the transfection operations and reagent dosage[43]. The control group was untreated HHDPCs, and 100 nmol/L DHT was used in the AGA cell model group. To investigate the effect of hADSC-Exos on HHDPC proliferation, the CCK8 assay was performed. Growth curve assay based on CCK8 analysis was tested at 24 and 48 hours after hADSC-Exo treatment (Figure 6B and C). hADSC-Exos increased HHDPC proliferation over 48 hours (Figure 6B). Proliferation of human DPCs was inhibited by DHT as compared with the control group at 48 hours (Figure 6C). hADSC-Exos rescued the proliferation of DHT-treated HHDPCs (Figure 6C). Migration of HHDPCs transfected with hADSC-Exos was assessed by scratch wound assay and Transwell assay. Likewise, the migratory capacity was restored by overexpressing hADSC-Exos in DHT-treated DPCs *in vitro* (Figure 6D-G). These findings suggested that hADSC-Exos played a beneficial role in promoting hair follicle development in an AGA cell model *in vitro*.

hADSC-Exo regulated DPC proliferation via the CDC42/Wnt/β-catenin pathway in AGA

The key genes in AGA are listed in Supplementary Table 2. By overlapping the cell cycle genes in hADSC-Exos with AGA-related genes, we identified six candidate genes (Figure 7A). CDC42 has been reported as the protein that promotes ADSC-derived insulin-producing cell proliferation *via* Wnt/β-catenin signaling[44]. In addition, the cell cycle related Wnt pathway in involved in 5 biological pathways for *CDC42* gene (Figure 7B). DHT signaling activates glycogen synthase kinase (GSK)-3β present in DPCs, whereas receptor AR signaling leads to phosphorylation of β-catenin to reduce its level, antagonizing the classical Wnt signaling pathway[45]. Therefore, we used Hair-GEL single cell databases and analyzed the expression of CDC42 and GSK-3β (Figure 7C and D). The expression of CDC42 in DPCs suggested the role of CDC42 in the DPC cell cycle, and GSK-3β was also expressed in DPCs. Under the effect of hADSC-Exos, expression level of Wnt3a and β-catenin in DPCs was significantly increased compared with the control group. Under the effect of DHT, expression of Wnt3a and β-catenin decreased compared with that of the control group. The expression of Wnt3a and β-catenin in the hADSC-Exo- and DHT-treated groups increased compared with that in the DHT-treated alone group (Figure 7E-H). By activating the Wnt/β-catenin signaling pathway through CDC42, hADSC-Exos can potentially suppress GSK-3β expression, counteracting the inhibitory impact of DHT, stimulating cell proliferation, and enhancing hair growth (Figure 8).

DISCUSSION

We explored the effect of hADSC-Exos on hair follicle development in AGA. It is believed that AGA is caused by both hereditary and androgenic factors. TP is one of the common androgens that induce AGA, which is a slow release formulation of testosterone. Testosterone is metabolized to DHT by steroid 5α-reductases[46]. DHT has a 10-fold higher

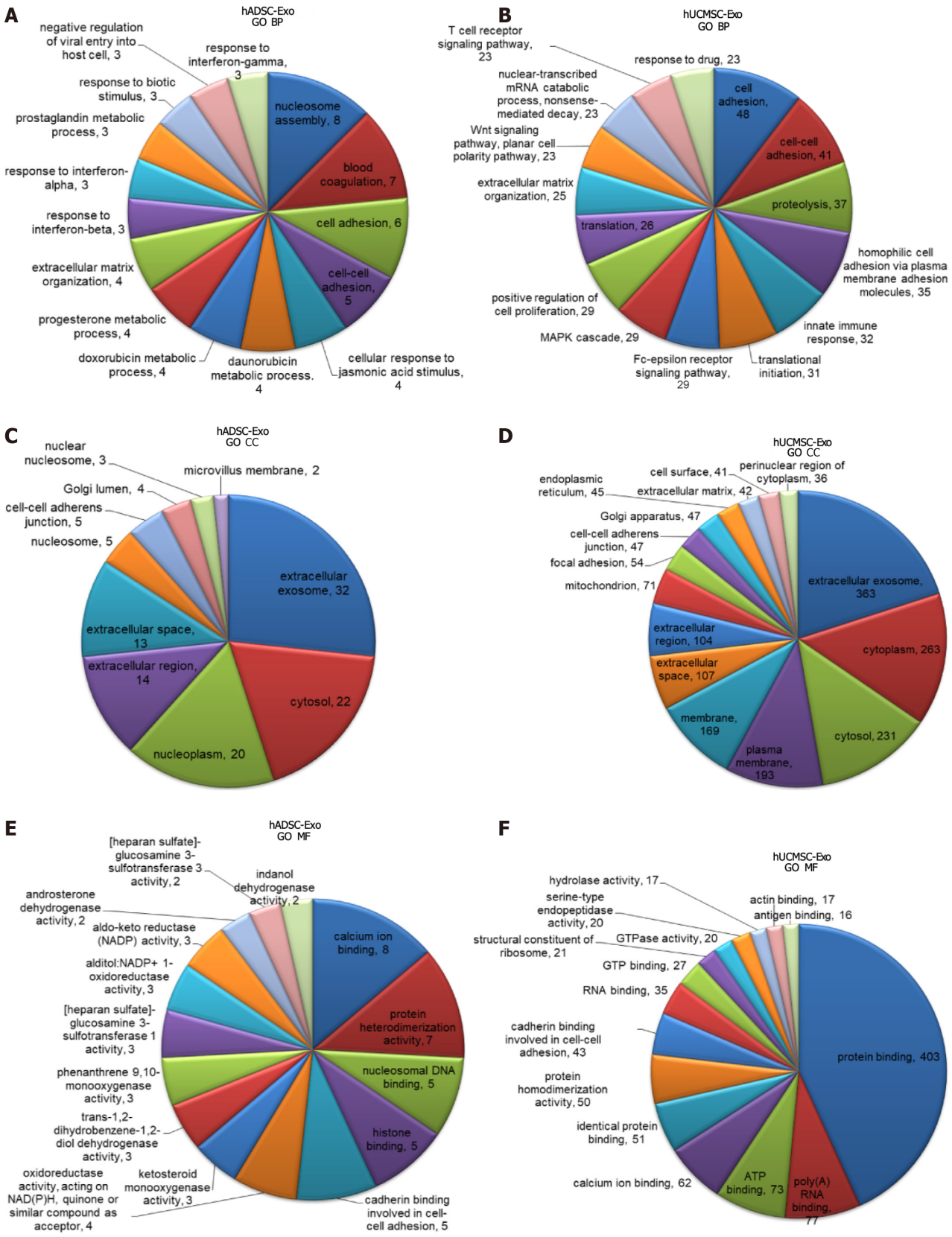
A
hADSC-Exo
GO BP
negative regulation of viral entry into host cell, 3
response to interferon-gamma, 3
response to biotic stimulus, 3
prostaglandin metabolic process, 3
response to interferon-alpha, 3
response to interferon-beta, 3
extracellular matrix organization, 4
progesterone metabolic process, 4
doxorubicin metabolic process, 4
daunorubicin metabolic process, 4
cellular response to jasmonic acid stimulus, 4
cell-cell adhesion, 5
cell adhesion, 6
blood coagulation, 7
nucleosome assembly, 8
B
hUCMSC-Exo
GO BP
T cell receptor signaling pathway, 23
response to drug, 23
nuclear-transcribed mRNA catabolic process, nonsense-mediated decay, 23
Wnt signaling pathway, planar cell polarity pathway, 23
extracellular matrix organization, 25
translation, 26
positive regulation of cell proliferation, 29
MAPK cascade, 29
Fc-epsilon receptor signaling pathway, 29
translational initiation, 31
innate immune response, 32
homophilic cell adhesion via plasma membrane adhesion molecules, 35
proteolysis, 37
cell-cell adhesion, 41
cell adhesion, 48
C
hADSC-Exo
GO CC
nuclear nucleosome, 3
microvillus membrane, 2
Golgi lumen, 4
cell-cell adherens junction, 5
nucleosome, 5
extracellular space, 13
extracellular region, 14
nucleoplasm, 20
cytosol, 22
extracellular exosome, 32
D
hUCMSC-Exo
GO CC
endoplasmic reticulum, 45
cell surface, 41
perinuclear region of cytoplasm, 36
extracellular matrix, 42
Golgi apparatus, 47
cell-cell adherens junction, 47
focal adhesion, 54
mitochondrion, 71
extracellular region, 104
extracellular space, 107
membrane, 169
plasma membrane, 193
cytosol, 231
cytoplasm, 263
extracellular exosome, 363
E
hADSC-Exo
GO MF
[heparan sulfate]-glucosamine 3-sulfotransferase 3 activity, 2
indanol dehydrogenase activity, 2
androsterone dehydrogenase activity, 2
aldo-keto reductase (NADP) activity, 3
alditol:NADP+ 1-oxidoreductase activity, 3
[heparan sulfate]-glucosamine 3-sulfotransferase 1 activity, 3
phenanthrene 9,10-monooxygenase activity, 3
trans-1,2-dihydrobenzene-1,2-diol dehydrogenase activity, 3
oxidoreductase activity, acting on NAD(P)H, quinone or similar compound as acceptor, 4
ketosteroid monooxygenase activity, 3
cadherin binding involved in cell-cell adhesion, 5
histone binding, 5
nucleosomal DNA binding, 5
protein heterodimerization activity, 7
calcium ion binding, 8
F
hUCMSC-Exo
GO MF
hydrolase activity, 17
serine-type endopeptidase activity, 20
structural constituent of ribosome, 21
GTPase activity, 20
GTP binding, 27
RNA binding, 35
cadherin binding involved in cell-cell adhesion, 43
protein homodimerization activity, 50
identical protein binding, 51
calcium ion binding, 62
ATP binding, 73
poly(A) RNA binding, 77
protein binding, 403
actin binding, 17
antigen binding, 16

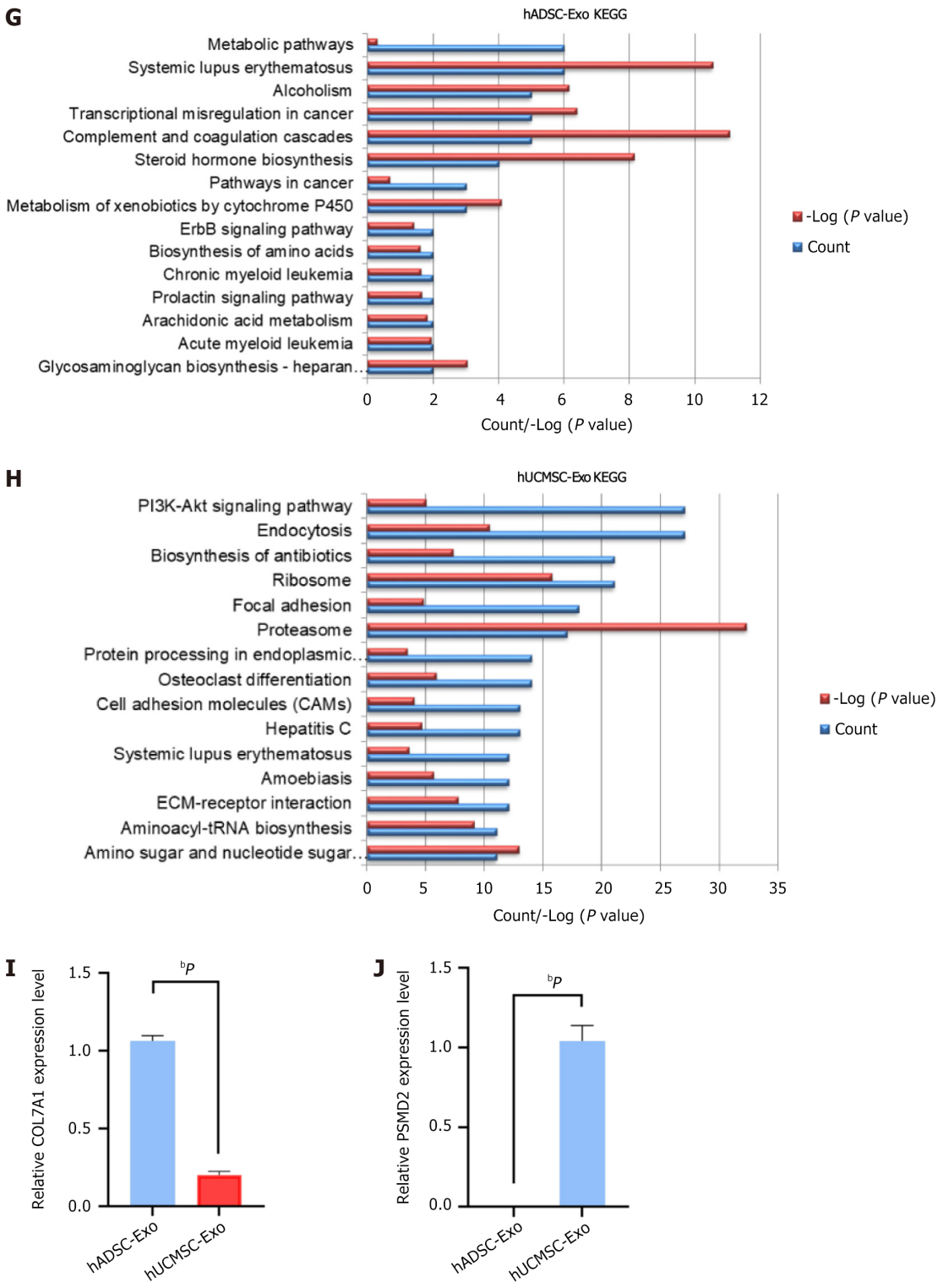

Figure 3 Gene Ontology and Kyoto Encyclopedia of Genes and Genomes analysis based on heterogeneous characteristics of human adipose-derived mesenchymal stem cell exosomes and human umbilical cord-derived mesenchymal stem cell exosome. A and B: Heterogeneous characteristics of human adipose-derived mesenchymal stem cell exosome (hADSC-Exo) (A) and human umbilical cord-derived mesenchymal stem cell exosome (hUCMSC-Exo) (B) function analyzed by biological process analysis; C and D: Heterogeneous characteristics of hADSC-Exo (C) and hUCMSC-Exo (D) function analyzed by cellular components analysis; E and F: Heterogeneous characteristics of hADSC-Exo (E) and hUCMSC-Exo (F) function analyzed by molecular function analysis; G and H: Heterogeneous characteristics of hADSC-Exo (G) and hUCMSC-Exo (H) function analyzed by Kyoto Encyclopedia of Genes and Genomes pathway analysis; I and J: The mRNA expression of COL7A1 (hADSC-Exo, I) and PSMD2 (hUCMSC-Exo, J) was detected by reverse transcription-polymerase chain reaction (data were presented as mean ± SD. $^{b}P < 0.01$, $n = 6$, unpaired *t*-test. hADSC-Exo: Human adipose-derived mesenchymal stem cell exosome; hUCMSC-Exo: Human umbilical cord-derived mesenchymal stem cell exosome; GO: Gene Ontology; KEGG: Kyoto Encyclopedia of Genes and Genomes; BP: Biological process; CC: Cellular component; MF: Molecular function.

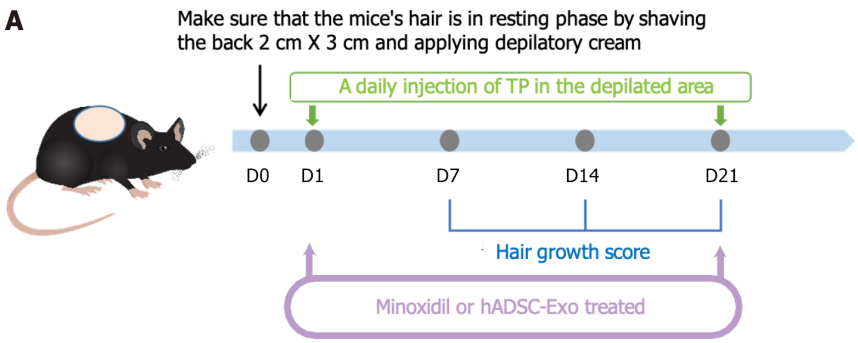
A
Make sure that the mice's hair is in resting phase by shaving the back 2 cm X 3 cm and applying depilatory cream
A daily injection of TP in the depilated area
D0
D1
D7
D14
D21
Hair growth score
Minoxidil or hADSC-Exo treated

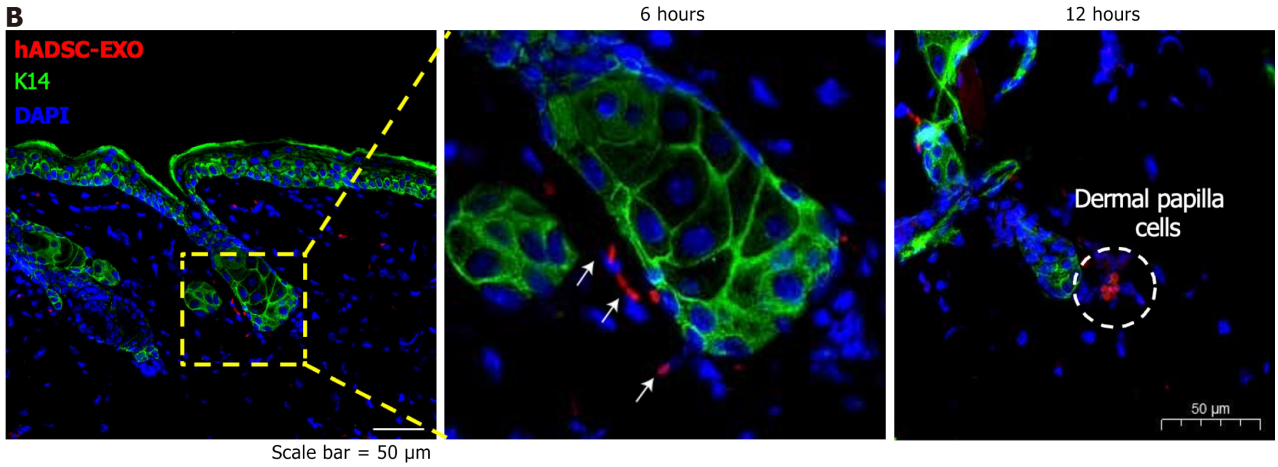
B
hADSC-EXO
K14
DAPI
6 hours
12 hours
Dermal papilla cells
50 μm
Scale bar = 50 μm

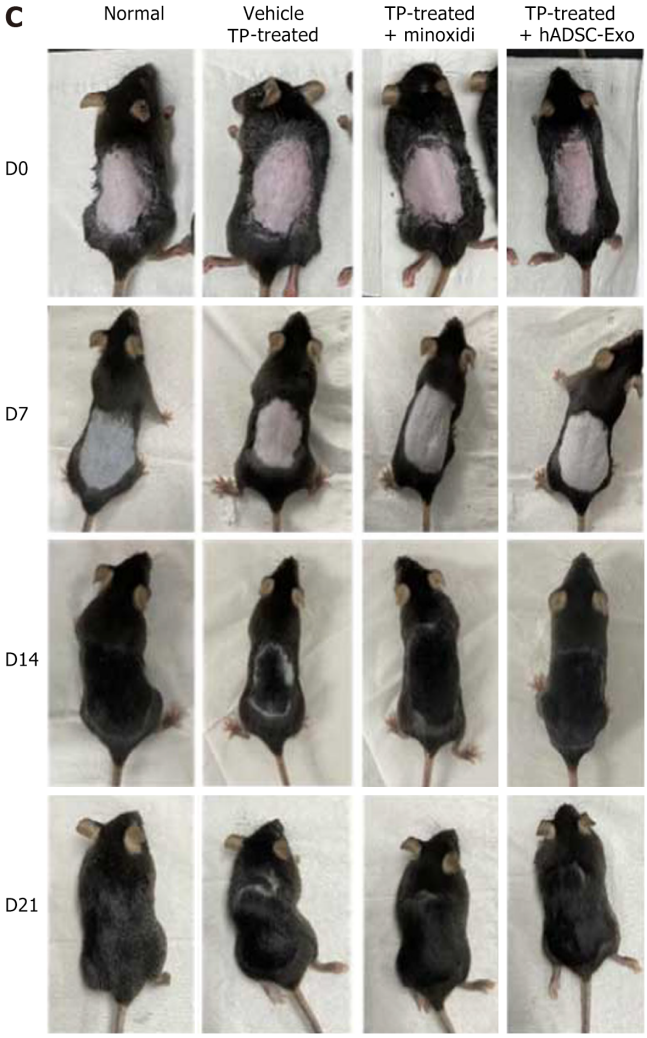
C
Normal
Vehicle TP-treated
TP-treated + minoxidi
TP-treated + hADSC-Exo
D0
D7
D14
D21

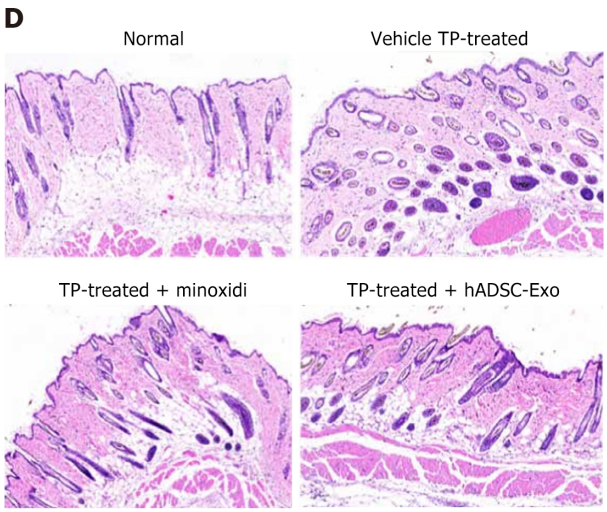
D
Normal
Vehicle TP-treated
TP-treated + minoxidi
TP-treated + hADSC-Exo

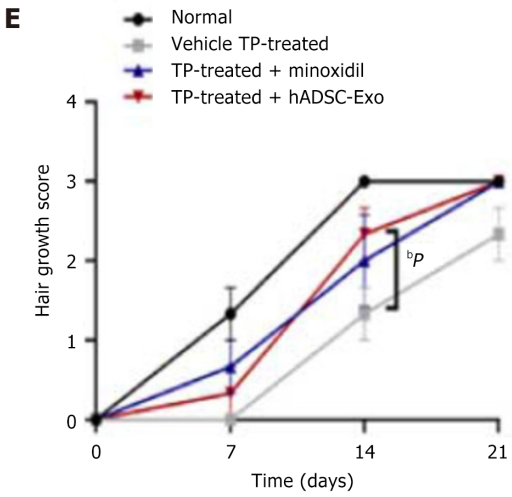
E
Normal
Vehicle TP-treated
TP-treated + minoxidil
TP-treated + hADSC-Exo
Hair growth score
0
1
2
3
4
0
7
14
21
Time (days)
bP

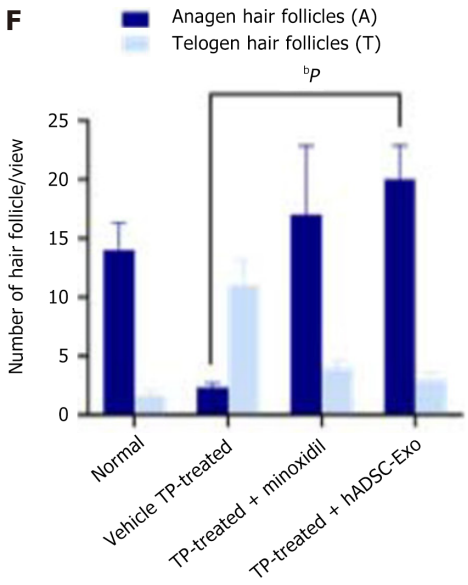

Figure 4 Human adipose-derived mesenchymal stem cell exosomes improve the hair regeneration in androgenetic alopecia mice model. A: Schematic flowchart of the experiment of testosterone propionate-treated and shaved in androgenetic alopecia mouse model; B: PKH26-labeled human adipose-derived mesenchymal stem cell exosome (red) retention in the site of hair follicle; C: Hair growth of C57BL/6 mice in each group; D: hematoxylin and eosin staining of mouse skin histopathological sections in each group; E: Hair growth score in each group; F: The number of follicles in each group. Differences among four groups were assessed by Tukey's multiple comparison test and one-way ANOVA; error bars represent SEM. $^{b}P < 0.01$, compared with testosterone propionate-treated group. Six mice were randomly selected from each group for histological examination. TP: Testosterone propionate; hADSC-Exo: Human adipose-derived mesenchymal stem cell exosome.

potency than testosterone as the primary AR ligand[47]. DHT inhibits proliferation of HaCaT keratinocytes in coculture with DPCs obtained from AGA patients, by suppressing the Wnt signaling pathway[48]. The Wnt/β-catenin signaling pathway plays an important role in cell proliferation, differentiation, apoptosis and stem cell renewal. Researchers have found that Wnt signaling can induce stem cells to differentiate into sebaceous glands and hair follicles[49]. In summary, compared with FDA-approved minoxidil, our results have proved that hADSC-Exos have an ameliorative effect. We found that hADSC-Exos inhibited the expression of GSK-3β by activating the Wnt/β-catenin signaling pathway through CDC42.

At present, the only therapeutic agents for AGA approved by the FDA in the United States are finasteride and minoxidil. However, finasteride is only effective in male subjects[50]. Minoxidil cannot prevent hair loss but may accelerate hair growth, but only 13%-40% of female subjects with AGA responded to minoxidil treatment[51]. The limitations of these drugs make it necessary to develop a more effective alternative. AGA treatments have significantly evolved over the past few decades, incorporating a range of techniques and technologies, such as platelet-rich plasma (PRP), microneedling, and low-level laser therapy and stem cell therapy[52]. PRP therapy utilizes autologous blood components enriched with growth factors, promoting hair regrowth by enhancing follicular health and stimulating hair follicle anagen phase. Clinical studies have demonstrated the effectiveness of PRP in enhancing hair density and thickness in both AGA and female alopecia[53,54]. Microneedling involves creating microinjuries in the scalp to stimulate hair follicles and improve the absorption of topical treatments. This technique improves scalp health and can be a valuable adjunct to other hair restoration methods[55]. Low-level laser therapy stimulates hair follicles with low-intensity lasers. It has been shown to increase hair density and promote regrowth through enhanced cellular metabolism and reduced inflammation[56]. Stem cell therapy may improve hair regrowth by reversing the pathological mechanisms or regulating cellular quiescence. HFSCs and MSCs are the most widely used stem cells for the study of AGA. HFSCs can effectively induce hair regrowth by reactivating the hair growth cycle and enhancing follicle development[57]. MSCs are another promising cell-based therapy for hair restoration, such as ADSCs and UCMSCs. Their regenerative potential stems from their ability to differentiate into various cell types and release growth factors that promote hair follicle development[58]. Despite the significant impact of MSCs on hair loss or thinning, there are some clinical limitations[59-61]. Compared to MSC therapy, exosome-based cell-free therapy is more stable in clinical application[61].

The importance of homogeneous MSC-Exos should be emphasized, which is one of the prerequisite steps in further clinical treatment of AGA. MSCs and their exosome have their own advantages and disadvantages in terms of isolation, differentiation capacity and cell count, as well as possible side effects[58]. This heterogeneity underscores the importance of establishing standardized quality control protocols for the clinical application of MSC-Exos. Incorporating proteomics as a quality control step may prove to be valuable in this regard. Here, we used a standardized method to obtain hADSC-Exos and hUCMSC-Exos with safety and stability, and selected hADSC-Exos by LC-MS proteomic analysis. The process of obtaining ADSCs involves liposuction, which is a less invasive procedure. This makes the procedure more acceptable to patients and reduces the risk of complications associated with the cell harvesting process. In addition, since ADSCs are derived from the patient's own adipose tissue, the risk of immunological rejection is minimal[62]. Our findings indicate that hADSC-Exos are more effective in promoting hair follicle development compared to hUCMSC-Exos. Several proteins

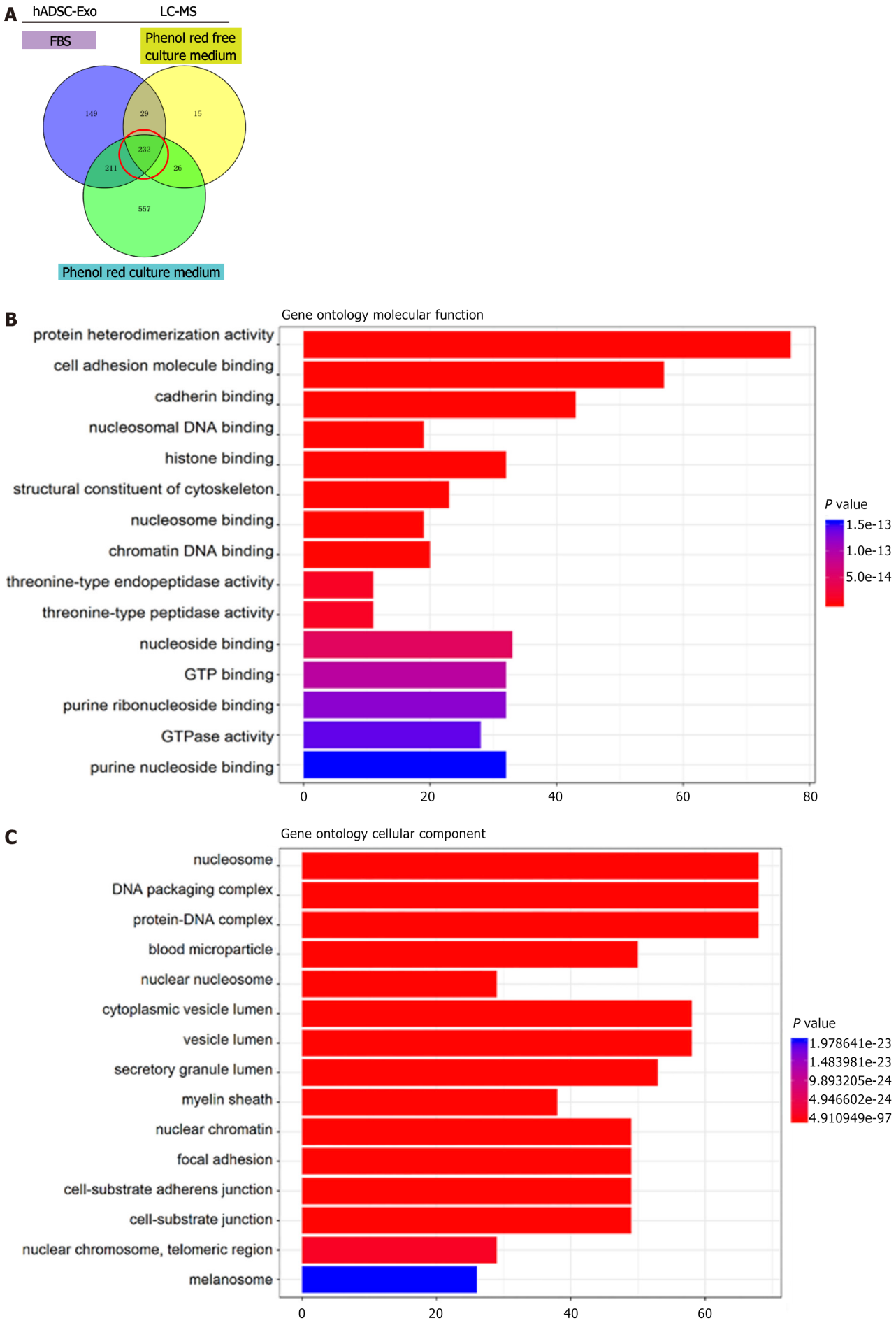
A
hADSC-Exo
LC-MS
FBS
Phenol red free culture medium
149
29
15
232
211
26
557
Phenol red culture medium
B
Gene ontology molecular function
protein heterodimerization activity
cell adhesion molecule binding
cadherin binding
nucleosomal DNA binding
histone binding
structural constituent of cytoskeleton
nucleosome binding
chromatin DNA binding
threonine-type endopeptidase activity
threonine-type peptidase activity
nucleoside binding
GTP binding
purine ribonucleoside binding
GTPase activity
purine nucleoside binding
0
20
40
60
80
P value
1.5e-13
1.0e-13
5.0e-14
C
Gene ontology cellular component
nucleosome
DNA packaging complex
protein-DNA complex
blood microparticle
nuclear nucleosome
cytoplasmic vesicle lumen
vesicle lumen
secretory granule lumen
myelin sheath
nuclear chromatin
focal adhesion
cell-substrate adherens junction
cell-substrate junction
nuclear chromosome, telomeric region
melanosome
0
20
40
60
P value
1.978641e-23
1.483981e-23
9.893205e-24
4.946602e-24
4.910949e-97

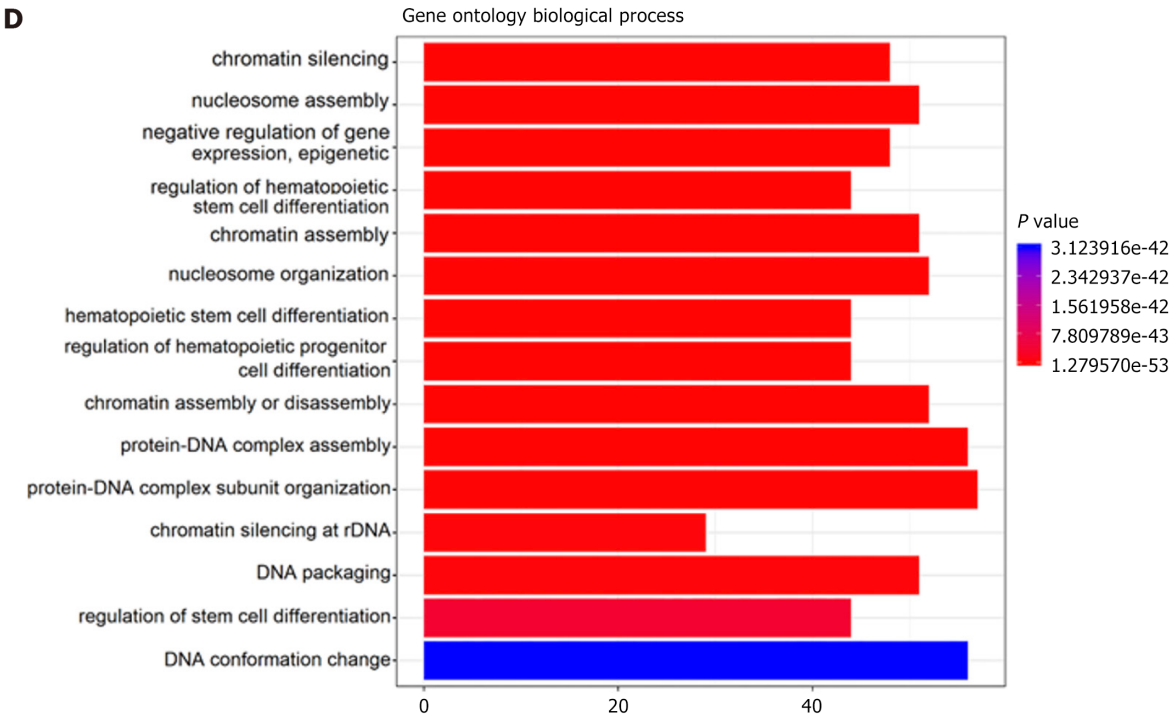
D
Gene ontology biological process
chromatin silencing
nucleosome assembly
negative regulation of gene expression, epigenetic
regulation of hematopoietic stem cell differentiation
chromatin assembly
nucleosome organization
hematopoietic stem cell differentiation
regulation of hematopoietic progenitor cell differentiation
chromatin assembly or disassembly
protein-DNA complex assembly
protein-DNA complex subunit organization
chromatin silencing at rDNA
DNA packaging
regulation of stem cell differentiation
DNA conformation change
0
20
40
P value
3.123916e-42
2.342937e-42
1.561958e-42
7.809789e-43
1.279570e-53

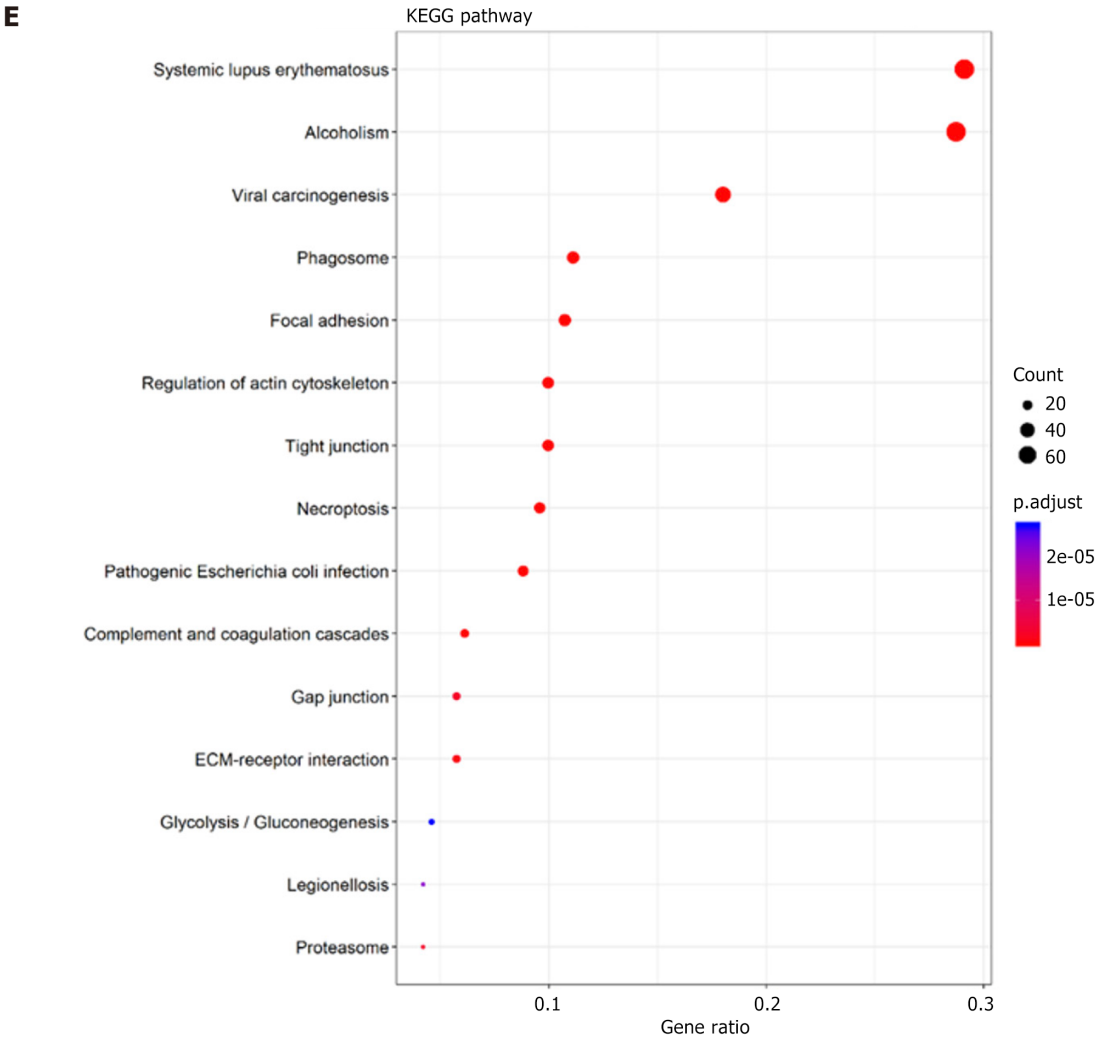
E
KEGG pathway
Systemic lupus erythematosus
Alcoholism
Viral carcinogenesis
Phagosome
Focal adhesion
Regulation of actin cytoskeleton
Tight junction
Necroptosis
Pathogenic Escherichia coli infection
Complement and coagulation cascades
Gap junction
ECM-receptor interaction
Glycolysis / Gluconeogenesis
Legionellosis
Proteasome
0.1
0.2
0.3
Gene ratio
Count
20
40
60
p.adjust
2e-05
1e-05

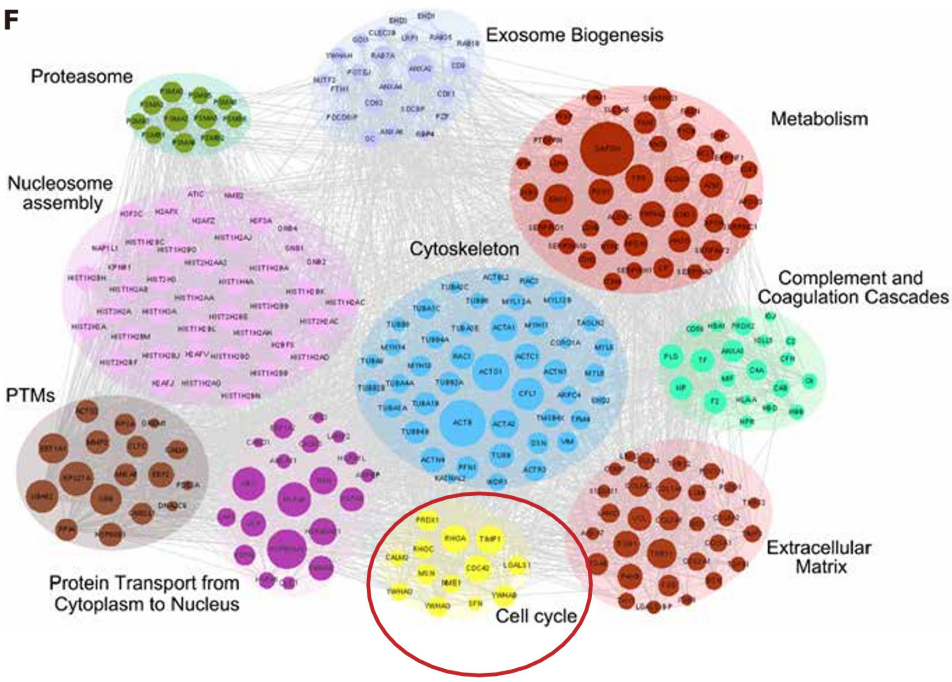

Figure 5 Gene Ontology and Kyoto Encyclopedia of Genes and Genomes analysis based on liquid chromatography-mass spectrometry proteome analysis data of human adipose-derived mesenchymal stem cell exosomes in different culture medium. A: Venn map showing the intersection of human adipose-derived mesenchymal stem cell exosomes (hADSC-Exo) proteins in different culture systems: Control medium (fetal bovine serum), phenol red free culture medium (Gibco, NY, United States), and phenol red culture medium (Takara, Japan); B-D: Gene Ontology analysis of hADSC-Exo liquid chromatography-mass spectrometry proteome analysis data. A chart indicates molecular function (B), cellular components (C) and biological process (D); E: Kyoto Encyclopedia of Genes and Genomes pathway of hADSC-Exo proteins; F: STRING network analysis of the intersection of hADSC-Exo proteins. hADSC-Exo: Human adipose-derived mesenchymal stem cell exosome; LC-MS: Liquid chromatography-mass spectrometry; FBS: Fetal bovine serum.

associated with angiogenesis, inflammation regulation, and ECM remodeling may also play an important role in hADSC-Exos, as there may be a potential impact of these proteins on HFSC activation, as well as on transition of hair follicles from the resting to the anagen phase. For instance, the aging of hair follicles is characterized by a reduction in the expression of cell adhesion and *ECM* genes in HFSCs, which are controlled by nuclear factor of activated T cells cytoplasmic 1 and forkhead box protein C1[63]. ADSCs have been shown to promote vascularization and regulate immunological responses through paracrine signaling, which could be beneficial in managing inflammation during the anagen phase[64]. Overall, hADSC-Exos can provide insights into potential therapeutic strategies for enhancing hair growth and regeneration.

The clinical applicability of hADSC-Exo therapy holds great promise, but it requires careful consideration of administration methods, dosage optimization, long-term effects, and safety[61]. Administration of hADSC-Exos can be performed through various routes, including topical, intravenous and subcutaneous methods. For instance, topical application may be more suitable for localized conditions such as hair growth and wound healing. Dose optimization is essential to maximize therapeutic benefits while minimizing potential side effects. This requires extensive preclinical and clinical studies to establish dose-response relationships and identify the most effective and safe dosage regimens[65]. The long-term effects of hADSC-Exo therapy are still under investigation. However, studies have shown that exosomes generally exhibit low immunogenicity, which is promising for their long-term use[66]. Lastly, safety considerations are paramount in the clinical translation of hADSC-Exo therapy. It is crucial to conduct comprehensive safety evaluations, including assessments of potential tumorigenicity, immunogenicity, and other adverse effects.

CONCLUSION

In summary, there are many advantages to ADSCs and their exosomes, such as their robust regenerative potential, minimal invasive harvesting, sustained efficacy, and synergistic potential. They can be used in combination with other hair regrowth treatments, such as PRP and microneedling, to enhance overall effectiveness. Here, we used needle roller administration. In the future, the effects of different modes of hADSC-Exo administration on hair follicle development should continue to be explored. Clinical trials must adhere to standardization of isolation techniques, culture media used, dose and other critical information.

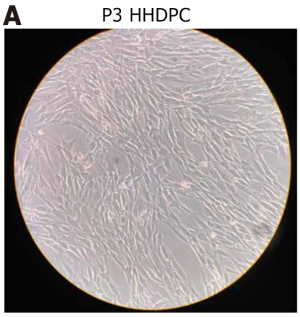
A
P3 HHDPC

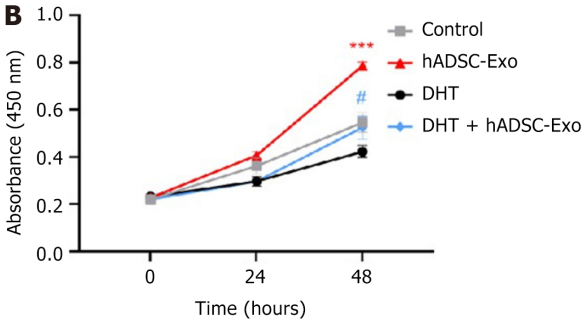
B
Absorbance (450 nm)
1.0
0.8
0.6
0.4
0.2
0.0
0
24
48
Time (hours)
***
#
Control
hADSC-Exo
DHT
DHT + hADSC-Exo

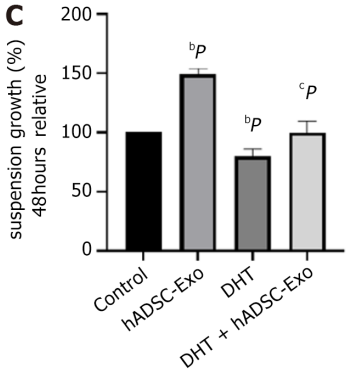
C
suspension growth (%)
48hours relative
200
150
100
50
0
bP
bP
cP
Control
hADSC-Exo
DHT
DHT + hADSC-Exo

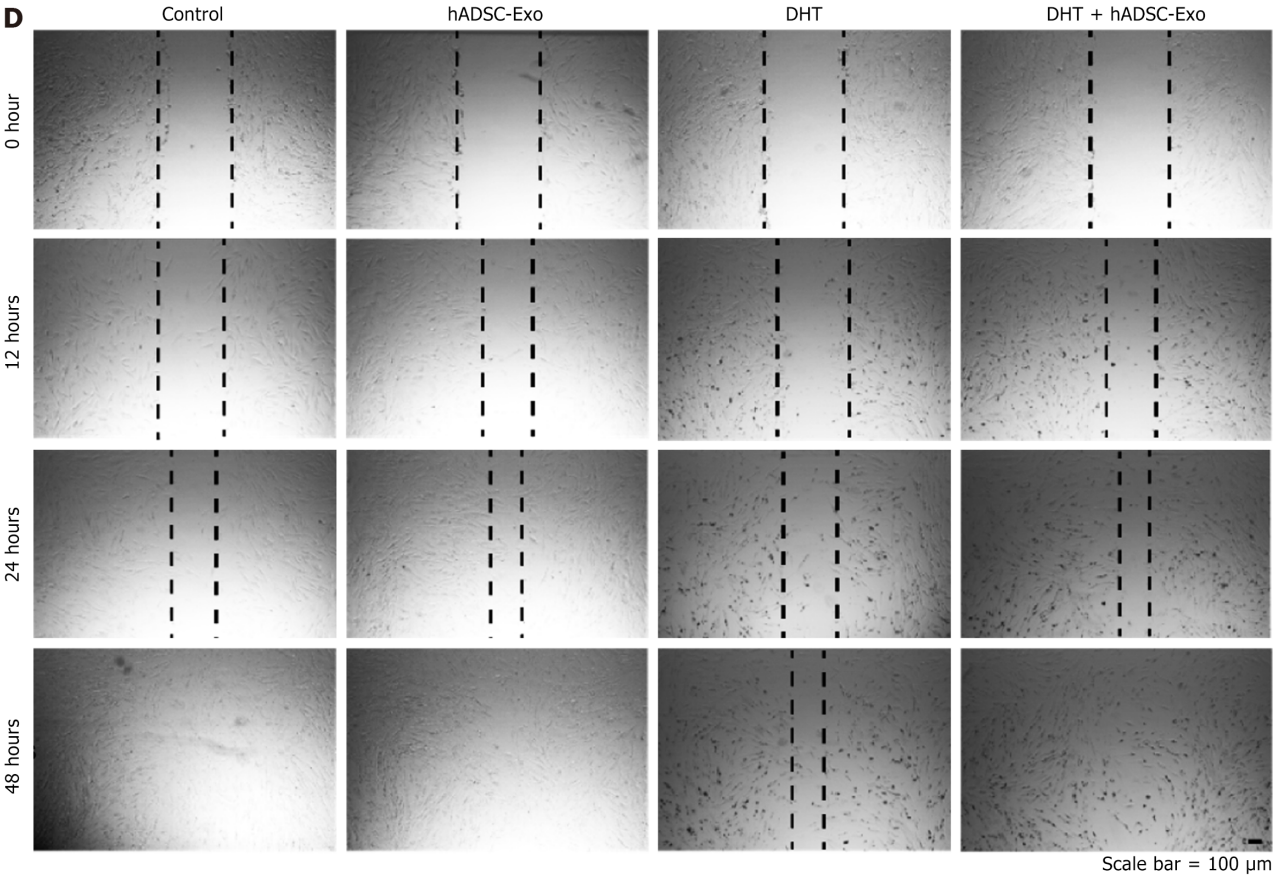
D
Control
hADSC-Exo
DHT
DHT + hADSC-Exo
0 hour
12 hours
24 hours
48 hours
Scale bar = 100 μm

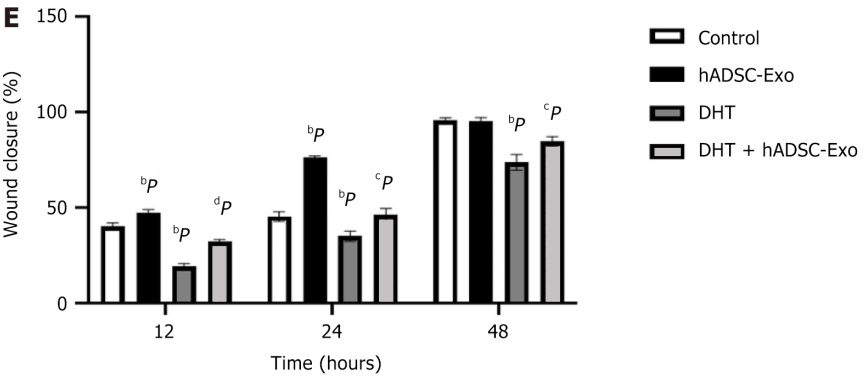
E
Wound closure (%)
150
100
50
0
12
24
48
Time (hours)
bP
bP
dP
bP
bP
cP
bP
cP
Control
hADSC-Exo
DHT
DHT + hADSC-Exo

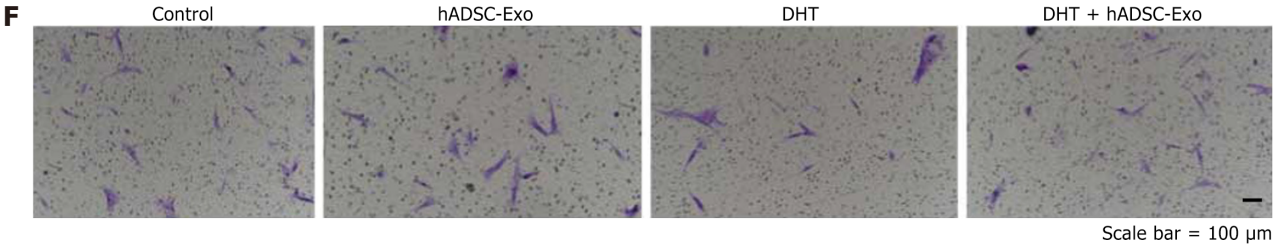
F
Control
hADSC-Exo
DHT
DHT + hADSC-Exo
Scale bar = 100 μm

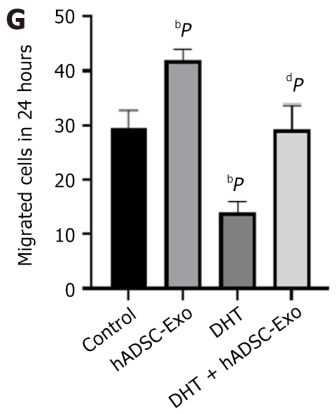

Figure 6 Human adipose-derived mesenchymal stem cell exosome improves the hair regeneration in androgenetic alopecia cell model. A: Human hair dermal papillary cells were used in subsequent analyses from passage 3 (P3); B and C: Cell counting kit-8 (CCK8) assay. CCK8 assay was carried out to measure the cell growth in 48 hours (B). Cell survival was determined by the CCK8 assay at 48 hours (C); D and E: The wound healing assay was used to assess migration in cells (D). Statistical analysis of the results of wound healing assay in each group (E); F and G: The migratory properties of human hair dermal papillary cells were analyzed using the Transwell migration assay with Transwell filter chambers (F). Statistical analysis of the results of Transwell migration assay in each group (G). $^{b}P < 0.01$, $^{c}P < 0.001$, $^{d}P < 0.0001$. HHDPC: Human hair dermal papillary cell; DHT: Dihydrotestosterone; hADSC-Exo: Human adipose-derived mesenchymal stem cell exosome.

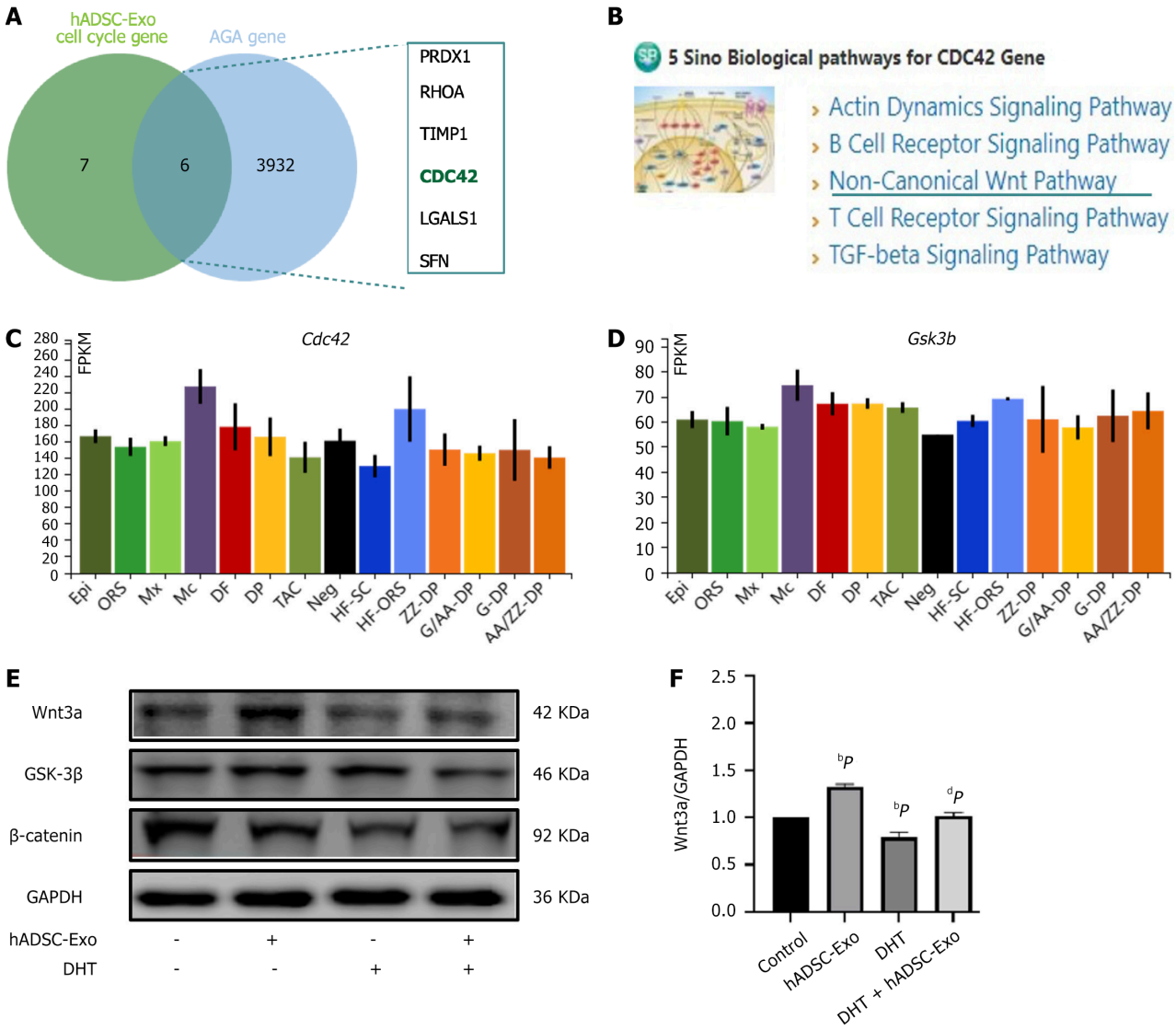

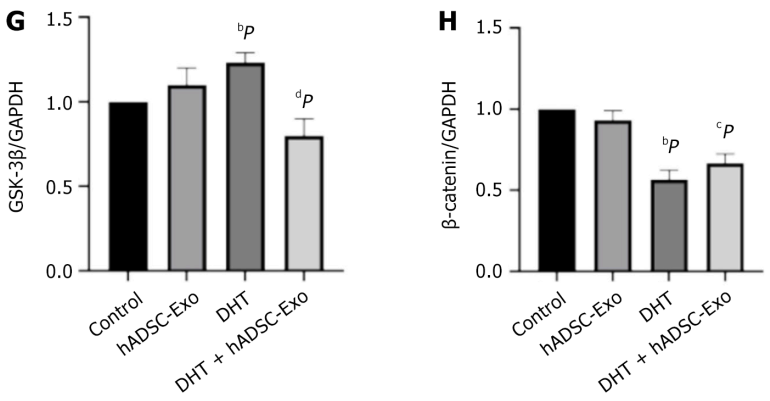

Figure 7 Human adipose-derived mesenchymal stem cell exosomes regulate dermal papillary cell proliferation *via* cell division cycle protein 42/Wnt/β-catenin pathway in androgenetic alopecia. A: Venn diagram demonstrating the intersections of genes from the androgenetic alopecia gene set and human adipose-derived mesenchymal stem cell exosomes cell cycle gene; B: Five-sino biological pathway enrichment diagram; C: Using single-cell mRNA-sequencing data from the Hair-GEL database, cell types expressing cell division cycle protein 42 (http://hair-gel.net/) were identified; D: Using single-cell mRNA-sequencing data from the Hair-GEL database, cell types expressing glycogen synthase kinase-3β (Gsk3β) (http://hair-gel.net/) were found; E: Representative western blotting image of GSK-3β after human adipose-derived mesenchymal stem cell exosomes was overexpressed in human hair dermal papillary cells; F-H: Statistical analysis of the western blotting in each group. Wnt3a (F), GSK-3β (G) and β-catenin (H). Differences among five groups were assessed by Tukey's multiple comparison test and one-way ANOVA, and error bars represent SEM. $^{b}P < 0.01$, $^{c}P < 0.001$, $^{d}P < 0.0001$, Compared with control group. hADSC-Exo: Human adipose-derived mesenchymal stem cell exosome; AGA: Androgenetic alopecia; Cdc42: Cell division cycle protein 42; Gsk3b: Glycogen synthase kinase-3β; DHT: Dihydrotestosterone.

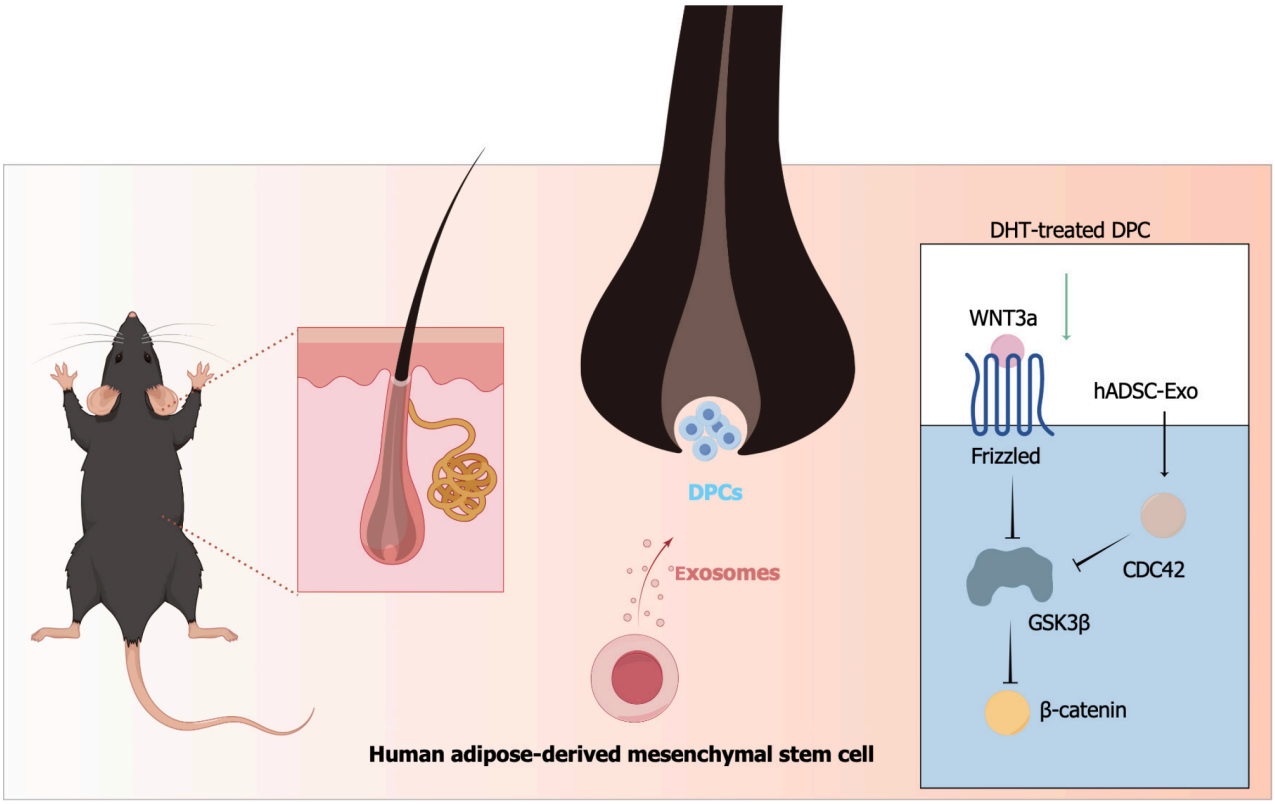

Figure 8 Human adipose-derived mesenchymal stem cell exosome regulate dermal papillary cells proliferation *via* Wnt/β-catenin/glycogen synthase kinase-3β in hair follicle development. DPC: Dermal papillary cell; hADSC-Exo: Human adipose-derived mesenchymal stem cell exosome; CDC42: Cell division cycle protein 42; GSK3β: Glycogen synthase kinase-3β; DHT: Dihydrotestosterone.

FOOTNOTES

Author contributions: Zhang J and Zhang J mainly designed and led the process of the project and as co-corresponding authors of this manuscript. Fu Y and Han YT wrote the manuscript and contributed equally to this manuscript as co-first authors of this manuscript. Fu Y, Xie JL, Liu RQ, Zhao B, and Zhang XL performed the experiments; Fu Y, Xie JL, Zhao B, and Zhang XL analyzed the data; Fu Y, Han YT, and Liu RQ performed statistical analysis. All authors read and approved the final manuscript.

Supported by the Peak Disciplines (Type IV) of Institutions of Higher Learning in Shanghai and the China Postdoctoral Science Foundation, No. 2022M722409.

Institutional review board statement: The study protocol conformed to the Declaration of Helsinki and was approved by the Committee of Ethics on Experimentation of Tongji University (Shanghai, China), approval No. [2024]094.

Institutional animal care and use committee statement: This study was approved by Tongji University, with the ethics approval No. TJAA09524102.

Conflict-of-interest statement: All the authors report no relevant conflicts of interest for this article.

Data sharing statement: All data can be supplied for reasonable requests.

ARRIVE guidelines statement: The authors have read the ARRIVE guidelines, and the manuscript was prepared and revised according to the ARRIVE guidelines.

Country of origin: China

ORCID number: Yu Fu 0000-0001-8058-6504; Jun Zhang 0000-0002-8473-1614; Jing Zhang 0000-0001-6241-5330.

S-Editor: Wang JJ
L-Editor: A
P-Editor: Zhang XD

REFERENCES

1 **Shimizu Y**, Ntege EH, Sunami H, Inoue Y. Regenerative medicine strategies for hair growth and regeneration: A narrative review of literature. *Regen Ther* 2022; **21**: 527-539 [PMID: 36382136 DOI: 10.1016/j.reth.2022.10.005]

2 **Alhanshali L**, Buontempo M, Shapiro J, Lo Sicco K. Medication-induced hair loss: An update. *J Am Acad Dermatol* 2023; **89**: S20-S28 [PMID: 37591561 DOI: 10.1016/j.jaad.2023.04.022]

3 **Alessandrini A**, Bruni F, Piraccini BM, Starace M. Common causes of hair loss - clinical manifestations, trichoscopy and therapy. *J Eur Acad Dermatol Venereol* 2021; **35**: 629-640 [PMID: 33290611 DOI: 10.1111/jdv.17079]

4 **Gao JL**, Streed CG Jr, Thompson J, Dommasch ED, Peebles JK. Androgenetic alopecia in transgender and gender diverse populations: A review of therapeutics. *J Am Acad Dermatol* 2023; **89**: 774-783 [PMID: 34756934 DOI: 10.1016/j.jaad.2021.08.067]

5 **Kim IY**, Kim JH, Choi JE, Yu SJ, Kim JH, Kim SR, Choi MS, Kim MH, Hong KW, Park BC. The first broad replication study of SNPs and a pilot genome-wide association study for androgenetic alopecia in Asian populations. *J Cosmet Dermatol* 2022; **21**: 6174-6183 [PMID: 35754308 DOI: 10.1111/jocd.15187]

6 **Ahlin R**, Nørskov NP, Nybacka S, Landberg R, Skokic V, Stranne J, Josefsson A, Steineck G, Hedelin M. Effects on Serum Hormone Concentrations after a Dietary Phytoestrogen Intervention in Patients with Prostate Cancer: A Randomized Controlled Trial. *Nutrients* 2023; **15**: 1792 [PMID: 37049632 DOI: 10.3390/nu15071792]

7 **Mai Q**, Han Y, Cheng G, Ma R, Yan Z, Chen X, Yu G, Chen T, Zhang S. Innovative Strategies for Hair Regrowth and Skin Visualization. *Pharmaceutics* 2023; **15**: 1201 [PMID: 37111686 DOI: 10.3390/pharmaceutics15041201]

8 **Morente-López M**, Mato-Basalo R, Lucio-Gallego S, Silva-Fernández L, González-Rodríguez A, De Toro FJ, Fafián-Labora JA, Arufe MC. Therapy free of cells vs human mesenchymal stem cells from umbilical cord stroma to treat the inflammation in OA. *Cell Mol Life Sci* 2022; **79**: 557 [PMID: 36264388 DOI: 10.1007/s00018-022-04580-z]

9 **Wang C**, Liu H, Yang M, Bai Y, Ren H, Zou Y, Yao Z, Zhang B, Li Y. RNA-Seq Based Transcriptome Analysis of Endothelial Differentiation of Bone Marrow Mesenchymal Stem Cells. *Eur J Vasc Endovasc Surg* 2020; **59**: 834-842 [PMID: 31874808 DOI: 10.1016/j.ejvs.2019.11.003]

10 **Liu C**, Hu F, Jiao G, Guo Y, Zhou P, Zhang Y, Zhang Z, Yi J, You Y, Li Z, Wang H, Zhang X. Dental pulp stem cell-derived exosomes suppress M1 macrophage polarization through the ROS-MAPK-NFκB P65 signaling pathway after spinal cord injury. *J Nanobiotechnology* 2022; **20**: 65 [PMID: 35109874 DOI: 10.1186/s12951-022-01273-4]

11 **Xu J**, Chen P, Yu C, Shi Q, Wei S, Li Y, Qi H, Cao Q, Guo C, Wu X, Di G. Hypoxic bone marrow mesenchymal stromal cells-derived exosomal miR-182-5p promotes liver regeneration *via* FOXO1-mediated macrophage polarization. *FASEB J* 2022; **36**: e22553 [PMID: 36111980 DOI: 10.1096/fj.202101868RRR]

12 **Vij R**, Stebbings KA, Kim H, Park H, Chang D. Safety and efficacy of autologous, adipose-derived mesenchymal stem cells in patients with rheumatoid arthritis: a phase I/IIa, open-label, non-randomized pilot trial. *Stem Cell Res Ther* 2022; **13**: 88 [PMID: 35241141 DOI: 10.1186/s13287-022-02763-w]

13 **Zhou T**, Yuan Z, Weng J, Pei D, Du X, He C, Lai P. Challenges and advances in clinical applications of mesenchymal stromal cells. *J Hematol Oncol* 2021; **14**: 24 [PMID: 33579329 DOI: 10.1186/s13045-021-01037-x]

14 **Zha K**, Li X, Yang Z, Tian G, Sun Z, Sui X, Dai Y, Liu S, Guo Q. Heterogeneity of mesenchymal stem cells in cartilage regeneration: from

characterization to application. *NPJ Regen Med* 2021; **6**: 14 [PMID: 33741999 DOI: 10.1038/s41536-021-00122-6]

15 **Zhou Y**, Zhao B, Zhang XL, Lu YJ, Lu ST, Cheng J, Fu Y, Lin L, Zhang NY, Li PX, Zhang J, Zhang J. Combined topical and systemic administration with human adipose-derived mesenchymal stem cells (hADSC) and hADSC-derived exosomes markedly promoted cutaneous wound healing and regeneration. *Stem Cell Res Ther* 2021; **12**: 257 [PMID: 33933157 DOI: 10.1186/s13287-021-02287-9]

16 **Zhao B**, Zhang X, Zhang Y, Lu Y, Zhang W, Lu S, Fu Y, Zhou Y, Zhang J, Zhang J. Human Exosomes Accelerate Cutaneous Wound Healing by Promoting Collagen Synthesis in a Diabetic Mouse Model. *Stem Cells Dev* 2021; **30**: 922-933 [PMID: 34167333 DOI: 10.1089/scd.2021.0100]

17 **Li J**, Zhao B, Yao S, Dai Y, Zhang X, Yang N, Bao Z, Cai J, Chen Y, Wu X. Dermal PapillaCell-Derived Exosomes Regulate Hair Follicle Stem Cell Proliferation *via* LEF1. *Int J Mol Sci* 2023; **24**: 3961 [PMID: 36835374 DOI: 10.3390/ijms24043961]

18 **Li J**, Zhao B, Dai Y, Zhang X, Chen Y, Wu X. Exosomes Derived from Dermal Papilla Cells Mediate Hair Follicle Stem Cell Proliferation through the Wnt3a/β-Catenin Signaling Pathway. *Oxid Med Cell Longev* 2022; **2022**: 9042345 [PMID: 36388171 DOI: 10.1155/2022/9042345]

19 **Gao Y**, Mi N, Zhang Y, Li X, Guan W, Bai C. Uterine macrophages as treatment targets for therapy of premature rupture of membranes by modified ADSC-EVs through a circRNA/miRNA/NF-κB pathway. *J Nanobiotechnology* 2022; **20**: 487 [PMID: 36402996 DOI: 10.1186/s12951-022-01696-z]

20 **Zhang J**, Qu X, Li J, Harada A, Hua Y, Yoshida N, Ishida M, Sawa Y, Liu L, Miyagawa S. Tissue Sheet Engineered Using Human Umbilical Cord-Derived Mesenchymal Stem Cells Improves Diabetic Wound Healing. *Int J Mol Sci* 2022; **23**: 12697 [PMID: 36293557 DOI: 10.3390/ijms232012697]

21 **García-Honduvilla N**, Cifuentes A, Ortega MA, Delgado A, González S, Bujan J, Alvarez-Mon M. High Sensitivity of Human Adipose Stem Cells to Differentiate into Myofibroblasts in the Presence of C. aspersa Egg Extract. *Stem Cells Int* 2017; **2017**: 9142493 [PMID: 29445405 DOI: 10.1155/2017/9142493]

22 **Fu Y**, Zhang YL, Liu RQ, Xu MM, Xie JL, Zhang XL, Xie GM, Han YT, Zhang XM, Zhang WT, Zhang J, Zhang J. Exosome lncRNA IFNG-AS1 derived from mesenchymal stem cells of human adipose ameliorates neurogenesis and ASD-like behavior in BTBR mice. *J Nanobiotechnology* 2024; **22**: 66 [PMID: 38368393 DOI: 10.1186/s12951-024-02338-2]

23 **Cheng Q**, Li X, Wang Y, Dong M, Zhan FH, Liu J. The ceramide pathway is involved in the survival, apoptosis and exosome functions of human multiple myeloma cells in vitro. *Acta Pharmacol Sin* 2018; **39**: 561-568 [PMID: 28858294 DOI: 10.1038/aps.2017.118]

24 **Zhao PY**, Ji J, Liu XH, Zhao H, Xue B, Jin LY, Fan YP, Zhao WJ, Wang L. Bu-Shen-Yi-Sui Capsule, an Herbal Medicine Formula, Promotes Remyelination by Modulating the Molecular Signals *via* Exosomes in Mice with Experimental Autoimmune Encephalomyelitis. *Oxid Med Cell Longev* 2020; **2020**: 7895293 [PMID: 32774683 DOI: 10.1155/2020/7895293]

25 **Tsunemi T**, Perez-Rosello T, Ishiguro Y, Yoroisaka A, Jeon S, Hamada K, Rammonhan M, Wong YC, Xie Z, Akamatsu W, Mazzulli JR, Surmeier DJ, Hattori N, Krainc D. Increased Lysosomal Exocytosis Induced by Lysosomal Ca(2+) Channel Agonists Protects Human Dopaminergic Neurons from α-Synuclein Toxicity. *J Neurosci* 2019; **39**: 5760-5772 [PMID: 31097622 DOI: 10.1523/JNEUROSCI.3085-18.2019]

26 **Jung YH**, Chae CW, Choi GE, Shin HC, Lim JR, Chang HS, Park J, Cho JH, Park MR, Lee HJ, Han HJ. Cyanidin 3-O-arabinoside suppresses DHT-induced dermal papilla cell senescence by modulating p38-dependent ER-mitochondria contacts. *J Biomed Sci* 2022; **29**: 17 [PMID: 35255899 DOI: 10.1186/s12929-022-00800-7]

27 **Bao L**, Sun Z, Dang L, Zhang Q, Zheng L, Yang F, Zhang J. LncRNA RP11-818O24.3 promotes hair-follicle recovery *via* FGF2-PI3K/Akt signal pathway. *Cytotechnology* 2024; **76**: 425-439 [PMID: 38933868 DOI: 10.1007/s10616-024-00624-3]

28 **Wang ZD**, Feng Y, Ma LY, Li X, Ding WF, Chen XM. Hair growth promoting effect of white wax and policosanol from white wax on the mouse model of testosterone-induced hair loss. *Biomed Pharmacother* 2017; **89**: 438-446 [PMID: 28249244 DOI: 10.1016/j.biopha.2017.02.036]

29 **Devjani S**, Ezemma O, Kelley KJ, Stratton E, Senna M. Androgenetic Alopecia: Therapy Update. *Drugs* 2023; **83**: 701-715 [PMID: 37166619 DOI: 10.1007/s40265-023-01880-x]

30 **Lee HJ**, Oh DW, Na MJ, Kim DW, Yuk DY, Choi HC, Lee YB, Han K, Park CW. Preparation and in vivo evaluation of lecithin-based microparticles for topical delivery of minoxidil. *Arch Pharm Res* 2017; **40**: 943-951 [PMID: 28770536 DOI: 10.1007/s12272-017-0934-x]

31 **Shi Y**, Zhao J, Li H, Yu M, Zhang W, Qin D, Qiu K, Chen X, Kong M. A Drug-Free, Hair Follicle Cycling Regulatable, Separable, Antibacterial Microneedle Patch for Hair Regeneration Therapy. *Adv Healthc Mater* 2022; **11**: e2200908 [PMID: 35817085 DOI: 10.1002/adhm.202200908]

32 **Li Y**, Wang G, Wang Q, Zhang Y, Cui L, Huang X. Exosomes Secreted from Adipose-Derived Stem Cells Are a Potential Treatment Agent for Immune-Mediated Alopecia. *J Immunol Res* 2022; **2022**: 7471246 [PMID: 35155688 DOI: 10.1155/2022/7471246]

33 **Zhang Y**, Zhang S, Long Y, Wang W, Du F, Li J, Jin F, Li Z. Stimulation of hair growth by Tianma Gouteng decoction: Identifying mechanisms based on chemical analysis, systems biology approach, and experimental evaluation. *Front Pharmacol* 2022; **13**: 1073392 [PMID: 36588691 DOI: 10.3389/fphar.2022.1073392]

34 **Kwon TR**, Oh CT, Park HM, Han HJ, Ji HJ, Kim BJ. Potential synergistic effects of human placental extract and minoxidil on hair growth-promoting activity in C57BL/6J mice. *Clin Exp Dermatol* 2015; **40**: 672-681 [PMID: 25787854 DOI: 10.1111/ced.12601]

35 **Wang J**, Cai J, Zhang Q, Wen J, Liao Y, Lu F. Fat transplantation induces dermal adipose regeneration and reverses skin fibrosis through dedifferentiation and redifferentiation of adipocytes. *Stem Cell Res Ther* 2022; **13**: 499 [PMID: 36210466 DOI: 10.1186/s13287-022-03127-0]

36 **Tampucci S**, Paganini V, Burgalassi S, Chetoni P, Monti D. Nanostructured Drug Delivery Systems for Targeting 5-α-Reductase Inhibitors to the Hair Follicle. *Pharmaceutics* 2022; **14**: 286 [PMID: 35214018 DOI: 10.3390/pharmaceutics14020286]

37 **Cai Y**, Jia Z, Zhang Y, Kang B, Chen C, Liu W, Li W, Zhang W. Cell-free fat extract restores hair loss: a novel therapeutic strategy for androgenetic alopecia. *Stem Cell Res Ther* 2023; **14**: 219 [PMID: 37612726 DOI: 10.1186/s13287-023-03398-1]

38 **Xiang P**, Li F, Ma Z, Yue J, Lu C, You Y, Hou L, Yin B, Qiang B, Shu P, Peng X. HCF-1 promotes cell cycle progression by regulating the expression of CDC42. *Cell Death Dis* 2020; **11**: 907 [PMID: 33097698 DOI: 10.1038/s41419-020-03094-5]

39 **Hercyk BS**, Rich-Robinson J, Mitoubsi AS, Harrell MA, Das ME. A novel interplay between GEFs orchestrates Cdc42 activity during cell polarity and cytokinesis in fission yeast. *J Cell Sci* 2019; **132**: jcs236018 [PMID: 31719163 DOI: 10.1242/jcs.236018]

40 **Wang P**, Hu G, Zhao W, Du J, You M, Xv M, Yang H, Zhang M, Yan F, Huang M, Wang X, Zhang L, Chen Y. Continuous ZnO nanoparticle exposure induces melanoma-like skin lesions in epidermal barrier dysfunction model mice through anti-apoptotic effects mediated by the oxidative stress-activated NF-κB pathway. *J Nanobiotechnology* 2022; **20**: 111 [PMID: 35248056 DOI: 10.1186/s12951-022-01308-w]

41 **Abraham CG**, Ludwig MP, Andrysik Z, Pandey A, Joshi M, Galbraith MD, Sullivan KD, Espinosa JM. ΔNp63α Suppresses TGFB2

Expression and RHOA Activity to Drive Cell Proliferation in Squamous Cell Carcinomas. *Cell Rep* 2018; **24**: 3224-3236 [PMID: 30232004 DOI: 10.1016/j.celrep.2018.08.058]

42 **Hammond NL**, Headon DJ, Dixon MJ. The cell cycle regulator protein 14-3-3σ is essential for hair follicle integrity and epidermal homeostasis. *J Invest Dermatol* 2012; **132**: 1543-1553 [PMID: 22377760 DOI: 10.1038/jid.2012.27]

43 **Li K**, Sun Y, Liu S, Zhou Y, Qu Q, Wang G, Wang J, Chen R, Fan Z, Liu B, Li Y, Mao X, Hu Z, Miao Y. The AR/miR-221/IGF-1 pathway mediates the pathogenesis of androgenetic alopecia. *Int J Biol Sci* 2023; **19**: 3307-3323 [PMID: 37496996 DOI: 10.7150/ijbs.80481]

44 **Xiao XH**, Huang QY, Qian XL, Duan J, Jiao XQ, Wu LY, Huang QY, Li J, Lai XN, Shi YB, Xiong LX. Cdc42 Promotes ADSC-Derived IPC Induction, Proliferation, And Insulin Secretion Via Wnt/β-Catenin Signaling. *Diabetes Metab Syndr Obes* 2019; **12**: 2325-2339 [PMID: 32009808 DOI: 10.2147/DMSO.S226055]

45 **Chen X**, Liu B, Li Y, Han L, Tang X, Deng W, Lai W, Wan M. Dihydrotestosterone Regulates Hair Growth Through the Wnt/β-Catenin Pathway in C57BL/6 Mice and In Vitro Organ Culture. *Front Pharmacol* 2019; **10**: 1528 [PMID: 32038233 DOI: 10.3389/fphar.2019.01528]

46 **Song KH**, Seo CS, Yang WK, Gu HO, Kim KJ, Kim SH. Extracts of Phyllostachys pubescens Leaves Represses Human Steroid 5-Alpha Reductase Type 2 Promoter Activity in BHP-1 Cells and Ameliorates Testosterone-Induced Benign Prostatic Hyperplasia in Rat Model. *Nutrients* 2021; **13**: 884 [PMID: 33803357 DOI: 10.3390/nu13030884]

47 **Chen CL**, Huang WY, Wang EHC, Tai KY, Lin SJ. Functional complexity of hair follicle stem cell niche and therapeutic targeting of niche dysfunction for hair regeneration. *J Biomed Sci* 2020; **27**: 43 [PMID: 32171310 DOI: 10.1186/s12929-020-0624-8]

48 **Park J**, Jun EK, Son D, Hong W, Jang J, Yun W, Yoon BS, Song G, Kim IY, You S. Overexpression of Nanog in amniotic fluid-derived mesenchymal stem cells accelerates dermal papilla cell activity and promotes hair follicle regeneration. *Exp Mol Med* 2019; **51**: 1-15 [PMID: 31273189 DOI: 10.1038/s12276-019-0266-7]

49 **Liu J**, Shu B, Zhou Z, Xu Y, Liu Y, Wang P, Xiong K, Xie J. Involvement of miRNA203 in the proliferation of epidermal stem cells during the process of DM chronic wound healing through Wnt signal pathways. *Stem Cell Res Ther* 2020; **11**: 348 [PMID: 32787903 DOI: 10.1186/s13287-020-01829-x]

50 **Diviccaro S**, Melcangi RC, Giatti S. Post-finasteride syndrome: An emerging clinical problem. *Neurobiol Stress* 2020; **12**: 100209 [PMID: 32435662 DOI: 10.1016/j.ynstr.2019.100209]

51 **Feldman PR**, Fiebig KM, Piwko C, Mints BM, Brown D, Cahan DJ, Guevara-Aguirre J. Safety and efficacy of ALRV5XR in women with androgenetic alopecia or telogen effluvium: A randomised, double-blinded, placebo-controlled clinical trial. *EClinicalMedicine* 2021; **37**: 100978 [PMID: 34235415 DOI: 10.1016/j.eclinm.2021.100978]

52 **Pozo-Pérez L**, Tornero-Esteban P, López-Bran E. Clinical and preclinical approach in AGA treatment: a review of current and new therapies in the regenerative field. *Stem Cell Res Ther* 2024; **15**: 260 [PMID: 39148125 DOI: 10.1186/s13287-024-03801-5]

53 **Papakonstantinou M**, Siotos C, Gasteratos KC, Spyropoulou GA, Gentile P. Autologous Platelet-Rich Plasma Treatment for Androgenic Alopecia: A Systematic Review and Meta-Analysis of Clinical Trials. *Plast Reconstr Surg* 2023; **151**: 739e-747e [PMID: 36729475 DOI: 10.1097/PRS.0000000000010076]

54 **Gentile P**, Garcovich S. Systematic review: The platelet-rich plasma use in female androgenetic alopecia as effective autologous treatment of regenerative plastic surgery. *J Plast Reconstr Aesthet Surg* 2022; **75**: 850-859 [PMID: 34872877 DOI: 10.1016/j.bjps.2021.11.004]

55 **Gentile P**, Garcovich S, Scioli MG, Bielli A, Orlandi A, Cervelli V. Mechanical and Controlled PRP Injections in Patients Affected by Androgenetic Alopecia. *J Vis Exp* 2018; 56406 [PMID: 29443105 DOI: 10.3791/56406]

56 **Gentile P**, Garcovich S. The Effectiveness of Low-Level Light/Laser Therapy on Hair Loss. *Facial Plast Surg Aesthet Med* 2024; **26**: 228-235 [PMID: 34546105 DOI: 10.1089/fpsam.2021.0151]

57 **Gentile P**. Autologous Cellular Method Using Micrografts of Human Adipose Tissue Derived Follicle Stem Cells in Androgenic Alopecia. *Int J Mol Sci* 2019; **20**: 3446 [PMID: 31337037 DOI: 10.3390/ijms20143446]

58 **Mathen C**, Dsouza W. In vitro and clinical evaluation of umbilical cord-derived mesenchymal stromal cell-conditioned media for hair regeneration. *J Cosmet Dermatol* 2022; **21**: 740-749 [PMID: 33780589 DOI: 10.1111/jocd.14114]

59 **Hoang DM**, Pham PT, Bach TQ, Ngo ATL, Nguyen QT, Phan TTK, Nguyen GH, Le PTT, Hoang VT, Forsyth NR, Heke M, Nguyen LT. Stem cell-based therapy for human diseases. *Signal Transduct Target Ther* 2022; **7**: 272 [PMID: 35933430 DOI: 10.1038/s41392-022-01134-4]

60 **Maldonado VV**, Patel NH, Smith EE, Barnes CL, Gustafson MP, Rao RR, Samsonraj RM. Clinical utility of mesenchymal stem/stromal cells in regenerative medicine and cellular therapy. *J Biol Eng* 2023; **17**: 44 [PMID: 37434264 DOI: 10.1186/s13036-023-00361-9]

61 **Zhuang WZ**, Lin YH, Su LJ, Wu MS, Jeng HY, Chang HC, Huang YH, Ling TY. Mesenchymal stem/stromal cell-based therapy: mechanism, systemic safety and biodistribution for precision clinical applications. *J Biomed Sci* 2021; **28**: 28 [PMID: 33849537 DOI: 10.1186/s12929-021-00725-7]

62 **Cruciani S**, Garroni G, Balzano F, Pala R, Bellu E, Cossu ML, Ginesu GC, Ventura C, Maioli M. Tuning Adipogenic Differentiation in ADSCs by Metformin and Vitamin D: Involvement of miRNAs. *Int J Mol Sci* 2020; **21**: 6181 [PMID: 32867201 DOI: 10.3390/ijms21176181]

63 **Zhang B**, Chen T. Local and systemic mechanisms that control the hair follicle stem cell niche. *Nat Rev Mol Cell Biol* 2024; **25**: 87-100 [PMID: 37903969 DOI: 10.1038/s41580-023-00662-3]

64 **Zhu Z**, Yuan ZQ, Huang C, Jin R, Sun D, Yang J, Luo XS. Pre-culture of adipose-derived stem cells and heterologous acellular dermal matrix: paracrine functions promote post-implantation neovascularization and attenuate inflammatory response. *Biomed Mater* 2019; **14**: 035002 [PMID: 30699384 DOI: 10.1088/1748-605X/ab0355]

65 **Golpanian S**, Schulman IH, Ebert RF, Heldman AW, DiFede DL, Yang PC, Wu JC, Bolli R, Perin EC, Moyé L, Simari RD, Wolf A, Hare JM; Cardiovascular Cell Therapy Research Network. Concise Review: Review and Perspective of Cell Dosage and Routes of Administration From Preclinical and Clinical Studies of Stem Cell Therapy for Heart Disease. *Stem Cells Transl Med* 2016; **5**: 186-191 [PMID: 26683870 DOI: 10.5966/sctm.2015-0101]

66 **Yaghoubi Y**, Movassaghpour A, Zamani M, Talebi M, Mehdizadeh A, Yousefi M. Human umbilical cord mesenchymal stem cells derived-exosomes in diseases treatment. *Life Sci* 2019; **233**: 116733 [PMID: 31394127 DOI: 10.1016/j.lfs.2019.116733]

World Journal of Stem Cells

Submit a Manuscript: https://www.f6publishing.com

World J Stem Cells 2025 March 26; 17(3): 102067

DOI: 10.4252/wjsc.v17.i3.102067

ISSN 1948-0210 (online)

SYSTEMATIC REVIEWS

Clinical experience with cryopreserved mesenchymal stem cells for cardiovascular applications: A systematic review

Moaz Safwan, Mariam Safwan Bourgleh, Khawaja Husnain Haider

Specialty type: Cell and tissue engineering

Provenance and peer review: Invited article; Externally peer reviewed.

Peer-review model: Single blind

Peer-review report's classification
Scientific Quality: Grade A, Grade A, Grade B, Grade C
Novelty: Grade A, Grade A, Grade B
Creativity or Innovation: Grade A, Grade A, Grade B
Scientific Significance: Grade A, Grade B, Grade C

P-Reviewer: Leone G; Li Y; Ventura C; Wan CL

Received: October 7, 2024
Revised: January 17, 2025
Accepted: February 24, 2025
Published online: March 26, 2025
Processing time: 164 Days and 14.5 Hours

Moaz Safwan, Mariam Safwan Bourgleh, Khawaja Husnain Haider, Department of Basic Sciences, Sulaiman Al Rajhi University, Al Bukairiyah 51941, AlQaseem, Saudi Arabia

Corresponding author: Khawaja Husnain Haider, PhD, Professor, Department of Basic Sciences, Sulaiman Al Rajhi University, PO Box 777, Al Bukairiyah 51941, AlQaseem, Saudi Arabia. kh.haider@sr.edu.sa

Abstract

BACKGROUND

As living biodrugs, mesenchymal stem cells (MSCs) have progressed to phase 3 clinical trials for cardiovascular applications. However, their limited immediate availability hampers their routine clinical use.

AIM

To validate our hypothesis that cryopreserved MSCs (^{Cryo}MSCs) are as safe and effective as freshly cultured MSC counterparts but carry logistical advantages.

METHODS

Four databases were systematically reviewed for relevant randomized controlled trials (RCTs) evaluating the safety and efficacy of ^{Cryo}MSCs from various tissue sources in treating patients with heart disease. A subgroup analysis was performed based on MSC source and post-thaw cell viability to determine treatment effects across different ^{Cryo}MSCs sources and viability status. Weighted mean differences (WMDs) and odds ratios were calculated to measure changes in the estimated treatment effects. All statistical analyses were performed using RevMan version 5.4.1 software.

RESULTS

Seven RCTs (285 patients) met the eligibility criteria for inclusion in the meta-analysis. During short-term follow-up, ^{Cryo}MSCs demonstrated a significant 2.11% improvement in left ventricular ejection fraction (LVEF) [WMD (95%CI) = 2.11 (0.66-3.56), P = 0.004, I^2 = 1%], with umbilical cord-derived MSCs being the most effective cell type. However, the significant effect on LVEF was not sustained over the 12 months of follow-up. Subgroup analysis demonstrated a substantial 3.44% improvement in LVEF [WMD (95%CI) = 3.44 (1.46-5.43), P = 0.0007, I^2 = 0%] when using MSCs with post-thaw viability exceeding 80%. There was no statistically significant difference in the frequency of major cardiac adverse events observed in rehospitalization or mortality in patients treated with ^{Cryo}MSCs *vs* the control group.

CONCLUSION

^{Cryo}MSCs are a promising option for heart failure patients, particularly considering the current treatment options for cardiovascular diseases. Our data suggest that ^{Cryo}MSCs could be a viable alternative or complementary treatment to the current options, potentially improving patient outcomes.

Key Words: Cardiovascular; Cryopreservation; Heart; Mesenchymal stem cells; Umbilical cord stem cells; Randomized controlled trials; Stem cells

Core Tip: Our study yields significant findings that are crucial for regenerative medicine and cardiology. Our findings revealed that cryopreserved mesenchymal stem cells (^{Cryo}MSCs) treatment, compared to the control group, resulted in a 2.11% improvement in left ventricular ejection fraction during six months of follow-up, offering hope for potential future therapies. Left ventricular ejection fraction improvement was higher when using umbilical cord-derived mesenchymal stem cells or ^{Cryo}MSCs with more than 80% post-thaw viability. The ^{Cryo}MSCs treatment was safe, as there was no significant difference in the incidence of major cardiac adverse events compared to the control group. In addition, no significant effects on mortality and readmission were observed in the ^{Cryo}MSCs group compared to the control group.

Citation: Safwan M, Bourgleh MS, Haider KH. Clinical experience with cryopreserved mesenchymal stem cells for cardiovascular applications: A systematic review. *World J Stem Cells* 2025; 17(3): 102067
URL: https://www.wjgnet.com/1948-0210/full/v17/i3/102067.htm
DOI: https://dx.doi.org/10.4252/wjsc.v17.i3.102067

INTRODUCTION

Cardiovascular diseases (CVDs), such as myocardial infarction and heart failure, are a pressing global health issue, contributing to 32% of all global deaths[1,2]. The current treatment options provide only symptomatic relief, failing to repair or regenerate the damaged myocardium or preserve declining cardiac function. In this context, cell-based therapy using mesenchymal stem cells (MSCs) has emerged as a promising solution for heart failure patients[3].

MSCs possess unique cell biology and characteristics, *i.e.*, multilineage differentiation potential, soluble and insoluble factor release as part of their paracrine activity, low immunogenicity upon transplantation, anti-inflammatory and immunomodulatory properties, *etc*[4]. They have a robust nature that withstands the rigors of genetic modulation and can carry transgenes during cell-based gene therapy. Combined with their ease of availability from diverse tissue sources, notably bone marrow, adipose tissue, and umbilical cord, non-invasive isolation without moral and ethical strings places them near the ideal cell type for use in the cell-based therapy approach[5]. These characteristic features of MSCs are critical for their diverse clinical applications and have been extensively studied during experimental animal studies and clinical trials[6]. Currently, nearly 1500 registrations with clinicaltrials.gov to assess MSCs from different tissue sources in clinical settings for diverse pathological conditions[7]. Despite these advantages, logistic issues regarding their off-the-shelf availability in large numbers remain a significant limitation that is a critical impediment in routine clinical use[8]. Moreover, repeated tissue sampling for isolation, purification, and *in vitro* expansion adds to the cost of each procedure, besides being time-intensive, which limits their routine use in clinical practice in general and especially in the emergency rooms[9].

The low-temperature storage or cryopreservation of MSCs offers a cost-effective solution to the logistical issues and ensures their ready-made availability. This significantly reduces the time needed to isolate, purify, and expand the cells *in vitro* before use for every patient. The currently available cryopreservation protocols are believed to preserve the cells' unique stemness characteristics, such as their ability to differentiate into multiple cell types and immunomodulatory properties. These characteristics are crucial for the therapeutic potential of MSCs. Despite the beneficial effects of cryopreservation's known impact on MSC biology and viability, standardized preservation methods do not lead to significant variability across preclinical data. Various techniques have been explored to mitigate cellular damage post-cryopreservation, with dimethyl sulfoxide (DMSO) being the most common cryoprotectant despite its associated adverse effects[10,11].

The potential of cryopreserved MSCs (^{Cryo}MSCs) in clinical trials treating CVDs has been reported as a significant advancement. A recent meta-analysis of six randomized controlled trials (RCTs) involving 263 heart failure patients found that bone marrow-derived MSCs (BM-MSCs) significantly increased left ventricular ejection fraction (LVEF) by 6.37% at the end of the follow-up period compared to the control group[3]. This promising potential not only instills hope and optimism for the future of cardiovascular medicine but also inspires further research and development in this area. The use of ^{Cryo}MSCs in clinical trials opens new doors for research and treatment, and their potential could significantly impact the field. Currently, several MSC-based products are available on the market, including Prochymal (Osiris Therapeutics, Canada), Cartistem (Medipost Co Ltd, Korea), and Stempeucel (Stempeutics Research), Cellgram-AMI (FCB Pharmicell, South Korea) (Alliance for Regenerative Medicine; https://alliancerm.org/available-products/), but their

functionality and clinical efficacy are still under scrutiny. Despite the commercial availability and recent use of MSC-based products, there is a scarcity of published data comparing ^{cryo}MSCs with freshly cultured MSCs as living biodrugs to assess their safety and efficacy for patients with CVD.

The present systematic review and meta-analysis of ^{cryo}MSCs in patients with myocardial infarction and heart failure compared to freshly cultured MSC-based therapies aim to significantly contribute to cardiovascular medicine and stem cell therapy. The evidence-based insights into the efficacy and safety of ^{cryo}MSCs could pave the way for improved treatment strategies using off-the-shelf MSCs. These findings can potentially revolutionize the field, bringing an exciting new approach to cardiovascular medicine and inspiring future research and innovation in stem cell therapy, potentially dramatically improving patient outcomes.

MATERIALS AND METHODS

Protocol registration

Before any formal literature search or data analysis, a complete protocol for this study was prospectively developed and registered on the International Prospective Register of Systematic Reviews database dated June 6, 2024. The protocol is available online under the registration ID: CRD42024555501.

Search strategy

A comprehensive and meticulous search strategy was conducted across four databases, including PubMed, Cochrane CENTRAL, ClinicalTrials.gov, and Embase, from their inception until June 2024 to identify relevant RCTs. The search strategy incorporated common text words and medical subject headings (MeSH) such as "Mesenchymal Stem Cells", "MSCs", "Cryopreserved", "Bone marrow Mesenchymal stem cells", "umbilical cord Mesenchymal stem cells", "myocardial infarction," "ischemic heart disease", "acute coronary syndrome", "heart failure", and "cardiomyopathy". These terms were combined using specific algorithms, such as "Mesenchymal stem cells" and "Myocardial infarction". Additionally, the reference lists of included studies were manually searched to identify any relevant RCTs not captured in the initial search. Our search was not restricted by language, and the strategy adhered to the Preferred Reporting Items for Systematic Reviews and Meta-Analysis 2020 statement[12], ensuring the thoroughness and validity of the research and instilling confidence in the validity of the findings.

Eligibility criteria

For inclusion in the current systematic review and meta-analysis, a study was required to meet the following eligibility criteria: (1) It must be an RCT; (2) It assessed the efficacy of ^{Cryo}MSCs; (3) It involved patients with myocardial infarction or heart failure; (4) It must include a control group; (5) The follow-up period was at least six months; and (6) It reported one of the following outcomes: Change in LVEF, six-minute walking distance test (6-MWD), major adverse cardiac events (MACE), or readmission for exacerbation of heart failure or myocardial infarction. Any study that did not fulfill these criteria or was not available in full text was considered ineligible for inclusion.

Outcome measures

The primary outcome evaluated the efficacy of ^{Cryo}MSCs, measured by the change in LVEF and 6-MWD compared to the change observed in the control arm. The secondary outcomes focused on the safety of ^{Cryo}MSCs, assessed by the frequency of MACE across both arms during treatment. MACE encompassed various events, including mortality, arrhythmias, heart failure, recurrence of myocardial infarction, and readmission for cardiac reasons.

Data extraction

Two co-authors (Safwan M and Bourgleh MS) independently evaluated the eligibility of studies for meta-analysis based on the inclusion/exclusion criteria and utilized a standardized data extraction sheet. Each included study was examined, with the extraction of the following variables: (1) First author and publication year; (2) Trial location (country); (3) Type of stem cells; (4) Sample size; (5) Gender distribution; (6) Mean sample age; (7) Presence of co-morbidities; (8) Duration of follow-up for key endpoint measurements; (9) Dosage (number of cells transferred in millions); (10) Method of cell delivery (*e.g.*, intravenous, intramyocardial, or intracoronary infusion); (11) New York Heart Association classification of study participants at baseline; (12) Assessment method/tools for study endpoints (*e.g.*, electrocardiogram, echocardiogram, magnetic resonance imaging, cardiac computed tomography, and single-photon emission computed tomography); (13) LVEF (mean ± SD); and (14) Occurrence of MACE.

Quality assessment

The same co-authors (Safwan M and Bourgleh MS) independently followed the Cochrane collaboration tool for bias assessment to evaluate the methodological quality of the included RCTs. The overall risk of bias was visually presented in a bias risk graph. In instances of disagreement between the authors, a third independent author (Haider KH) was consulted for resolution, ensuring the objectivity and independence of the quality assessment process and reassuring the authors about the results' reliability. This rigorous quality assessment process adds further credibility to the findings, providing the audience with confidence in the reliability of the results.

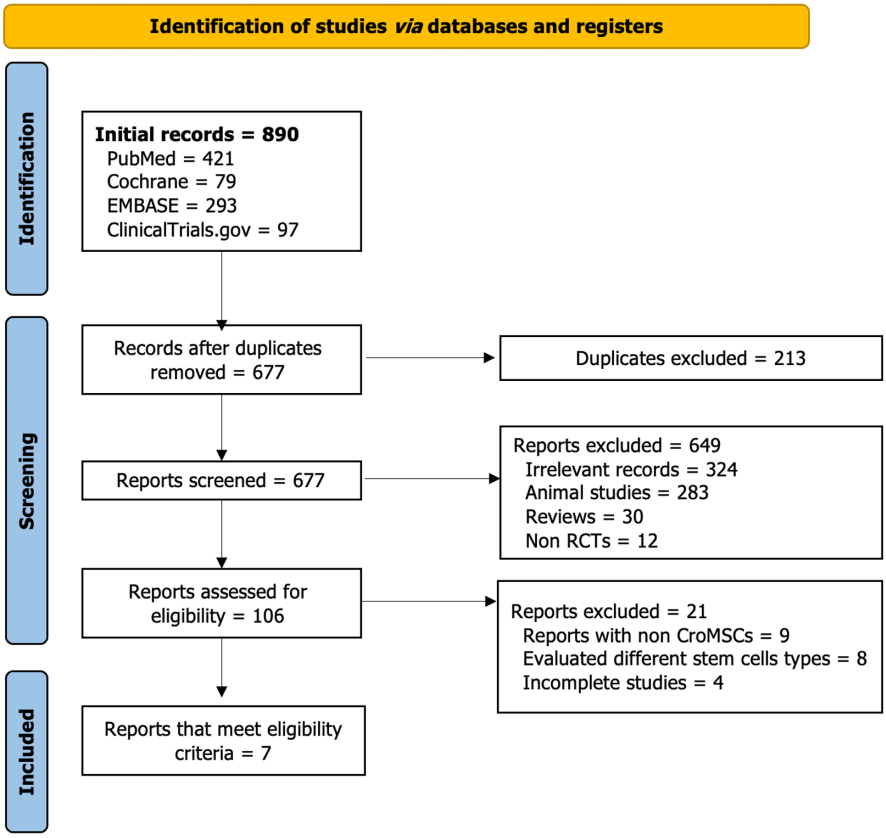

Figure 1 Study selection flow diagram (PRISMA chart). RCTs: Randomized controlled trials; Cryo-MSCs: Cryopreserved mesenchymal stem cells.

Statistical analysis

Statistical data analysis was performed using Review Manager (RevMan) 5.4.1 software. The odds ratio (OR) was calculated and presented with confidence intervals (CI) for dichotomous outcomes, mortality, MACE, and readmission. For continuous outcomes, LVEF and 6MWD, any data extracted in mean ± SE or mean and CI were converted into mean ± SD using equations of the Cochrane Handbook[13]. Weighted mean difference (WMD) analysis was performed due to the consistent measurement units across all the studies for LVEF and 6MWD. Considering the expected heterogeneity between studies due to variations in sample sizes, countries, and doses, a random effect model was employed. To explore the potential variations in efficacy and safety based on the cell source, subgroup analysis was performed using two different cell sources: Bone marrow and umbilical cord tissue. Additionally, a subgroup analysis was conducted based on the release criteria for post-thaw viability, comparing groups with viability rates above 80% to those below 80%. Between-study heterogeneity was assessed using the I^2 statistic and interpreted as follows: 25% < I^2 < 75%: Low and unimportant heterogeneity; I^2 25%-75%: Moderate heterogeneity; 75% < I^2 < 100%: High heterogeneity. The significance cutoff for statistical significance was set at a P value of less than 0.05. A sensitivity analysis was conducted in case high heterogeneity was observed between the studies.

RESULTS

Eligible studies

Figure 1 summarizes the process of systematically searching for eligible RCTs. Initially, a search was conducted across various databases, resulting in 890 records. After removing duplicates and performing title and abstract screening, 28 RCTs remained for full-text screening. Seven RCTs were included, and the remaining 21 were excluded based on the reasons outlined in Figure 1. The risk of bias for the included studies was assessed using the Cochrane collaboration tool [14]. The assessment was based on selection, performance, detection, attrition, and reporting biases. Figure 2 presents a graphical summary of the bias assessment.

Characteristics of included studies

The baseline characteristics of the included RCTs are detailed in Tables 1 and 2. The 7 RCTs included 285 heart disease patients, with 178 patients in the intervention and 107 in the control arms[15-21]. Four of the included RCTs used ^{Cryo}BM-MSCs for the intervention[15-18], involving 164 patients, 103 in the intervention arm and 61 in the control arm. The percentage of male participants in the BM-MSCs studies ranged from 43% to 100% in the intervention group and 24% to 80% in the control group. The remaining three RCTs used cryopreserved umbilical cord-derived MSCs (^{Cryo}UC-MSCs)[19-

Table 1 Baseline characteristics of randomized clinical trials with cryopreserved human umbilical cord-derived mesenchymal stem cells for heart disease, *n* (%)

Ref.		He *et al*[20], 2020, China	Bartolucci *et al*[21], 2017, Chile	Ulus *et al*[19], 2020, Turkey
Study type		RCT	RCT	Open-label RCT
Phase		I	I/II	I/II
Condition		MI	HF	MI
Sample size	Total	50	30	41
	Intervention (% male)	35 (71.42)	15 (80.0)	25 (100)
	Control (% male)	15 (46.67)	15 (93.3)	16 (100)
Age (mean ± SD)	Intervention	61 ± 8.2	57.33 ± 10.05	61.8 ± 10
	Control	65.2 ± 7.9	57.20 ± 11.64	65.3 ± 6.8
BMI (mean ± SD)	Intervention	25 ± 3.35	29.12 ± 2.88	26.5 ± 4.5
	Control	23.59 ± 2.28	29.52 ± 4.00	26.6 ± 4.8
Number of smokers	Intervention	11 (31.43)	7 (46.7)	21 (84)
	Control	3 (25.0)	4 (26.7)	15 (88.2)
HTN	Intervention	24 (68.57)	7 (46.7)	15 (60)
	Control	9 (75.0)	8 (53.3)	11 (64.7)
DM	Intervention	12 (34.29)	5 (33.3)	16 (66.7)
	Control	8 (66.7)	7 (46.7)	9 (52.9)
NYHA; I (*n*), II (*n*), III (*n*), IV (*n*)	Intervention	III (4/8), IV (12/8)	N/S: 2.03 ± 0.61	N/S: 1.9 ± 0.44
	Control	III (7) IV (5)	N/S: 1.67 ± 0.49	N/S: 2.1 ± 0.37
Comparison		CABG only	Placebo	CABG only
Follow-up		3, 6, and 12 months	3, 6, and 12 months	1, 3, 6, and 12 months
Assessment modality (yes/no)	ECG	No	Yes	Yes
	Echo	No	Yes	Yes
	MRI	Yes (CMR)	Yes (CMR)	Yes
	Cardiac CT	No	No	No
	SPECT	No	No	Yes
Measured outcomes		Serious adverse events at 12 months (primary), the efficacy of hUC-MSCs and collagen scaffold assessed according to the CV-CMR–based LVEF and infarct size at 3, 6, and 12 months after treatment, and NYHA (secondary)	Safety: Adverse events after IV infusion -/-. Efficacy: Primary, changes in LVEF, LVESV & LVEDV by Echo; LVEF, LVESV, and LVEDV by CMR; NYHA score (secondary)	LVEF, LV remodeling, myocardial mass, 6MWD, NYHA score change

RCT: Randomized controlled trial; MI: Myocardial infarction; HF: Heart failure; BMI: Body mass index; HTN: Hypertension; DM: Diabetes mellitus; NYHA: New York Heart Association; N/S: Not specified; CABG: Coronary artery bypass graft; ECG: Electrocardiogram; MRI: Magnetic resonance imaging; CT: Computed tomography; SPECT: Single-photon emission computed tomography; CMR: Cardiac magnetic resonance; hUC-MSCs: Human umbilical cord-derived mesenchymal stem cells; LV: Left ventricle; LVEF: Left ventricular ejection fraction; LVESV: Left Ventricular end-systolic volume; LVEDV: Left ventricular end-diastolic volume; 6MWD: Six-minute walk distance.

21] with 121 patients, 75 in the intervention group and 46 in the control group. The percentage of male participants in the UC-MSCs studies ranged from 71% to 100% in the intervention group and 46% to 100% in the control groups. The included studies were published between 2009 and 2020 and were conducted across several countries: One each in India [16], Turkey[19], China[20], and Chile[21], while three RCTs were conducted in the United States[15,17,18]. The route of cell delivery varied among the included studies. Four studies employed the intramyocardial route[15,18-20], while the remaining three used the intravenous route[16,17,21].

In the included studies, the control group received a placebo treatment besides standard pharmacological or adjunct surgical intervention. For example, in three studies[15,18,21], the control group also received standard heart failure therapy, including beta blockers, angiotensin-converting enzyme inhibitors, angiotensin II receptor blockers, or

Table 2 Baseline characteristics of randomized clinical trials with cryopreserved human bone marrow mesenchymal stem cells for heart disease, *n* (%)

Ref.		Chullikana *et al*[16], 2015, India	Hare *et al*[17], 2009, United States	Bolli *et al*[15], 2020, United States	Perin *et al*[18], 2015, United States
Study type		RCT	RCT	RCT	RCT
Phase		I/II	I	I	II
Condition		MI	MI	HF	HF
Sample size	Total	20	53	31	60
	Intervention (% male)	10 (100)	34 (82.4)	14 (43)	45 (97.8)
	Control (% male)	10 (80)	19 (78.9)	17 (24)	15 (73.3)
Age (mean ± SD)	Intervention	47.31 ± 12.10	59 ± 12.3	54.7 ± 12.8	62.2 ± 10.3
	Control	47.79 ± 6.48	55 ± 10.2	58.2 ± 11.2	62.7 ± 11.2
BMI (mean ± SD)	Intervention	23.32 ± 3.74	29.8 ± 6.7	30.2 ± 9.0	29.8 ± 4.1
	Control	24.86 ± 1.88	30.3 ± 4.3	30.4 ± 6.5	31.3 ± 9.2
Number of smokers	Intervention	N/A	3 (8.8)	5 (36)	7 (15.6)
	Control	N/A	2 (10.5)	3 (18)	2 (13.3)
HTN	Intervention	N/A	16 (17.6)	6 (43)	29 (64.4)
	Control	N/A	9 (47.4)	10 (59)	9 (60)
DM	Intervention	N/A	6 (17.6)	3 (21)	13 (28.9)
	Control	N/A	1 (5.3)	5 (29)	2 (13.3)
NYHA; I (*n*), II (*n*), III (*n*), IV (*n*)	Intervention	N/A	N/A	II (13), III (1)	II (31), III (14)
	Control	N/A	N/A	II (13), III (4)	II (6), III (9)
Comparison		Placebo (multiple electrolytes injection)	Placebo	Placebo	Placebo
Follow-up, months		Six months till two years	Six months	6 and 12 months	3, 6, 12 months
Assessment modality (yes/no)	ECG	No	Yes	Yes	No
	Echo	Yes	Yes	No	Yes
	MRI	Yes	Yes	Yes (CMR)	No
	Cardiac CT	No	Yes	No	No
	SPECT	Yes	No	No	Yes
Measured outcomes		Adverse events, LVEF (Echo & SPECT), total perfusion score, and total volume of infarct	Safety, adverse events, LVEF (Echo), and 6MWD	Safety and feasibility of allogenic MSC administration in this population (primary). Effects of allogenic MSC administration on LV function (LVEF, LVEDV, LVESV, scar morphology) and functional status (6MWD, MLHFQ) (secondary)	Safety (primary), LV volume, LVEF, 6MWD (secondary)

RCT: Randomized controlled trial; MI: Myocardial infarction; HF: Heart failure; BMI: Body mass index; N/A: Not applicable; HTN: Hypertension; DM: Diabetes mellitus; NYHA: New York Heart Association; ECG: Electrocardiogram; MRI: Magnetic resonance imaging; CT: Computed tomography; SPECT: Single-photon emission computed tomography; CMR: Cardiac magnetic resonance; MSCs: Mesenchymal stem cells; LV: Left ventricle; LVEF: Left ventricular ejection fraction; LVESV: Left Ventricular end-systolic volume; LVEDV: Left ventricular end-diastolic volume; 6MWD: Six-minute walk distance; MLHFQ: Minnesota Living with Heart Failure Questionnaire.

aldosterone antagonists. In two studies[19,20], the control group underwent coronary artery bypass graft surgery, while in one study[16], the control group received percutaneous coronary intervention. The remaining study[17] did not provide specific information on the medications or procedures administered to the control group.

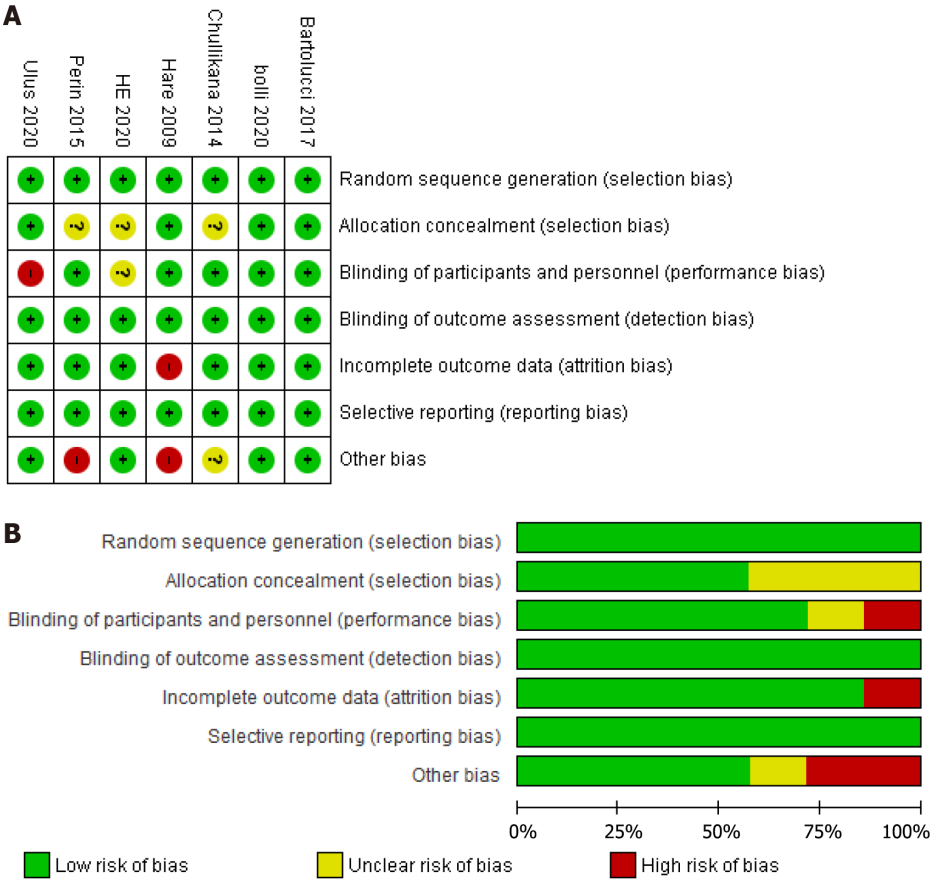

Figure 2 Risk of bias summary and graph. A: Risk of bias summary; B: Risk of bias graph. Symbols: (+) low risk of bias, (?) unclear risk of bias, (-) high risk of bias.

The functional outcome

LVEF: Seven studies[15-21] reported changes in LVEF after six months of ^{Cryo}MSCs-based treatment, including three studies[19-21] using UC-MSCs and four studies[15-18] using BM-MSCs. The pooled analysis showed a significant 2.11% improvement in LVEF in the MSC treatment groups compared to the control [WMD (95%CI) = 2.11 (0.66-3.56), P = 0.004, I^2 = 1%]. In the subgroup analysis by cell type, the pooled 6-month LVEF changes recorded a significant 3.53% increase in the UC-MSCs studies [WMD (95%CI) = 3.53 (1.38-5.67), P = 0.001, I^2 = 0%]. At the same time, the BM-MSCs treatment did not demonstrate any significant improvement compared to the control [WMD (95%CI) = 0.92 (-1.03 to 2.88), P = 0.35, I^2 = 0%] (Figure 3A). Seven studies measured the LVEF change before and after 12 months of ^{Cryo}MSCs treatment, including 3 UC-MSCs and 4 BM-MSCs studies. However, the pooled change in the treatment group was a 1.99% improvement compared to the control, which was not statistically significant [WMD (95%CI) = 1.99 (-0.02 to 3.99), P = 0.05, I^2 = 14%) (Figure 3B).

In the subgroup analysis based on post-thaw viability, the group with more than 80% post-thaw viable cells demonstrated a significant 3.44% increase in LVEF after six months of follow-up compared to the placebo group [WMD (95%CI) = 3.44 (1.46-5.43), P = 0.0007, I^2 = 0%]. On the contrary, the group with less than 80% post-thaw viable cells did not show a significant difference at six months [WMD (95%CI) = 0.37 (-2.89 to 2.14), P = 0.77, I^2 = 0%] (Figure 4A). Moreover, at the 12-month follow-up, neither the > 80% viable cell group nor the < 80% viable cell group showed any statistically significant improvement in LVEF compared to the control group [WMD (95%CI) = 2.25 (-1.36 to 5.86), P = 0.22, I^2 = 53%] and [WMD (95%CI) = 0.79 (-3.74 to 5.32), P = 0.73] respectively (Figure 4B).

6MWD test: The 6MWD test results were reported in four included studies, one involving UC-MSCs and three involving BM-MSCs. The pooled analysis demonstrated no significant difference in 6MWD between the MSCs group and control group [WMD (95%CI) = 20.73 (-3.40.10 to 44.86), P = 0.09, I^2 = 0%] for either the UC-MSCs studies [WMD (95%CI) = 28.36 (-37.10 to 93.82), P = 0.40] or the BM-MSCs studies [WMD (95%CI) = 19.53 (-6.43 to 45.49), P = 0.14, I^2 = 0%] (Figure 5A). Furthermore, the subgroup analysis according to cellular post-thaw viability demonstrated no significant difference in 6MWD between the intervention and control groups, regardless of whether the viable cells were > 80% [WMD (95%CI) = 14.15 (-33.31 to 61.60), P = 0.56, I^2 = 0%] or < 80% [WMD (95%CI) = 22.74 (-9.09 to 54.57), P = 0.16, I^2 = 22%] (Figure 5B).

The safety outcomes

Rehospitalization: The rehospitalization incidence was reported during the follow-up period in two UC-MSCs and two BM-MSCs studies. The analysis showed no significant reduction in the overall OR of rehospitalization [OR (95%CI) = 0.51 (0.20-1.28), P = 0.15, I^2 = 0%] for both UC-MSCs and BM-MSCs treated groups compared to the respective control groups

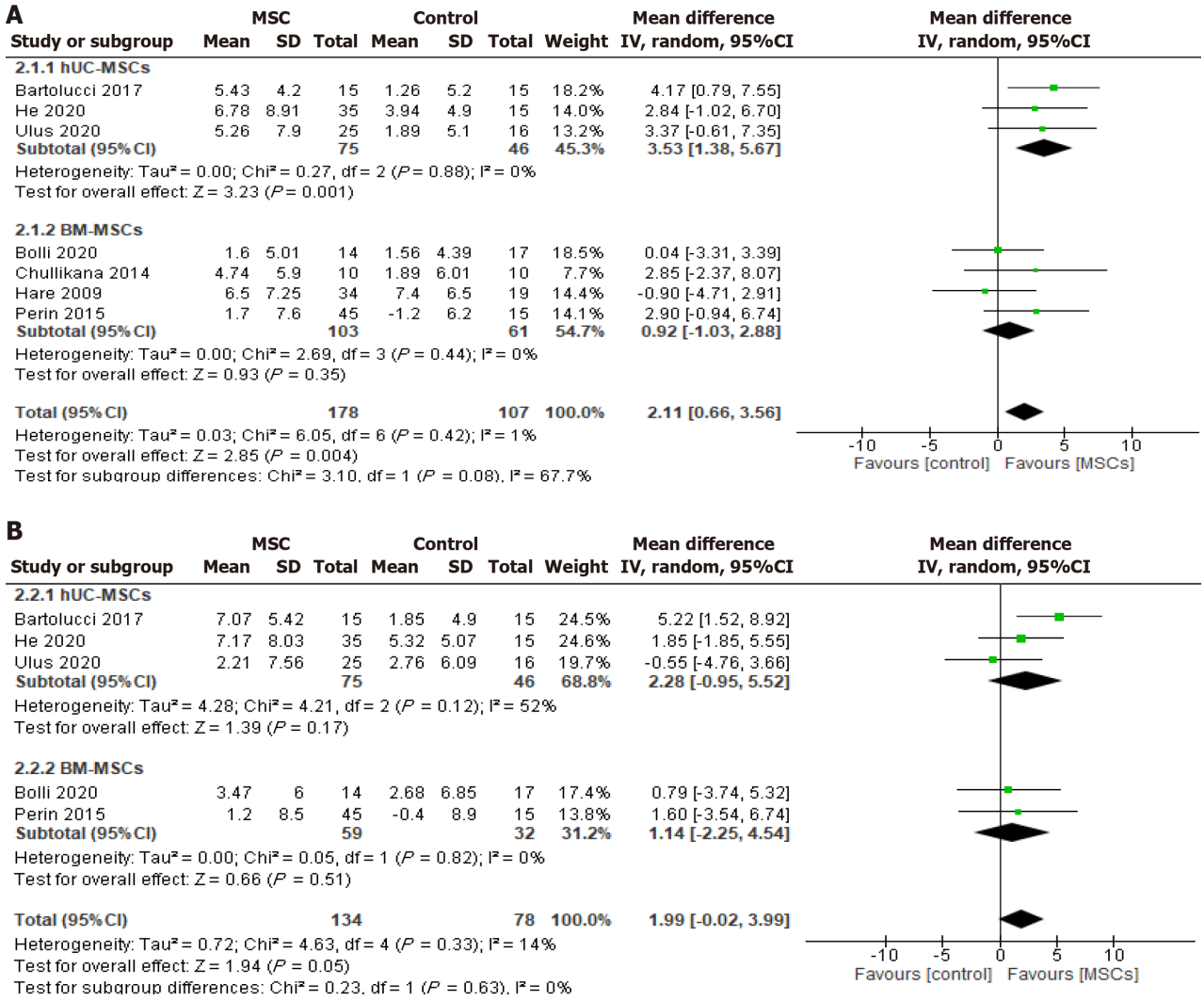

Figure 3 Effect of cryopreserved mesenchymal stem cell therapy on left ventricular ejection fraction sub-grouped according to cell source: Umbilical cord-derived mesenchymal stem cells and bone marrow-derived mesenchymal stem cells. A: Change from the baseline to six months of follow-up; B: Change from the baseline to twelve months of follow-up; hUC-MSC: Human umbilical cord-derived mesenchymal stem cell; BM-MSC: Bone marrow-derived mesenchymal stem cell.

[OR (95%CI) = 0.64 (0.09-4.72), P = 0.66, I^2 = 9%] and [OR (95%CI) = 0.47 (0.16-1.38), P = 0.17, I^2 = 0%] (Figure 6A).

Mortality: Two UC-MSCs RCTs and three BM-MSCs RCTs reported mortality from the included RCTs (Figure 6B). There were no significant differences in the OR of mortality between the intervention group and control group with either UC-MSCs studies [OR (95%CI) = 0.79 (0.10-5.95), P = 0.82, I^2 = 0%] and BM-MSCs studies [OR (95%CI) = 0.64 (0.17-2.35), P = 0.50, I^2 = 0%].

MACEs

Six included studies reported the incidence of MACE, 2 UC-MSCs studies, and 4 BM-MSCs studies, such as ventricular tachycardia, supraventricular tachycardia, and angina and revascularization of myocardial infarction. The pooled analysis did not show a statistically significant difference in the overall MACE [OR (95%CI) = 0.80 (0.39-1.67), P = 0.56, I^2 = 0%] between the [Cryo]MSCs and the control group. Similarly, no statistically significant effect was seen when sub-grouping into UC-MSCs and BM-MSCs compared to the control [OR (95%CI) = 0.90 (0.24-3.33), P = 0.87, I^2 = 0%] and [OR (95%CI): 0.72 (0.24-2.12), P = 0.55, I^2 = 29%] respectively (Figure 6C).

The effect of cellular post-thaw viability on adverse events

Based on cellular post-thaw viability, a subgroup analysis was conducted on adverse events, including rehospitalization, mortality, and MACE. The analysis found no significant differences between the MSCs and the control groups for either the > 80% viable cells or < 80% viable cells groups regarding rehospitalization, mortality, or MACE (Figure 7).

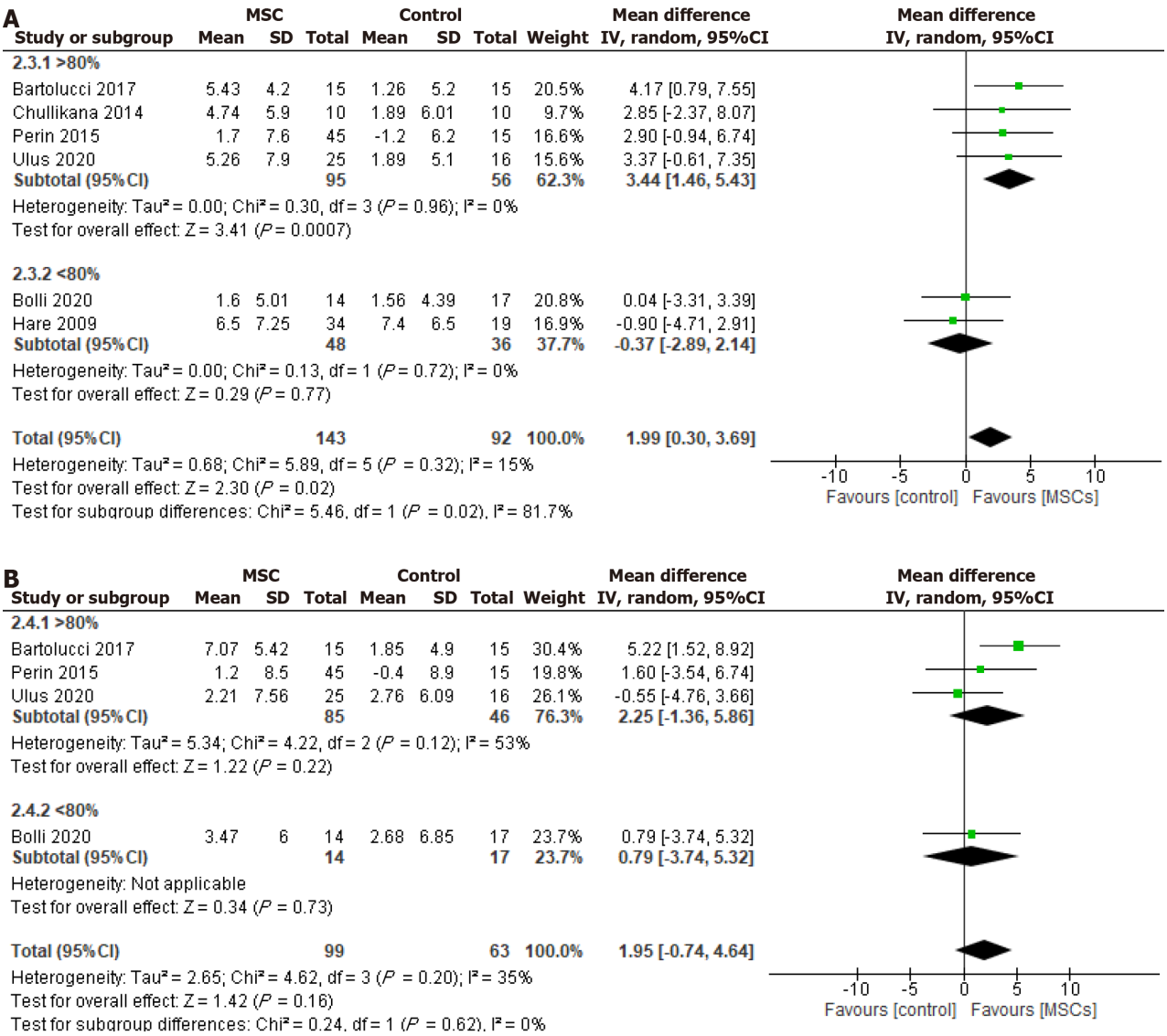

Figure 4 Effect of cryopreserved mesenchymal stem cell therapy on left ventricular ejection fraction sub-grouped according to cellular post-thaw viability as > 80% and < 80%. A: Change from the baseline to 6 mo of follow-up; B: Change from the baseline to 12 mo of follow-up. MSC: Mesenchymal stem cell; CI: Confidence interval.

DISCUSSION

Our systematic review and meta-analysis are aimed at evaluating the safety and efficacy of the ^{Cryo}MSCs for treating patients with myocardial infarction and heart failure. The significant findings of our study are: (1) ^{Cryo}MSC treatment resulted in an overall 2.11% improvement in LVEF during 6 mo of follow-up compared to the control group; (2) The LVEF improvement was higher when using UC-MSCs or ^{Cryo}MSCs with more than 80% post-thaw viability; (3) The functional benefits of treatment with ^{Cryo}MSCs were not sustained during the 12-mo follow-up; (4) Treatment with ^{Cryo}MSCs did not result in a statistically significant improvement of the 6MWD test compared to control; (5) Treatment with ^{Cryo}MSCs was safe, as there was no significant difference in the incidence of MACE compared to the control group; and (6) No significant effects on mortality and readmission were observed in the ^{Cryo}MSC group compared to the control group.

Unlike conventional drugs, which are mostly natural or synthetic, and modern-day biologics, which are substances of biological origin, pharmacology has advanced to the next generation of drugs: The living biodrugs, *i.e.*, a novel fast-emerging group of medications for which product viability is a primary requirement. Depending upon their subsequent therapeutic application, living biodrugs can also be genetically modified to enhance their efficacy, such as chimeric antigen receptors-T cells nick-named TRUCKs and hematopoietic progenitor cells-based Food and Drug Administration-approved products (Allocord, Hemacord, Ducord, *etc*)[22]. MSCs are novel living biodrugs that may be used naïve or modified to deliver transgenes and drugs as payloads[23]. Logistic considerations for living biodrugs, especially off-the-shelf ready-to-use availability, differ from conventional pharmaceuticals and impede their clinical progress. Firstly, such an arrangement will mainly necessitate an allogenic source of cells. Although the published clinical data supports the use of allogenic MSCs on par with their autologous counterparts[24,25], the donor-related factors affecting their biology and functional heterogeneity, especially for long-term benefits, add to the potential uncertainty about their clinical outcome

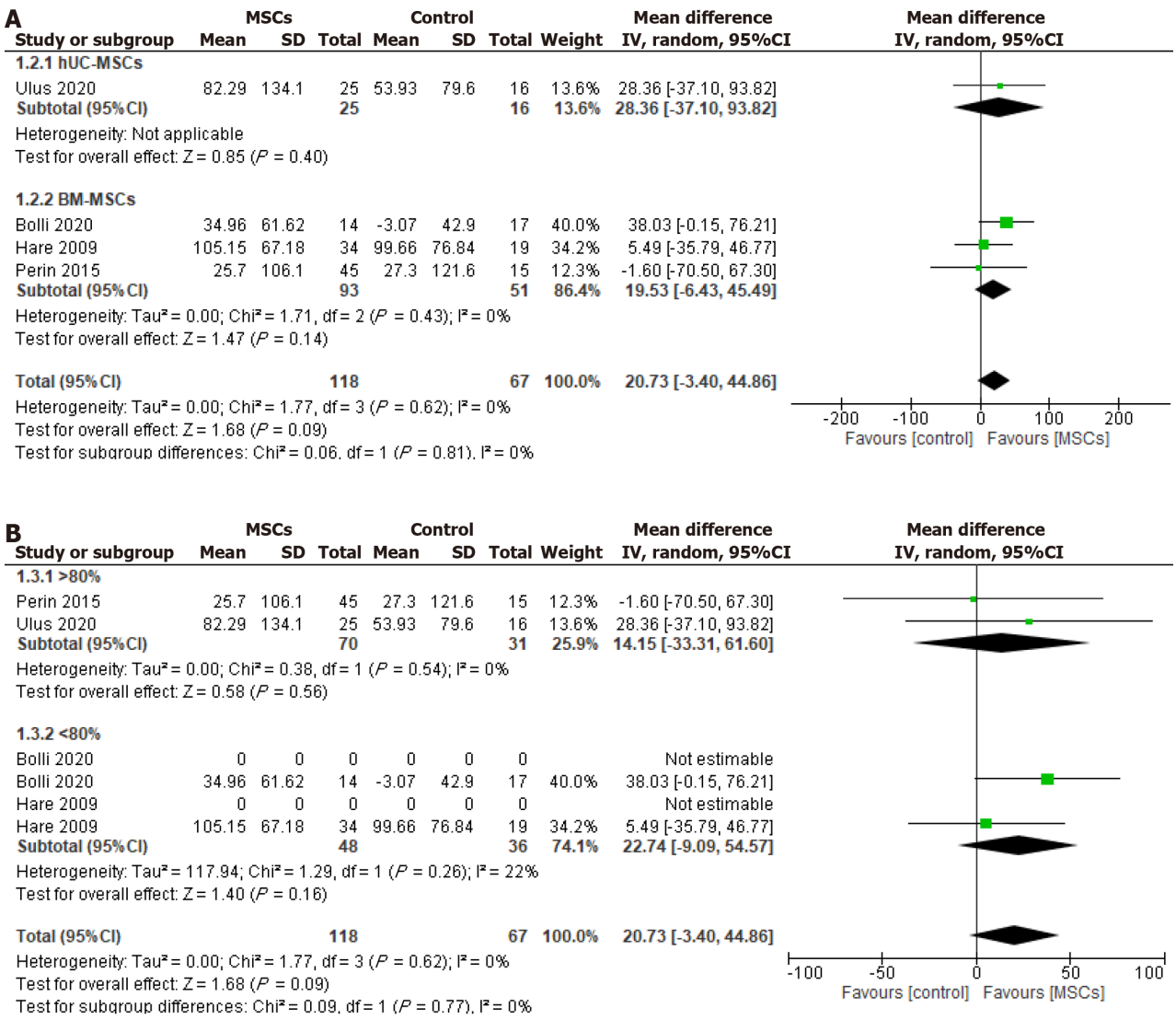

Figure 5 Effect of cryopreserved mesenchymal stem cell therapy on 6 min walk distance sub-grouped according to cell source. A and B: Umbilical cord-derived mesenchymal stem cells (A) and bone marrow-derived mesenchymal stem cells (B) cellular post-thaw viability as > 80% and < 80%. MSC: Mesenchymal stem cell; CI: Confidence interval; hUC-MSC: Human umbilical cord-derived mesenchymal stem cell; BM-MSC: Bone marrow-derived mesenchymal stem cell.

[26]. Their cryopreservation increases the uncertainty regarding their post-transplantation performance.

The factors affecting the safety and efficacy of cryopreserved cells encompass almost everything from tissue source[27] and cryo-banking to thawing and delivery. For example, whether the cryopreserved cells post-thaw be cultured or used directly after washing to remove the cryoprotectant remains an important consideration. Similarly, their viability post-thaw is critical to their safety and efficacy. The current study represents the first evaluation of ^{Cryo}MSCs' efficacy in patients with CVD and reveals a notable connection between MSCs viability post-thawing and their impact on LVEF. A subgroup analysis based on MSC type and post-thaw viability showed that treatment with UC-MSCs resulted in a significant 3.53% improvement in LVEF during 6 mo of follow-up compared to the control group. On the contrary, no significant LVEF change was observed after treatment with BM-MSCs. It is essential to mention that neither cell type significantly impacted the 12-mo follow-up, although UC-MSCs demonstrated better efficacy. The considerable variations in LVEF improvement observed between MSCs from two tissue sources may be attributed to the relatively primitive nature of UC-MSCs compared to the BM-MSCs[5,27]. These are significant findings as UC-MSCs, with their better efficacy, primitive nature, and non-invasive availability, are being widely cryopreserved to ensure ready-to-use obtainability. The preclinical studies support these data to indicate that MSCs isolated from healthy donors and cryopreserved in liquid nitrogen for extended periods can sustain their biology and stemness characteristics, *i.e.*, paracrine signaling, differentiation potential, and proliferation capabilities[10,28]. This underscores the potential of UC-MSCs for future cryopreservation efforts, instilling a sense of optimism and hope for further research and development.

Changes in LVEF remain a significant predictor of prognosis in heart failure patients. Previous studies have shown that the hazard ratio for all-cause mortality increases by 39% for every 10% reduction in LVEF below 45%[29]. Despite this, relatively few studies have assessed the effectiveness of heart failure medications in improving LVEF. One study demonstrated that beta-blocker treatment led to an LVEF improvement of 4% to 4.9% in patients with a baseline LVEF below 40% and 1.9% in those with a baseline LVEF between 40% and 50%[30]. Another study on the impact of renin-

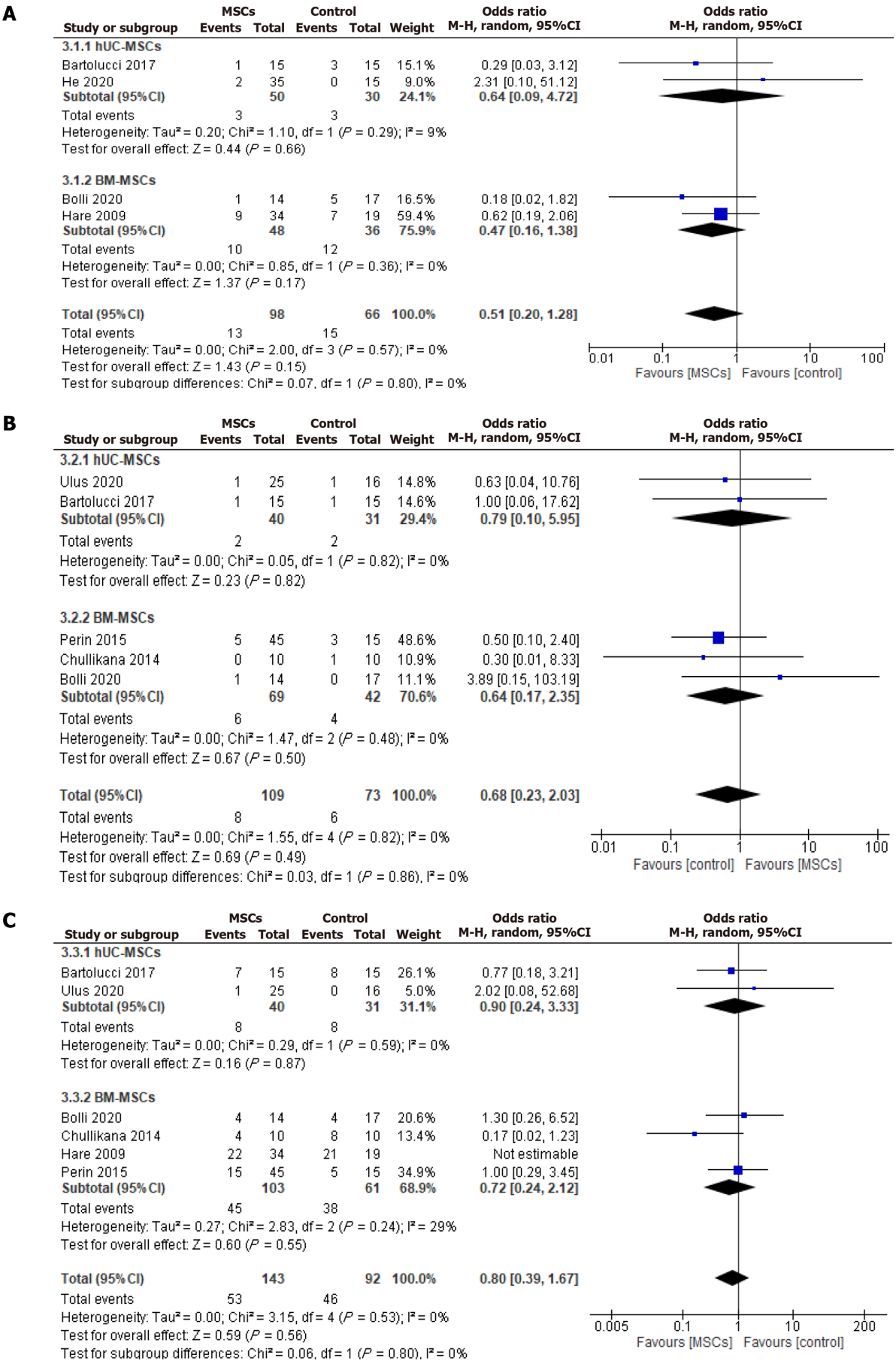

Figure 6 Odds ratio of the safety outcomes. A: Rehospitalization; B: Mortality; C: Major adverse cardiac events. MSC: Mesenchymal stem cell; CI: Confidence interval; hUC-MSC: Human umbilical cord-derived mesenchymal stem cell; BM-MSC: Bone marrow-derived mesenchymal stem cell.

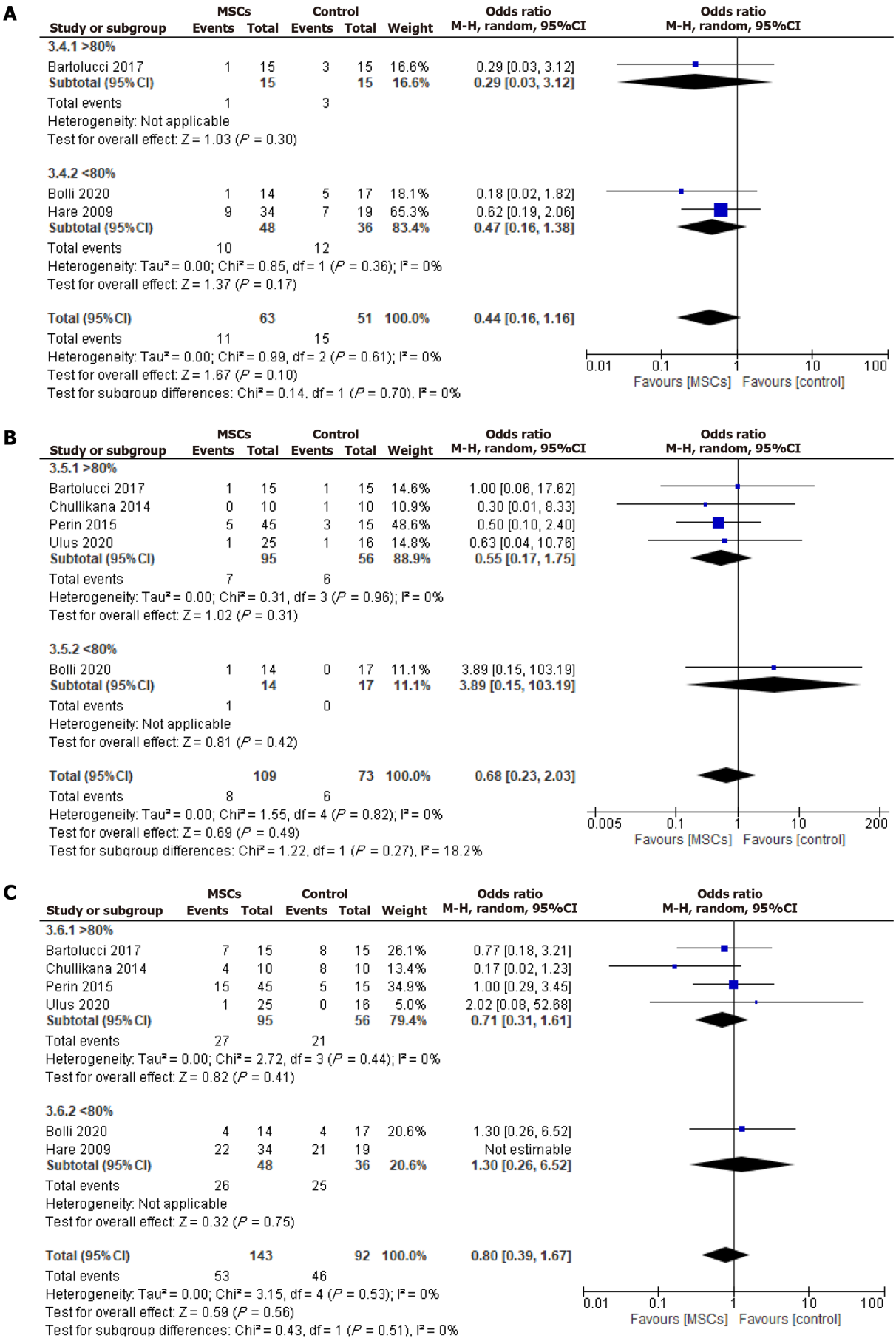

Figure 7 Odds ratio of the safety outcomes sub-grouped according to post-thaw cellular viability. A: Rehospitalization; B: Mortality; C: Major adverse cardiac events. MSC: Mesenchymal stem cell; CI: Confidence interval.

angiotensin system inhibition in heart failure with preserved LVEF found a significant LVEF improvement (2.18%) after treatment[31]. Based on this evidence, the improvements observed in our analysis with ^{Cryo}MSCs appear promising. However, it is important to note that in three of the included studies, both the intervention and control groups received standard therapy (*e.g.*, beta blockers and/or renin-angiotensin system inhibitors). Consequently, we found that treatment with ^{Cryo}MSCs resulted in a more sustained and pronounced improvement in LVEF compared to those receiving standard therapy alone. Moreover, it is difficult to delineate the effects of cell therapy from those of standard therapy during concomitant treatment.

The lack of sustained treatment effects with ^{Cryo}MSCs after 12 months suggests that a single dose is insufficient for long-term cardiac improvement, and administering a second dose may sustain long-term outcomes. Possible explanations for the lack of sustained long-term effects include the progressive nature of heart failure, which often worsens insidiously due to the underlying neurohormonal imbalance and endothelial dysfunction, even in the absence of overt clinical symptoms[32]. Secondly, the permanence of the long-term therapeutic benefits may require the sustenance of the cell graft. Loss of cell graft may contribute to the loss of therapeutic benefits, which can be benefited by repeated cell administration until the recovery from heart failure is reached. Moreover, some studies have employed intravenous administration of cells, which offers advantages such as safety, ease of administration, and lower cost than intracoronary or intramyocardial routes. Although these alternative routes may be more effective, there is a need for specialized centers and a 1%-2% risk of complications like perforation and tamponade that hamper their routine application. Intravenous administration is associated with lower engraftment, which can limit the therapeutic benefits, especially when a single dose is used[33]. Lastly, due to the clinical trial design of the included studies, labeling the injected cells and tracking their migration to the myocardium proved challenging[17]. These factors underscore the potential advantages of administering multiple doses over time. A recent study by Attar *et al*[34] showed that administering repeated MSC doses led to a 4% improvement in LVEF at 6 months compared to a single dose. Although there is no data on a second dose administered after 6 mo for myocardial infarction or heart failure patients, studies have shown that a second dose given 6 months after the first can lead to significant functional improvements in knee osteoarthritis patients compared to a single dose[35,36]. These findings emphasize the potential of repeated MSC doses at various intervals to optimize treatment in cardiac patients, sparking further interest and research. We did not find a significant difference in the adverse cardiac events between the ^{Cryo}MSCs and the control groups, suggesting the clinical safety of the cryopreserved cells. However, the included RCTs lack details regarding the cryopreservation methods, underscoring the need for further research.

Our study results were limited by the relatively small number of RCTs and the small sample size in the included RCTs. Another significant limitation of our study is the absence of RCTs that directly assess the clinical effectiveness of ^{Cryo}MSCs. Given the topic's significance, it is strongly recommended that future clinical studies explore this area further. Hence, there is a pressing need for more extensive RCTs to validate these findings and establish standardized cell preservation protocols. This urgent need for further research underscores the importance of our findings and the potential impact on cardiology and regenerative medicine.

CONCLUSION

In conclusion, our systematic review of the literature's meta-analysis reveals that ^{Cryo}MSCs significantly improved LVEF by an average of 2.11%, with superior outcomes observed when employing ^{Cryo}MSCs with post-thaw viability exceeding 80%. Furthermore, the safety profile of ^{Cryo}MSCs did not show a significant incidence of adverse events compared to the control. This suggests that ^{Cryo}MSCs hold promise as a viable cell product for off-the-shelf use in patients with CVD, offering a positive outlook for the future of this treatment[37]. This promising outlook should encourage further research and development in this area.

FOOTNOTES

Author contributions: Haider KH designed and produced the study and its methodology; Safwan M and Bourgleh MS performed database research and screened the extracted records against eligibility criteria, performed the data extraction and plotted and validated the extracted data, performed the quality assessment of the included trials, and conducted the statistical analysis; Safwan M and Haider KH drafted the first manuscript; Safwan M, Bourgleh MS, and Haider KH reviewed the final manuscript; and all the authors contributed to the final manuscript. All authors have read and agreed to the published version of the manuscript.

Conflict-of-interest statement: The authors report no relevant conflicts of interest for this article.

PRISMA 2009 Checklist statement: The authors have read the PRISMA 2009 Checklist, and the manuscript was prepared and revised according to the PRISMA 2009 Checklist.

Country of origin: Saudi Arabia

ORCID number: Khawaja Husnain Haider 0000-0002-7907-4808.

S-Editor: Wang JJ
L-Editor: Filipodia
P-Editor: Zhao S

REFERENCES

1 **World Health Organization**. Cardiovascular diseases (CVDs). [cited 15 August 2024]. Available from: https://www.who.int/news-room/fact-sheets/detail/cardiovascular-diseases-(cvds)

2 **Vaduganathan M**, Mensah GA, Turco JV, Fuster V, Roth GA. The Global Burden of Cardiovascular Diseases and Risk: A Compass for Future Health. *J Am Coll Cardiol* 2022; **80**: 2361-2371 [PMID: 36368511 DOI: 10.1016/j.jacc.2022.11.005]

3 **Kalou Y**, Al-Khani AM, Haider KH. Bone Marrow Mesenchymal Stem Cells for Heart Failure Treatment: A Systematic Review and Meta-Analysis. *Heart Lung Circ* 2023; **32**: 870-880 [PMID: 36872163 DOI: 10.1016/j.hlc.2023.01.012]

4 **Alvarez-Viejo M**, Haider KH (2022). Mesenchymal Stem Cells. In: Haider, K.H. (eds) Handbook of Stem Cell Therapy. Springer, Singapore. https://doi.org/10.1007/978-981-16-6016-0_6-12

5 **Mebarki M**, Abadie C, Larghero J, Cras A. Human umbilical cord-derived mesenchymal stem/stromal cells: a promising candidate for the development of advanced therapy medicinal products. *Stem Cell Res Ther* 2021; **12**: 152 [PMID: 33637125 DOI: 10.1186/s13287-021-02222-y]

6 **Guo Y**, Yu Y, Hu S, Chen Y, Shen Z. The therapeutic potential of mesenchymal stem cells for cardiovascular diseases. *Cell Death Dis* 2020; **11**: 349 [PMID: 32393744 DOI: 10.1038/s41419-020-2542-9]

7 **National Library of Medicine**. Search results for "mesenchymal stem cells". [cited 18 February 2025]. Available from: https://clinicaltrials.gov/search?intr=mesenchymal%20stem%20cells

8 **Zhou T**, Yuan Z, Weng J, Pei D, Du X, He C, Lai P. Challenges and advances in clinical applications of mesenchymal stromal cells. *J Hematol Oncol* 2021; **14**: 24 [DOI: 10.1186/s13045-021-01037-x]

9 **Linkova DD**, Rubtsova YP, Egorikhina MN. Cryostorage of Mesenchymal Stem Cells and Biomedical Cell-Based Products. *Cells* 2022; **11**: 2691 [PMID: 36078098 DOI: 10.3390/cells11172691]

10 **Bahsoun S**, Coopman K, Akam EC. The impact of cryopreservation on bone marrow-derived mesenchymal stem cells: a systematic review. *J Transl Med* 2019; **17**: 397 [PMID: 31783866 DOI: 10.1186/s12967-019-02136-7]

11 **Whaley D**, Damyar K, Witek RP, Mendoza A, Alexander M, Lakey JR. Cryopreservation: An Overview of Principles and Cell-Specific Considerations. *Cell Transplant* 2021; **30**: 963689721999617 [PMID: 33757335 DOI: 10.1177/0963689721999617]

12 **Page MJ**, McKenzie JE, Bossuyt PM, Boutron I, Hoffmann TC, Mulrow CD, Shamseer L, Tetzlaff JM, Akl EA, Brennan SE, Chou R, Glanville J, Grimshaw JM, Hróbjartsson A, Lalu MM, Li T, Loder EW, Mayo-Wilson E, McDonald S, McGuinness LA, Stewart LA, Thomas J, Tricco AC, Welch VA, Whiting P, Moher D. The PRISMA 2020 statement: An updated guideline for reporting systematic reviews. *Int J Surg* 2021; **88**: 105906 [PMID: 33789826 DOI: 10.1016/j.ijsu.2021.105906]

13 **Cumpston MS**, McKenzie JE, Welch VA, Brennan SE. Strengthening systematic reviews in public health: guidance in the Cochrane Handbook for Systematic Reviews of Interventions, 2nd edition. *J Public Health (Oxf)* 2022; **44**: e588-e592 [PMID: 35352103 DOI: 10.1093/pubmed/fdac036]

14 **Higgins JP**, Altman DG, Gøtzsche PC, Jüni P, Moher D, Oxman AD, Savovic J, Schulz KF, Weeks L, Sterne JA; Cochrane Bias Methods Group; Cochrane Statistical Methods Group. The Cochrane Collaboration's tool for assessing risk of bias in randomised trials. *BMJ* 2011; **343**: d5928 [PMID: 22008217 DOI: 10.1136/bmj.d5928]

15 **Bolli R**, Perin EC, Willerson JT, Yang PC, Traverse JH, Henry TD, Pepine CJ, Mitrani RD, Hare JM, Murphy MP, March KL, Ikram S, Lee DP, O'Brien C, Durand JB, Miller K, Lima JA, Ostovaneh MR, Ambale-Venkatesh B, Gee AP, Richman S, Taylor DA, Sayre SL, Bettencourt J, Vojvodic RW, Cohen ML, Simpson LM, Lai D, Aguilar D, Loghin C, Moyé L, Ebert RF, Davis BR, Simari RD; Cardiovascular Cell Therapy Research Network (CCTRN). Allogeneic Mesenchymal Cell Therapy in Anthracycline-Induced Cardiomyopathy Heart Failure Patients: The CCTRN SENECA Trial. *JACC CardioOncol* 2020; **2**: 581-595 [PMID: 33403362 DOI: 10.1016/j.jaccao.2020.09.001]

16 **Chullikana A**, Majumdar AS, Gottipamula S, Krishnamurthy S, Kumar AS, Prakash VS, Gupta PK. Randomized, double-blind, phase I/II study of intravenous allogeneic mesenchymal stromal cells in acute myocardial infarction. *Cytotherapy* 2015; **17**: 250-261 [PMID: 25484310 DOI: 10.1016/j.jcyt.2014.10.009]

17 **Hare JM**, Traverse JH, Henry TD, Dib N, Strumpf RK, Schulman SP, Gerstenblith G, DeMaria AN, Denktas AE, Gammon RS, Hermiller JB Jr, Reisman MA, Schaer GL, Sherman W. A randomized, double-blind, placebo-controlled, dose-escalation study of intravenous adult human mesenchymal stem cells (prochymal) after acute myocardial infarction. *J Am Coll Cardiol* 2009; **54**: 2277-2286 [PMID: 19958962 DOI: 10.1016/j.jacc.2009.06.055]

18 **Perin EC**, Borow KM, Silva GV, DeMaria AN, Marroquin OC, Huang PP, Traverse JH, Krum H, Skerrett D, Zheng Y, Willerson JT, Itescu S, Henry TD. A Phase II Dose-Escalation Study of Allogeneic Mesenchymal Precursor Cells in Patients With Ischemic or Nonischemic Heart Failure. *Circ Res* 2015; **117**: 576-584 [PMID: 26148930 DOI: 10.1161/CIRCRESAHA.115.306332]

19 **Ulus AT**, Mungan C, Kurtoglu M, Celikkan FT, Akyol M, Sucu M, Toru M, Gul SS, Cinar O, Can A. Intramyocardial Transplantation of Umbilical Cord Mesenchymal Stromal Cells in Chronic Ischemic Cardiomyopathy: A Controlled, Randomized Clinical Trial (HUC-HEART Trial). *Int J Stem Cells* 2020; **13**: 364-376 [PMID: 32840230 DOI: 10.15283/ijsc20075]

20 **He X**, Wang Q, Zhao Y, Zhang H, Wang B, Pan J, Li J, Yu H, Wang L, Dai J, Wang D. Effect of Intramyocardial Grafting Collagen Scaffold With Mesenchymal Stromal Cells in Patients With Chronic Ischemic Heart Disease: A Randomized Clinical Trial. *JAMA Netw Open* 2020; **3**: e2016236 [PMID: 32910197 DOI: 10.1001/jamanetworkopen.2020.16236]

21 **Bartolucci J**, Verdugo FJ, González PL, Larrea RE, Abarzua E, Goset C, Rojo P, Palma I, Lamich R, Pedreros PA, Valdivia G, Lopez VM, Nazzal C, Alcayaga-Miranda F, Cuenca J, Brobeck MJ, Patel AN, Figueroa FE, Khoury M. Safety and Efficacy of the Intravenous Infusion of Umbilical Cord Mesenchymal Stem Cells in Patients With Heart Failure: A Phase 1/2 Randomized Controlled Trial (RIMECARD Trial [Randomized Clinical Trial of Intravenous Infusion Umbilical Cord Mesenchymal Stem Cells on Cardiopathy]). *Circ Res* 2017; **121**: 1192-

1204 [PMID: 28974553 DOI: 10.1161/CIRCRESAHA.117.310712]

22 **Holzinger A**, Abken H. Treatment with Living Drugs: Pharmaceutical Aspects of CAR T Cells. *Pharmacology* 2022; **107**: 446-463 [PMID: 35696994 DOI: 10.1159/000525052]

23 **Litvinova LS**, Shupletsova VV, Khaziakhmatova OG, Daminova AG, Kudryavtseva VL, Yurova KA, Malashchenko VV, Todosenko NM, Popova V, Litvinov RI, Korotkova EI, Sukhorukov GB, Gow AJ, Weissman D, Atochina-Vasserman EN, Khlusov IA. Human Mesenchymal Stem Cells as a Carrier for a Cell-Mediated Drug Delivery. *Front Bioeng Biotechnol* 2022; **10**: 796111 [PMID: 35284410 DOI: 10.3389/fbioe.2022.796111]

24 **Omar T**. Ahmed OT, Ahmed ZT, Dairi AW, Zain Al-Abeden MS, Alkahlot MH, Alkahlot RH, Al Jowf GI, Eijssen LMT, Haider KH. The Inconclusive Superiority Debate of Allogeneic Vs. Autologous MSCs in Treating Patients with HFrEF: A Systematic Review and Meta-Analysis of RCTs. *Stem Cell Res Ther* 2025

25 **Li C**, Zhao H, Cheng L, Wang B. Allogeneic vs. autologous mesenchymal stem/stromal cells in their medication practice. *Cell Biosci* 2021; **11**: 187 [PMID: 34727974 DOI: 10.1186/s13578-021-00698-y]

26 **Safwan M**, Bourgleh MS, Alshakaki H, Molhem A, Haider KH (2024a). Morbid Cell Status and Donor Age Significantly Alter Mesenchymal Stem Cell Functionality and Reparability. In: K. H. Haider (ed.), Handbook of Stem Cell Applications, Springer Nature Singapore Pte Ltd., pp.1359-1387, 2024. https://doi.org/10.1007/978-981-99-7119-0_6227

27 **Safwan M**, Bourgleh MS, Aldoush M, Haider KH. Tissue-source effect on mesenchymal stem cells as living biodrugs for heart failure: Systematic review and meta-analysis. *World J Cardiol* 2024; **16**: 469-483 [PMID: 39221190 DOI: 10.4330/wjc.v16.i8.469]

28 **Bárcia RN**, Santos JM, Teixeira M, Filipe M, Pereira ARS, Ministro A, Água-Doce A, Carvalheiro M, Gaspar MM, Miranda JP, Graça L, Simões S, Santos SCR, Cruz P, Cruz H. Umbilical cord tissue-derived mesenchymal stromal cells maintain immunomodulatory and angiogenic potencies after cryopreservation and subsequent thawing. *Cytotherapy* 2017; **19**: 360-370 [PMID: 28040463 DOI: 10.1016/j.jcyt.2016.11.008]

29 **Solomon SD**, Anavekar N, Skali H, McMurray JJ, Swedberg K, Yusuf S, Granger CB, Michelson EL, Wang D, Pocock S, Pfeffer MA; Candesartan in Heart Failure Reduction in Mortality (CHARM) Investigators. Influence of ejection fraction on cardiovascular outcomes in a broad spectrum of heart failure patients. *Circulation* 2005; **112**: 3738-3744 [PMID: 16330684 DOI: 10.1161/CIRCULATIONAHA.105.561423]

30 **Cleland JGF**, Bunting KV, Flather MD, Altman DG, Holmes J, Coats AJS, Manzano L, McMurray JJV, Ruschitzka F, van Veldhuisen DJ, von Lueder TG, Böhm M, Andersson B, Kjekshus J, Packer M, Rigby AS, Rosano G, Wedel H, Hjalmarson Å, Wikstrand J, Kotecha D; Beta-blockers in Heart Failure Collaborative Group. Beta-blockers for heart failure with reduced, mid-range, and preserved ejection fraction: an individual patient-level analysis of double-blind randomized trials. *Eur Heart J* 2018; **39**: 26-35 [PMID: 29040525 DOI: 10.1093/eurheartj/ehx564]

31 **Fukuta H**, Goto T, Wakami K, Kamiya T, Ohte N. Effect of renin-angiotensin system inhibition on cardiac structure and function and exercise capacity in heart failure with preserved ejection fraction: a meta-analysis of randomized controlled trials. *Heart Fail Rev* 2021; **26**: 1477-1484 [PMID: 32562021 DOI: 10.1007/s10741-020-09969-1]

32 **Anand I**. Stable but Progressive Nature of Heart Failure: Considerations for Primary Care Physicians. *Am J Cardiovasc Drugs* 2018; **18**: 333-345 [PMID: 29761293 DOI: 10.1007/s40256-018-0277-0]

33 **Traverse JH**. Is There a Role for Intravenous Stem Cell Delivery in Nonischemic Cardiomyopathy? *Circ Res* 2017; **120**: 256-258 [PMID: 28104762 DOI: 10.1161/CIRCRESAHA.116.310342]

34 **Attar A**, Farjoud Kouhanjani M, Hessami K, Vosough M, Kojuri J, Ramzi M, Hosseini SA, Faghih M, Monabati A. Effect of once versus twice intracoronary injection of allogeneic-derived mesenchymal stromal cells after acute myocardial infarction: BOOSTER-TAHA7 randomized clinical trial. *Stem Cell Res Ther* 2023; **14**: 264 [PMID: 37740221 DOI: 10.1186/s13287-023-03495-1]

35 **Matas J**, Orrego M, Amenabar D, Infante C, Tapia-Limonchi R, Cadiz MI, Alcayaga-Miranda F, González PL, Muse E, Khoury M, Figueroa FE, Espinoza F. Umbilical Cord-Derived Mesenchymal Stromal Cells (MSCs) for Knee Osteoarthritis: Repeated MSC Dosing Is Superior to a Single MSC Dose and to Hyaluronic Acid in a Controlled Randomized Phase I/II Trial. *Stem Cells Transl Med* 2019; **8**: 215-224 [PMID: 30592390 DOI: 10.1002/sctm.18-0053]

36 **Freitag J**, Bates D, Wickham J, Shah K, Huguenin L, Tenen A, Paterson K, Boyd R. Adipose-derived mesenchymal stem cell therapy in the treatment of knee osteoarthritis: a randomized controlled trial. *Regen Med* 2019; **14**: 213-230 [PMID: 30762487 DOI: 10.2217/rme-2018-0161]

37 **Yong KW**, Wan Safwani WK, Xu F, Wan Abas WA, Choi JR, Pingguan-Murphy B. Cryopreservation of Human Mesenchymal Stem Cells for Clinical Applications: Current Methods and Challenges. *Biopreserv Biobank* 2015; **13**: 231-239 [PMID: 26280501 DOI: 10.1089/bio.2014.0104]

World Journal of Stem Cells

Submit a Manuscript: https://www.f6publishing.com

World J Stem Cells 2025 March 26; 17(3): 101376

DOI: 10.4252/wjsc.v17.i3.101376

ISSN 1948-0210 (online)

LETTER TO THE EDITOR

Cyclodextrin host-guest complex to facilitate sinomenine-based osteoporosis therapy

Meng-Qin Guo, Ping Hu, Zheng-Wei Huang

Specialty type: Cell and tissue engineering

Provenance and peer review: Unsolicited article; Externally peer reviewed.

Peer-review model: Single blind

Peer-review report's classification
Scientific Quality: Grade B
Novelty: Grade B
Creativity or Innovation: Grade B
Scientific Significance: Grade B

P-Reviewer: He HS

Received: September 12, 2024
Revised: December 9, 2024
Accepted: March 6, 2025
Published online: March 26, 2025
Processing time: 189 Days and 21.1 Hours

Meng-Qin Guo, Ping Hu, Zheng-Wei Huang, College of Pharmacy, Jinan University, Guangzhou 511443, Guangdong Province, China

Co-corresponding authors: Ping Hu and Zheng-Wei Huang.

Corresponding author: Zheng-Wei Huang, PhD, Associate Professor, College of Pharmacy, Jinan University, No. 855 East Xingye Dadao, Panyu District, Guangzhou 511443, Guangdong Province, China. huangzhengw@jnu.edu.cn

Abstract

Xiao *et al* reported on the natural product sinomenine (SIN), which is a traditional Chinese medicine for treating osteoporosis *via* its modulation of autophagy; however, SIN was dissolved in dimethyl sulfoxide prior to administration, which is not conducive to the development of clinical injectables. By comparing solubilization techniques, including amorphisation, emulsification, micellisation, nanocrystallisation and host-guest inclusion, we found that the solubilization of SIN by host-guest inclusion can enhance solubility and improve stability and has an increased release rate and enhanced bioavailability. Therefore, we conclude that host-guest inclusion holds promise for SIN solubilization. To solubilise SIN, we selected β-cyclodextrin as the host agent considering its excellent biocompatibility, efficient encapsulation ability, mature preparation process and adequate drug stability. If the prerequisites of SIN-β-cyclodextrin complexes in terms of safety, efficacy, stability and the relevant laws and regulations are met, its clinical application for the treatment of osteoporosis may be achieved.

Key Words: Sinomenine; Cyclodextrin; Osteoporosis; Autophagy; Solubilization

Core Tip: Sinomenine (SIN) inhibits phosphorylation processes in the phosphatidylinositol 3-kinase/protein kinase B/mammalian target of the rapamycin pathway, increases autophagic capacity and promotes osteogenic differentiation, hence effectively treating osteoporosis. Nevertheless, the insolubility of SIN is a limitation to its clinical application. Here, we proposed the use of host-guest inclusion instead of dimethyl sulfoxide (DMSO) to solubilise SIN by preparing SIN-β-cyclodextrin complexes. Compared with direct dissolution in DMSO, the SIN-β-cyclodextrin complexes circumvent the safety concerns associated with DMSO, providing higher water solubility, improved drug stability, lower toxicity and side effects and optimal drug release properties. We conclude the clinical application of SIN-β-cyclodextrin complexes to treat osteoporosis may be achieved.

Citation: Guo MQ, Hu P, Huang ZW. Cyclodextrin host-guest complex to facilitate sinomenine-based osteoporosis therapy. *World J Stem Cells* 2025; 17(3): 101376
URL: https://www.wjgnet.com/1948-0210/full/v17/i3/101376.htm
DOI: https://dx.doi.org/10.4252/wjsc.v17.i3.101376

TO THE EDITOR

Xiao *et al*[1] reported on the anti-osteoporosis activity of the natural product sinomenine (SIN), which is a traditional Chinese medicine. The major underlying mechanism of SIN involves the inhibition of phosphorylation of the phosphatidylinositol 3-kinase/protein kinase B/mammalian target of the rapamycin signalling pathway in bone marrow mesenchymal stromal cells, which increases the autophagic capacity and promotes osteogenic differentiation. Bone loss antagonism, osteogenic differentiation promotion, autophagy induction and phosphatidylinositol 3-kinase/protein kinase B/mammalian target of the rapamycin inhibition were assessed. The overall outline of this work is shown in Figure 1 (modified from the original work).

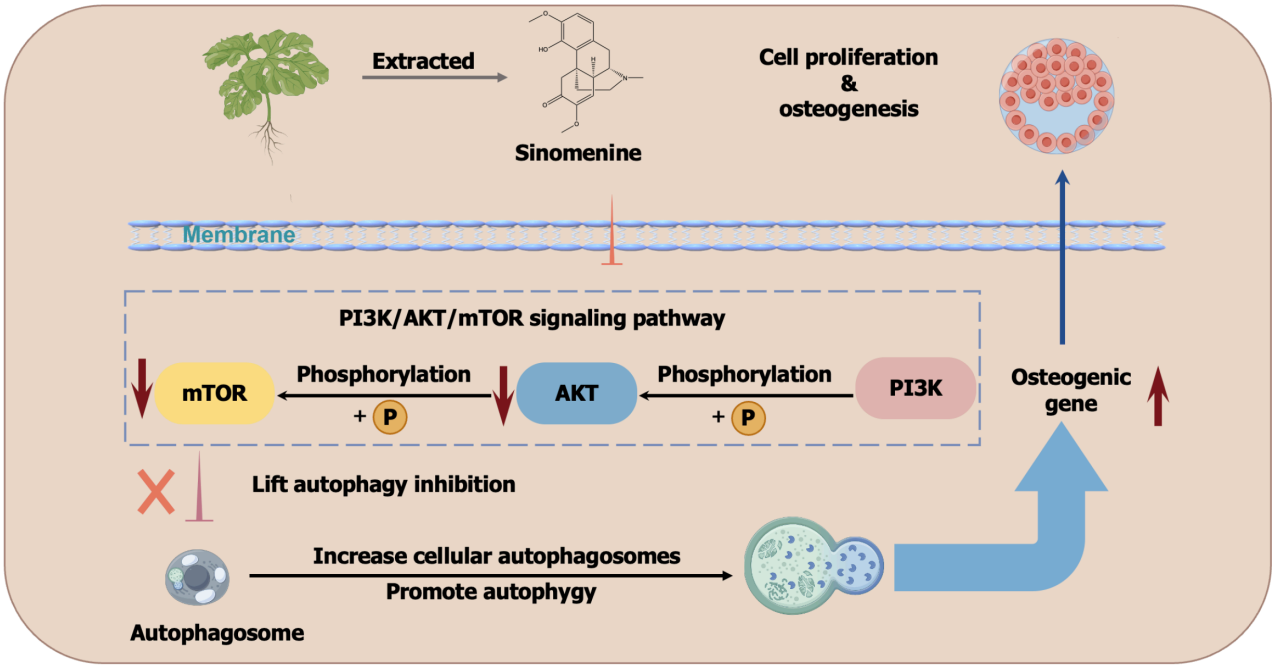

Figure 1 Scheme of the study by Xiao *et al*[1]. This figure is modified from the original work[1]. mTOR: Mammalian target of the rapamycin; AKT: Protein kinase B; PI3K: Phosphatidylinositol 3-kinase.

It is important to consider the delivery of SIN to bone marrow mesenchymal stromal cells or ovariectomised mice in the original study. Based on the methodology, SIN was dissolved in dimethyl sulfoxide (DMSO) and subsequently diluted to the required concentration for injection. In animal studies, the resulting SIN solution was administrated *via* intraperitoneal injection. For clinical application, intraperitoneal injection must be modified to intravenous or intramuscular injection. A more challenging problem is that DMSO-containing solvents are not favourable for developing an injection formulation because it has several safety concerns. First, DMSO is highly permeable in the mucous membranes[2]. For injectable formulations, DMSO may be utilised for other ingredients, which include potentially harmful impurities, into the body along with it, thus increasing the risk of side effects or unpredictable systemic reactions.

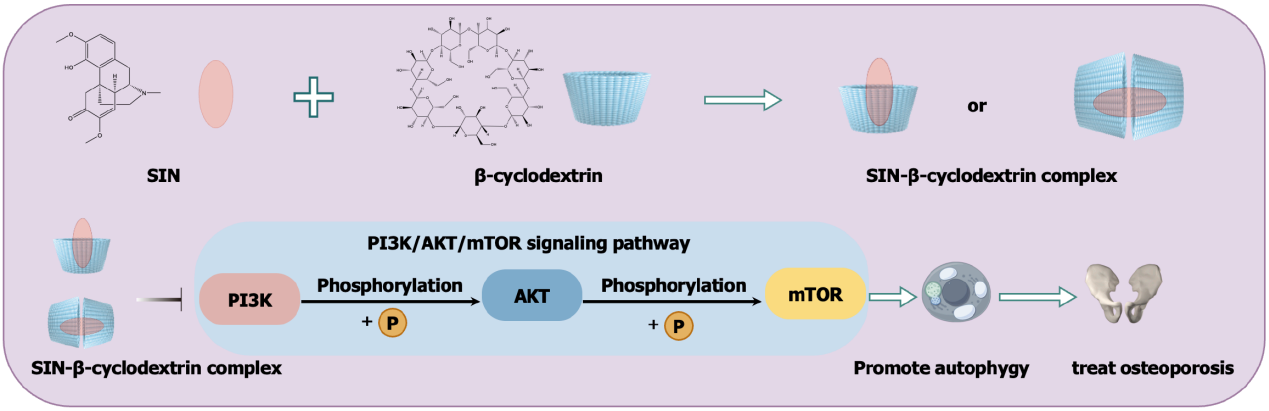

Figure 2 Illustration of the scheme to solubilise sinomenine with β-cyclodextrin and its application. SIN: Sinomenine; mTOR: Mammalian target of the rapamycin; AKT: Protein kinase B; PI3K: Phosphatidylinositol 3-kinase.

Second, DMSO irritates the skin and mucous membranes and may cause discomfort or inflammation at the injection site [3]. Such irritation renders the use of the injection unsuitable or unsafe. Third, DMSO may react with other components from the injectables to affect the stability and potency of the drug. For instance, it may cause chemical degradation of the drug[4]. The reason for using DMSO by Xiao *et al*[1] was that SIN showed a low water solubility[5] and dissolving it in DMSO could achieve higher solubility. We have developed alternative techniques to solubilise SIN in water, which can avoid the use of DMSO and reduce safety concerns.

From the perspective of pharmaceutics, several techniques for solubilization, including amorphisation, emulsification, micellisation, nano-crystallisation and host-guest inclusion exist. Notably, amorphisation does not significantly improve the solubility of SIN (with only an approximate 7% increment), as shown previously[6]. Although emulsification optimises the solubility of SIN, emulsifiers have stability issues and may interact with the drug to affect its bioavailability [7]. Micellisation involves the encapsulation of SIN in micelles to improve solubility; however, the material utilised to prepare micelles may affect the rate of drug release, whereas the formulation and concentration of the micelles must be optimised to avoid potential interactions[8]. Nano-crystallisation can significantly enhance the solubility and dissolution rate of SIN; however, the preparation process for nano-crystallisation is complex and costly[9]. Additionally, the stability of the nanoparticles and potential particle aggregation must be addressed. Host-guest inclusion improves the solubility of SIN[10], which effectively prevents recrystallisation of the drug in an aqueous phase by encapsulating SIN in the hydrophobic inner cavity of the host molecule, thus optimising its solubility and bioavailability. Compared with the solubilization methods listed above, host-guest inclusion has the advantages of improved stability, lower cost and an increased release rate and bioavailability of the drug. Therefore, we conclude that host-guest inclusion holds promise for SIN solubilization.

Host-guest inclusion is defined as a drug molecule wholly or partially encapsulated into the molecular cavity of the encapsulation agent[11]. Herein, the 'host' and 'guest' refer to the encapsulation agent and the drug, respectively. Materials that are commonly utilised as encapsulation agents include cyclodextrins, calixarene and cucurbits. Of these, cyclodextrins are widely considered to be the best materials for host-guest inclusion because of their excellent biocompatibility, efficient encapsulation ability, mature preparation process and good drug stability[12]. There are three major categories of cyclodextrins, namely α-, β-, and γ-cyclodextrin. β-cyclodextrin has a larger cavity inner diameter compared to α-cyclodextrin and a lower production cost compared to γ-cyclodextrin, and therefore it has rapidly become a research hotspot in recent years. According to the literature[13], β-cyclodextrin is widely employed because of its strong interaction with various guest molecules. Several derivatives of β-cyclodextrin have been developed, such as 2-hydroxypropyl-β-cyclodextrin, sulfobutyl aether-β-cyclodextrin and amino-β-cyclodextrin. They exhibit superior solubilization effects, better drug stability, lower toxicity and side effects and optimised drug release properties compared with common β-cyclodextrin[14]. Some commercially available injections use cyclodextrin as the solubiliser, such as Cylert® (containing 2-hydroxypropyl-β-cyclodextrin), DepoCyte® (containing sulfobutyl aether-β-cyclodextrin) and Kytril® (containing a mixture of α, β, and γ-cyclodextrins)[15]. Noteworthily, a previous study synthesised a β-cyclodextrin-grafted polymer to encapsulate SIN, which showed a high interaction intensity with the guest molecule. Overall, we believe that the β-cyclodextrin inclusion complex can effectively solubilise SIN, thus circumventing the need for DMSO and facilitating its clinical application (Figure 2).

To facilitate the clinical translation of the SIN-β-cyclodextrin complex, several prerequisites must be fulfilled. First, a safety assessment, which includes toxicity and allergic reactions, must be carried out on the SIN-β-cyclodextrin complex. Second, pharmacodynamic evaluation is required to ensure that the complex has the desired therapeutic effect. Stability testing studies are also required to ensure that it is stable during storage and use. Finally, compliance and regulatory approvals are required and SIN-β-cyclodextrin complexes must comply with relevant drug regulations and clinical trial requirements to obtain official approval. Once all the above are achieved, the clinical application of the relevant products will be possible.

In conclusion, in the study of Xiao *et al*[1] evaluating SIN to modulate autophagy for the treatment of osteoporosis, considering the safety issue of DMSO solubilization, we proposed a safer method, which involves the preparation of SIN-β-cyclodextrin complexes instead of DMSO co-solubilization. After comparing different methods of solubilising SIN, we

contend that the use of the host-guest inclusion method with β-cyclodextrin and its derivatives is superior for the solubilization of SIN. However, host-guest inclusion technology has several disadvantages such as limited release control, stability issues and toxicity risks. These disadvantages can affect the clinical transformation of SIN-β-cyclodextrin complexes by complicating dose optimization, controlling release profiles, and ensuring long-term safety. Considering the future clinical application of SIN-β-cyclodextrin complexes, issues including safety, efficacy, stability and the relevant laws and regulations must be addressed. Once these issues are resolved, the clinical application of SIN-β-cyclodextrin complexes to treat osteoporosis may be achieved.

FOOTNOTES

Author contributions: Guo MQ contributed to the manuscript writing and artwork preparation; Hu P and Huang ZW participated in the conceptualisation, supervision, and proofreading of this manuscript, and they contributed equally to this manuscript as co-corresponding authors. All authors have read and agreed to the published version of the manuscript.

Supported by Guangdong Basic and Applied Basic Research Foundation, No. 2024A1515011236; and General Program of Administration of Traditional Chinese Medicine of Guangdong Province, No. 20241071.

Conflict-of-interest statement: All the authors report no relevant conflicts of interest for this article.

Country of origin: China

ORCID number: Zheng-Wei Huang 0000-0003-2351-7347.

S-Editor: Wang JJ
L-Editor: A
P-Editor: Zhang XD

REFERENCES

1 **Xiao HX**, Yu L, Xia Y, Chen K, Li WM, Ge GR, Zhang W, Zhang Q, Zhang HT, Geng DC. Sinomenine increases osteogenesis in mice with ovariectomy-induced bone loss by modulating autophagy. *World J Stem Cells* 2024; **16**: 486-498 [PMID: 38817333 DOI: 10.4252/wjsc.v16.i5.486]

2 **Patil M**. Pharmacology and Clinical Use of Dimethyl Sulfoxide (DMSO): A Review. *Int J Mol Vet Res* 2013 [DOI: 10.5376/ijmvr.2013.03.0006]

3 **Kollerup Madsen B**, Hilscher M, Zetner D, Rosenberg J. Adverse reactions of dimethyl sulfoxide in humans: a systematic review. *F1000Res* 2018; **7**: 1746 [PMID: 31489176 DOI: 10.12688/f1000research.16642.2]

4 **den Brok MW**, Nuijen B, Lutz C, Opitz HG, Beijnen JH. Pharmaceutical development of a lyophilised dosage form for the investigational anticancer agent Imexon using dimethyl sulfoxide as solubilising and stabilising agent. *J Pharm Sci* 2005; **94**: 1101-1114 [PMID: 15793808 DOI: 10.1002/jps.20331]

5 **Chen X**, Li D, Zhang H, Duan Y, Huang Y. Sinomenine-phenolic acid coamorphous drug systems: Solubilization, sustained release, and improved physical stability. *Int J Pharm* 2021; **598**: 120389 [PMID: 33609724 DOI: 10.1016/j.ijpharm.2021.120389]

6 **Chen X**, Li D, Zhang H, Duan Y, Huang Y. Co-amorphous systems of sinomenine with nonsteroidal anti-inflammatory drugs: A strategy for solubility improvement, sustained release, and drug combination therapy against rheumatoid arthritis. *Int J Pharm* 2021; **606**: 120894 [PMID: 34280485 DOI: 10.1016/j.ijpharm.2021.120894]

7 **Zou L**, Liu W, Liu C, Xiao H, McClements DJ. Designing excipient emulsions to increase nutraceutical bioavailability: emulsifier type influences curcumin stability and bioaccessibility by altering gastrointestinal fate. *Food Funct* 2015; **6**: 2475-2486 [PMID: 26165514 DOI: 10.1039/c5fo00606f]

8 **Ahmad Z**, Shah A, Siddiq M, Kraatz HB. Polymeric micelles as drug delivery vehicles. *RSC Adv* 2014; **4**: 17028-17038 [DOI: 10.1039/C3RA47370H]

9 **Muller RH**, Keck CM. Challenges and solutions for the delivery of biotech drugs--a review of drug nanocrystal technology and lipid nanoparticles. *J Biotechnol* 2004; **113**: 151-170 [PMID: 15380654 DOI: 10.1016/j.jbiotec.2004.06.007]

10 **Wankar J**, Kotla NG, Gera S, Rasala S, Pandit A, Rochev YA. Recent Advances in Host–Guest Self-Assembled Cyclodextrin Carriers: Implications for Responsive Drug Delivery and Biomedical Engineering. *Adv Funct Mater* 2020; **30**: 1909049 [DOI: 10.1002/adfm.201909049]

11 **Hu Y**, Jiang L, Xing K, Li X, Sang S, Mcclements DJ, Chen L, Long J, Jiao A, Xu X, Wang J, Jin Z, Shang M, Qiu C. Cyclodextrins promoting the analysis and application of food-grade protein/peptides. *Trends Food Sci Tech* 2023; **137**: 63-73 [DOI: 10.1016/j.tifs.2023.05.009]

12 **Păduraru DN**, Niculescu AG, Bolocan A, Andronic O, Grumezescu AM, Bîrlă R. An Updated Overview of Cyclodextrin-Based Drug Delivery Systems for Cancer Therapy. *Pharmaceutics* 2022; **14**: 1748 [PMID: 36015374 DOI: 10.3390/pharmaceutics14081748]

13 **Singh G**, Singh PK. Complexation of a cationic pyrene derivative with sulfobutylether substituted β-cyclodextrin: Towards a stimulus-

responsive supramolecular material. *J Mol Liq* 2020; **305**: 112840 [DOI: 10.1016/j.molliq.2020.112840]

14 **Zhang Z**, Niu J, Wang J, Zheng Q, Miao W, Lin Q, Li X, Jin Z, Qiu C, Sang S, Ji H. Advances in the preparation and application of cyclodextrin derivatives in food and the related fields. *Food Res Int* 2024; **195**: 114952 [PMID: 39277230 DOI: 10.1016/j.foodres.2024.114952]

15 **Jacob S**, Nair AB. Cyclodextrin complexes: Perspective from drug delivery and formulation. *Drug Dev Res* 2018; **79**: 201-217 [PMID: 30188584 DOI: 10.1002/ddr.21452]

World Journal of Stem Cells

Submit a Manuscript: https://www.f6publishing.com

World J Stem Cells 2025 March 26; 17(3): 104566

DOI: 10.4252/wjsc.v17.i3.104566

ISSN 1948-0210 (online)

LETTER TO THE EDITOR

Efficacy equivalence but hidden hurdles: Can serum-free human umbilical cord mesenchymal stem cells translate to clinically superior osteoarthritis therapy

Fang Lin, Ke-Xin Ma, Yue Ding, Xiao-Ting Liang

Specialty type: Cell and tissue engineering

Provenance and peer review: Invited article; Externally peer reviewed.

Peer-review model: Single blind

Peer-review report's classification
Scientific Quality: Grade B, Grade B
Novelty: Grade A, Grade B
Creativity or Innovation: Grade A, Grade B
Scientific Significance: Grade B, Grade B

P-Reviewer: Liu S; Wen L

Received: December 25, 2024
Revised: January 21, 2025
Accepted: February 18, 2025
Published online: March 26, 2025
Processing time: 87 Days and 1.7 Hours

Fang Lin, Ke-Xin Ma, Xiao-Ting Liang, Translational Medical Center for Stem Cell Therapy and Institute for Regenerative Medicine, Shanghai East Hospital, Tongji University School of Medicine, Shanghai 200120, China

Fang Lin, Xiao-Ting Liang, Shanghai Heart Failure Research Center, Shanghai East Hospital, Tongji University School of Medicine, Shanghai 200120, China

Yue Ding, Department of Organ Transplantation, Changzheng Hospital, Naval Medical University, Shanghai 200000, China

Xiao-Ting Liang, Shenzhen Ruipuxun Academy for Stem Cell and Regenerative Medicine, Shenzhen 515100, Guangdong Province, China

Co-first authors: Fang Lin and Ke-Xin Ma.

Co-corresponding authors: Yue Ding and Xiao-Ting Liang.

Corresponding author: Xiao-Ting Liang, Translational Medical Center for Stem Cell Therapy and Institute for Regenerative Medicine, Shanghai East Hospital, Tongji University School of Medicine, No. 150 Jimo Road, Shanghai 200120, China. liangxt@tongji.edu.cn

Abstract

This article discusses the study by Xiao *et al*, which investigated the therapeutic efficacy of serum-free cultured human umbilical cord mesenchymal stem cells (N-hUCMSCs) in a mouse model of knee osteoarthritis. The results showed that N-hUCMSCs alleviated osteoarthritis-related cartilage damage and inflammation comparably to both serum-cultured hUCMSCs and hyaluronic acid. While these findings broaden the potential clinical utility of N-hUCMSCs by circumventing certain drawbacks of serum-based cultures, the equivalence in efficacy raises important questions. First, how do N-hUCMSCs differ phenotypically from serum-cultured hUCMSCs, particularly in terms of proliferation rate, replicative capacity, and senescence profile? Second, what advantages might N-hUCMSCs offer over hyaluronic acid - a well-established therapy - beyond avoiding xenogeneic components and ethical concerns? Future research should focus on long-term phenotypic stability, sustained functional benefits, safety profiles, and mechanistic insights to ascertain whether N-hUCMSCs can surpass current standards of care.

Key Words: Mesenchymal stem cells; Serum-free culture; Osteoarthritis; Cartilage repair; Regenerative medicine

Core Tip: This article evaluates the study by Xiao *et al* on using serum-free cultured human umbilical cord mesenchymal stem cells (N-hUCMSCs) to treat knee osteoarthritis in a mouse model. Although N-hUCMSCs matched the efficacy of both serum-cultured hUCMSCs and hyaluronic acid, future research must clarify how N-hUCMSCs differ in long-term proliferative capacity and senescence profiles compared to their serum-cultured counterparts. Additionally, since hyaluronic acid is an established osteoarthritis treatment, demonstrating clear advantages, such as fewer side effects, more durable outcomes, or enhanced cartilage regeneration, will be crucial for justifying the clinical adoption of N-hUCMSCs.

Citation: Lin F, Ma KX, Ding Y, Liang XT. Efficacy equivalence but hidden hurdles: Can serum-free human umbilical cord mesenchymal stem cells translate to clinically superior osteoarthritis therapy. *World J Stem Cells* 2025; 17(3): 104566
URL: https://www.wjgnet.com/1948-0210/full/v17/i3/104566.htm
DOI: https://dx.doi.org/10.4252/wjsc.v17.i3.104566

TO THE EDITOR

We read with great interest the recent study by Xiao *et al*[1], which demonstrated that intra-articular injection of serum-free cultured human umbilical cord mesenchymal stem cells (N-hUCMSCs) effectively alleviates cartilage damage and inflammation in a mouse model of knee osteoarthritis (OA). By comparing N-hUCMSCs with both serum-cultured hUCMSCs (S-hUCMSCs) and hyaluronic acid (HA), the authors present evidence that a serum-free cell culture system can achieve therapeutic outcomes equivalent to well-established treatments. This advance is noteworthy, given that traditional fetal bovine serum-based systems pose ethical concerns, xenogeneic risks, and regulatory challenges.

The study showed that N-hUCMSCs retained regenerative capacity and anti-inflammatory properties. However, because N-hUCMSCs performed similarly to S-hUCMSCs, it raises the question of whether and how the serum-free approach influences key cellular phenotypes. Recent research has indicated that while serum free-expanded MSCs demonstrate higher proliferative capacity, this trait does not always correlate with their chondrogenic potential or cartilage repair efficacy[2]. Other studies showed that UCMSCs cultured in serum-free and serum-containing media exhibit similar proliferation, morphology, MSC surface marker expression, and stemness[3]. However, exosomes derived from UCMSCs cultured in different media display variations in growth factor and cytokine levels, which could impact their therapeutic potential[4]. These findings underscore the importance of thoroughly evaluating the effects of serum-free media on intrinsic properties and functional characteristics of MSC. Another important aspect is that over multiple passages, MSCs typically face replicative senescence, reduced proliferative capacity, and altered paracrine function[5]. A comparison of N-hUCMSCs and S-hUCMSCs - focusing on proliferation rates, maximum population doublings, senescence markers, and differentiation potential - would provide insights into whether serum-free conditions confer any long-term advantages. If N-hUCMSCs maintain a more stable phenotype over successive passages, this could justify their use despite any additional complexity and cost in their production process.

Furthermore, while N-hUCMSCs matched HA in reducing OA-related symptoms, HA already serves as a common and relatively simple OA therapy. HA injections can, however, have variable efficacy and may cause injection-site pain or inflammation[6]. A key question is whether N-hUCMSCs can surpass HA by offering more durable benefits, fewer adverse effects, or superior cartilage regeneration. Addressing this is critical, as cell-based therapies will likely be more resource-intensive. To be adopted clinically, N-hUCMSCs must demonstrate clear advantages in terms of safety, long-term outcomes, and mechanistic benefits - such as enhanced cartilage repair or more robust modulation of the joint's immune environment - beyond what HA can achieve.

Strength and limitation

The comparative approach of the study is a clear strength. However, the small cohort size and noted mortality in the stem cell-treated groups limit generalizability and suggest that delivery protocols may need refinement. Identifying optimal dosages and delivery methods to minimize stress-related mortality will be essential. More importantly, the study's primary reliance on histological and biochemical endpoints, while informative, leaves mechanistic details unexplored. Understanding how N-hUCMSCs regulate local inflammation, extracellular matrix remodeling, and host immune responses at the molecular level could uncover unique therapeutic targets and clarify how these cells differ from conventional treatments.

Future directions

Looking ahead, long-term culture studies comparing N-hUCMSCs and S-hUCMSCs would determine whether serum-free conditions preserve proliferative capacity, delay senescence, or enhance functional properties over successive passages. Employing transcriptomics, proteomics, and metabolomics could elucidate the pathways driving N-hUCMSC-

mediated tissue repair and highlight how these pathways differ from those of HA or S-hUCMSCs. Such large-scale omics approaches would also facilitate the identification of novel biomarkers for monitoring therapeutic outcomes. Furthermore, using advanced imaging techniques such as magnetic resonance imaging or micro-computed tomography at multiple time points would enable precise and longitudinal visualization of cartilage repair, offering a more comprehensive assessment of N-hUCMSC-mediated tissue regeneration.

Additionally, systematic dose-response studies, improved cell delivery methods, and standardized anesthetic conditions will help reduce adverse events, increase reproducibility, and better underscore N-hUCMSCs' potential advantages over HA. Moreover, in assessing the broader clinical feasibility of N-hUCMSCs, cost implications and scalability of serum-free systems should be carefully evaluated. Demonstrating that this approach is both economically viable and capable of supporting large-scale production will be pivotal for translating serum-free cultured MSCs into routine clinical practice.

Conclusion

Xiao *et al*'s study underscores the potential of N-hUCMSCs as a viable OA therapy[1]. The serum-free approach holds promise, but further validation is needed. Establishing whether N-hUCMSCs maintain superior phenotypic stability compared to S-hUCMSCs and confirming their capacity to outperform HA in terms of longevity of effect, safety, and regenerative efficacy will be pivotal. By addressing these questions and enhancing mechanistic insight, future research could position N-hUCMSCs as a transformative option for patients with OA.

FOOTNOTES

Author contributions: Lin F and Ma KX contributed equally to this work and as co-first authors of this manuscript. Lin F, Ma KX, and Ding Y wrote the original draft; Ding Y and Liang XT contributed to reviewing and editing the manuscript, and supervised the project. Ding Y and Liang XT are co-corresponding authors. All the authors have read and approved the manuscript.

Supported by the Natural Science Foundation of Shanghai, No. 24ZR1459300 (to Xiao-Ting Liang); and the Pyramid Talent Project, No. YQ677 (to Yue Ding).

Conflict-of-interest statement: All the authors report no relevant conflicts of interest for this article.

Country of origin: China

ORCID number: Fang Lin 0000-0001-8008-7764; Yue Ding 0009-0003-8552-1381; Xiao-Ting Liang 0000-0003-3262-1859.

S-Editor: Wang JJ
L-Editor: Filipodia
P-Editor: Zhao YQ

REFERENCES

1 **Xiao KZ**, Liao G, Huang GY, Huang YL, Gu RH. Efficacy of serum-free cultured human umbilical cord mesenchymal stem cells in the treatment of knee osteoarthritis in mice. *World J Stem Cells* 2024; **16**: 944-955 [PMID: 39619871 DOI: 10.4252/wjsc.v16.i11.944]

2 **Kang M**, Yang Y, Zhang H, Zhang Y, Wu Y, Denslin V, Othman RB, Yang Z, Han J. Comparative Analysis of Serum and Serum-Free Medium Cultured Mesenchymal Stromal Cells for Cartilage Repair. *Int J Mol Sci* 2024; **25**: 10627 [PMID: 39408956 DOI: 10.3390/ijms251910627]

3 **Wu X**, Ma Z, Wu D. Derivation of clinical-grade mesenchymal stromal cells from umbilical cord under chemically defined culture condition - platform for future clinical application. *Cytotherapy* 2020; **22**: 377-387 [PMID: 32439307 DOI: 10.1016/j.jcyt.2020.03.431]

4 **Dao HH**, Nguyen TH, Hoang DH, Vu BD, Tran MA, Le MT, Hoang NTM, Bui AV, Than UTT, Nguyen XH. Manufacturing exosomes for wound healing: Comparative analysis of culture media. *PLoS One* 2024; **19**: e0313697 [PMID: 39541412 DOI: 10.1371/journal.pone.0313697]

5 **Wang J**, Zhang M, Wang H. Emerging Landscape of Mesenchymal Stem Cell Senescence Mechanisms and Implications on Therapeutic Strategies. *ACS Pharmacol Transl Sci* 2024; **7**: 2306-2325 [PMID: 39144566 DOI: 10.1021/acsptsci.4c00284]

6 **Ferkel E**, Manjoo A, Martins D, Bhandari M, Sethi P, Nicholls M. Intra-articular Hyaluronic Acid Treatments for Knee Osteoarthritis: A Systematic Review of Product Properties. *Cartilage* 2023; **14**: 424-432 [PMID: 37314014 DOI: 10.1177/19476035231154530]

Published by **Baishideng Publishing Group Inc**
7041 Koll Center Parkway, Suite 160, Pleasanton, CA 94566, USA
Telephone: +1-925-3991568
E-mail: office@baishideng.com
Help Desk: https://www.f6publishing.com/helpdesk
https://www.wjgnet.com